



# Modelling and Solving the Single-Airport Slot Allocation Problem

By

Fotios A. Katsigiannis

THESIS SUBMITTED FOR  
THE DEGREE OF DOCTOR OF PHILOSOPHY (PhD)

Centre for Transport and Logistics (CENTRAL)

Department of Management Science

Lancaster University Management School

Lancaster, UK

March 2022



This thesis is dedicated to Maria.

*For supporting and helping me in all things great and small.*



# Declaration

This thesis is my own work and has not been submitted elsewhere for the award of any other degree at this or any other university. Except where stated otherwise by reference or acknowledgement the work presented is original and entirely my own.

The main body of this thesis consists of three research papers that are either published, submitted for publication or are in preparation for submission.

- Chapter 2 has been published in Transportation Research Part B: Methodological as Katsigiannis, F. A., Zografos, K. G. (2021a). *Optimising airport slot allocation considering flight-scheduling flexibility and total airport capacity constraints*. In chapters 3 and 4, references to this paper (which appear as [Katsigiannis and Zografos., 2021a]) can be interpreted as references to chapter 2.
- Chapter 3 has been submitted for publication as Katsigiannis, F. A., and Zografos K. G. (2022a). *Multi-objective airport slot scheduling incorporating operational delays and multi-stakeholder preferences*.
- Chapter 4 has been submitted for publication as Katsigiannis, F. A., and Zografos K. G. (2022b). *On the stable allocation of airport slots*.

*Fotios A. Katsigiannis*  
*March 2022*



# Acknowledgements

First and foremost, I would like to express my sincere gratitude to Prof Konstantinos G. Zografos, who gave me the opportunity to join Lancaster University and devoted his time unfailingly in countless meetings and discussions. Your rigour and research integrity instilled into me patience and values that are scarce and difficult to obtain in our days.

My gratitude is extended to my second supervisor Prof Guglielmo Lulli and all faculty members and researchers across the University with whom I engaged during the past four years.

In addition, I am grateful for the doctoral studentship provided by Lancaster University Management School in the context of the OR-MASTER programme grant (EP/M020258/1) funded by the Engineering and Physical Sciences Research Council (EPSRC).

I am indebted to my family for their sacrifices, unconditional love, and support. During difficult times they provided safety and allowed me to pursue my dreams undistracted. Μάνα, Πατέρα you are my heroes. Παππού, thank you for the life lessons that you taught me. Γιαγιά, thank you for the childhood tales and the time that you spent with me.

Finally, enduring thanks go to my friends that supported my personal life in Lancaster. Without you, things would have been a lot more difficult for me.

Addendum: I would like to thank Prof Julia Bennell and Prof Kevin Glazebrook for examining this thesis. Their rigorous review led to the improvement of this document. It was a true pleasure to discuss my work with them.





# Abstract

Currently, there are about 200 overly congested airports where airport capacity does not suffice to accommodate airline demand. These airports play a critical role in the global air transport system since they concern 40% of global passenger demand and act as a bottleneck for the entire air transport system. This imbalance between airport capacity and airline demand leads to excessive delays, as well as multi-billion economic, and huge environmental and societal costs. Concurrently, the implementation of airport capacity expansion projects requires time, space and is subject to significant resistance from local communities. As a short to medium-term response, Airport Slot Allocation (ASA) has been used as the main demand management mechanism.

The main goal of this thesis is to improve ASA decision-making through the proposition of models and algorithms that provide enhanced ASA decision support. In doing so, this thesis is organised into three distinct chapters that shed light on the following questions (I–V), which remain untapped by the existing literature. In parentheses, we identify the chapters of this thesis that relate to each research question.

- I. How to improve the modelling of airline demand flexibility and the utility that each airline assigns to each available airport slot? (Chapters 2 and 4)
- II. How can one model the dynamic and endogenous adaptation of the airport's landside and airside infrastructure to the characteristics of airline demand? (Chapter 2)
- III. How to consider operational delays in strategic ASA decision-making? (Chapter 3)

- IV. How to involve the pertinent stakeholders into the ASA decision-making process to select a commonly agreed schedule; and how can one reduce the inherent decision-complexity without compromising the quality and diversity of the schedules presented to the decision-makers? (Chapter 3)
- V. Given that the ASA process involves airlines (submitting requests for slots) and coordinators (assigning slots to requests based on a set of rules and priorities), how can one jointly consider the interactions between these two sides to improve ASA decision-making? (Chapter 4)

With regards to research questions (I) and (II), the thesis proposes a Mixed Integer Programming (MIP) model that considers airlines' timing flexibility (research question I) and constraints that enable the dynamic and endogenous allocation of the airport's resources (research question II). The proposed modelling variant addresses several additional problem characteristics and policy rules, and considers multiple efficiency objectives, while integrating all constraints that may affect airport slot scheduling decisions, including the asynchronous use of the different airport resources (runway, aprons, passenger terminal) and the endogenous consideration of the capabilities of the airport's infrastructure to adapt to the airline demand's characteristics and the aircraft/flight type associated with each request. The proposed model is integrated into a two-stage solution approach that considers all primary and several secondary policy rules of ASA. New combinatorial results and valid tightening inequalities that facilitate the solution of the problem are proposed and implemented.

An extension of the above MIP model that considers the trade-offs among schedule displacement, maximum displacement, and the number of displaced

requests, is integrated into a multi-objective solution framework. The proposed framework holistically considers the preferences of all ASA stakeholder groups (research question IV) concerning multiple performance metrics and models the operational delays associated with each airport schedule (research question III). The delays of each schedule/solution are macroscopically estimated, and a subtractive clustering algorithm and a parameter tuning routine reduce the inherent decision complexity by pruning non-dominated solutions without compromising the representativeness of the alternatives offered to the decision-makers (research question IV). Following the determination of the representative set, the expected delay estimates of each schedule are further refined by considering the whole airfield's operations, the landside, and the airside infrastructure. The representative schedules are ranked based on the preferences of all ASA stakeholder groups concerning each schedule's displacement-related and operational-delay performance.

Finally, in considering the interactions between airlines' timing flexibility and utility, and the policy-based priorities assigned by the coordinator to each request (research question V), the thesis models the ASA problem as a two-sided matching game and provides guarantees on the stability of the proposed schedules. A *Stable Airport Slot Allocation Model* (SASAM) capitalises on the flexibility considerations introduced for addressing research question (I) through the exploitation of data submitted by the airlines during the ASA process and provides functions that proxy each request's value considering both the airlines' timing flexibility for each submitted request and the requests' prioritisation by the coordinators when considering the policy rules defining the ASA process. The thesis argues on the compliance of the proposed functions with the primary regulatory requirements of the ASA process and demonstrates their applicability for different types of slot requests. SASAM guarantees stability through sets of inequalities that

prune allocations blocking the formation of stable schedules. A multi-objective *Deferred-Acceptance* (DA) algorithm guaranteeing the stability of each generated schedule is developed. The algorithm can generate all stable non-dominated points by considering the trade-off between the spilled airline and passenger demand and maximum displacement.

The work conducted in this thesis addresses several problem characteristics and sheds light on their implications for ASA decision-making, hence having the potential to improve ASA decision-making. Our findings suggest that the consideration of airlines' timing flexibility (research question I) results in improved capacity utilisation and scheduling efficiency. The endogenous consideration of the ability of the airport's infrastructure to adapt to the characteristics of airline demand (research question II) enables a more efficient representation of airport declared capacity that results in the scheduling of additional requests. The concurrent consideration of airlines' timing flexibility and the endogenous adaptation of airport resources to airline demand achieves an improved alignment between the airport infrastructure and the characteristics of airline demand, ergo proposing schedules of improved efficiency. The modelling and evaluation of the peak operational delays associated with the different airport schedules (research question III) provides allows the study of the implications of strategic ASA decision-making for operations and quantifies the impact of the airport's declared capacity on each schedule's operational performance. In considering the preferences of the relevant ASA stakeholders (airlines, coordinators, airport, and air traffic authorities) concerning multiple operational and strategic ASA efficiency metrics (research question IV) the thesis assesses the impact of alternative preference considerations and indicates a commonly preferred schedule that balances the stakeholders' preferences. The proposition of representative subsets of alternative schedules reduces decision-complexity without significantly compromising the

quality of the alternatives offered to the decision-making process (research question IV). The modelling of the ASA as a two-sided matching game (research question V), results in stable schedules consisting of request-to-slot assignments that provide no incentive to airlines and coordinators to reject or alter the proposed timings. Furthermore, the proposition of stable schedules results in more intensive use of airport capacity, while simultaneously improving scheduling efficiency.

The models and algorithms developed as part of this thesis are tested using airline requests and airport capacity data from coordinated airports. Computational results that are relevant to the context of the considered airport instances provide evidence on the potential improvements for the current ASA process and facilitate data-driven policy and decision-making. In particular, with regards to the alignment of airline demand with the capabilities of the airport's infrastructure (questions I and II), computational results report improved slot allocation efficiency and airport capacity utilisation, which for the considered airport instance translate to improvements ranging between 5-24% for various schedule performance metrics. In reducing the difficulty associated with the assessment of multiple ASA solutions by the stakeholders (question IV), instance-specific results suggest reductions to the number of alternative schedules by 87%, while maintaining the quality of the solutions presented to the stakeholders above 70% (expressed in relation to the initially considered set of schedules). Meanwhile, computational results suggest that the concurrent consideration of ASA stakeholders' preferences (research question IV) with regards to both operational (research question III) and strategic performance metrics leads to alternative airport slot scheduling solutions that inform on the trade-offs between the schedules' operational and strategic performance and the stakeholders' preferences. Concerning research question (V), the application of SASAM and the DA algorithm suggest improvements to the number of unaccommodated flights and passengers (13 and 40% improvements) at

the expense of requests concerning fewer passengers and days of operations (increasing the number of rejected requests by 1.2% in relation to the total number of submitted requests).

The research conducted in this thesis aids in the identification of limitations that should be addressed by future studies to further improve ASA decision-making. First, the thesis focuses on exact solution approaches that consider the landside and airside infrastructure of the airport and generate multiple schedules. The proposition of pre-processing techniques that identify the bottleneck of the airport's capacity, i.e., landside and/or airside, can be used to reduce the size of the proposed formulations and improve the required computational times. Meanwhile, the development of multi-objective heuristic algorithms that consider several problem characteristics and generate multiple efficient schedules in reasonable computational times, could extend the capabilities of the models propositioned in this thesis and provide decision support for some of the world's most congested airports. Furthermore, the thesis models and evaluates the operational implications of strategic airport slot scheduling decisions. The explicit consideration of operational delays as an objective in ASA optimisation models and algorithms is an issue that merits investigation since it may further improve the operational performance of the generated schedules. In accordance with current practice, the models proposed in this work have considered deterministic capacity parameters. Perhaps, future research could propose formulations that consider stochastic representations of airport declared capacity and improve strategic ASA decision-making through the anticipation of operational uncertainty and weather-induced capacity reductions. Finally, in modelling airlines' utility for each submitted request and available time slot the thesis proposes time-dependent functions that utilise available data to approximate airlines' scheduling preferences. Future studies wishing to improve the accuracy of the proposed functions could utilise commercial

data sources that provide route-specific information; or in cases that such data is unavailable, employ data mining and machine learning methodologies to extract airlines' time-dependent utility and preferences.





# Table of Contents

Chapter 1: Introduction and Background .....	1
1.1 Motivation .....	1
1.2 The Airport Slot Allocation process and literature .....	4
1.2.1 Overview of the ASA process as per the WASG .....	4
1.2.2 Related work .....	7
1.3 Contributions.....	13
1.4 Overview and structure of the thesis .....	13
Chapter 2: Optimising airport slot allocation considering flight-scheduling flexibility and total airport capacity constraints.....	20
2.1 Introduction.....	20
2.2 Previous related work .....	27
2.3 Summary of the proposed modelling and solution framework.....	32
2.4 Airport slot allocation model .....	36
2.4.1 Base model.....	36
2.4.2 Terminal and airport capacity modelling .....	42
2.4.3 Dynamic capacity utilisation expressions .....	50
2.5 The Timing Flexibility Identifier Model (TFIM) .....	55
2.5.1 Timing flexibility membership functions .....	57
2.5.2 Description of the TFIM .....	60
2.6 Formulation strengthening.....	61

---

2.6.1	Requests having only lower turnaround times.....	62
2.6.2	Requests with lower and upper turnaround times that are equal to the requested time separation .....	65
2.6.3	Performance and impact of the proposed inequalities on linear relaxation, nodes, and computational time .....	69
2.7	A computational study .....	73
2.7.1	Data and experimental setup .....	74
2.7.2	Computational results .....	77
2.8	Concluding remarks .....	111
Chapter 3: Multi-objective airport slot scheduling incorporating operational delays and multi-stakeholder preferences .....		115
3.1	Introduction.....	115
3.1.1	Background .....	117
3.1.2	Previous related work.....	121
3.1.3	Contributions .....	126
3.2	Overview of the proposed framework.....	127
3.3	A multi-objective, multi-stakeholder airport slot allocation framework .....	131
3.3.1	A multi-objective airport slot allocation model for constructing airport slot schedules .....	132
3.3.2	Schedule generation module .....	139
3.3.3	Clustering module: selecting a subset of representative solutions.....	143

---

3.3.4	Delay estimation modules: estimation of the expected delays associated with the non-dominated and the representative schedules.....	147
3.3.5	Schedule elicitation module .....	154
3.4	Application .....	163
3.4.1	Data and experimental setup .....	164
3.4.2	Results from the application of the AHP model.....	168
3.4.3	Computational results and analysis of the schedules obtained from the proposed framework.....	176
3.5	Concluding remarks .....	214
Chapter 4:	On the stable allocation of airport slots .....	219
4.1	Introduction.....	219
4.1.1	Previous related work.....	222
4.1.2	Contributions .....	225
4.2	Summary of the proposed approach.....	227
4.3	The stable Airport slot Allocation Model (SASAM).....	230
4.3.1	Modelling foundations .....	230
4.3.2	Enforcing stability in ASA decisions .....	234
4.4	Solution methodology .....	259
4.4.1	MIP solution approach.....	259
4.4.2	Deferred acceptance algorithm .....	261
4.5	Application and computational results .....	280
4.5.1	Data and computational setup .....	280

---

4.5.2	Sensitivity of the functions with respect to different parameters .....	286
4.5.3	Comparisons between the schedules obtained by u-MIP and s-MIP ...	300
4.5.4	Assessment of the schedules obtained by the DA algorithm and comparison with s-MIP and u-MIP .....	307
4.5.5	Sample output and decision-making support .....	321
4.6	Concluding remarks .....	323
Chapter 5:	Conclusion .....	328
5.1	Summary .....	328
5.2	Recommendations for future research .....	332
Bibliography	.....	335



# List of Figures

<b>Figure 2-1:</b> Overview of the slot coordination process .....	26
<b>Figure 2-2:</b> Flowchart summarising the modelling components of this chapter .... .....	33
<b>Figure 2-3:</b> Example on the asynchronous interaction between runways, apron, and terminals .....	49
<b>Figure 2-4:</b> Graphical representation of Example 2.2 .....	58
<b>Figure 2-5:</b> Performance profile of the different models and comparison when tightened by expressions (2.59) .....	72
<b>Figure 2-6:</b> Radar plot comparing the <i>no-TFI</i> and the <i>TFI</i> schedule.....	80
<b>Figure 2-7:</b> Distribution of the gains/losses per airline and objective.....	85
<b>Figure 2-8:</b> Distribution of total displacement and the number of displaced requests per airline and request priority.....	88
<b>Figure 2-9:</b> Distribution of maximum displacement and displaced passengers per airline and priority .....	89
<b>Figure 2-10:</b> Comparison of the airport's capacity under the static and dynamic apron/passenger terminal constraints .....	93
<b>Figure 2-11:</b> Comparison of the dynamic and static capacity constraints under alternative scenarios.....	95
<b>Figure 2-12:</b> Radar chart comparing the performance of the capacity constraints and the <i>TFI</i> .....	106
<b>Figure 2-13:</b> Comparison between the base schedules given under alternative policy considerations .....	108
<b>Figure 3-1:</b> Overview of the proposed framework.....	131

---

<b>Figure 3-2:</b> Schematic overview of the macroscopic operational delay estimation module .....	149
<b>Figure 3-3:</b> Illustration of the proposed <i>AHP</i> model.....	157
<b>Figure 3-4:</b> Example of the structure of the <i>AHP</i> questionnaire (artificial response) .....	169
<b>Figure 3-5:</b> Objectives' priorities derived by the application of the <i>AHP</i> .....	172
<b>Figure 3-6:</b> Sensitivity analysis – Mean relative error of the objectives' priority weights.....	174
<b>Figure 3-7:</b> Determination of the representative points and the clustering parameters for the <i>H</i> level.....	181
<b>Figure 3-8:</b> Demonstration of the complete and the representative frontiers for each stakeholder group ( <i>H</i> priority) .....	182
<b>Figure 3-9:</b> Diagrammatical representation of the frontiers generated from the selected <i>H</i> schedules .....	185
<b>Figure 3-10:</b> Determination of the representative points and the clustering parameters for the CH, NE, and O level.....	187
<b>Figure 3-11:</b> Comparisons between the selected schedules of the different stakeholder groups .....	194
<b>Figure 3-12:</b> Value path diagrams displaying the trade-offs between the reported solutions.....	198
<b>Figure 3-13:</b> Comparison of the estimated delays of the requested and the allocated slots during the peak day .....	201
<b>Figure 3-14:</b> Comparative analysis of airlines' objectives under the different representative schedules .....	205
<b>Figure 3-15:</b> Screenshot illustrating the use of the interactive tool for comparing schedules .....	208

---

<b>Figure 3-16:</b> Screenshots showcasing the functionalities of the interactive visualisation tool .....	212
<b>Figure 3-17:</b> Inspecting the arrivals and the corresponding departures for a single schedule.....	213
<b>Figure 3-18:</b> Comparing the arrival requests/allocations of multiple schedules for one or multiple airlines.....	214
<b>Figure 4-1:</b> Overview of the proposed approach .....	229
<b>Figure 4-2:</b> Graphical representation of each request's function .....	245
<b>Figure 4-3:</b> Plots of the proposed functions for requests of different priorities .....	254
<b>Figure 4-4:</b> Demonstration of the memory property of Algorithm 4-1 .....	270
<b>Figure 4-5:</b> Demonstration of the multi-objective <i>DA</i> algorithm for the ASA problem .....	278
<b>Figure 4-6:</b> Distribution of demand exponent's values for each airline under different load factor scenarios.....	288
<b>Figure 4-7:</b> Scatter plot demonstrating the relationship between the components of $\xi'_m$ .....	290
<b>Figure 4-8:</b> Heatmap illustrating the correlation among multiple metrics and the value of $\xi'_m$ .....	292
<b>Figure 4-9:</b> Impact of alternative load factors on $\psi'_m$ .....	293
<b>Figure 4-10:</b> Scatter plot studying the relationships among the components of $\psi'_m$ .....	295
<b>Figure 4-11:</b> Correlation heatmap between the components of $\psi'_m$ .....	296
<b>Figure 4-12:</b> Schematic representation on the trade-off between airport capacity utilisation and scheduling performance for the schedules obtained by <i>s-MIP</i> and <i>u-MIP</i> .....	303



---

<b>Figure 4-13:</b> Bar-chart/table assessing the implications of stability for multiple airlines.....	306
<b>Figure 4-14:</b> Comparison among the schedules generated by different slot allocation schemes.....	313
<b>Figure 4-15:</b> Value paths of alternative solution reduction scenarios .....	316
<b>Figure 4-16:</b> Selection of schedules that are different from <i>s-MIP</i> and <i>u-MIP</i> .....	317
<b>Figure 4-17:</b> Performance profiles of <i>DA</i> and <i>h-DA-MIP</i> as a function of the requests' preference list size .....	320
<b>Figure 4-18:</b> Sample output from the execution of the proposed <i>DA</i> algorithm .....	322



# List of Tables

<b>Table 2-1:</b> Literature overview and gaps addressed by this chapter .....	31
<b>Table 2-2:</b> Overview of the parameters submitted by airlines as per the <i>SSIM</i> format .....	38
<b>Table 2-3:</b> Computational performance of expressions (2.59) .....	71
<b>Table 2-4:</b> Airport capacity parameters .....	74
<b>Table 2-5:</b> Parameters used in the experiments .....	76
<b>Table 2-6:</b> Comparison of the <i>no-TFI</i> and <i>TFI</i> schedules for each slot priority	83
<b>Table 3-1:</b> Input data and decision variables for the base model.....	133
<b>Table 3-2:</b> Declared capacity parameters of the two airports .....	165
<b>Table 3-3:</b> Requests' distribution and priority code for the two airports.....	165
<b>Table 3-4:</b> Parameters used in the <i>MACAD</i> model.....	167
<b>Table 3-5:</b> Comparison of the <i>H</i> schedules selected by considering the complete and the representative schedule sets .....	184
<b>Table 3-6:</b> Comparison of the <i>CH</i> , <i>NE</i> , <i>O</i> schedules selected under the complete and the representative schedule sets .....	188
<b>Table 4-1:</b> A toy instance of the preferences of the airlines and the priority assigned by the coordinator based on <i>WASG</i> .....	235
<b>Table 4-2:</b> Distribution of requests and the concerned passengers across the different request priorities .....	281
<b>Table 4-3:</b> Model parameters .....	282
<b>Table 4-4:</b> Description of the slot allocation schemes considered for the computational experiments .....	284
<b>Table 4-5:</b> Statistical comparison between the mean value of $\xi'_m$ under alternative load factor scenarios.....	289

<b>Table 4-6:</b> Statistical comparison between the mean values of $\psi'_m$ under alternative load factor scenarios.....	294
<b>Table 4-7:</b> Comparison between the mean values of $\psi'_m$ and $\xi'_m$ under alternative load factor scenarios.....	298
<b>Table 4-8:</b> Comparison between the schedules obtained by solving $s$ -MIP and $u$ -MIP .....	301

# Chapter 1: Introduction and Background

## 1.1 Motivation

Currently, there are about 200 airports where airline demand exceeds the available airport capacity (annex 12.7; IATA/ACI/WWACG, 2020). These airports constitute major links for the global air transport system since they account for 40% of global passenger demand and more than 55% of the total aircraft movements outside the United States (Odoni, 2020). Concurrently, these airports continue facing increased demand both in terms of aircraft and passenger movements (ACI, 2019). This signifies that congested airports face a demand-capacity imbalance which affects both their airside and landside infrastructure.

The airport capacity supply and airline passenger demand imbalance described above acts as a bottleneck to the sustainable and efficient growth of air travel, inflicting multi-billion delay-related costs to airlines, passengers, airports, and other airspace users, as well as significant CO<sub>2</sub> emissions. It is estimated that system-wide delay-related costs surpassed €11 billion in Europe and \$32.9 billion in the United States during 2013 (IATA, 2013) and 2007 (Ball et al., 2010) respectively. The situation is expected to exacerbate as the industry recovers from the COVID-19 pandemic and returns to normalcy.

Increasing capacity supply through the implementation of airport capacity expansion projects is the only sustainable solution to the aforementioned supply-demand imbalance. However, the resistance of local communities that reside close to the airports, spatial constraints, and the long-term implementation horizon of airport infrastructure expansion projects, suggest that in the short term the

attention of researchers and practitioners should be shifted to demand-side interventions. Demand-side interventions may be classified into three broad categories (Zografos et al., 2017b; Zografos and Jiang, 2019). These are:

- a) administrative approaches that allocate the available capacity using rules and regulations;
- b) market-based approaches that consider pricing mechanisms; and
- c) hybrid approaches that propose solutions consisting of both market and administrative schemes.

The work developed in this thesis pertains to single-airport administrative approaches since it proposes models and algorithms that consider the Airport Slot Allocation (ASA) process defined by the World Airport Scheduling Guidelines (WASG) (IATA/ACI/WWACG, 2020). The WASG-based ASA is the main administrative demand-management mechanism and is currently being applied in the majority of the worlds' congested airports residing outside the United States (U.S.)<sup>1</sup>. Seeking to improve the existing WASG-based ASA process, airports, air traffic authorities, airlines, and slot coordinators have engaged in a lengthy revision<sup>2</sup> of the regulatory framework defining the ASA process. The revised regulatory

---

<sup>1</sup> Airports within the U.S. do not manage demand for airport capacity (with the exception of airports that follow the High-Density Rule (HDR)). Instead, airlines schedule their flights based on a mechanism which considers expected delays.

<sup>2</sup> Before the revision of WASG, the industry used to refer to this policy framework as the World Scheduling Guidelines (WSG) of the International Air Transport Association (IATA) (IATA WSG). However, after the revision, in addition to IATA, the document is maintained by the Airport Council International (ACI) and the Worldwide Airport Coordinator Group (WWACG). Hence, the terms IATA WSG and WASG are used throughout this document to refer to the policy rules defining the ASA process as per the old set of policy rules and criteria (IATA WSG) and its revised version (WASG).

framework introduces increased flexibility and collaboration among the pertinent parties, i.e., airlines, coordinators, airport, and air traffic authorities.

On par with the industry and policy side, a considerable corpus of academic literature studying the administrative ASA process defined by WASG has appeared during the last decade. WASG-based ASA studies have evolved from single-objective studies (Zografos et al., 2012), to models considering multiple efficiency objectives (Zografos et al., 2017a; Ribeiro et al., 2018; Jorge et al., 2021; Katsigiannis et al., 2021). In addition, there are multi-objective formulations that introduce fairness objectives in conjunction with displacement-related objectives (Zografos and Jiang, 2016, 2019; Fairbrother et al., 2019; Androutsopoulos and Madas, 2019; Katsigiannis et al., 2021; Jiang and Zografos, 2021); and models examining alternative definitions of policy-related concepts (Ribeiro et al., 2019b; Fairbrother and Zografos, 2020).

Despite the numerous papers studying the WASG-based ASA decision-making, there is a series of research questions that have not yet been addressed by the literature. These are identified as follows:

- I. How to improve the modelling of airline demand flexibility and the utility that each airline assigns to each available airport slot? (Chapters 2 and 4)
- II. How can one model the dynamic and endogenous adaptation of the airport's landside and airside infrastructure to the characteristics of airline demand? (Chapter 2)
- III. How to consider operational delays in strategic ASA decision-making? (Chapter 3)
- IV. How to involve the pertinent stakeholders into the ASA decision-making process to select a commonly agreed schedule; and how can one reduce the

inherent decision-complexity without compromising the quality and diversity of the schedules presented to the decision-makers? (Chapter 3)

- V. Given that the ASA process involves airlines (submitting requests for slots) and coordinators (assigning slots to requests based on a set of rules and priorities), how can one jointly consider the interactions between these two sides to improve ASA decision-making? (Chapter 4)

The current doctoral thesis aims to answer the above research questions through the development of mathematical models and algorithms for the single-airport ASA problem defined by the policy framework of WASG. The following section provides a brief background on the current ASA process and further elaborates on the research questions that are addressed by this work.

## **1.2 The Airport Slot Allocation process and literature**

Before presenting a brief overview of the relevant literature (subsection 1.2.2) and its relationship to the identified research questions (as identified in section 1.1), the following subsection provides an overview of the main rules, priorities, and processes of the ASA process as defined in the WASG.

### **1.2.1 Overview of the ASA process as per the WASG**

ASA is an administrative process for managing airline access to congested airports. The main ASA paradigm that is used in practice is the process defined by WASG and is currently applied in 190-207 airports (depending on the season).

#### **1.2.1.1 Pre-season activity**

As per the WASG, each calendar year is divided into two scheduling seasons. At the outset of the calendar year, each airport carries out a capacity analysis that determines the *declared capacity* of the airport, i.e., the capacity that is available



under an acceptable service level. In cases where the capacity does not suffice to accommodate airline demand, airports are classified into two main categories.

First, level 2 airports (also referred to as *schedule facilitated*) may experience occasional congestion (e.g., weekends), which can be mitigated by mutual schedule adjustments that are agreed between the airlines and the appointed schedule facilitator. Second, level 3 airports (also referred to as *schedule coordinated*) concern airports where the declared capacity is systematically insufficient to satisfy airline demand. In level 3 airports, a slot/schedule coordinator manages access to airport capacity by considering airline demand and the scheduling parameters defined during the airport's capacity assessment (e.g., load factors per flight type, the maximum number of movements, passengers, parked aircraft).

The work conducted in this thesis relates to level 3 airports since they concern more passengers and face severe congestion.

### 1.2.1.2 Initial slot allocation

At the core of schedule coordination lies the *initial slot allocation* process. In the context of ASA, a slot represents the air carriers' right to access airport capacity during landing or take-off (IATA/ACI/WWACG, 2020). Hence, in level 3 airports, airport slots represent the right to use the airport capacity during a specific time. During the initial slot allocation process, the appointed coordinator defines the *initial slot pool* and informs airlines about the available capacity. Respectively, airlines wishing to access the airport submit their requests for the next scheduling season/period. Airline requests are submitted bi-annually before the summer and winter Schedule Coordination Conferences (SCC) using the *Standard Schedules Information Manual* (SSIM) format. During the initial slot allocation, coordinators allocate slots to requests using expert systems software (e.g., [PDC score](#)), which consider the rules and priorities of WASG. As per the main principles of WASG,

requests for *series-of-slots* (requests that are repeated for more than five weeks) pre-empt *ad-hoc requests* (ad-hoc requests concern less than 5 weeks of operations).

In considering requests for series-of-slots, the first set of requests to be allocated by the coordinator, are requests for pre-existing operations. These requests are referred to as *historic (H)* and receive their requested times. Up to 50% of the remaining capacity after the allocation of *H* requests is reserved for *new entrant (NE)* requests which concern requests submitted by airlines with a minimum presence at the airport. The remainder of the airport capacity is allocated to requests amending historic operations (also referred to as *changes to historic (CH)*) and *other (O)* requests. Additional primary criteria differentiate between two different types of *CH* requests and are further analysed in the main body of the thesis. At this point, it is worth noting that prior to 2019, *CH* requests pre-empted *NE* movements. A recent revision to the policy framework resulted in a new prioritisation of airline requests. A comparison between the previous and the current prioritisation schemes (before and after the revision) and their modelling implications is conducted in chapter 3.

Within each of the *H, NE, CH* and *O* priorities, requests wishing to extend operations from/to other seasons receive increased priority in relation to requests concerning a single season of operations (referred to as year-round requests). In addition to this set of primary criteria, coordinators should consider local or regional guidelines. An example drawn from European airports is the prioritisation for routes with *Public Service Obligations (PSO)*. As per the PSO rule, operations that are essential for the connectivity and development of remote areas receive an increased priority (Bråthen and Eriksen, 2018; European Commission, 2018). Besides, there exist secondary criteria which are used for tie-breaking purposes to determine requests' prioritisation within each of the main request priorities. These secondary

criteria suggest among others the consideration of competition, connectivity, passengers' needs, and the frequency of operations.

### **1.2.1.3 Activities following the initial slot allocation**

Following the initial allocation, the airlines and the coordinators engage in a series of discussions to resolve potential scheduling conflicts before the SCC. During the SCCs the interested stakeholders (airlines, coordinators, airport, and air-traffic authorities) meet and discuss adjustments to the coordinators' initial allocation so as to resolve timing discrepancies between the times allocated in different airports. Following the SCC, air carriers should decide on whether they will retain, return, or modify each of the slots that they received.

A holistic graphical overview of the activities composing the airport slot allocation process is provided in Figure 2-1. The studies discussed in the remainder of this section concern the initial slot allocation process since it defines – to a great extent – the basis of the schedules that will be operated during the scheduling seasons.

## **1.2.2 Related work**

This section provides a concise overview of the most relevant literature (papers that consider the administrative airport slot scheduling as per WASG at a single airport) and elaborates on the importance of research questions (I)–(V) (as identified in section 1.1) for ASA decision-making. More detailed discussions on the literature and the specific modelling and problem characteristics addressed by chapters 2-4 are provided in sections 2.2, 3.1.2 and 4.1.1.

Hereby, it is worth noting that in addition to administrative airport demand management mechanisms, there exist market-based or hybrid (using both administrative and market-based methods) instruments. Moreover, it is worth acknowledging that in parallel to the WASG-based ASA process, another set of

---

administrative ASA studies considers the U.S. slot scheduling context (Jacquillat and Odoni, 2015; Pyrgiotis and Odoni, 2015; Jacquillat and Vaze, 2018). This research stream exhibits several commonalities with the work presented in this thesis but is characterised by some distinguishing differences. Instead of considering ASA for an entire slot scheduling season (as required by WASG), U.S.-based models generate schedules that concern a single day of operations and do not consider the request prioritisation scheme defined by WASG. Furthermore, the U.S. decision context mostly relates to the tactical decision level, meaning that slots are allocated a few days before operations. Concurrently, the U.S. decision context does not consider prioritisation rules for the allocation of airport slots (as detailed in section 1.2.1). For the sake of completeness and whenever deemed applicable, in the chapters that follow, the modelling characteristics of network-wide and tactical U.S.-based models are further discussed.

The first mathematical model to consider the ASA defined by the WASG (previously IATA WSG) was the model of Zografos et al., (2012) which considered the allocation of slots at a single airport by minimising schedule displacement (Koesters, 2007), i.e. the sum of the absolute deviations between the requested and the allocated times, subject to turnaround time constraints (defining the precedence of the arrival request in relation to the departure request) and rolling runway capacity constraints that defined the maximum number of arrivals, departures and total movements during different interval lengths. In Zografos et al., (2012), requests were prioritised based on three main priorities. Requests with historic usage rights, i.e., requests concerning operations that are previously existent in the airport are classified as ‘*historic*’ and pre-empt other requests. Requests submitted by airlines without previous presence at the airport (classified as ‘*new entrant*’ requests) which pre-empt other requests but follow historic requests. The final priority considered is the ‘*other*’ requests which are treated after the allocation of

---

the historic and the new entrant requests. This model minimised the total displacement of the requests of each of the above priorities and provide a feasible schedule that ensures a minimum time difference between the arrival and departure leg of each request and respects the runway capacity of the airport. The model of Zografos et al., (2012) has provided the basis and the core components of the multi-objective studies detailed below, which regardless of the objective set that they consider, they integrate rolling runway capacity constraints, turnaround times and consider the main ASA request priorities (historic, new entrant, other).

Despite the expansion of the WASG-based administrative ASA literature in terms of objective functions and expressions modelling airlines' timing flexibility (Zografos et al., 2017a; Fairbrother et al., 2019), we note that there are currently no studies that can provide comprehensive expressions of the flexibility of airline demand and the utility that each airline assigns to each available airport slot (research question I). For instance, there are currently no formulations that can explicitly consider airlines' earliness/tardiness preferences, the distance covered, and the available seats of each flight. The modelling of airlines' flexibility, besides being a policy requirement (IATA/ACI/WWACG, 2020), it enables the allocation of airport capacity to the airspace users that value it the most and provides improved allocation efficiency. This research question is addressed in chapters 2 and 4. Chapter 2 develops time-dependent flexibility functions which model the policy requirements that relate to the Timing Flexibility Indicator (TFI) (IATA/ACI/WWACG, 2020). Chapter 4 builds upon the functions proposed in chapter 2 and provides functions that provide a comprehensive modelling of the factors that determine airlines' time-dependent utility (aircraft, frequency, distance, effective period, competition, and connectivity).

Furthermore, in considering airport terminal and apron capacity constraints, current formulations (Ribeiro et al., 2019b) propose static expressions that do not consider the alignment of the landside and airside capacity with the demand characteristics; and do not encompass the complete set of the airport's capacity requirements. Hence, current models do not take into account that in various airport instances the designation of airport resources is dynamically reconfigured based on the characteristics of the flights, i.e., aircraft type, Schengen vs. Non-Schengen flights. The dynamic, demand-based configuration of the airside (aprons, runways) and landside (passenger terminals) resources (research question II) leads to the improved representation of airport capacity and addresses the mismatch between airport infrastructure configurations (related to physical and operational constraints) and airline demand characteristics (de Neufville and Odoni, 2013; Mirković and Tošić, 2014). Chapter 2 provides an endogenous modelling of the capability of the airport infrastructure to adapt to the characteristics of airline demand.

The simultaneous consideration of the above issues (as stated in research questions I and II) enables the study of the joint consideration of airlines' flight timing flexibility and the dynamic and endogenous allocation of total airport capacity and allow one to study their combined or separate effect on ASA decision-making.

With regards to the objectives considered in the ASA literature, most studies employ multi-objective formulations. In doing so, existing formulations either generate a single schedule through the lexicographic ordering of the considered objective functions (Ribeiro et al., 2018), or produce multiple airport slot schedules by considering the trade-offs among the considered objectives (Zografos et al., 2017a; Fairbrother et al., 2019; Zografos and Jiang, 2019; Jiang and Zografos, 2021;

Jorge et al., 2021; Katsigiannis et al., 2021). The latter formulation typology provides enhanced support to decision-makers since it informs on the alternative solutions that are available. An initial complication relating to models generating multiple schedules, is that current algorithms cannot produce the complete efficient frontier for multi-objective ASA problems exceeding two objective functions. Meanwhile, the generation of multiple airport slot schedules results in increased decision complexity since the decision makers need to assess each available alternative (concerning multiple days of operations and movements). To address this complication there is need to provide mechanisms that reduce decision complexity without compromising the quality and diversity of the schedules presented to the decision-makers (research question IV). This complication is addressed by chapter 3, which besides generating the complete set of non-dominated schedules for any tri-objective ASA model, proposes a solution-space reduction technique that can reduce the number of alternative schedules that are made available to the decision-makers without compromising their representativeness in relation to the complete set of generated schedules.

Concerning the schedule performance metrics considered for assessing the multiple schedules, one notes that existing formulations are limited to strategic performance metrics that refer to the displacement (maximum or total schedule displacement) and the number of displaced passengers and requests reported by each schedule. However, there are currently no strategic ASA studies to provide a lookahead on the operational implications of strategic airport slot allocation decisions (research question III). The consideration of operational delays constitutes a fundamental objective of airport demand management (Swaroop et al., 2012), while the integration of operational delay estimates in strategic ASA decision-making has been acknowledged as an important research gap (Zografos et al., 2017b). Albeit, operational delays have solely been considered in tactical re-timing

models that introduce scheduling interventions a few days prior to operations (Jacquillat and Odoni, 2015) or impose constraints on the anticipated queues (Jacquillat and Vaze, 2018). Chapter 3 models and evaluates the peak operational delays associated with each generated schedule, hence providing improved insights on the implications of strategic ASA scheduling for operations.

Meanwhile, in the presence of the multiple ASA stakeholder groups (airlines, coordinators, airport, and air traffic authorities) the assessment of the alternative airport slot schedules and the selection of a commonly agreed solution that will be considered for operations, require the consideration of the diverging views of the stakeholder groups that relate to ASA decision-making (research question IV) and their consolidation so as to reach to a commonly preferable schedule. The only study to consider stakeholders' preferences regarding alternative performance metrics, is the model of Jiang and Zografos (2021) that selects the most preferable fairness objective and subsequent frontier using a voting mechanism that considers airlines' and coordinators' views. Chapter 3 considers and consolidates the preferences of ASA stakeholders with respect to multiple strategic and operational scheduling performance metrics, assesses multiple alternative slot schedules and proposes a preferable schedule reflecting the expectations of all ASA stakeholders.

With respect to individual request-to-slot assignments, existing ASA studies model the ASA as a single-sided problem without considering the interactions between airlines' timing flexibility and utility, and the WASG-based priorities assigned by the coordinator to each request. In view of this gap, an issue that remains untapped by the existing literature relates to the proposition of stable request-to-slot assignments that provide no incentives to both airlines and coordinators to alter or reject the proposed schedules (research question V). In the context of ASA, the notion of stability becomes a synonym of allocation



acceptability since under a stable schedule the time-dependent utility achieved for each request cannot be improved without compromising the allocation of a more important request (Pareto optimal request-to-slot assignments). Schedule stability may lead to more consistent operations within the scheduling season of interest but also to improved continuity and inter-season scheduling consistency. Chapter 4 models the ASA problem as a two-sided matching game and provides insights on the trade-offs between scheduling efficiency and the spilled airline/passenger demand required to obtain stable airport slot schedules. Chapter 4 optimises an objective function that the multi-stakeholder preferences introduced in chapter 3 and enforces request-to-slot stability by modelling the interactions between airline demand and the WASG-based priorities assigned by the coordinators to each request.

### 1.3 Contributions

Despite the wealth of ASA studies developed in recent years, the multiple objectives, and the additional constraints and policy considerations, there exist unaddressed problem aspects and questions (identified in I–V) that have the potential to improve the efficiency of ASA decision-making. This thesis is trying to address these questions through the development of mathematical models and solution algorithms for ASA decision-making. The contributions of this thesis are summarised as follows:

In addressing research question (I), chapter 2 of the thesis introduces a new modelling and solution approach, referred to as the Timing Flexibility Indicator Model (TFIM) integrating time-dependent functions that consider airlines' earliness/tardiness flexibility. Besides, chapter 4 capitalises on the TFIM formulation and provides functions that provide a comprehensive approximation of airlines' utility for each available airport slot and consider several operational

characteristics, competition and connectivity dynamics. Furthermore, chapter 2 proposes constraints that enable the dynamic allocation of the airport's resources (research question II). The added value of the model proposed in chapter 2 stems from the improved alignment between airline demand and airport capacity, thus leading to improved capacity utilisation and reduced displacement.

The thesis addresses research questions (III)–(IV) through the proposition of a multi-objective decision-making framework that incorporates operational delays and multi-stakeholder scheduling preferences. In particular, chapter 3 provides an extension of the model presented in chapter 2 and generates the complete set of non-dominated schedules for any ASA model considering three linear objective functions. To alleviate the decision-making complexity that arises from the multiple non-dominated solutions, the framework is complemented by a suitable clustering algorithm that is tuned based on the shape of the non-dominated set so as to propose a high-quality subset of non-dominated points (research question IV). In addition, chapter 3 models the expected delays associated with each generated schedule (research question III) and allows the consideration of the operational implications of strategic ASA decisions. Chapter 3 moves beyond the generation of airport slot schedules and the evaluation of the associated operational delays, through the consideration of multi-stakeholder preferences (research question IV) with respect to each schedule's operational and strategic performance. The proposed framework is tested using empirical preference data obtained through a survey with multiple industry experts. The proposed framework facilitates more collaborative ASA decision-making and allows all interested parties to review the impact of their preferences on the displacement and the expected delays associated with each schedule. Further, it enables the quantification of the impact associated with the airport's current declared capacity setting.

Finally, the thesis introduces a game-theoretic model that considers ASA decision-making as a two-sided matching game (research question V). The resulting model (presented in chapter 4) is referred to as the *Stable Airport Slot Allocation Model* (SASAM) since it results in equilibria between airline demand and the coordinators' perspective in considering the policy rules defining ASA. SASAM extends the time-dependent airline utility functions introduced in chapter 2 and considers several factors that can proxy airlines' timing utility. By integrating time-dependent prioritisation functions for each request considering both the coordinators and the airlines' perspectives, SASAM provides a structured and consistent mechanism that can propose Pareto optimal request-to-slot assignments and guarantee the stability of the generated airport schedules. In order to study the trade-offs required so as to achieve a stable schedule, a *Deferred Acceptance* (DA) algorithm generates multiple schedules in reasonable computational times.

Computational analyses using data from coordinated airports shed light on the potential implications of this thesis for ASA decision-making. Instance-specific results suggest that the joint consideration of airlines' timing flexibility and the dynamic capabilities of airport capacity (research questions I and II) result to a more intensive use of airport capacity and improved scheduling efficiency (improvements ranging between 5-24% with respect to multiple displacement-related efficiency metrics). With regards to the decision-complexity associated with the assessment of multiple airport slot schedules (research question IV), computational results suggest that by using 17% of the initially generated schedules, one can achieve a comparable quality and divergence (exceeding 70%) in relation to the initially considered set of schedules. The consideration of operational delays and multi-stakeholder preferences (research questions III and IV) allows the examination of the impact of stakeholders' views on ASA decision-making and provides a lookahead on the operational implications of the selected

schedules. Results based on the considered airport instance, suggest that the framework developed to address questions III – IV results to non-dominated points and enhances decision-support. Finally, regarding the two-sided modelling of ASA and the interactions between airlines’ timing flexibility and the WASG-based prioritisation of airport slot coordinators (research question V), computational results using data from an airport concerning more than 70,000 flight movements suggest more intensive use of airport capacity, ergo allowing the scheduling of additional flights and passengers (improvements of 12% and 40% respectively). This improvement is achieved by rejecting requests concerning a few days of operations and a limited number of passengers (increase to the number of rejected requests by 1.2%).

## 1.4 Overview and structure of the thesis

The following chapters of this thesis consist of three research articles. A brief description of each chapter is provided below.

- Chapter 2 considers airlines’ timing flexibility, in conjunction to total airport capacity constraints and the rules, and priorities of WASG. It is entitled:

*Optimising airport slot allocation considering flight  
scheduling flexibility and total airport capacity constraints.*

Its focus lies on the development of a new model that considers airlines’ timing-flexibility and integrates dynamic and asynchronous runway, apron, and passenger terminal constraints. The chapter proposes new valid inequalities which tighten turnaround time constraints and alleviate computational complexity and considers several secondary and regional rules of the WASG.

- Chapter 3 considers the operational implications of strategic airport slot schedules and addresses the need for explicitly considering the needs of the

multiple stakeholder groups that are pertinent to the ASA process. It is entitled:

*Multi-objective airport slot scheduling incorporating operational delays and multi-stakeholder preferences.*

This chapter proposes a multi-objective, multi-stakeholder solution framework that elicits airport slot schedules by considering the preferences of multiple stakeholders with respect to the expected delays and the strategic performance metrics associated with each schedule. An intrinsic aspect of this chapter is that it reduces decision-making complexity by selecting subsets of representative schedules. In considering multi-stakeholder preferences the chapter employs empirical preference data obtained through a study with ASA professionals and experts.

- Chapter 4 argues on the stability of optimisation-based airport slot schedules and models the ASA problem as a two-sided matching game by considering the interactions between airlines' time-dependent utility and the coordinators' perspective when considering the policy rules of WASG. It is entitled:

*On the stable allocation of airport slots.*

This chapter introduces a Stable Airport Slot Allocation Model (SASAM) that guarantees the stability of the proposed airport slot schedules by proposing request-to-slot assignments that are Pareto optimal per se. This chapter introduces a Deferred Acceptance (DA) algorithm that generates multiple stable airport slot schedules.

The final part of the thesis (Chapter 5) draws overall conclusions and provides suggestions for future research.

This thesis is an interdisciplinary body of work. Whilst the main methodologies developed and used in the thesis lie in the field of *Multi-objective Optimisation*, its application lies traditionally in the field of *Civil Engineering*. On top of that, chapter 3 makes use of *Data Analysis*, *Visualisation*, and *Machine Learning* techniques, while chapter 4 employs techniques that are widely used in the *Game Theory* literature. The methodologies developed in this thesis stand as an attestation of the complexity of the ASA problem and the challenges faced by the research community in improving ASA decision-making.



# **Chapter 2:**

## **Optimising airport slot allocation considering flight-scheduling flexibility and total airport capacity constraints**

### **2.1 Introduction**

The shortage of airport capacity acts as bottleneck to global air-travel and obstructs its sustainable and efficient growth, inflicting more than €11 billion of delay-related costs to airlines, airports and passengers (IATA, 2013, p. 201). Given the excessive time needed to plan and implement airport capacity expansion projects, Airport Slot Allocation (ASA) has been proposed as a short-term measure for dealing with the demand-capacity imbalance at congested airports. In overly congested airports (Level 3 coordinated airports), ASA is expressed by a regulatory framework defined in the World Schedule Guidelines of the International Air Transport Association (IATA WSG) (IATA, 2019a). More than 200 airports with capacity shortages manage airline demand for their resources based on the IATA WSG. Interestingly more than half of these airports are located in Europe (IATA, 2018). Appointed slot coordinators use IATA WSG to manage the allocation of airport resources, by prioritising requests for airport slots based on historical usage rights.

The first step of the ASA process is the determination of the coordination parameters, i.e. the declared runway, passenger and apron capacity of the airport (IATA, 2019a). The declared capacity depends on the maximum throughput of the airport (Morisset and Odoni, 2011) (typically set to be between 80-90% of the maximum capacity) and is determined based on certain factors (e.g. the airport infrastructure) and assumptions after the realisation of a capacity assessment analysis (Ball et al., 2010; Stamatopoulos et al., 2004). The airport capacity



parameters given by the capacity assessment are used by coordinators with the aid of a guide exemplifying their instantiation in different airports (WWACG, 2019). WWACG (2019) recognises that in certain airports, the utilisation of airport resources can be configured based on the demand's characteristics, i.e., aircraft type (e.g., 1 additional apron for heavy aircraft can be given by using an apron for medium aircraft), location of origin (Schengen/Non-Schengen).

Once the coordinator receives the declared capacity parameters of the airport, they confirm and input them to their coordination systems and communicate them to the airlines. The capacity is then distributed using the initial slot allocation process, which is the primary focus of this study, and recognises a set of criteria assigning different priorities to each slot request. A graphical overview of the slot coordination processes, indicating the focus of the current study is provided in Figure 2-1.

Slot requests are classified by coordinators within four distinct slot priorities, i.e., Historic requests (H), Changes to Historic requests (CH), requests of New Entrants (NE) and Other requests (O). For more information on the specifications of these priorities, the reader is referred to IATA WSG. In addition, for slot requests associated with routes connecting airports located in isolated or developing regions of European Union member states, an additional request priority referred to as Public Service Obligations (PSO), pre-empts other requests (Council Regulation (EEC) No 95/93, 1993), and is used to guarantee the 'continuity, regularity, pricing or minimum capacity to ensure access' to these regions (European Commission, 2017, 2018). IATA WSG require within each of the above priorities, that requests for flights that will operate at the same time and day for more than four weeks (considered as series-of-slots) should be prioritised over requests with smaller effective periods (considered as ad-hoc operations).

Likewise, requests that wish to extend operations of other scheduling seasons (year-round requests) should receive priority over requests submitted for a single season of operations (single-period requests). In considering these priorities, coordinators seek to allocate time slots as close as possible to the requested times. However, in the case that there is inadequate capacity during the requested time, alternative slot offerings should be made based on the Timing Flexibility Indicator (TFI). Requests that could not be accommodated within the TFI are placed in the pending list awaiting approval from the airline. TFI is voluntarily supplied by the airlines during the initial slot allocation in order to disclose their operational constraints (e.g., curfews in other airports) and flexibility. An essential rule relating to the TFI, is that airlines that choose to disclose this information, should not be placed in a disadvantageous position (receive worse allocations) for having done so.

From a methodological perspective, researchers working on the ASA deriving from IATA WSG, have introduced formulations that optimise airport slot scheduling decisions by considering different slot scheduling objectives, i.e. total displacement (Zografos et al., 2012, 2017a; Ribeiro et al., 2018), weighted displacement (Zografos and Jiang, 2016), maximum displacement (Zografos et al., 2017a; Ribeiro et al., 2018), fairness (Jiang and Zografos, 2017; Zografos and Jiang, 2019; Fairbrother et al., 2019), displaced requests (Ribeiro et al., 2018), rejected requests (Ribeiro et al., 2018). Despite the expansion of the literature in terms of considering alternative objectives, existing studies do not consider the rules and processes associated to the TFI. Hence, in suggesting alternative slot timings, previous studies pretermite the operational requirements that the airlines disclose through the TFI. The integration of TFI has the potential to improve the ASA outcome and increase the acceptability of alternative slot offerings. The modelling of the TFI concept, apart from being an IATA requirement, it introduces an approach whose importance is recognised by the relevant literature. For instance,

Barnhart et al. (2012) suggest that the consideration of airlines' flexibility is an important gap that will allow the proposition of mechanisms that allocate '*capacity to the airlines that value it most and will best use it to transport passengers*'. The importance of modelling air carriers' flexibility extends to other air transport problems. For instance, in the context of air traffic management, Mavoian et al. (2016) indicate that integrating air carriers' flexibility improves the utilisation of airspace and airport resources. The modelling of airlines' timing flexibility through the consideration of each request's TFI, constitutes the first methodological component of work.

In addition, existing models consider the airport's capacity parameters exogenously and do not adjust, where needed, the configuration of passenger and apron capacity according to the characteristics of the slot requests and the operating procedures of the airport. Recent studies (Ribeiro et al., 2019b) have proposed apron and passenger capacity constraints that do not consider the alignment of the landside and airside supply and demand characteristics; and do not encompass the complete set of the airport's capacity requirements. Hence, current models do not consider that in various airport instances the designation of airport resources is dynamically reconfigured based on the characteristics of the flights, i.e., aircraft type, Schengen vs. Non-Schengen flights. From a methodological standpoint, the importance of the dynamic allocation of airport capacity is recognised since it leads to the improved utilisation of the airport's resources (Mirković and Tošić, 2017, 2014). Besides being a requirement in several airports (WWACG, 2019), the dynamic allocation of airport capacity extends beyond the confines of the ASA problem. For instance, the dynamic capacity allocation can deal with potential demand-capacity imbalances and capacity bottlenecks caused by the '*mismatch between apron configuration (related to*

*physical and operational constraints) and demand characteristics'* (Mirković and Tošić, 2014).

Furthermore, the demand-based configuration of the airside (aprons, runways) and landside (passenger terminals) resources leads to the improved representation of airport capacity as opposed to the static capacity allocation, which is merely a 'snapshot' of the airport's resources (de Neufville and Odoni, 2003). From a practical standpoint, the dynamic allocation of airport capacity is an issue that is considered by airport slot coordinators (WWACG, 2019) and is aligned with IATA's strategic goals which seek to '*realise the full potential of the airport infrastructure*' (IATA, 2019b). In this chapter, this literature gap is addressed by introducing constraint expressions that enable the dynamic allocation of the airport's resources and the improved utilisation of its capacity. This constitutes the second methodological component of this work.

Overall, this chapter contributes to the literature by integrating the above untapped methodological issues in a modelling and solution framework. The kernel of this chapter's methodological contribution that signifies the importance of this work stems from the joint consideration of airlines' flight flexibility, modelled using the TFI; and its seamless integration with the dynamic allocation of total airport capacity, enabled by the alignment of the landside and airside supply and demand characteristics. The proposed integrated methodology benefits from valid inequalities that reduce the computational times required for its solution. From a policy perspective, a secondary contribution of this work is that it addresses all primary policy rules, as well as additional requirements relating to routes with PSO, ad-hoc operations and year-round requests (see section 2.2). In modelling these primary rules, the chapter provides a well-defined priority structure that enhances the acceptability of this model and its compliance with IATA WSG.

The remainder of this chapter is composed by 7 sections. Section 2.2 provides a compact discussion on the studies relating to this work and situates the aforementioned contributions based on methodological literature gaps. Section 2.3 wraps the modelling components introduced in the paper and summarises the proposed solution methodology. Section 2.4 introduces an airport slot allocation model that considers all primary rules discussed in IATA WSG (section 2.4.1) In addition, section 2.4 develops the asynchronous<sup>3</sup> apron and passenger constraints (section 2.4.2) and generalised dynamic airside and landside constraints (section 2.4.3). The TFI model is introduced in section 2.5. Section 2.6 presents the valid tightening inequalities and discusses their performance. The application of the proposed approach to a real-world slot coordinated airport is presented and discussed in section 2.7. Finally, section 2.8 concludes the chapter and provides suggestions for future research.

---

<sup>3</sup> The term *asynchronous* is used throughout the document to denote that the utilisation of the airport's resources (runways, aprons, terminals) by the same aircraft will occur in different time intervals as per the time lag parameters defined in section 2.4. For instance, when an aircraft is arriving it will use the runway at time  $t_0$ , then it will use the apron at time  $t_1 > t_0$ , and finally it will use the passenger terminal at a later time  $t_2 > t_1 > t_0$  (the order is reversed for departing aircraft, i.e.,  $t_0 > t_1 > t_2$ ).

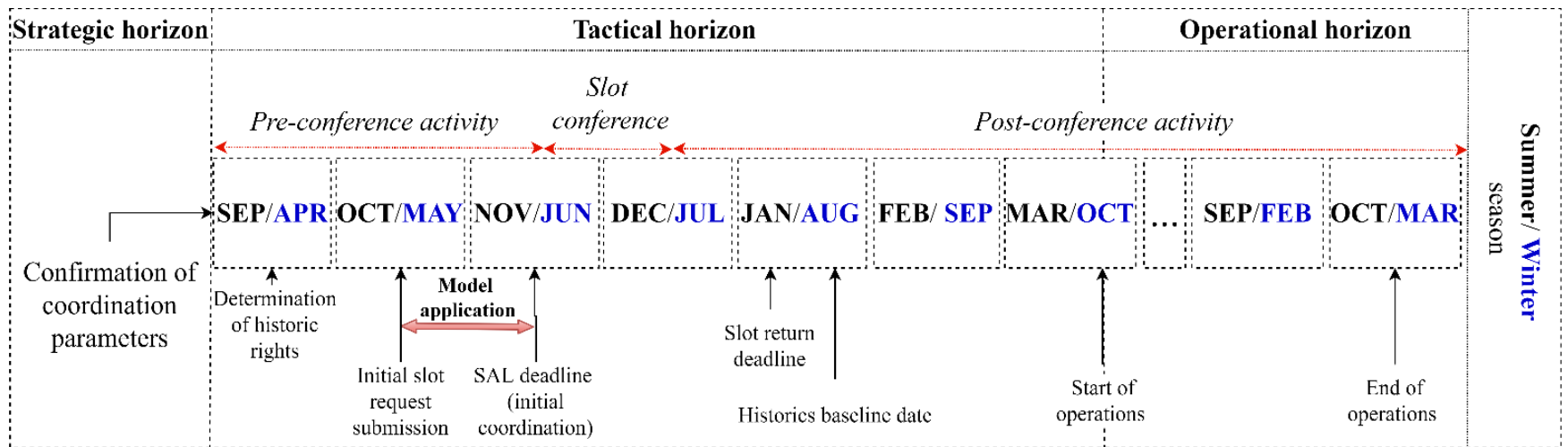


**Figure 2-1:** Overview of the slot coordination process

## 2.2 Previous related work

The research presented in this chapter addresses the scheduling of slots at a single airport using the administrative rules described in IATA WSG and the European regulations relating to the PSO routes (European Commission, 2018). Other streams of research address ASA from a market-based or hybrid (using both administrative and market-based methods) perspective or consider the scheduling of slots at network-wide level (Pellegrini et al., 2017); albeit, the aim of this section is to discuss selected research papers that relate the most to the proposed approach, i.e. papers that consider the administrative airport slot scheduling as per IATA WSG at a single airport.

For a recent and inclusive review of the literature relating to ASA, the reader is referred to the work of Zografos et al. (2017b). Even so the review focuses on administrative approaches deriving from the IATA WSG, it is worth noting the existence of models that address ASA in the United States' slot scheduling context (Jacquillat and Odoni, 2015; Jacquillat and Vaze, 2018; Pyrgiotis and Odoni, 2015). The main features that distinguish this body of literature from the models encompassing IATA WSG, is that instead of considering ASA for an entire slot scheduling season, they schedule slots for a single day of operations, and they do not consider any slot prioritisation rules.

The first paper to address ASA from a mathematical modelling perspective was the single-objective formulation of Zografos et al. (2012). Being the first attempt to address the modelling complexity of the IATA WSG slot scheduling context, the model minimised total/schedule displacement by considering the allocation of series-of-slots for an entire scheduling season subject to rolling runway capacity and aircraft turnaround time constraints. Zografos et al. (2017a) extended the formulation of Zografos et al. (2012) by proposing two bi-objective formulations

minimising total and maximum displacement, and total displacement and the number of violated slot assignments respectively. The number of violated slot assignments was implemented by using a displacement threshold called ‘maximum acceptable displacement’. Based on this concept, the proposed formulation minimised the number of requests which receive displacements that are larger than the ‘maximum acceptable displacement’. However, this model does not consider airlines’ flexibility for each of their requests, does not consider carriers’ aversion towards larger displacements and does not distinguish whether an airline prefers to be displaced to an earlier or a later time period (earliness and tardiness preferences).

The model of Zografos et al. (2012) was also extended by the work of Jiang and Zografos (2017, 2021) and Zografos and Jiang (2016, 2019), which in addition to total displacement, they considered a fairness objective. An interesting aspect of the work of Zografos and Jiang (2019) is that they presented their computational results at a disaggregate level for each airline. The presentation of the disaggregate results aims to inform discussions among the interested stakeholders and improve the transparency of the slot scheduling decisions (Zografos and Jiang, 2019). In Jiang and Zografos (2021) the authors consider alternative fairness objectives and a voting mechanism that incorporates stakeholders' preferences, which facilitate the selection of the airport schedule that will be implemented.

Fairbrother et al. (2019) built on the fairness considerations of Jiang and Zografos (2017) and Zografos and Jiang (2016, 2019) and introduced a fairness objective which considers slot requests made during periods that demand exceeds the available capacity. Another aspect of this work was that it introduced a budget-displacement mechanism. The mechanism’s first stage determines a base schedule based on the total displacement and fairness objectives and allocates to each airline its fair share of displacement, referred to as the displacement budget. During



the second stage of the mechanism, airlines may re-allocate their displacement budget based on a super-additive preference function which represents airlines' aversion towards large displacements (Fairbrother et al., 2019). This super-additive preference function penalises large displacements using a parameter that applies to all airlines without considering their individual earliness/tardiness preferences for each of their requests. An interesting aspect of the proposed mechanism is that it does not require airlines to disclose their internal valuation of slots.

The papers discussed so far do not differentiate between the historic's and changes to historic's slot request priorities. This literature gap was recently addressed by Ribeiro et al. (2018) who introduced a formulation which models the IATA hierarchical allocation in a more detailed manner. In particular, they extended the priority considerations of existing research attempts and explicitly considered the changes to historic's slot priority. They used a quadr-objective weighted function that minimised lexicographically the number of rejected requests, maximum displacement, total displacement, and the number of displaced slots. The authors suggest that the format of their objective function adheres to the preferences of airport slot coordinators (Ribeiro et al., 2018, 2019b). Despite the explicit modelling of changes to historic's priority, this paper does not consider the priorities relating to PSO routes and year-round requests. Katsigiannis et al. (2021) proposed a multi-level, multi-objective formulation that captures the trade-offs among the scheduling objectives for all slot scheduling priorities and the airport schedule as a whole.

Current literature comprises formulations which are optimised subject to runway, aircraft turnaround and priority constraints. In large airports that have sufficient terminal and apron capacity, runway capacity is the main bottleneck of the system. However, in airports with limited landside infrastructure or regional

airports that have limited apron and/or passenger terminal capacity, the efficiency of airport operations can be hindered (Airport Coordination Limited, 2018). Ribeiro et al. (2019) addressed this gap by incorporating static passenger terminal and apron capacity constraints, which do not allow dynamic allocation of the capacity of the airport and the optimum alignment of the airport's demand and supply characteristics. The consideration of flexible capacity capabilities is of significant importance, since it enables the improved utilisation of the airport's resources (Mirković and Tošić, 2014).

Table 2-1 summarises the modelling components that are introduced by the existing single-airport ASA literature relating to the IATA WSG and the current study. The problem modelling requirements stemming from the IATA WSG (columns) that are addressed by each study (rows) are represented by ticks. Table 2-1 underlines two main groups of problem specifications which are insufficiently addressed by the existing literature and that this work attempts to address. From a methodological perspective, this work contributes to the state-of-the-art by introducing an integrated modelling and solution approach that comprises the joint consideration of airlines' flexibility and the endogenously considered and dynamically allocated total airport capacity. The integrated methodology proposed in this chapter is strengthened by valid inequalities relating to the turnaround time constraints which reduce the required computational times. From a policy perspective, the existing literature does not differentiate between PSO routes, year-round versus single period and series-of-slots versus ad-hoc requests. These primary rules and criteria are addressed in this study.

Research paper	Addressed problem characteristics											
	Multiple objectives	<i>Compliance with priority rules</i>						<i>Capacity constraints</i>				
		<i>H</i>	<i>CH</i>	<i>NE</i>	<i>O</i>	Year-round <i>PSO</i> Ad-hoc	TFI	Runway	Apron	Passenger	Dynamic	Asynchronous
Zografos et al. (2012)	X	✓	X	✓	✓	X	X	✓	X	X	X	X
Zografos et al. (2017a)	✓	✓	X	✓	✓	X	X	✓	X	X	X	X
Ribeiro et al. (2018)	✓	✓	✓	✓	✓	X	X	✓	X	X	X	X
Zografos and Jiang (2016, 2019)	✓	✓	X	✓	✓	X	X	✓	X	X	X	X
Fairbrother et al. (2019)	✓	✓	X	✓	✓	X	X	✓	X	X	X	X
Ribeiro et al. (2019)	✓	✓	✓	✓	✓	X	X	✓	✓	✓	X	X
Katsigiannis et al. (2021)	✓	✓	✓	✓	✓	X	X	✓	X	X	X	X
<b>Proposed approach</b>	✓	✓	✓	✓	✓	✓	✓	✓	✓	✓	✓	✓

**Table 2-1:** Literature overview and gaps addressed by this chapter

## 2.3 Summary of the proposed modelling and solution framework

The proposed framework (summarised in Figure 2-2) takes as input the declared capacity parameters of the airport for each day ( $d$ ) and time interval ( $t$ ). The declared capacity parameters consist of the:

- runway capacity ( $u_{d,t,c}^k$ ) which is expressed using rolling constraints of duration  $c$  for each movement type  $k$  (arrivals, departures, total movements);
- apron capacity ( $\delta_{d,t}^{f,r}$ ) of each terminal  $f$  with respect to aircraft type  $r$ ;
- passenger terminal capacity ( $E_{d,t,c,o}^{f,k}$ ) expressed using rolling constraints of duration  $c$  for each passenger type  $o$  (Schengen/Domestic, Non-Schengen) on board movement type  $k$  (arrivals, departures, total movements);
- expected load factor of each request ( $\xi_m$ ); and
- time lags used for estimating the time difference between the use of each resource (apron, passenger terminal) and the associated runway movement ( $l_k^{f,o,pas}$  for the passenger terminals,  $l_k^{f,apr}$  for the aprons).

The second dataset that is provided to the proposed framework are the initial slot requests ( $M$ ) submitted by the airlines and the sequence of the priorities, i.e., historic requests, changes to historic, new entrants and others, based on which they will be allocated ( $Q$ ). In Figure 2-2 this step is referred to as *Modelling phase*. The solution of the model built using the input described above is composed by two stages. The first solution stage carries out the initial slot allocation via the lexicographic optimisation of three slot scheduling objectives (number of rejected requests, maximum and total displacement) for each priority  $q \in Q$  hierarchically.  $Q$  is used to define the sequence based on which the model enforces the primary prioritisation rules of WSG.

In particular, this step comprises the solution of 3 Mixed Integer Programs (MIP) for each priority ( $q$ ) in the priority sequence ( $Q$ ) (with each of them solely considering the requests of this priority as per Figure 2-2). Once the requests falling into priority  $q$  are allocated, the capacity of the airport is updated (the remaining capacity after the allocation of  $q$  is determined) and the model proceeds to the allocation of the requests of the following request priority. The process is repeated

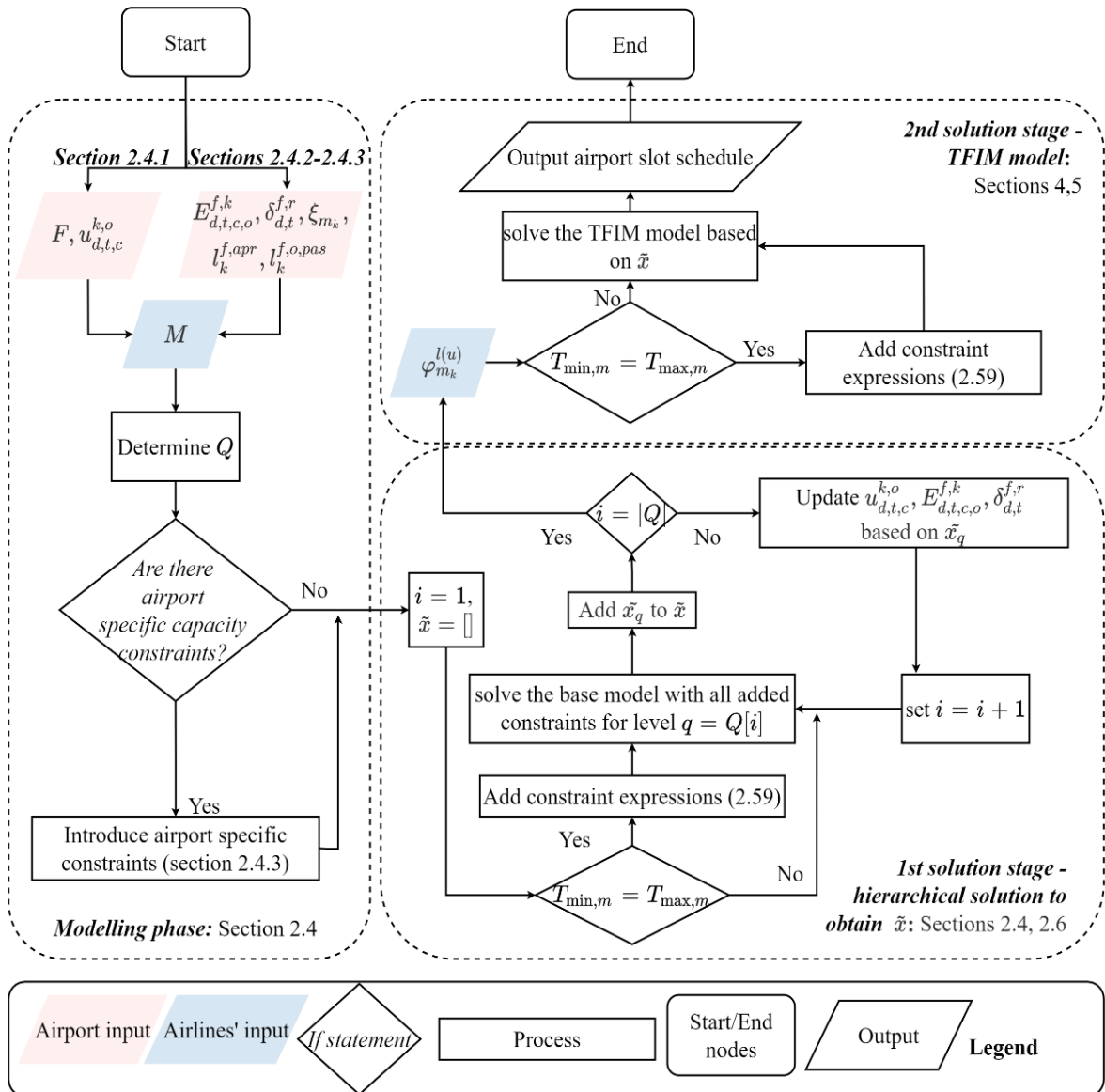


**Figure 2-2:** Flowchart summarising the modelling components of this chapter

for all  $q \in Q$ , thus resulting to an initial schedule (denoted by  $\tilde{x}^4$ ) that considers all request priorities. Hereafter, this initial schedule will be referred to as the *no-TFI schedule* since it does not consider the timing flexibility indicator (TFI) of each request.

The second part of the proposed solution framework considers the operational flexibility of the airlines (expressed for each request  $m \in M$  through the TFI denoted by  $\varphi_m^{l(u)}$ ) and solves the *Timing Flexibility Indicator Model* (TFIM) so as to optimise the number of slot requests which fall into the flexibility bounds  $(l, u)$  provided by the airline submitting each request. The schedule that is obtained after the solution of the TFIM is hereafter referred to as the *TFI schedule*. In contrast to the first step of the approach, this step requires the solution of a single MIP consisting of all the requests ( $M$ ) submitted to the airport. At this point, the maximum displacement, and the number of rejected slots are constrained based on the *no-TFI* schedule given by the first stage (through the addition of constraint (2.37)) of the framework. By constraining the number of rejected requests and the maximum displacement of the schedule, it is ensured that the outcome of the first stage will not deteriorate after the disclosure of the TFI information. In addition, the total displacement of each airline is constrained by the displacement allocated by the *no-TFI* schedule, such that airlines will not be placed in a disadvantageous position (this is safeguarded by adding one constraint per airline as per expressions (2.38)). The increased timing flexibility provided by the consideration of each

---

<sup>4</sup>  $\tilde{x}$  is a data structure (dictionary) that contains all binary decision variables ( $x_{t,m}^f$  as defined in section 2.4.1) that have a value that is different from 0. Hence,  $\tilde{x} = \{x_{t,m}^f \forall t \in T, f \in F, m \in M: x_{t,m}^f = 1\}$  can be used so as to represent a schedule and obtain its performance for different performance metrics.

request's TFI coupled with the addition of dynamic apron and passenger capacity constraints that allow additional feasible cases of apron and passenger terminal utilisation (see section 2.4.3), result in improved capacity utilisation and superior slot scheduling decisions. The schedule obtained after the solution of the TFIM is the airport slot schedule which can be used during the Slot Scheduling Conference (SCC) and the post conference activities. Please note that in the case that the turnaround times are set to be equal to the initially requested time difference between the departure and the arrival of each request, the valid expressions introduced in section 2.6 can be used to tighten the models and reduce the required computational times. Given that the proposed solution approach (a) captures airlines' operational requirements and flexibility for each slot request; and (b) complies with IATA WSG, the resulting schedule constitutes a solution which will require fewer amendments during and after the SCC.

The proposed solution approach assumes that the objective functions considered for obtaining the no-TFI and schedule (see section 2.4) are optimised lexicographically based on prior preference information given by the coordinators (*a-priori articulation of preferences*). Hence, by minimising lexicographically the number of rejected requests, maximum displacement and total displacement, the model proxies coordinators' scheduling behaviour as per Ribeiro et al. (2018, 2019) and produces a single airport schedule which benefits from flexible capacity constraints. Therefore, the priority structure of the objective function considered for obtaining the no-TFI schedule, depends on the preferences of the decision makers. The proposed framework may be used under alternative objective structures so as to study the impact of stakeholders' preferences on the efficiency of the airport slot schedule.

## 2.4 Airport slot allocation model

In this section, a slot allocation model which considers lexicographically the number of rejected slots, maximum displacement and total displacement is proposed. This objective function is used since it encompasses the preferences and the processes applied by airport slot coordinators (Ribeiro et al., 2018, 2019b). In what follows the section presents the mathematical structure and notation of an original ASA model (section 2.4.1) and detail the sequence ( $Q$ ) based on which the different slot request priorities are allocated. Furthermore, asynchronous apron and passenger capacity expressions (section 2.4.2) are introduced, which are then extended so as to allow the dynamic allocation of the capacity of the airport and the optimum alignment of the airport's demand and supply characteristics (section 2.4.3). The parameters used to build the models described in this section, are provided by the airlines during the initial slot allocation based on the Standard Schedule Information Manual (SSIM) of IATA WSG (IATA, 2019a). A condensed description of the parameters submitted by the airlines during the initial ASA as per the SSIM format is provided in Table 2-2.

### 2.4.1 Base model

#### Input data sets

$F$ : set of terminals available at the airport indexed by  $f$  with  $|F|$  being the number of terminals of the airport

$P$ :  $\{PSO, H, CH, NE, Oth\}$  set of slot request priorities indexed by  $p$  where  $p = p_{YR} \cup p_{SP}$  with  $p_{YR}$  being the requests extending a request from a previous season or requesting to operate for two consecutive slot scheduling seasons; and  $p_{SP} = p - p_{YR}$  being the request which are intended for a single season of operations. In addition,  $p_{YR} = p_{YR}^{\sigma} \cup p_{YR}^h$  and  $p_{SP} = p_{SP}^{\sigma} \cup p_{SP}^h$  with  $\sigma$  indicating requests considered as series of slots and  $h$  requests which are considered as ad-hoc operations



The hierarchical allocation of slots based on IATA WSG requires that airport slots are allocated hierarchically based on the following sequenced order of  $P$ :  $Q = \{PSO, H_{YR}^\sigma, H_{SP}^\sigma, CH_{YR}^\sigma, CH_{SP}^\sigma, NE_{YR}^\sigma, NE_{SP}^\sigma, Oth_{YR}^\sigma, Oth_{SP}^\sigma, H_{YR}^h, H_{SP}^h, CH_{YR}^h, CH_{SP}^h, NE_{YR}^h, NE_{SP}^h, Oth_{YR}^h, Oth_{SP}^h\}$ , indexed by  $q$ . For more information on the regulations that determine  $Q$  the reader is referred to Council Regulation (EEC) No 95/93 (1993) and IATA WSG

$K$ :  $\{Arr, Dep, Total\}$  set of movement types indexed by  $k$

$A$ : set of airlines submitting requests indexed by  $\alpha$

$M$ : set of requests indexed by  $m$ . In differentiating between the legs of a request,  $ma$  and  $md$  are used for arrival and departures respectively

$M_\alpha$ : set of requests submitted by airline  $\alpha$

$M_q$ : set of requests of slot priority  $q \in Q$  (as defined above) with  $|M_q|$  being the number of requests falling into request priority  $q$

$M^k$ : set of requests  $m$  of movement type  $k$ . Consequently, the request set may be sliced to obtain the sets of arrival (departure) requests  $M^{Arr(Dep)}$ :  $M^{Arr} \cup M^{Dep} = M^{Total} = M$

$D$ : set of days in scheduling season indexed by  $d$

$W$ : set of weeks in scheduling season indexed by  $w$  where  $|W| = (D \text{ div } 7) + 1$

$W_m$ :  $\{w_{n_m}, \dots, w_{N_m}\}$  set of weeks in scheduling season that slot  $m$  is to operate with  $W_m \subseteq W$ ,  $n_m$  being the starting week of operation  $m$  and  $N_m$  being the index of the last week that slot  $m$  will operate such that  $n_m \leq N_m \leq |W|$ .  $W_m = \{w_{n_m+\rho} \omega_m : w \in W, \rho \in [0, \frac{N_m-n_m}{\omega_m}]\}$ , where  $\omega_m$  is the frequency of operations of request  $m$ . Note that an arrival and a departure can't be requested for different durations ( $W_{mArr} = W_{mDep} = W_m$ ). Obviously, if  $N_m = n_m$  then  $|W_m| = 1$

$D_m$ : set of days that request  $m$  is to operate

$C$ : set of capacity time interval lengths indexed by  $c, \tilde{c}$

$T_{\tilde{c}} = \{0, \dots, |T_{\tilde{c}}|\}$ : set of time intervals per day calculated based on interval length  $\tilde{c}$  indexed by  $t/t'$  with cardinality  $|T_{\tilde{c}}|$  with  $\tilde{c} = \min_{c \in C} c$

<b>ID</b>	<b>1</b>	<b>2</b>	<b>3</b>	<b>4</b>	<b>5</b>	<b>6</b>	<b>7</b>	<b>8</b>	<b>9</b>	<b>10</b>	<b>11</b>	<b>12</b>	<b>13</b>	<b>14</b>	<b>15</b>	<b>16</b>
<i>Label</i>	AC	ANU	DC	DNU	HF	MHF	HT	MHT	M	T	W	H	F	S	U	SEN
1	A1	1111	A1	1112	16	JUN	13	OCT	0	2	0	4	0	0	0	231
...	...	...	...	...	...	...	...	...	...	...	...	...	...	...	...	...
$ M $	AN	9998	AN	9999	30	MAY	03	OCT	0	0	0	0	0	6	0	167
<b>ID</b>	<b>17</b>	<b>18</b>	<b>19</b>	<b>20</b>	<b>21</b>	<b>22</b>	<b>23</b>	<b>24</b>	<b>25</b>	<b>26</b>	<b>27</b>	<b>28</b>	<b>29</b>	<b>30</b>	<b>31</b>	<b>21</b>
<i>Label</i>	TYP	AFR	BFR	AH	AM	DH	DM	V	ADE	BDE	FY	Q	ADOF	ADOT	AAOF	AAOT
1	737	PRG	PRG	12	55	13	55	0	PRG	PRG	JJ	3	0	0	0	0
...	...	...	...	...	...	...	...	...	...	...	...	...	...	...	...	...
$ M $	321	BLL	BLL	08	40	9	40	0	BLL	BLL	CC	1	0	0	0	0
Notes:	Arrival / Departure Company (AC/DC), Arrival/ Departure Number (ANU/DNU), first/ last day of operations (HF/HT), first/ last month of operations (MHF/MHT), Monday (M), Tuesday (T), Wednesday (W), Thursday (H), Friday (F), Saturday (S), Sunday (U), Seats Expected (SEN), type of aircraft (TYP), airport of origin (AFR), last stopover airport (BFR), Arrival/Departure Hour (AH/DH), Arrival/ Departure Minute (AM/DM), Overnight indicator (can be 1 if the aircraft will depart the next day, or 0 if it departs the same day) (V), next stopover airport (ADE), destination airport (BDE), Service codes for the arrival and departure flights (FY where J/F: schedule passenger/ cargo flight, C/H: chartered passenger/cargo flight, P: positional, X: technical, D: general or private, N: Business aviation/ air taxi), frequency indicator (Q), Alternative Departure/Arrival Offers From (To) (ADOF(T)/AAOF(T)).															

**Table 2-2:** Overview of the parameters submitted by airlines as per the SSIM format

### Input parameters

$t_m$ : requested time for slot request  $m$

$$\lambda_m = \begin{cases} 1, & \text{if request } m \text{ concerns positioning or maintenance operations} \\ 0, & \text{otherwise} \end{cases}$$

Defined based on column 27 of Table 2-2

$T_{\max(\min),m}$ : maximum (minimum) turnaround time of request  $m$ . For this chapter's computational experiments, turnaround times are set to be equal to the initially requested time difference between the arrival and the departure movements associated with request  $m$ , i.e.,  $T_{\min,m} = t_{md} - t_{ma} + |T_c|v_m = T_{\max,m}$

$u_{d,t,c}^k$ : runway capacity for movement  $k$  for period  $[t, t + c)$  on day  $d$  based on time interval length  $c$

$$a_{d,m} = \begin{cases} 1, & \text{if } m \text{ is requested on day } d \\ 0, & \text{otherwise} \end{cases}$$

$h_m = \begin{cases} 1, & \text{if } |W_m| < 5 \\ 0, & \text{otherwise} \end{cases}$ : is a parameter determining whether a request is considered as an ad-hoc operation or not based on the *series of slots* definition of (IATA, 2019a)

$\sigma_m = 1 - h_m$ : a parameter that determines whether a request is considered as a series of slots or not

$v_m = \begin{cases} 1, & \text{if } a_{d,md} = a_{d,ma} + 1 \\ 0, & \text{if } a_{d,md} = a_{d,ma} \end{cases}$ : is listed in the SSIM format as overnight indicator (column 24 of Table 2-2) stating whether the departure of request  $m$  ( $md$ ) is requested to be scheduled a day after the arrival ( $ma$ )

$\psi_{t,m} = t - t_m$ : the displacement of slot request  $m$

### Decision variables, parameters, and expressions

$$x_{t,m}^f = \begin{cases} 1, & \text{if request } m \text{ is allocated to time } t \text{ on terminal } f \\ 0, & \text{otherwise} \end{cases}$$

$\Psi$ : auxiliary variable defining the maximum displacement objective as a set of linear constraints (see (2.1))

### Base model constraints and cost function

The following expressions define the base model of this chapter.

$$\sum_{f \in F} \sum_{t \in T_{\bar{c}}} x_{t,ma}^f = \sum_{f \in F} \sum_{t \in T_{\bar{c}}} x_{t,md}^f \leq 1 \quad \forall m \in M_q \quad (2.1)$$

$$\left( \sum_{t \in T_{\bar{c}}} x_{t,ma}^f - \sum_{t \in T_{\bar{c}}} x_{t,md}^f \right) (1 - \lambda_m) = 0 \quad \forall f \in F, m \in M_q \quad (2.2)$$

$$\sum_{m \in M_q^k} \sum_{t' \in [t, t+c-1]} \sum_{f \in F} a_{d,m} x_{t',m}^f \leq u_{d,t,c}^k \quad \forall k \in K, d \in D, c \in C, t \in [0, |T_{\bar{c}}| - c] \quad (2.3)$$

$$T_{min,m} \leq \sum_{f \in F} \sum_{t \in T_{\bar{c}}} [x_{t,md}^f t + v_m |T_{\bar{c}}|] - \sum_{f \in F} \sum_{t \in T_{\bar{c}}} x_{t,ma}^f t \leq T_{max,m} \quad \forall m \in M_q \quad (2.4)$$

$$\sum_{t \in T_{\bar{c}}} x_{t,m}^f |\psi_{t,m}| \leq \Psi \quad \forall m \in M_q \quad (2.5)$$

$$Z_q = \text{lexmin} \begin{cases} |M_q| - \sum_{f \in F} \sum_{m \in M_q} \sum_{t \in T_{\bar{c}}} x_{t,m}^f \\ \max_{\forall m \in M_q} \{ |\psi_{t,m}| x_{t,m}^f \} = \Psi \\ \sum_{f \in F} \sum_{m \in M_q} |D_m| \sum_{t \in T_{\bar{c}}} (x_{t,m}^f |\psi_{t,m}|) \end{cases} \quad (2.6)$$

Constraints (2.1) ensure that each of the slots will be allocated to a time and a terminal at most once. In addition, expression (2.1) states that if the arrival leg of a request is scheduled/rejected, then the departure will be scheduled/rejected as well. Constraints (2.2) state that the arrival and the departure of a request, must be scheduled at the same terminal  $f$ . Please note that (2.2) become inactive with the use of  $\lambda_m$ . Constraints (2.3) are runway capacity constraints for each type of movement i.e., arrival, departure, or total movements ensuring that at each time of the day the scheduled aircraft movements will not exceed the runway capacity of the airport. The subscripts  $t, d$  of capacity parameter  $u_{d,t,c}^k$  allows the explicit

consideration of different capacity levels throughout each time and day of the scheduling season.

Hence, expressions (2.3) allow the consideration of curfews and noise-related constraints applying to the airport (WWACG, 2019). Furthermore, constraints (2.4) are turnaround time constraints which ensure that the time difference between two paired movements should not be less than the initially requested difference between them (minimum turnaround time) and larger than a specified limit (maximum turnaround time). In the absence of preferences regarding the maximum turnaround time, its value can be set equal to an operationally viable value or infinity. Constraints (2.4) differentiate from existing formulations since they consider the overnight indicator ( $v_m$ ) of each request. The last set of constraints (2.5), are auxiliary expressions that help the introduction of the maximum displacement objective used in the objective function denoted by expression (2.6).

The objective function of the model captures slot coordinators' behaviour and preferences, minimising lexicographically the total number of rejected/unsatisfied slot requests of priority  $q$  ( $Z_{1,q}$ ), the maximum displacement across all satisfied slot requests of priority  $q$  ( $Z_{2,q}$ ) and the total displacement objective ( $Z_{3,q}$ ). In what follows the model expressed in (2.1)-(2.6) is referred to as *base model*.

The lexicographic optimisation of the objective set ( $Z_q$ ) minimises each objective  $Z_{i,q}$ ,  $i = 1, 2$  and then proceeds to the minimisation of the next objective  $Z_{i+1,q}$  by constraining the value of  $Z_{i,q}$  to be above its optimum value previously obtained. Hence, there is need to solve the following optimisation problems:  $\min Z_{i,q}(x)$  subject to (1) – (6) and  $Z_{j,q} \leq Z_{j,q}^*$ ,  $j = 1, 2, i - 1: i > 1$ . Herein,  $i$  represents the order of the objectives and  $Z_{j,q}^*$  is the optimum value of the objective function  $j$  found in the  $j^{th}$  iteration.

### 2.4.2 Terminal and airport capacity modelling

The base model (expressions (2.1)-(2.6)) can be enriched by adding constraints modelling the terminal and apron capacity requirements of the airport. The motivation behind the use of such capacity constraints stems from the fact that the bottleneck of airport infrastructure may lie in the terminal's passenger capacity, or the apron stands which can serve parking aircraft during their stay at the airport. That is an observation made by practitioners in some of the busiest European airports (Airport Coordination Limited, 2018). To model such requirements, below additional notation is introduced. Let:

$O = \{Schengen, Non - Schengen, Domestic \text{ etc.}\}$ : be the set of flight types indexed by  $o, o'$

$R = \{Light, Medium, Heavy\}$ : be the set of aircraft categories indexed by  $r$

$e_m$ : be the number of seats requested for  $m$  (based on column 16 of Table 2-2)

$\xi_m$ : be the load factor for slot request  $m$  (percentage of expected occupied seats)

$E_{d,t,c,o}^{f,k}$ : be the passenger capacity for type  $o$ , movement  $k$  and period  $[t, t + c)$  at terminal  $f$  on day  $d$

$\delta_{d,t}^{f,r}$ : be the apron capacity for aircraft type  $r$  at terminal  $f$  on day  $d$  and time interval  $t$

$Air_{t,-1(|D|+1),f,r}$ : be the number of arriving (departing) aircraft of type  $r$  at terminal  $f$  at time  $t$  of the last day of the previous scheduling season (first day of the next scheduling season);

$Pas_{-1(|D|+1),t,o}^{f,Arr(Dep)}$ : be the estimated number of passengers on arrival (departure) movements of type  $o$  at terminal  $f$  at time interval  $t$  on the last day of

the previous scheduling season (first day of the following scheduling season)

$l_k^{f,apr}, l_k^{f,o,pas}$ : be lag parameters representing the time difference between the use of the runways, the aprons, and the passenger terminals of the airport. These parameters are used in the apron and passenger capacity constraints to determine when movement  $k \in (Arr, Dep)$  of request  $m$  and type  $o$  (used for passengers) will consume resources at terminal  $f$ . One may safely assume that  $0 < l_{Dep}^{f,apr} < l_{Dep}^{f,pas}$  and  $l_{Arr}^{f,o,pas} < l_{Arr}^{f,o,apr} < 0$ . That is because if an arrival (departure) consumes apron capacity on time  $t$ , then the aircraft should have landed on time  $t' = t + l_{Arr}^{f,apr} < t$  ( $t' = t + l_{Dep}^{f,apr} > t$ ). Similarly, for each time  $t$  the passengers that each movement of a request concerns, make use the terminal on time  $t' = t + l_{Arr}^{f,o,pas} < t + l_{Arr}^{f,apr} < t$  ( $t' = t + l_{Dep}^{f,o,pas} > t + l_{Dep}^{f,apr} > t$ )

$\pi_{t,d,f,r}$ : be the number of aircraft of type  $r$  which are parked at terminal  $f$  on day  $d$  at time  $t$

Given the additional notation detailed above, one may construct and add to the base model the following passenger constraint expressions (2.7)-(2.11).

$$\begin{aligned}
 & \forall k \in \{Arr, Dep\}, c \\
 & \in C, d \in D, o \\
 & \in O, f \in F, t \\
 & \in T_{\bar{c}}: t + l_k^{f,o,pas} \\
 & \in [0, |T_{\bar{c}}| - c] \\
 & \sum_{m \in M_{f,o}^k} \sum_{t' \in [t + l_k^{f,o,pas}, t + l_k^{f,o,pas} + c - 1]} a_{d,m} x_{t',m}^f e_m \xi_m \leq E_{d,t,c,o}^{f,k} \quad (2.7)
 \end{aligned}$$

$$\begin{aligned}
& \sum_{m \in M_{f,o}^{Arr}} \sum_{t' \in [|\bar{T}_{\bar{c}}| + t - l_{Arr}^{f,o,pas}, |\bar{T}_{\bar{c}}| + t - l_{Arr}^{f,o,pas} + c - 1]} a_{d-1,m} x_{t',m}^f e_m \xi_m & \forall c \in C, d \in D/\{0\}, o \in O, f \in F, t \in T_{\bar{c}}: t + \\
& \leq E_{d,t,c,o}^{f,Arr} & l_{Arr}^{f,o,pas} < 0
\end{aligned} \tag{2.8}$$

$$\begin{aligned}
& \sum_{t' \in [|\bar{T}_{\bar{c}}| + t - l_{Arr}^{f,o,pas}, |\bar{T}_{\bar{c}}| + t - l_{Arr}^{f,o,pas} + c - 1]} Pas_{-1,t',o}^{f,Arr} \leq E_{0,t,c,o}^{f,Arr} & \forall c \in C, o \in O, f \in F, t \in [0, |\bar{T}_{\bar{c}}| - c]: t + l_{Arr}^{f,o,pas} < 0
\end{aligned} \tag{2.9}$$

$$\begin{aligned}
& \sum_{m \in M_{f,o}^{Dep}} \sum_{t' \in [t + l_{Dep}^{f,o,pas} - |\bar{T}_{\bar{c}}|, t + l_{Dep}^{f,o,pas} - |\bar{T}_{\bar{c}}| + c - 1]} a_{d+1,m} x_{t',m}^f e_m \xi_m & \forall c \in C, d \in D/\{0\}, o \in O, f \in F, t \in T_{\bar{c}}: t + \\
& \leq E_{d,t,c,o}^{f,Dep} & l_k^{f,o,pas} > |\bar{T}_{\bar{c}}| - c
\end{aligned} \tag{2.10}$$

$$\begin{aligned}
& \sum_{t' \in [t + l_{Dep}^{f,o,pas} - |\bar{T}_{\bar{c}}|, t + l_{Dep}^{f,o,pas} - |\bar{T}_{\bar{c}}| + c - 1]} Pas_{|D|+1,t',o}^{f,Dep} \leq E_{|D|,t,c,o}^{f,Dep} & \forall c \in C, o \in O, f \in F, t \in T_{\bar{c}}: t + \\
& & l_k^{f,o,pas} > |\bar{T}_{\bar{c}}| - c
\end{aligned} \tag{2.11}$$

(2.7)-(2.11) ensure that the number of passengers coming from Schengen or non-Schengen areas in each terminal, will be kept below the operational limits of parts of the terminal serving respectively Schengen and non-Schengen flights at each time.

Constraints (2.7) consider the time difference that separates the usage of terminal capacity by the passengers served by movements that used runway capacity in earlier or later time periods by considering  $l_k^{f,o,pas}$  parameters. Please note that these lag parameters depend on the flight type, since international passengers travelling to non-Schengen destinations, should arrive at the terminal significantly earlier than passengers flying to domestic or Schengen destinations. As



a result, passengers that are present in the terminal at time  $t$  have either arrived on an arrival movement which made use of runway capacity on time  $t + l_{Arr}^{f,o,pas} < t$ , or will depart from it on a departure movement using the airport's runways on time  $t + l_{Dep}^{f,o,pas} > t$ . In the case that the arrival (departure) of the passengers that are present in the terminal on time  $t$  happened during the previous (following) day such that  $t + l_{Arr}^{f,o,pas} < 0$  ( $t + l_{Dep}^{f,o,pas} > |T_{\bar{c}}|$ ), constraints (2.8)((2.10)) are used to extend and generalise (2.7).

However, the number of passengers that are present in the terminal during the first (last) time intervals of the first (last) day of the scheduling season, cannot be defined without knowing the number of arrivals (departures) that were (will be) scheduled during the last (first) intervals of the last (first) day of the previous (following) scheduling season. Therefore, parameters  $Pas_{-1(|D|+1),t,c,o}^{f,Arr(Dep)}$  are used as estimates for these measures. Fortunately,  $Pas_{-1,t,c,o}^{f,Arr}$  are defined during the previous scheduling season and can be perceived as input parameters. Alternatively, they can be estimated by the passengers that will be scheduled on the closest similar day (sixth)<sup>5</sup> of the current season i.e.,  $Pas_{-1,t,o}^{f,Arr} = \sum_{m \in M_{f,o}^{Arr}} a_{6,m} x_{t,m}^f e_m \xi_m$ .

Similarly, given that the number of departures on the first-time intervals of the following season are not known *a priori*, an estimate on the number of

---

<sup>5</sup> If the last day of the previous season that is indexed by -1 is a Wednesday, then the first Wednesday of the current season can be found after seven positions of the index of  $D$ . Hence, the first Wednesday of the current season will have  $d = 6$ . The same holds for the end of the current season. If the first day of the next season with index  $n+1$  is a Friday, then the last Friday of the current season can be found seven positions before the index  $d = n + 1$ . Hence, the index of the last Friday of the current season is  $d = n - 6$ . As a result, in estimating the passengers/aircraft during the last/first intervals of the season the model considers 6 days.

passengers can be given as  $Pas_{|D|+1,t,o}^{f,Dep} = \sum_{m \in M_{f,o}^{Dep}} a_{|D|-6,m} x_{t,m}^f e_m \xi_m$ , where  $|D| - 6$  is the closest similar weekday of the current season (e.g. Monday) with respect to the first day of the following scheduling season. Expressions (2.9) and (2.11) use  $Pas_{-1(|D|+1),t,c,o}^{f,Arr(Dep)}$  parameters to define the passenger capacity constraints during the first and last time-intervals of the scheduling season. Please note, that in most airports these time intervals are not heavily congested; hence, the accuracy of the estimated parameters is not expected to influence the slot scheduling outcome.

In addition to the passenger capacity constraints discussed above, apron capacity constraints which also consider an appropriate time difference between the time of the runway movement are introduced, i.e., landing, take-off and the use of the apron stands ( $l_k^{f,apr}$ ).

$$\begin{aligned} & \sum_{m \in M_{f,r}^{Arr}} x_{t+l_{Arr}^{f,apr},m}^f a_{d,m} \\ & - \sum_{m \in M_{f,r}^{Dep}} x_{t+l_{Dep}^{f,apr},m}^f a_{d,m} \\ & + \pi_{t-1,d,f,r} = \pi_{t,d,f,r} \end{aligned} \quad \begin{aligned} & \forall d \in D, f \in F, r \in R, t \in \\ & (0, |T_{\bar{c}}|]: t + l_{Arr}^{f,apr} \geq 0, t + \\ & l_{Dep}^{f,apr} \leq |T_{\bar{c}}| \end{aligned} \quad (2.12)$$

$$\begin{aligned} & \sum_{m \in M_{f,r}^{Arr}} x_{|T_{\bar{c}}|+t-l_{Arr}^{f,apr},m}^f a_{d-1,m} \\ & - \sum_{m \in M_{f,r}^{Dep}} x_{t+l_{Dep}^{f,apr},m}^f a_{d,m} \\ & + \pi_{t-1,d,f,r} = \pi_{t,d,f,r} \end{aligned} \quad \begin{aligned} & \forall d \in D/\{0\}, f \in F, r \in R, t \in \\ & (0, |T_{\bar{c}}|]: t + l_{Arr}^{f,apr} < 0 \end{aligned} \quad (2.13)$$

$$\begin{aligned} & \sum_{m \in M_{f,r}^{Arr}} x_{t+l_{Arr}^{f,apr},m}^f a_{d,m} \\ & - \sum_{m \in M_{f,r}^{Dep}} x_{t+l_{Dep}^{f,apr}-|T_{\bar{c}}|,m}^f a_{d+1,m} \\ & + \pi_{t-1,d,f,r} = \pi_{t,d,f,r} \end{aligned} \quad \begin{aligned} & \forall d \in D/\{|D|\}, f \in F, r \in \\ & R, t \in (0, |T_{\bar{c}}|]: t + l_{Dep}^{f,apr} > \\ & |T_{\bar{c}}| \end{aligned} \quad (2.14)$$



and (2.16) respectively. Similar to the passenger constraints (2.9) and (2.11),

$$Air_{|T_{\bar{c}}|-|t+l_{Arr}^{f,apr}|,-1,f,r} = \sum_{m \in M_{f,r}^{Arr}} x_{|T_{\bar{c}}|+t-l_{Arr}^{f,apr},m}^f a_{6,m} \quad \text{and} \quad Air_{t+l_{Dep}^{f,apr}-|T_{\bar{c}}|,|D|+1,f,r} = \sum_{m \in M_{f,r}^{Dep}} x_{t+l_{Dep}^{f,apr}-|T_{\bar{c}}|,m}^f a_{|D|-6,m}.$$

(2.17) initialise the number of aircraft of type  $r$  that are parked in terminal  $f$  at the beginning ( $t = 0$ ) of each day  $d \neq 0$ . Please note that (2.17) consider and depend on the aircraft parked in this terminal during the last period ( $t = |T_{\bar{c}}|$ ) of the previous day ( $d - 1$ ). In the case that  $d = 0$ , the number of aircraft parked at the aprons of each terminal can be given as parameter, or it can be calculated based on the slot schedule of the previous season. In the absence of such data an approximation can be supplied based on  $\pi_{|T_{\bar{c}}|,|D|-6,f,r}$ . Finally, constraints (2.18) ensure that the parked aircraft of type  $r$  in terminal  $f$  should not exceed its capacity for that aircraft type at all time intervals. In the following sections, expressions (2.7)-(2.18) are referred to as *apron and passenger capacity constraints*.

To demonstrate how the time difference (lag) parameters ( $l_k^{f,apr}, l_k^{f,o,pas}$ ) used in the constraints of this section may influence the solution of the models, an illustrative example is provided (see Example 2.1 and Figure 2-3).

### Example 2.1

Suppose that the average time of each arrival (departure) movement to reach its apron or parking spot (runway) from the runway (apron or parking spot) is between 0-15 minutes, i.e., 1 interval (15-30 minutes, i.e., 2 intervals). Hence,  $l_{Arr}^{f,apr} = -1$  ( $l_{Dep}^{f,apr} = 2$ ). In addition, since passengers flying to international destinations must be at the terminal at least two hours before gate closure, one can set  $l_{Dep}^{f,Non-schengen,pas} = 8 + l_{Dep}^{f,apr} = 10$  (15-minute time intervals).

For Schengen and domestic departures, suppose that passengers arrive in the terminal 45 minutes before the departure time, i.e.,  $l_{Dep}^{f,Domestic,pas} = l_{Dep}^{f,Schengen,pas} + l_{Dep}^{f,apr} = 5$ . For international arrivals one can assume that the passengers will be in the terminal within 15-30 minutes ( $l_{Arr}^{f,Non-schengen,pas} = -2 + l_{Arr}^{f,apr} = -3$ ) while for domestic and Schengen arrivals the setting is  $l_{Arr}^{f,Domestic,pas} = l_{Arr}^{f,Schengen,pas} = -1 + l_{Arr}^{f,apr} = -2$ .

Based on this setup, assume two slot requests ( $m1$  and  $m2$ ) which are submitted for the same day  $d$  (with each day being discretised in 96 15-minute time intervals).  $m1Arr$  and  $m1Dep$  are requested for  $t_{m1Arr} = 1$  (00:15) and  $t_{m1Dep} = 4$  (01:00), and  $m2Arr$  and  $m2Dep$  for  $t_{m2Arr} = 93$  (23:15) and  $t_{m2Dep} = 1$  (00:15) of the next day ( $d + 1$ ) having an overnight indicator  $v_{m1} = 1$ .  $m1$  concerns international non-Schengen movements while  $m2$  two Schengen/Domestic movements. Also, suppose that all movements concerned get their requested slots.

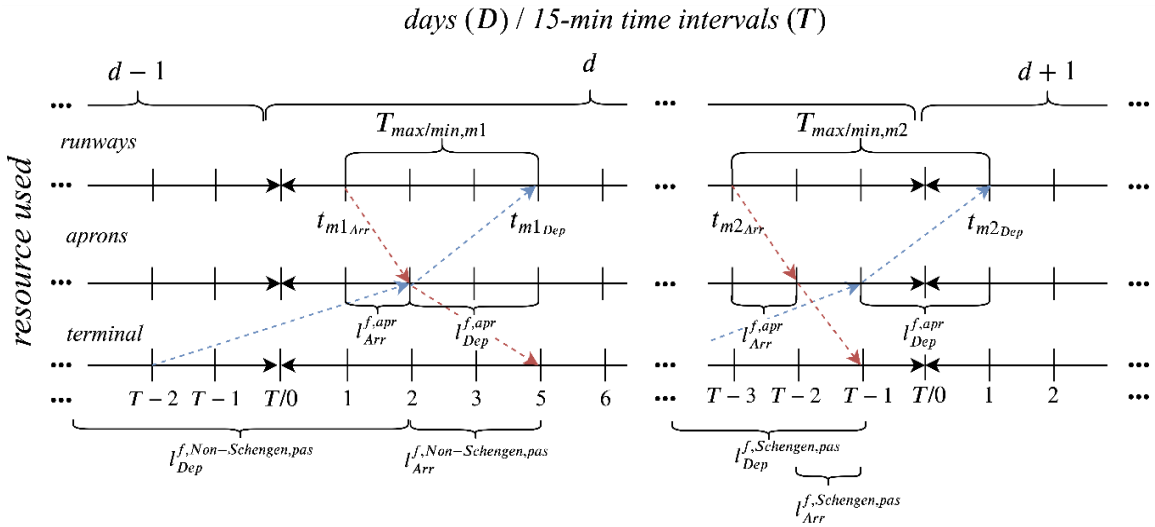


**Figure 2-3:** Example on the asynchronous interaction between runways, apron, and terminals

Given the parametrisation detailed above, the aircraft concerned in  $m1Arr$  will arrive at the apron one time-interval after its arrival, i.e., 00:30. Since it is a

non-Schengen flight its passengers will reach the terminal after their border check at 01:00. Similarly, the passengers that will depart with *m1Dep* have to be in the terminal at least 8 intervals (2 hours) before the departure of the airplane from the apron. Hence, they will arrive at the terminal at 22:30 the day before ( $d - 1$ ). Accordingly, the airplane will depart from the parking/apron 30-45 minutes before departing from the runway at 01:00, i.e., at 12.15-12.30. Similar, dynamics are given for *m2*.

### 2.4.3 Dynamic capacity utilisation expressions

The capacity parameters, layout and capacity utilisation specifications of each airport and terminal are given in the declared capacity parameters supplied before the beginning of each slot scheduling season (IATA, 2019a). Existing literature considers the runway, apron and passenger terminal capacity parameters of each airport and its terminals without acknowledging that the facilities of the airport can be reconfigured dynamically based on the demand's characteristics.

Hence, existing studies do not enable the full utilisation of airport capacity resources. For instance, in airports having MARS (Multiple Aircraft Ramp System) stands, aprons can be configured so as to accommodate one heavy aircraft (category E) or two medium/small aircraft (categories C or below) (WWACG, 2019; p. 5). Based on this dynamic reconfiguration of the airport's airside and landside facilities, apron capacity of the airport/terminal depends on the types of the aircraft scheduled to park in the apron stands of the airport and result in improved apron utilisation (Mirković and Tošić, 2014). Accordingly, the capacity of each airport/terminal may depend on the types of passengers arriving in the terminal (e.g., passengers arriving from Schengen or Non-Schengen areas). A comprehensive analysis on the benefit of the dynamic allocation of airport capacity with regard to the apron and passenger terminal capacity is provided in section 2.7.2.4.

In airports/terminals where the declared capacity parameters include demand-based capacity specifications, in the case that more aircraft of type  $r$  need to be accommodated, additional aprons can be used by aircraft of type  $r$  using aprons for other aircraft types ( $r'$ ) and *vice versa*. In airports where this requirement is active, expressions (2.18) are complemented by the following expressions:

$$\pi_{t,d,f,r} \leq \sum_{r' \in R/\{r\}} \left( \frac{\delta_{d,t}^{f,r'} - \pi_{t,d,f,r'}}{CA_f^{r',r}} \right) + \delta_{d,t}^{f,r} \quad \forall d \in D, t \in T_{\bar{c}}, f \in F, r \in R \quad (2.19)$$

Constraints (2.19) define the capacity of terminal  $f$  for aircraft type  $r$  with respect to its apron stands at each time. Expressions (2.19) differ from inequalities (2.18) since they allow the use of slack capacity ( $\delta_{d,t}^{f,r'} - \pi_{t,d,f,r'} > 0$ ) of other aircraft types ( $r'$ ) to accommodate additional aircraft of type  $r$ . In (2.19),  $CA_f^{r',r}$  represent the number of stands of type  $r'$  required for parking aircraft of type  $r$  in terminal  $f$ . Note that  $CA_f^{r',r} = 1/CA_f^{r,r'}$ . For instance, if there are only two aircraft types using the airport ( $r, r'$ ), expressions (2.19) become  $\pi_{t,d,f,r} \leq (\delta_{d,t}^{f,r'} - \pi_{t,d,f,r'})/CA_f^{r',r} + \delta_{d,t}^{f,r}$ . In the case that  $\delta_{d,t}^{f,r'} - \pi_{t,d,f,r'} = 0$ , then (2.19) become equal to (2.18). If,  $\delta_{d,t}^{f,r'} - \pi_{t,d,f,r'} > 0$ , for each stand made available to  $r'$ , the capacity for  $r$  is increased by  $1/CA_f^{r',r}$ . When  $\delta_{d,t}^{f,r'} - \pi_{t,d,f,r'} < 0$ , for each stand of made available to  $r'$ , the capacity for  $r$  is decreased by  $1/CA_f^{r',r}$ .

In addition, the configuration of airport terminals that can accommodate different types of passengers (e.g., one terminal that will accept all Schengen arrivals and one for non-Schengen arrivals), is adapted based on the demands of the flights that are about to arrive or depart. Therefore, in the absence of a certain type of passengers, the capacity for this passenger type may be used by movements

concerning other flight types. At such airports, the described operational requirement can be modelled by altering constraints (2.7) using the following variables and constraint expressions

Let  $\zeta_{d,t,o}^{f,k}$  be equal to 1, if passengers on flight  $o$  depart (arrive) from (to) terminal  $f$  on time  $t$  and day  $d$  and 0, otherwise. The passenger constraints (2.7) are modified and replaced by expressions (2.20) and (2.21) that are interconnected by variables  $\zeta_{d,t,o}^{f,k}$ .

$$\sum_{m \in M_{f,o}^k} \sum_{t' \in [t+l_k^{f,o,pas}, t+l_k^{f,o,pas}+c-1]} a_{d,m} x_{t',m}^f e_m \xi_m \leq \zeta_{d,t,o}^{f,k} E_{d,t,c,o}^{f,k} \quad (2.20)$$

$\forall d \in D, c$   
 $\in C, k$   
 $\in \{Arr, Dep\}, o$   
 $\in O, f \in F, t$   
 $\in T_{\bar{c}}: t + l_k^{f,o,pas}$   
 $\in [0, |T_{\bar{c}}| - c]$

$$\sum_{m \in M_{f,o}^k} \sum_{t' \in [t+l_k^{f,o,pas}, t+l_k^{f,o,pas}+c-1]} a_{d,m} x_{t',m}^f e_m \xi_m \leq \sum_{o' \in O/\{o\}} [(1 - \zeta_{d,t,o'}^{f,k}) E_{d,t,c,o'}^{f,k}] + E_{d,t,c,o}^{f,k} \quad (2.21)$$

$\forall d \in D, k$   
 $\in \{Arr, Dep\}, o$   
 $\in O, c \in C, f$   
 $\in F, t$   
 $\in T_{\bar{c}}: t + l_k^{f,o,pas}$   
 $\in [0, |T_{\bar{c}}| - c]$

As per (2.20) and (2.21), when passengers on board flights of type  $o$  are about to depart/arrive in terminal  $f$  on time  $t$  and day  $d$ , expressions (2.20) are only satisfied if  $\zeta_{d,t,o}^{f,k} = 1$ . When  $\zeta_{d,t,o}^{f,k} = 1$ , constraints (2.21) ensure that the capacity for flight type  $o$  will not be used to accommodate passengers of other flight types. However, in the occasion that there are no flights (and therefore passengers) of type  $o$  ( $\zeta_{d,t,o}^{f,k} = 0$ ), then constraints (2.21) allow the passenger capacity dedicated to  $o$  to be used for other flight types. In a similar fashion, the following expressions can be used to substitute constraints (2.8)-(2.11).



$$\begin{aligned}
& \sum_{m \in M_{f,o}^{Arr}} \sum_{t' \in [|\bar{T}_{\bar{c}}| + t - l_{Arr}^{f,o,pas}, |\bar{T}_{\bar{c}}| + t - l_{Arr}^{f,o,pas} + c - 1]} a_{d-1,m} x_{t',m}^f e_m \xi_m & \forall c \in C, d \in D/\{0\}, o \in O, f \in F, t \in T_{\bar{c}}: t + l_{Arr}^{f,o,pas} < 0 \\
& \leq \zeta_{d,t,o}^{f,Arr} E_{d,t,c,o}^{f,Arr} & (2.22)
\end{aligned}$$

$$\begin{aligned}
& \sum_{m \in M_{f,o}^{Arr}} \sum_{t' \in [|\bar{T}_{\bar{c}}| + t - l_{Arr}^{f,o,pas}, |\bar{T}_{\bar{c}}| + t - l_{Arr}^{f,o,pas} + c - 1]} a_{d-1,m} x_{t',m}^f e_m \xi_m & \forall c \in C, d \in D/\{0\}, o \in O, f \in F, t \in T_{\bar{c}}: t + l_{Arr}^{f,o,pas} < 0 \\
& \leq \sum_{o' \in O/\{o\}} \left[ (1 - \zeta_{d,t,o'}^{f,Arr}) E_{d,t,c,o'}^{f,Arr} \right] + E_{d,t,c,o}^{f,Arr} & (2.23)
\end{aligned}$$

$$\begin{aligned}
& \sum_{t' \in [|\bar{T}_{\bar{c}}| + t - l_{Arr}^{f,o,pas}, |\bar{T}_{\bar{c}}| + t - l_{Arr}^{f,o,pas} + c - 1]} Pas_{-1,t',o}^{f,Arr} \leq \zeta_{0,t,o}^{f,Arr} E_{0,t,c,o}^{f,Arr} & \forall c \in C, o \in O, f \in F, t \in [0, |\bar{T}_{\bar{c}}| - c]: t + l_{Arr}^{f,o,pas} < 0 \\
& (2.24)
\end{aligned}$$

$$\begin{aligned}
& \sum_{t' \in [|\bar{T}_{\bar{c}}| + t - l_{Arr}^{f,o,pas}, |\bar{T}_{\bar{c}}| + t - l_{Arr}^{f,o,pas} + c - 1]} Pas_{-1,t',o}^{f,Arr} & \forall c \in C, o \in O, f \in F, t \in [0, |\bar{T}_{\bar{c}}| - c]: t + l_{Arr}^{f,o,pas} < 0 \\
& \leq \sum_{o' \in O/\{o\}} \left[ (1 - \zeta_{0,t,o'}^{f,Arr}) E_{0,t,c,o'}^{f,Arr} \right] + E_{0,t,c,o}^{f,Arr} & (2.25)
\end{aligned}$$

$$\begin{aligned}
& \sum_{m \in M_{f,o}^{Dep}} \sum_{t' \in [t + l_{Dep}^{f,o,pas} - |\bar{T}_{\bar{c}}|, t + l_{Dep}^{f,o,pas} - |\bar{T}_{\bar{c}}| + c - 1]} a_{d+1,m} x_{t',m}^f e_m \xi_m & \forall c \in C, d \in D/\{D\}, o \in O, f \in F, t \in T_{\bar{c}}: t + l_{Dep}^{f,o,pas} > |\bar{T}_{\bar{c}}| - c \\
& \leq \zeta_{d,t,o}^{f,Dep} E_{d,t,c,o}^{f,Dep} & (2.26)
\end{aligned}$$

$$\begin{aligned}
& \sum_{m \in M_{f,o}^{Dep}} \sum_{t' \in [t + l_{Dep}^{f,o,pas} - |\bar{T}_{\bar{c}}|, t + l_{Dep}^{f,o,pas} - |\bar{T}_{\bar{c}}| + c - 1]} a_{d+1,m} x_{t',m}^f e_m \xi_m & \forall c \in C, d \in D/\{D\}, o \in O, f \in F, t \in T_{\bar{c}}: t + l_{Dep}^{f,o,pas} > |\bar{T}_{\bar{c}}| - c \\
& \leq \sum_{o' \in O/\{o\}} \left[ (1 - \zeta_{d,t,o'}^{f,Dep}) E_{d,t,c,o'}^{f,Dep} \right] + E_{d,t,c,o}^{f,Dep} & (2.27)
\end{aligned}$$

$$\begin{aligned}
& \sum_{t' \in [t + l_{Dep}^{f,o,pas} - |T_{\bar{c}}|, t + l_{Dep}^{f,o,pas} - |T_{\bar{c}}| + c - 1]} Pas_{|D|+1,t',o}^{f,Dep} & \forall c \in C, o \in \\
& \leq \zeta_{|D|,t,o}^{f,Dep} E_{|D|,t,c,o}^{f,Dep} & O, f \in F, t \in \\
& & T_{\bar{c}}: t + \\
& & l_{Dep}^{f,o,pas} > \\
& & |T_{\bar{c}}| - c
\end{aligned} \tag{2.28}$$

$$\begin{aligned}
& \sum_{t' \in [t + l_{Dep}^{f,o,pas} - |T_{\bar{c}}|, t + l_{Dep}^{f,o,pas} - |T_{\bar{c}}| + c - 1]} Pas_{|D|+1,t',o}^{f,Dep} & \forall c \in C, o \in \\
& \leq \sum_{o' \in O/\{o\}} \left[ (1 - \zeta_{|D|,t,o'}^{f,Dep}) E_{|D|,t,c,o'}^{f,Dep} \right] & O, f \in F, t \in \\
& + \zeta_{|D|,t,o}^{f,Dep} E_{|D|,t,c,o}^{f,Dep} & T_{\bar{c}}: t + \\
& & l_{Dep}^{f,o,pas} > \\
& & |T_{\bar{c}}| - c
\end{aligned} \tag{2.29}$$

Respectively, constraints (2.8) are substituted by expressions (2.22) and (2.23), expressions (2.9) by (2.24) and (2.25), expressions (2.10) by (2.26) and (2.27). Finally, expressions (2.11) are replaced by (2.28) and (2.29).

When constraints (2.8)-(2.11) are replaced by (2.22)-(2.29), expressions (2.30)-(2.34) are needed to ensure that the total number of passengers departing/arriving from/to each terminal at any time, does not exceed the total departure capacity of the terminal.

$$\begin{aligned}
& \sum_{o \in O} \sum_{m \in M_{f,o}^k} \sum_{t' \in [t + l_k^{f,o,pas}, t + l_k^{f,o,pas} + c - 1]} a_{d,m} x_{t',m}^f e_m \xi_m & \forall d \in D, k \\
& \leq \sum_{o \in O} E_{d,t,c,o}^{f,k} & \in \{Arr, Dep\}, c \\
& & \in C, f \in F, t \\
& & \in T_{\bar{c}}: t \\
& & + l_k^{f,o,pas} \\
& & \in [0, |T_{\bar{c}}| - c]
\end{aligned} \tag{2.30}$$

$$\begin{aligned}
& \sum_{o \in O} \sum_{m \in M_{f,o}^k} \sum_{t' \in [t + l_{Dep}^{f,o,pas} - |T_{\bar{c}}|, t + l_{Dep}^{f,o,pas} - |T_{\bar{c}}| + c - 1]} a_{d+1,m} x_{t',m}^f e_m \xi_m & \forall d \in D / \{|D|\}, c \in C, f \in F, t \in T_{\bar{c}}: t & (2.31) \\
& \leq \sum_{o \in O} E_{d,t,c,o}^{f,Dep} & + l_{Dep}^{f,o,pas} > |T_{\bar{c}}| - c
\end{aligned}$$

$$\begin{aligned}
& \sum_{o \in O} \sum_{t' \in [|T_{\bar{c}}| + t - l_{Arr}^{f,o,pas}, |T_{\bar{c}}| + t - l_{Arr}^{f,o,pas} + c - 1]} Pas_{-1,t',o}^{f,Arr} \leq \sum_{o \in O} E_{0,t,c,o}^{f,Arr} & \forall c \in C, f \in F, t \in [0, |T_{\bar{c}}| - c]: t & (2.32) \\
& & + l_{Arr}^{f,o,pas} < 0
\end{aligned}$$

$$\begin{aligned}
& \sum_{o \in O} \sum_{m \in M_{f,o}^{Arr}} \sum_{t' \in [|T_{\bar{c}}| + t - l_{Arr}^{f,o,pas}, |T_{\bar{c}}| + t - l_{Arr}^{f,o,pas} + c - 1]} a_{d-1,m} x_{t',m}^f e_m \xi_m & c \in C, d \in D / \{0\}, f \in F, t \in [0, |T_{\bar{c}}| - c]: t & (2.33) \\
& \leq \sum_{o \in O} E_{d,t,c,o}^{f,Arr} & + l_{Arr}^{f,o,pas} < 0
\end{aligned}$$

$$\begin{aligned}
& \sum_{o \in O} \sum_{t' \in [t + l_{Dep}^{f,o,pas} - |T_{\bar{c}}|, t + l_{Dep}^{f,o,pas} - |T_{\bar{c}}| + c - 1]} Pas_{|D|+1,t',o}^{f,Dep} & \forall c \in C, f \in F, t \in T_{\bar{c}}: t & (2.34) \\
& \leq \sum_{o \in O} E_{|D|,t,c,o}^{f,Dep} & + l_{Dep}^{f,o,pas} > |T_{\bar{c}}| - c
\end{aligned}$$

## 2.5 The Timing Flexibility Identifier Model (TFIM)

The solution given by the base model (expressions (2.1)-(2.6)) with dynamic apron and passenger capacity constraints (based on (2.19)-(2.34)) for all slot priorities as per sequence  $Q$ , is herein denoted by  $\tilde{x}$ . The objective values associated with  $\tilde{x}$  are represented by  $Z_i(\tilde{x}), i = 1, 2, 3$ .  $\tilde{x}$  represents a slot schedule that is drafted by the appointed slot coordinator of the airport without considering airlines' preferences. In the remainder of the document,  $\tilde{x}$  denotes the *no-TFI schedule*.

During the days following this initial slot allocation, the coordinators communicate the outcome of the initial slot schedule to the airlines. The airlines can then validate the allocation and accept it or object to it. In the latter case, the resolution of the conflict will happen in the Slot Coordination Conference (SCC) which takes place about four months prior to the start of the season's operations (IATA, 2019a). However, the acceptability of  $\tilde{x}$  can be improved by considering the airlines' scheduling flexibility preferences.

These preferences of the airlines are made voluntarily available to slot coordinators during the pre-conference period through the Timing Flexibility Identifier (TFI)(IATA, 2019a). The TFI is represented in request messages by an 8-digit format specifying the times between which offers should be accepted (e.g., 09001015 specifies a range between 09:00-10:15). This standard of information sharing is part of the current practice and is defined in the Standard Schedule Information Manual (SSIM) of IATA (see Table 2-2). TFI can be considered so as to minimise the number of requests which do not abide by the preferences of the airlines and therefore minimise the conflicts arising from the different demands of each airline.

In addition, TFI is a key policy aspect of IATA's WSG which is essential for devising detailed models for optimising airport slot allocation decisions since:

- Requests for operations that are constrained by operational factors or a curfew, should have priority over other requests where the air carrier may have operational flexibility;
- In occasions that the requested slot is not available, alternative slot offerings should be made within the TFI range as this is disclosed by airlines;

- Coordinators should consider the timing flexibility range indicated by an airline; and
- Airlines disclosing their TFI should not be placed in unfavourable conditions.

To consider TFI and airlines' preferences without putting them in unfavourable conditions, in what follows, the building blocks of a Timing Flexibility Identifier Model (TFIM) for optimising slot scheduling decisions are introduced.

### 2.5.1 Timing flexibility membership functions

The proposed model considers airlines' TFI using additional parameters denoted by  $\varphi_m^{l(u)}$ . These parameters act as soft lower (upper) flight scheduling flexibility bounds of request  $m$  where  $\varphi_m^l < 0$  ( $\varphi_m^u > 0$ ). They represent the number of intervals that request  $m$  is flexibly allowed to be displaced to an earlier (later) time interval.

Using the TFI parameters, the following membership function, and its properties (see examples below) can be used to address the policy requirements associated with the TFI. The following functions receive values based on the displacement and the flexibility parameters provided by the airline submitting request  $m$ .

$$\mu_m(\psi_{t,m}) = \begin{cases} -\frac{1}{(\varphi_m^l - 1)}\psi_{t,m} + 1, & \text{if } \psi_{t,m} \leq 0 \text{ and } \psi_{t,m} > \varphi_m^l - 1 \\ -\frac{1}{(\varphi_m^u + 1)}\psi_{t,m} + 1, & \text{if } \psi_{t,m} > 0 \text{ and } \psi_{t,m} < \varphi_m^u + 1 \\ 0, & \text{if } \psi_{t,m} \leq \varphi_m^l - 1 \text{ or } \psi_{t,m} \geq \varphi_m^u + 1 \end{cases} \quad (2.35)$$

Expression (2.35) takes value 0 when a request  $m$  is displaced outside the TFI range defined by  $\varphi_m^l$  and  $\varphi_m^u$ . When  $m$  is not displaced ( $\psi_{t,m} = 0$ ),  $\mu_m$  receives its maximum value ( $\mu_m(0) = 1$ ). For displacements within the TFI range, the

membership functions receive values  $\mu_m \in (0,1)$ . To further illustrate the properties of (2.35), an illustrative toy example is provided.

### Example 2.2

Assume that an airline has indicated that slot request  $m$  should not be displaced by more than 2 intervals earlier (earliness preference) and 3 intervals later (tardiness preference), i.e.,  $\varphi_m^l = -2$  and  $\varphi_m^u = 3$ . Therefore, the membership function of  $m$  is:

$$\mu_m(\psi_{t,m}) = \begin{cases} \frac{1}{3}\psi_{t,m} + 1, & \text{if } \psi_{t,m} \leq 0 \text{ and } \psi_{t,m} > -3 \\ -\frac{1}{4}\psi_{t,m} + 1, & \text{if } \psi_{t,m} > 0 \text{ and } \psi_{t,m} < 4 \\ 0, & \text{otherwise} \end{cases}$$

Assume now an allocation where  $m$  is allocated to time  $t'$  receiving displacement  $\psi_{t',m} = -2$ . This allocation satisfies partially the earliness preferences of the airline submitting this request since  $\mu_m(-2) = 1/3$ . In the case that  $\psi_{t',m} = 2$ , this allocation satisfies the tardiness preferences since  $\mu_m(2) = 0.5$ . When  $\psi_{t',m} = 0$ , the TFI preferences are satisfied entirely having  $\mu_m(0) = 1$ . The example provided above is further illustrated in Figure 2-4.

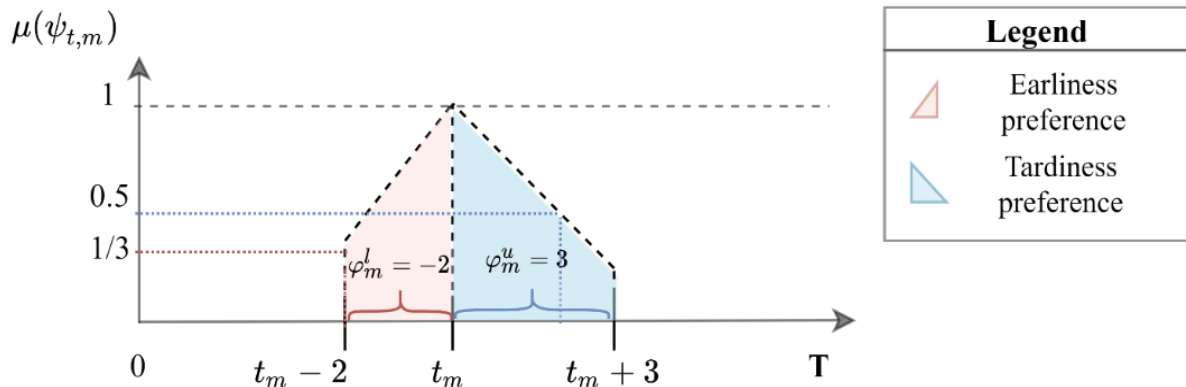


Figure 2-4: Graphical representation of Example 2.2

Another interesting aspect of the proposed membership functions is that they can be adjusted based on the available TFI information. Since it is not mandatory for airlines to disclose their TFI preferences, the proposed membership function should be able to capture occasions where the airline submitting request  $m$  does not disclose its preferences. Therefore, under this setting  $\varphi_m^l = \varphi_m^u = 0$  are substituted into (2.35) and (2.35) becomes:

$$\mu_m(\psi_{t,m}) = \begin{cases} 1, & \text{if } \psi_{t,m} = 0 \\ 0, & \text{otherwise} \end{cases}$$

Note that under this example (2.35) monitors whether request  $m$  is displaced or not. Therefore, for requests that airlines do not disclose their preferences,  $\mu_m$  becomes automatically an auxiliary expression representing whether the request is displaced or not. This property of (2.35) is rather useful since it can be used to model the absence of flexibility preferences for  $H$  or  $CH$  requests that are not willing to accept alternative slot offerings (denoted by  $L$  action code in the SSIM format). In addition, this property of (2.35) can encompass the lack of flexibility of requests that are constrained by curfews either at the origin or the destination airport.

On the other hand, requests that fall into the  $CH$  priority and are willing to accept alternative offerings (denoted by  $R$  action code in the SSIM format), should either get the requested slot or get displaced at any time between the requested or the historic slot ( $t_m^H$ ). Therefore, under this setting (2.35) may be modified and consider this setting as follows:

$$\mu_m(\psi_{t,m}) = \begin{cases} -\frac{1}{(t_m^H - t_m - 1)}\psi_{t,m} + 1, & \text{if } t_m^H - t_m \leq 0 \text{ and } \psi_{t,m} > t_m^H - t_m - 1 \\ -\frac{1}{(t_m^H - t_m + 1)}\psi_{t,m} + 1, & \text{if } t_m^H - t_m > 0 \text{ and } \psi_{t,m} < t_m^H - t_m + 1 \\ 0, & \text{otherwise} \end{cases}$$

In this case, the membership function of request  $m$  does not require the TFI parameters since it can be calculated based on the requested amendments to the historic timing of the concerned request.

## 2.5.2 Description of the TFIM

The TFIM consists of the following expressions.

$$Z = \max \sum_{f \in F} \sum_{m \in M} \sum_{t \in T_{\tilde{z}}} \left[ x_{t,m}^f \mu_m(\psi_{t,m}) \frac{e_m W_m}{\max_{\forall m \in M} \{e_m\} \max_{\forall m \in M} \{W_m\}} \right] \quad (2.36)$$

Subject to (2.1)-(2.4) and (2.7)-(2.18) and/or (2.19)-(2.34) and:

$$\sum_{f \in F} \sum_{m \in M} \sum_{t \in [t_m \pm Z_2(\tilde{x})]} x_{t,m}^f \geq (|M| - Z_1(\tilde{x})) \quad (2.37)$$

$$\sum_{f \in F} \sum_{m \in M_a} |D_m| \sum_{t \in T_{\tilde{z}}} (x_{t,m}^f |\psi_{t,m}|) \leq Z_3^\alpha(\tilde{x})(1 + tol) \quad \forall \alpha \in A \quad (2.38)$$

The objective function (2.36) of the TFIM maximises the number of slot allocations which satisfy the provided membership functions  $\mu_m(\psi_{t,m})$ . In addition, to consider the relative importance of each request based on factors that value for airport slot coordinators, expression (2.36) is weighted by the normalised passenger capacity of the aircraft (Fairbrother et al., 2019; Vossen and Ball, 2006) and the effective period of operations (number of weeks) of each request. As a result, the TFIM considers two of the additional criteria of airport slot allocation which demand that: (i) requests for operations that are effective for longer periods within the same season, should have priority; and (ii) the needs of requests serving more of the travelling public and/or shippers should be met as far as possible.

Constraints (2.37) are efficient linear expressions ensuring that the number of scheduled requests and the maximum displacement across all requests will not deteriorate after the disclosure of the TFI indicators. The joint consideration of the



maximum displacement and the number of rejected requests is ensured by requiring that the number of requests scheduled within time period  $[t_m \pm Z_2(\tilde{x})]$  will be at least equal to the number of scheduled requests in  $\tilde{x}$  (base schedule).

Similarly, constraints (2.38) ensure that the total displacement of the allocations received by each airline (as provided by the TFIM) will not be larger than a threshold given based on  $\tilde{x}$  and a tolerance parameter  $tol$ . Parameter  $tol$  represents the percentage by which the coordinator wants to increase the total displacement of each airline and receive improvements with respect to (2.36). In the case that  $tol = 0$  (like current practice), each airline's total displacement will be at most equal to the displacement that it received in  $\tilde{x}$ . Hence, in the case that  $tol = 0$ , TFIM guarantees that airlines will not deteriorate their allocations as they will receive at most the displacement that they received without disclosing their TFI.

## 2.6 Formulation strengthening

Herein a set of *valid linear inequalities* is provided. The proposed inequalities strengthen ASA formulations and improve the computational times required for their solution. The terms *valid linear inequalities/expressions* refer to linear expressions which are not violated by any feasible solution lying within the feasible space of the airport slot allocation models of sections 2.4 and 2.5. The proposed inequalities concern models which require that the turnaround time of each request is equal to the initially requested differences between the arrival and the departure. Despite being quite restrictive, this is a setting that complies with the requirements of the airlines which request their turnaround times based on cost factors (aircraft utilisation/airtime), their operating model (low cost, legacy carrier) the aircraft type and their agreements with the ground-handling agents.

Section 2.6.1 provides valid expressions when the turnaround times are required to be greater than or equal to the initially requested time difference between the arrival and the departure of a request ( $T_{min,m} = t_{md} - t_{ma} + v_m |T_{\bar{c}}|$ ). Section 2.6.2 builds on the expressions provided in section 2.6.1 and provides inequalities that strengthen slot allocation models that require the turnaround times to be equal to the initially requested time difference of a pair of requests ( $T_{min,m} = t_{md} - t_{ma} + v_m |T_{\bar{c}}| = T_{max,m}$ ).

### 2.6.1 Requests having only lower turnaround times

If a request's arrival time is displaced at a later time than the one requested ( $\psi_{t,m,Arr} \geq 0$ ), then, to maintain the minimum turnaround time at a feasible value, the departure time will have to receive equal or more tardiness. Analogously, when the departure movement of a request is displaced at an earlier time the arrival will have to receive equal or more earliness displacement. Therefore, the following expressions must be satisfied:

$$\text{if } \psi_{t,ma} \geq 0, \text{ then } \psi_{t,md} \geq 0 \text{ and if } \psi_{t,md} \leq 0, \text{ then } \psi_{t,ma} \leq 0 \quad (2.a)$$

**Remark 2.1** (2.a) is equivalent to  $\psi_{t,ma} < 0$  or  $\psi_{t,md} \geq 0$  and equivalently  $\psi_{t,md} > 0$  or  $\psi_{t,ma} \leq 0$  (2.b).

*Proof.* Let A denote that the statement  $\psi_{t,ma} \geq 0$  is true, and B denote that  $\psi_{t,md} \geq 0$ . Expression (2.a) can be restated as: *A implies B*. Then if  $\neg A$  and  $\neg B$  represent the negation of A and B, it is logical equivalent to writing *not(A and  $\neg B$ )*, i.e.m  $\neg A$  or B. Therefore, *A implies B =  $\neg A$  or B*. Therefore (2.a) is equivalent to (2.b).

As per Remark 2.1 expression (2.b) is valid since it is equivalent to (2.a). Interestingly, in contrast to expression (2.a), (2.b) can be expressed as “either-or” constraints with the use of the following linear expressions:

$$x_{t,m}^f \psi_{t,m} < |\psi_{t,m}| w_{t,ma}^+ \quad \forall m \in M_{Arr}, t \in T_{\bar{c}}, f \in F \quad (2.39)$$

$$x_{t,m}^f \psi_{t,m} \geq -|\psi_{t,m}| (1 - w_{t,ma}^+) \quad \forall m \in M_{Dep}, t \in T_{\bar{c}}, f \in F \quad (2.40)$$

$$x_{t,m}^f \psi_{t,m} > -|\psi_{t,m}| w_{t,md}^- \quad \forall m \in M_{Dep}, t \in T_{\bar{c}}, f \in F \quad (2.41)$$

$$x_{t,m}^f \psi_{t,m} \leq |\psi_{t,m}| (1 - w_{t,md}^-) \quad \forall m \in M_{Arr}, t \in T_{\bar{c}}, f \in F \quad (2.42)$$

Where  $w_{t,ma}^+, w_{t,md}^- \in \{0,1\}$ .

Please note that in expressions (2.39)-(2.42) act as auxiliary variables that help the introduction of binding conditions between the arrival and departure times of each request as per (2.b). Based on (2.39)-(2.42),  $w_{t,ma(md)}^{+(-)}$  is equal to one if the arrival (departure) movement of request  $m$  is displaced to a later (earlier) time period.

**Proposition 2.1** Constraints (2.39)-(2.42) satisfy the base model with passenger and apron constraints when the minimum turnaround times  $\forall m \in M$  are  $T_{min,m} = t_{m_{Dep}} - t_{m_{Arr}} + |T_{\bar{c}}| v_m$ .

*Proof.* Assume any feasible solution given by the base model (expressions (2.1)-(2.6)) with passenger and apron constraints. Then, each slot request may fall into the two following cases with respect to its overnight indicator ( $v_m$ ):

**Case 1:** Requests having  $v_m = 1$ .

Let  $\tau_{ma}$  be  $\sum_{f \in F} \sum_{t \in T} x_{t,ma}^f t$  and  $\tau_{md}$  be  $\sum_{f \in F} \sum_{t \in T_{\bar{c}}} (x_{t,md}^f t + |T_{\bar{c}}|)$  (i).

$\tau_{md(md)}$  can be expressed as a function of the displacement of movement  $md(md)$ , i.e.,  $t_{md(md)} + |T_{\bar{c}}| + \sum_{t \in T_{\bar{c}}} x_{t,md(md)}^f \psi_{t,md(md)}$  (ii). Since (2.4)

must hold, then  $t_{md} - t_{ma} + |T_{\bar{c}}| \leq \tau_{md} - \tau_{ma}, \forall m \in M$  (iii). By

substituting (i) and (ii) into (iii) one obtains  $\sum_{t \in T_{\bar{c}}} x_{t,ma}^f \psi_{t,ma} \leq$

$\sum_{t \in T_{\bar{c}}} x_{t,md}^f \psi_{t,md}$ .

Also, by (2.1) there will be at most a time interval  $t' \in T_{\bar{c}}: x_{t',m}^f = 1$ . Therefore,  $\psi_{t',ma} \leq \psi_{t',md}, \forall m \in M$ . Then, if the displacement of the arrival is non-negative ( $\psi_{t',ma} \geq 0$ ) then the same must happen for the departure ( $\psi_{t',md} \geq 0$ ). Similarly, if  $\psi_{t',md} \leq 0$  then  $\psi_{t',ma} \leq 0$ .

**Case 2:** Requests having  $v_m = 0$ .

Let  $\tau_{md(ma)} = \sum_{f \in F} \sum_{t \in T_{\bar{c}}} x_{t,md(ma)}^f t$  (i). In addition, similar to previous case  $\tau_{md(ma)}$  can be written as a function of the displacement as follows  $t_{md(ma)} + \sum_{t \in T_{\bar{c}}} x_{t,md(ma)}^f \psi_{t,md(ma)}$  (ii). Since (2.4) must hold, the following expression must hold  $t_{md} - t_{ma} \leq \tau_{md} - \tau_{ma}, \forall m \in M$  (iii). By substituting (i) and (ii) in (iii) it follows that the displacement of the arrival should be less than or equal to the displacement of the departure ( $\sum_{t \in T_{\bar{c}}} x_{t,ma}^f \psi_{t,ma} \leq \sum_{t \in T_{\bar{c}}} x_{t,md}^f \psi_{t,md}$ ).

Also, by (2.1) there will exist at most a time interval  $t' \in T_{\bar{c}}: x_{t',m}^f = 1$ . Therefore, the following inequality is true  $\psi_{t',ma} \leq \psi_{t',md}, \forall m \in M$ . Then obviously, if the arrival has a non-negative displacement ( $\psi_{t',ma} \geq 0$ ) the departure must also have a non-negative displacement ( $\psi_{t',md} \geq 0$ ). Similarly, if  $\psi_{t',md} \leq 0$  then  $\psi_{t',ma} \leq 0$ .

By (2.4), the arrival of a request cannot be scheduled later if its departure is displaced to an earlier time and *vice versa*. Therefore, the following expressions may be introduced.

$$w_{t,ma}^+ + w_{t,md}^- = 1 \quad \forall m \in M, t \in T_{\bar{c}} \quad (2.43)$$

**Corollary 2.1** When expressions (2.43) hold, it can be proved by substitution that expressions (2.40) and (2.42) become redundant.

*Proof.* As per (2.43),  $w_{t,ma}^+ = 1 - w_{t,md}^-$ ,  $\forall m \in M, t \in T_{\bar{c}}$  (i). Using (i) in (2.39),  $w_{t,ma}^+$  is substituted with  $1 - w_{t,md}^-$ . Hence, expression (2.39) becomes  $x_{t,ma}^f \psi_{t,ma} < |\psi_{t,ma}|(1 - w_{t,md}^-)$  and renders expression (2.42) redundant. By using (i) to substitute  $w_{t,md}^-$  in (2.41) by  $1 - w_{t,ma}^+$ , becomes  $x_{t,md}^f \psi_{t,md} > -|\psi_{t,md}|(1 - w_{t,ma}^+)$ , thus rendering expression (2.40) redundant.

## 2.6.2 Requests with lower and upper turnaround times that are equal to the requested time separation

Similar constraints may be introduced when the upper turnaround times must be the same as those requested. Tightening constraints capturing turnaround times' upper bound when those are equal to the initially requested time difference, are given in the following linear expressions.

$$x_{t,m}^f \psi_{t,m} > -|\psi_{t,m}|w_{t,ma}^- \quad \forall m \in M_{Arr}, t \in T_{\bar{c}}, f \in F \quad (2.44)$$

$$x_{t,m}^f \psi_{t,m} \leq |\psi_{t,m}|(1 - w_{t,ma}^-) \quad \forall m \in M_{Arr}, t \in T_{\bar{c}}, f \in F \quad (2.45)$$

$$x_{t,m}^f \psi_{t,m} < |\psi_{t,m}|w_{t,md}^+ \quad \forall m \in M_{Dep}, t \in T_{\bar{c}}, f \in F \quad (2.46)$$

$$x_{t,m}^f \psi_{t,m} \geq -|\psi_{t,m}|(1 - w_{t,md}^+) \quad \forall m \in M_{Dep}, t \in T_{\bar{c}}, f \in F \quad (2.47)$$

Where  $w_{t,ma}^-, w_{t,md}^+ \in \{0,1\}$

Note that in expressions (2.44)-(2.47),  $w_{t,ma}^-$  and  $w_{t,md}^+$  act as auxiliary variables that help the introduction of binding conditions between the arrival and departure times of each request as per (2.b) which is similar to (2.a). Based on (2.44)-(2.47),  $w_{t,ma}^{-(+)}$  is equal to one if the arrival (departure) movement of request  $m$  is displaced to an earlier (later) time period.

(2.44)-(2.47) may be further strengthened by setting:

$$w_{t,ma}^+ + w_{t,md}^- = 1 \quad \forall m \in M, t \in T_{\bar{c}} \quad (2.48)$$

Conditions (2.48) render constraints (2.45) and (2.47) redundant. In addition, since slot requests cannot be displaced simultaneously at a later and an earlier time, one can introduce:

$$w_{t,ma}^- + w_{t,ma}^+ = 1 \quad \forall m \in M_{Arr}, t \in T_{\bar{c}} \quad (2.49)$$

$$w_{t,md}^- + w_{t,md}^+ = 1 \quad \forall m \in M_{Dep}, t \in T_{\bar{c}} \quad (2.50)$$

**Remark 2.2** Similar to Corollary 2.1 by integrating (2.48) in (2.50) and (2.43) in (2.49) it is trivially proved that  $w_{t,md}^+ = w_{t,ma}^+$  and  $w_{t,md}^- = w_{t,ma}^-$   $\forall m \in M, t \in T_{\bar{c}}$ .

As a result, the number of auxiliary variables and constraints needed can be reduced. This is formalised in the following proposition.

**Proposition 2.2** Given expressions (2.43), Remark 2.2 and expressions (2.49) and (2.50), auxiliary variables  $w_{t,md}^-, w_{t,ma}^-, w_{t,md}^+, w_{t,ma}^+$  can be substituted by a single auxiliary variable  $w_{t,m}$ . Hence, constraints (2.39)-(2.50) can be replaced by:

$$x_{t,m}^f \psi_{t,m} < |\psi_{t,m}| w_{t,m} \quad \forall m \in M_{Arr}, t \in T_{\bar{c}}, f \in F \quad (2.51)$$

$$x_{t,m}^f \psi_{t,m} > -|\psi_{t,m}|(1 - w_{t,m}) \quad \forall m \in M_{Dep}, t \in T_{\bar{c}}, f \in F \quad (2.52)$$

$$x_{t,m}^f \psi_{t,m,Arr} > -|\psi_{t,m}|(1 - w_{t,m}) \quad \forall m \in M_{Arr}, t \in T_{\bar{c}}, f \in F \quad (2.53)$$

$$x_{t,m}^f \psi_{t,m} < |\psi_{t,m}| w_{t,m} \quad \forall m \in M_{Dep}, t \in T_{\bar{c}}, f \in F \quad (2.54)$$

*Proof.* In addition to Corollary 2.1, Using Remark 2.2 it is trivially proved that (2.47) becomes redundant. Furthermore, by using inequality (2.48) in (2.46), expression (2.45) becomes redundant. Therefore, 4 expressions suffice to represent the desired either-or conditions see (2.b) for both arrival and departure movements. Hence

$$x_{t,ma}^f \psi_{t,m} < |\psi_{t,m}| w_{t,ma}^+ \quad \forall m \in M_{Arr}, t \in T_{\bar{c}}, f \in F \quad (2.55)$$

$$x_{t,md}^f \psi_{t,m} > -|\psi_{t,m}| w_{t,md}^- \quad \forall m \in M_{Dep}, t \in T_{\bar{c}}, f \in F \quad (2.56)$$

$$x_{t,mArr}^f \psi_{t,m} > -|\psi_{t,m}| w_{t,ma}^- \quad \forall m \in M_{Arr}, t \in T_{\bar{c}}, f \in F \quad (2.57)$$

$$x_{t,mDep}^f \psi_{t,m} < |\psi_{t,m}| w_{t,md}^+ \quad \forall m \in M_{Dep}, t \in T_{\bar{c}}, f \in F \quad (2.58)$$

Based on Remark 2.2  $w_{t,ma}^+ = w_{t,md}^+ = 1 - w_{t,md}^- = 1 - w_{t,ma}^-$ . Therefore, constraints (2.55)-(2.58) can be written using a single variable ( $w_{t,m} \in \{0,1\}$ ) and can be replaced by (2.51)-(2.54).

Furthermore, the following constraints can be used to substitute (2.51)-(2.54).

$$\begin{aligned} & -\max\{|\psi_{t,ma}|, |\psi_{t,md}|\} (1 - w_{t,m}) \\ & \leq \left( \sum_{t'=t}^{\min\{t+T_{\max,m}-1, |T_{\bar{c}}|\}} x_{t',ma}^f \right) \psi_{t,ma} \quad \forall m \\ & \quad \in M_{Arr}, t \quad (2.59) \\ & \quad \in T_{\bar{c}}, f \in F \\ & + \left( \sum_{t'=\max\{t-T_{\max,m}+1, 0\}}^t x_{t',md}^f \right) \psi_{t,md} \\ & \leq \max\{|\psi_{t,ma}|, |\psi_{t,md}|\} w_{t,m} \end{aligned}$$

**Proposition 2.3** Constraints (2.59) are valid for any version of the base problem substituting expressions (2.51)-(2.54).

*Proof.* By adding (2.51) and (2.54) one obtains  $x_{t,ma}^f \psi_{t,ma} + x_{t,md}^f \psi_{t,md} < (|\psi_{t,ma}| + |\psi_{t,md}|) w_{t,m}, \forall m \in M, t \in T_{\bar{c}}, f \in F$ . However, given that  $T_{\max,m} = T_{\min,m} > 0$ , the time of the arrival cannot be the same with the time of the departure. Therefore, the maximum displacement that both legs can have during the same  $t \in T_{\bar{c}}$  will be at most  $\max\{|\psi_{t,ma}|, |\psi_{t,md}|\}$ . Hence,  $x_{t,ma}^f \psi_{t,ma} + x_{t,md}^f \psi_{t,md} \leq \max\{|\psi_{t,ma}|, |\psi_{t,md}|\} w_{t,m}$  (i). Similarly, by adding (2.53) and (2.52), it can be proved that  $x_{t,ma}^f \psi_{t,ma} + x_{t,md}^f \psi_{t,md} \geq -\max\{|\psi_{t,ma}|, |\psi_{t,md}|\} (1 - w_{t,m})$  (ii).

By using Proposition 2.2, expressions (i) and (ii) one obtains:

$$\begin{aligned}
-\max\{|\psi_{t,ma}|, |\psi_{t,md}|\}(1 - w_{t,m}) &\leq x_{t,ma}^f \psi_{t,ma} + x_{t,md}^f \psi_{t,md} \\
&\leq \max\{|\psi_{t,ma}|, |\psi_{t,md}|\} w_{t,m}, \forall m \in M, t \in T_{\bar{c}}, f \in F \text{ (iii)}
\end{aligned}$$

(iii) trivially satisfy all capacity constraints. Since the time of the arrival of each slot request  $m$  must differ from the time of the departure by  $T_{\max,m}$ ,  $\forall t \in T_{\bar{c}}$ :  $[t, t + T_{\max,m})$  or  $(t - T_{\max,m}, t]$ , only one of the arrival or the departure of  $m$  will be scheduled. Meanwhile, based on (2.1), the arrival and the departure of each  $m$  cannot be allocated to a slot more than one times. As a result, expression (iii) is transformed to (2.59).

Expressions (2.59) tighten turnaround time constraints (2.4) and eliminate fractional solutions where the displacement of two paired requests violates the initially requested difference between the arrival and the departure legs of each request  $m$ . The following example exhibits how the elimination of fractional solutions by constraints (2.59) strengthens the formulation of the base model by improving the solution to its linear relaxation.

### Example 2.3

Assume a singleton of slot requests. The request ( $m$ ) is composed by both an arrival ( $ma$ ) and a departure leg ( $md$ ) both of whom need to be scheduled for a single day that consists of ten slot scheduling intervals ( $t_1 = 1, t_2 = 2, \dots, t_9 = 9, t_{10} = 10$ ). The requested times for the arrival and the departure are  $t_1$  and  $t_5$  accordingly (turnaround time is 4 intervals). Now assume a solution to the Linear Programming (LP) relaxation of the model given by expressions (2.1)-(2.6) where for the arrival leg  $x_{t_1,ma} = 0.8$ ,  $x_{t_2,ma} = 0.1$  and  $x_{t_3,ma} = 0.1$ , and for the departure leg,  $x_{t_3,md} = 0.1$ ,  $x_{t_5,md} = 0.8$  and  $x_{t_{10},md} = 0.1$ . This solution satisfies constraints (2.1) and (2.4) (by solving for one request all capacity constraints are trivially satisfied). However, by substituting this solution into (2.59) it is obvious that it becomes infeasible.



Please note, that in larger problem instances additional fractional solutions may occur and therefore more nodes will have to be explored for solving the problem. Hence, the proposed valid expressions may reduce the number of nodes, as well as the memory requirements and computational times for reporting the optimal solution.

The following section comprises experiments demonstrating the influence of the proposed valid expressions on the computational time and complexity for solving the models of varying complexities.

### **2.6.3 Performance and impact of the proposed inequalities on linear relaxation, nodes, and computational time**

This section reports on computational experiments with respect to the application of (2.59) and their impact on the linear programming (LP) relaxation and the computational times for solving to optimality different formulations whose common modelling platform is given by the models presented in section 2.4. It is important to stress at the outset, that the goal of the experiments included in the remainder of this section, is to provide comparisons regarding the computational performance of the tightened and untightened variants of the studied formulations rather than solving the slot priorities defined in  $Q$  sequentially (further experiments on the hierarchical/sequential solution approach are given in section 2.7). Therefore, computational results are solved for all requests submitted to the airport (data presented in section 2.7.1) by comparing the influence of the proposed valid inequalities to the computational times required for solving the following models:

- The constraints of the base model (expressions (2.1)-(2.5));
- The constraints of the base model with the addition of airport specific passenger constraints;

- The constraints of the base model with the addition of airport specific apron constraints; and
- The constraints of the base model with the addition of airport specific passenger and apron constraints.

For simplicity and ease of comparisons, all modelling variants are solved by considering a single-objective expression minimising the total displacement objective across all slot requests in  $Q$ , i.e.,  $Z = \sum_{f \in F} \sum_{m \in M} |D_m| \sum_{t \in T_c} (x_{t,m}^f |\psi_{t,m}|)$ . Please note, that all displacement metrics are expressed in 15-minute time intervals and that the experimental setup is identical to the one described in section 2.7.1.

Furthermore, all variants are solved using exact turnaround time considerations (the time separation between the arrival and departure legs of each request is equal to the initially requested time difference) and compare the computational times, the number of nodes explored and the LP relaxation of the formulations when valid inequalities (2.59) are present or not. A concise summary of the results is given in Table 2-3.

The introduction of expressions (2.59) reduces the gap between the LP relaxation and the optimum objective value by 2.4% on average. The greatest improvement (3%) is observed when solving the base model with apron constraints (LP relaxation is increased from 8848.1 to 8940.43, i.e., an increase of 92.33 units of total displacement). Even though the gap between the optimal integer value and the linear relaxation remains significantly large, it is observed that small improvements regarding the LP relaxation of the models lead to improved computational times.

An interesting observation stems from the significant reduction in terms of nodes required for obtaining the optimal solutions. An average reduction in the

number of nodes of 38.2% across all examined models is observed. Interestingly, the model with apron and passenger constraints could not produce feasible solutions without the addition of tightening expressions (2.59), since it exceeded the memory of the computer used for its solution after exploring almost 19000 nodes and spending more than 9.5 hours. The addition of (2.59) limited the number of nodes to 5347 and allowed to find an optimal solution in 3.65 hours. In addition, when added to the model with passenger constraints, constraints (2.59) reduced the number of nodes and the computational time required (by 16.7% and 37.3% respectively). For the base model and its variant with apron constraints the conducted experiments report reduced nodes (24.9% respectively) but increased computational times (7.8%).

Simultaneous consideration of all requests in $Q$		Turnaround time setting			
		$T_{min,m} = t_{md} - t_{ma} +  T_c v_m = T_{max,m}$			
		LP relaxation	$Z_3^*$	Nodes	Solution times (s)
Model	Base (expressions (2.1)-(2.5))	<b>8613.12</b> <i>(8519.77)</i>	11972	<b>2247</b> <i>(3723)</i>	2056.6 <i>(2052.4)</i>
	Base + Apron constraints (expressions (2.1)-(2.5)+ (2.19))	<b>8940.43</b> <i>(8848.1)</i>	11972	<b>3927</b> <i>(5231)</i>	3675 <i>(3409.9)</i>
	Base + Passenger constraints (expressions (2.1)-(2.5)+ (2.20)-(2.34))	<b>9020.44</b> <i>(8961.5)</i>	12308	<b>4419</b> <i>(5303)</i>	<b>9050.9</b> <i>(14440.2)</i>
	Base + Apron & Passenger constraints (expressions (2.1)-(2.5)+ (2.19)-(2.34))	<b>9195.17</b> <i>(9135.26)</i>	<b>12308</b> <i>(-)</i>	<b>5347</b> <i>(&gt;18919)</i>	<b>13149.2</b> <i>(&gt;34464)</i>

**Notes:** In parentheses and italics are the results from the untightened variants of the models: tightened (untightened), if not reported the metrics are identical;  $Z_3^*$ : value of the total displacement objective after solving the MIP to optimality. **bold** font denotes occasions where the models tightened by the considered valid expressions resulted in improvements; ‘>’ denotes a memory error that did not allow the solution of the instance to optimality.

**Table 2-3:** Computational performance of expressions (2.59)

Further insights on the influence of (2.59) on the solution of the different models can be extracted by observing Figure 2-5. The performance profiles reveal that the tightened formulations demand more time in order to start exploring nodes. However, in doing so they benefit from tighter bounds occurring from the improved LP relaxation and the reduced feasible space. Moreover, for the standard versions of the models that solved to optimality (subplots a, b, and c), a large

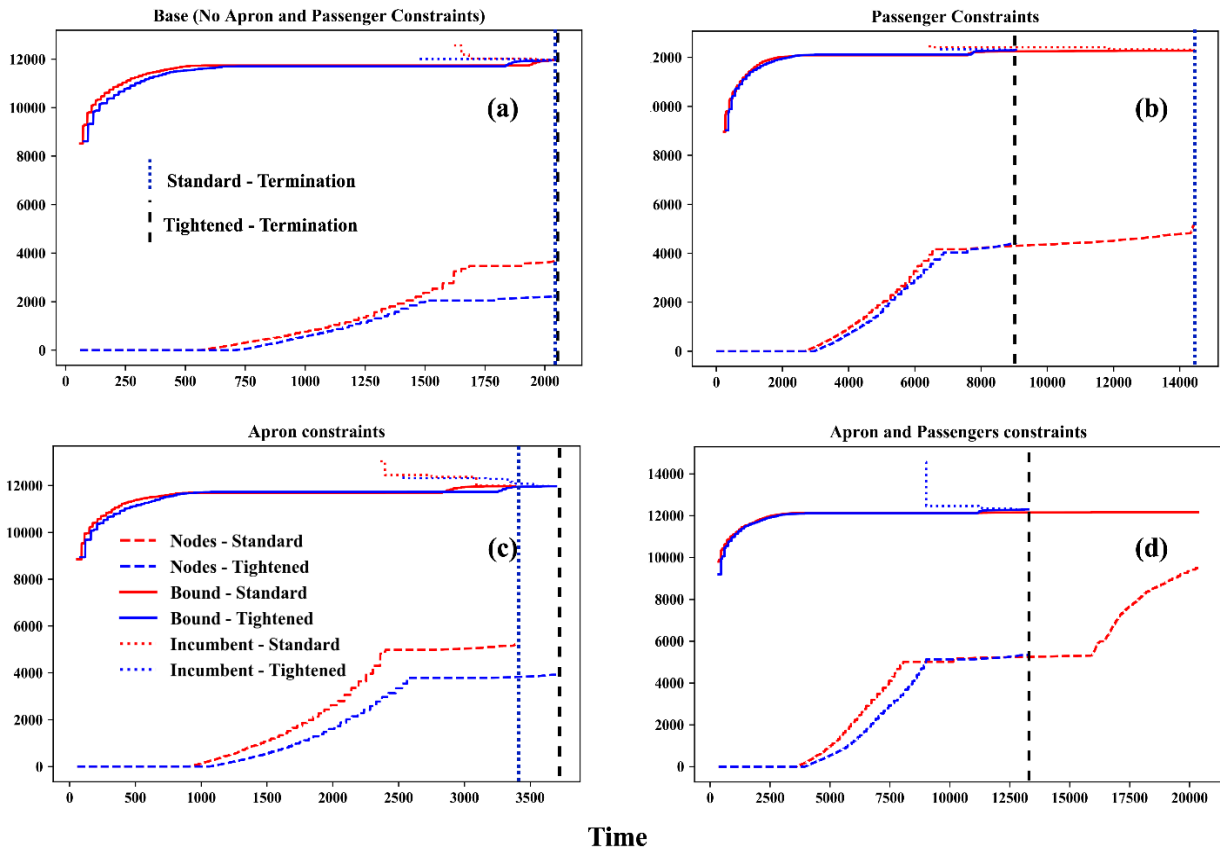


**Figure 2-5:** Performance profile of the different models and comparison when tightened by expressions (2.59)

increase in the numbers of explored nodes after finding an initial feasible solution (incumbent) is reported.

On the other hand, under the tightened formulations, the improved quality of the initial solutions rendered most of the unexplored nodes redundant, thus limiting the number of nodes required in order to converge to an optimal solution.

Hence, in all subplots of Figure 2-5, it is observed that the tightened versions of the considered models demanded less than 500 nodes in order to find the optimal solution after reporting the initial incumbent solution, while the untightened variants that managed to yield optimal solutions required the exploration of up to 1250 nodes in order to prove optimality. Another interesting aspect of the tightened variants is that for the base model and its variant with passenger constraints, the initial incumbent solution was also the optimal solution (subplots (a) and (b)).

## 2.7 A computational study

The application of the proposed modelling and solution framework to a real-world coordinated airport provides valuable insights regarding the impact of TFI considerations on the allocation of the slot requests of each airline, slot priority or the airport slot schedule.

It is important to underline that the goal of the computational analyses that follow is to demonstrate how the methodological contributions of this chapter improve the ASA process. Detailed comparative analyses between the solutions of the two stages of the TFIM may allow the interested stakeholders, i.e., coordinators, airport authorities and airlines to study how the outcome of the airport slot coordination changes after the disclosure of the airlines' operational and flexibility preferences. In addition, the following subsections comprise results of computational experiments that demonstrate the improved capacity utilisation that is enabled by the addition of the dynamic capacity constraints of section 2.4.3.

Hence, the goal of the following sections is to examine how the proposed concepts and solution framework, improve ASA decisions, catalyse, and inform discussions among the interested stakeholders; and therefore, reduce their conflicts before, during and after the SCC. The comparative presentation of the results at the airport-wide, priority-wide and individual airline levels informs and supports

negotiations, and improves the transparency of the resulting slot scheduling decisions (Zografos and Jiang, 2019).

In what follows the section presents the problem data and the experimental setup (section 2.7.1) as well as comprehensive computational experiments (section 2.7.2).

### 2.7.1 Data and experimental setup

Our approach is tested on data obtained from a coordinated regional European airport. The capacity parameters of the airport regarding its runways, apron, and passenger terminals, are expressed in 15-minute, 30-minute and 60-minute time intervals. Hence, day of the scheduling season is discretised using 15-minute coordination intervals, since  $\tilde{c} = \min\{15, 30, 60\} = 15$ . The studied airport consists of one terminal ( $|F| = 1$ ). The capacity parameters of the airport are presented in the following table (Table 2-4). In addition, the airport declared capacity parameters include capacity specifications with respect to the configuration of the passenger terminal and the use of the apron stands.

Resource (model parameter)	Movement( $k$ ) and/or Type( $r, o$ )	Capacity time intervals ( $C$ )		
		15 min (1 interval)	30 min (2 intervals)	60 min (4 intervals)
Runways ( $u_{d,t,c}^k$ )	Arrivals	-	-	8
	Departures	-	-	12
	Total	5	-	20
Passenger Terminal ( $E_{d,t,c,o}^{f,k}$ )	Arrivals (S/NS)	-	1150	2300 (1470/830)
	Departures (S/NS)	-	1150	2300 (1470/830)
	Total	-	-	-
Aprons ( $\pi_{t,d,f,r}$ )	Light	8	-	-
	Medium	3(2)	-	-
	Heavy	2(3)	-	-
<b>Notes</b>	S: <i>Schengen and Domestic</i> ; NS: <i>Non-Schengen</i> ; Apron capacity is expressed based on IATA's aircraft wake category ( <i>Light (H)</i> / <i>Medium (M)</i> / <i>Heavy (H)</i> ).			

**Table 2-4:** Airport capacity parameters

Firstly, the declared capacity of the considered instance indicates that in the exclusive presence of flights same category only (e.g., exclusively Schengen), then the full arrival or departure capacity can be used to accommodate the flights of this category. In addition, it is a-priori known that the airport has a MARS (Multiple Apron Ramp System) apron (WWACG, 2019). Hence, an additional heavy aircraft may be parked (further to the two apron stands already available for this category) by using one of the apron stands designated for medium aircraft (by reducing the available stands for medium aircraft from 3 to 2).

Modelling of this demand-based capability of the airport's apron system, provides 27 additional feasible cases/combinations of apron capacity utilisation (see Figure 2-10 in section 2.7.2.4). Therefore, there is need to make use of the airport-specific constraints presented in section 2.4.3. In order to illustrate how (2.19) are adapted to the capacity specification of the studied airport (since,  $CA_1^{Heavy,Medium} = 1/CA_1^{Medium,Heavy} = 1$ ), expressions (2.18) and (2.19) provide their instantiation for heavy and medium aircraft:

$$\pi_{t,d,f,Heavy} \leq 3 \quad \forall d \in D, t \in T_{\bar{c}}, f \in F \quad (2.60)$$

$$\pi_{t,d,f,Heavy} \leq 2 + (3 - \pi_{t,d,f,Medium}) \quad \forall d \in D, t \in T_{\bar{c}}, f \in F \quad (2.61)$$

$$\pi_{t,d,f,Medium} \leq (2 - \pi_{t,d,f,Heavy}) + 3 \quad \forall d \in D, t \in T_{\bar{c}}, f \in F \quad (2.62)$$

The second dataset that is required to carry out the initial slot allocation, is the set of slot requests submitted by the airlines ( $M$ ). In this case, a total of 80 airlines ( $A = \{A1, \dots, A80\}$ ) submitted a total of 1057 paired requests composed by an arrival and departure movement (2114 single-movement request series). Please note that for all request priorities only requests for single period operations ( $p_{SP}$ ) are present. The absence of year-round requests is justified by the fact that the airport under consideration is only coordinated during the summer scheduling

season. As a result, there are 9 distinct priorities in  $Q$  which have to be allocated hierarchically according to the following sequence:

$$Q = \{PSO_{SP}^\sigma, H_{SP}^\sigma, CH_{SP}^\sigma, NE_{SP}^\sigma, O_{SP}^\sigma, H_{SP}^h, CH_{SP}^h, NE_{SP}^h, O_{SP}^h\}$$

On another note, requests with public service obligations ( $PSO$ ) represent under 5% of the individual slot requests submitted to the airport. However, since the slot coordination process has to abide by European regulations (Council Regulation (EEC) No 95/93, 1993; European Commission, 2018),  $PSO$  routes have to be considered explicitly.

Parameter	Description	Value/Assumption
$T_{max,m}, T_{min,m}$	Turnaround times	$T_{min,m} = t_{md} - t_{ma} + v_m  T_{\bar{c}}  = T_{max,m}$
$l_k^{1,apr}, l_k^{1,o,pas}$	Time-difference (lag) parameters for apron and passenger capacity constraints	$l_{Arr}^{1,apr} = -1, l_{Arr}^{1,apr} = 2,$ $l_{Arr}^{1,Schengen,pas} = l_{Arr}^{1,apr} - 1, l_{Arr}^{1,Non-Schengen,pas} = l_{Arr}^{1,apr} - 2,$ $l_{Dep}^{1,Schengen,pas} = l_{Dep}^{1,apr} + 3, l_{Dep}^{1,Non-Schengen,pas} = l_{Arr}^{1,apr} + 8$
$Q$	Sequence used for the hierarchical allocation of the requests	$\{PSO_{SP}^\sigma, H_{SP}^\sigma, CH_{SP}^\sigma, NE_{SP}^\sigma, O_{SP}^\sigma, H_{SP}^h, CH_{SP}^h, NE_{SP}^h, O_{SP}^h\}$
$\xi_m$	Load factor (%)	$\xi_{ma} = \xi_{md} = 0.8 \forall m \in M$
$tol$	Percentage of tolerance towards increases to the total displacement of each airline	$tol = 0$
$\varphi_m^{l(u)}$	Timing flexibility bounds	$\varphi_m^{l(u)} = 0 \forall m \in \cup M_{PSO}, M_H, M_{CH};$ $\varphi_{ma}^u = \varphi_{md}^u = -\varphi_{ma}^l = -\varphi_{md}^l = 4 \forall m \in M_{NE};$ $\varphi_{ma}^u = \varphi_{md}^u = -\varphi_{ma}^l = -\varphi_{md}^l \sim Uniform \in \{1, \dots, 8\} \forall m \in M_O$

**Table 2-5:** Parameters used in the experiments

Computational experiments are set using the parameters presented in Table 2-5. Turnaround times are constrained to be equal to the ones requested by the airlines so as to accommodate their operational needs and avoid unnecessary use of



apron capacity. Therefore, expressions (2.59) are added to tighten the model. Since airport slot scheduling is a strategic problem solved many months in advance, the lag parameters can only rely on historical data or coordinators' experience and depend on the airport under consideration. Hence, the lag parameters for the apron and passenger capacity constraints are decided based on the logic presented in the first example (see Figure 2-3).

The described data and experimental setup are used to test the proposed models and solution approach. For all results presented in the remainder of the chapter, Gurobi 8.1 is the selected mathematical programming solver (Gurobi Optimization, 2018). All MIP models are solved to optimality the standard settings of the solver (optimality gap less than  $1e-4$ ). The models and solution approach are implemented using version 3.7 of the Python programming language (Rossum, 1995) running on the Anaconda distribution. All computational experiments are carried out on a laptop with a 1.9-GHz Intel® i7-8650U central processing unit and 31.8 GB of RAM.

## 2.7.2 Computational results

This section consists of 6 subsections. Section 2.7.2.1 compares the TFI and the no-TFI schedules and demonstrates the benefits of the proposed framework for the airport slot schedule as a whole. Section 2.7.2.2 dives deeper and analyses the benefits of the proposed approach for each slot scheduling priority. A disaggregate analysis studying the effect of the proposed framework on each airline's objectives is presented in 2.7.2.3. Section 2.7.2.4, studies the impact of the dynamic capacity constraints in separation to the TFI and tests their performance under alternative passenger capacity scenarios. 2.7.2.5 demonstrates the synergies between the TFI and the dynamic capacity constraints. This is achieved by conducting a comparative analysis of multiple alternative modelling considerations by pivoting

on the application of the TFI and the dynamic capacity constraints. Finally, section 2.7.2.6 includes computational results that test alternative slot prioritisation scenarios, thus studying the implications of the policy constraints that are introduced in this chapter and are active in the studied airport.

### 2.7.2.1 Comparison between the TFI and the no-TFI schedules

This section compares the performance of the no-TFI slot schedule obtained after solving the first stage of the solution approach ( $\tilde{x}$ ) and the *TFI schedule* (solution obtained after solving the TFIM denoted by  $\hat{x}$ ). The motivation here is to demonstrate the potential improvement in terms of several schedule quality metrics after solving the TFIM. The design of the TFIM guarantees that the alternative allocations given after the consideration of TFI will be at most weakly dominated (since the total displacement of each airline is less than or equal to the displacement obtained at the base schedule).

In addition, based on (2.37) and (2.38) the resulting allocation will lead to better or equal values for total and maximum displacement in relation to the base schedule. The no-TFI schedule is obtained after 3173.9 seconds (53 minutes) of solution time and the TFI schedule after 20064.6 seconds, i.e., 5.57 hours (total computational time required for  $\hat{x}$  was 23238.5 seconds). As a result, the total computational time required for running the solution approach presented in Figure 2-2 was under 6.5 hours. The resulting computational time although significant, is not prohibitive given the strategic nature of these decisions, their frequency (twice a year) and the time available to make them (3 weeks) (see Figure 2-1) (IATA, 2019a). The comparison of the two schedules is facilitated by the following schedule quality metrics:

- Rejected slot requests (Ribeiro et al., 2018, 2019b):

$$Z_{1,q}(x) = |M_q| - \sum_{f \in F} \sum_{m \in M_q} \sum_{t \in T_c} x_{t,m}^f$$

- Maximum displacement (Jacquillat and Odoni, 2015; Pyrgiotis and Odoni, 2015; Zografos et al., 2017a; Jacquillat and Vaze, 2018; Ribeiro et al., 2018, 2019b):

$$Z_{2,q}(x) = \max_{\forall m \in M_q} \{|\psi_{t,m}| x_{t,m}^f\}$$

- Total displacement (Zografos et al., 2012; Jacquillat and Odoni, 2015; Pyrgiotis and Odoni, 2015; Ribeiro et al., 2018; Zografos et al., 2017a; Jacquillat and Vaze, 2018; Zografos and Jiang, 2019; Ribeiro et al., 2019b; Fairbrother et al., 2019):

$$Z_{3,q}(x) = \sum_{f \in F} \sum_{m \in M_q} |D_m| \sum_{t \in T_c} (x_{t,m}^f |\psi_{t,m}|)$$

- Number of displaced slot requests (Ribeiro et al., 2018, 2019b):

$$Z_{4,q}(x) = \sum_{f \in F} \sum_{t \in T_c} \sum_{m \in M_q: |\psi_{t,m}| > 0} x_{t,m}^f$$

- Average displacement per displaced request:

$$Z_{5,q}(x) = \frac{Z_{3,q}(x)}{\max\{Z_{4,q}(x), 1\}}$$

- Number of displaced passengers:

$$Z_{6,q}(x) = \sum_{f \in F} \sum_{t \in T_c} \sum_{m \in M_q: |\psi_{t,m}| > 0} x_{t,m}^f e_m \xi_m$$

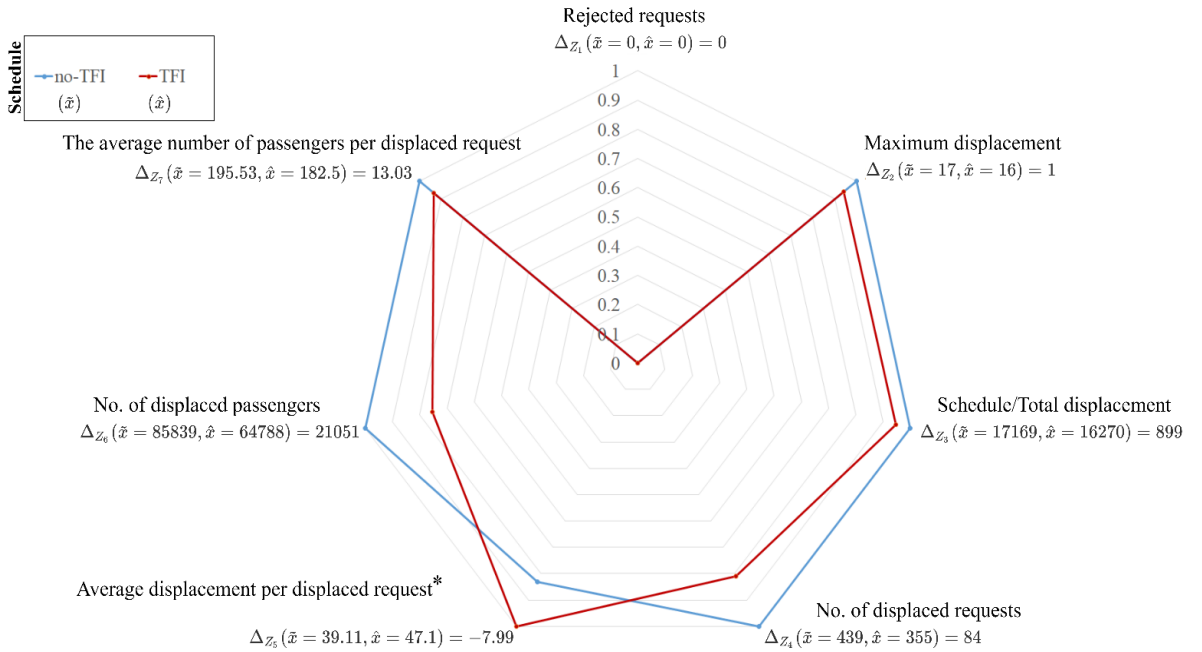
- Average number of displaced passengers per displaced request:

$$Z_{7,q}(x) = \frac{Z_{6,q}(x)}{\max\{Z_{4,q}(x), 1\}}$$

Herein, passenger related metrics are introduced as a proxy of passengers' welfare, since airlines requesting slot timings optimise their operations so as to satisfy passenger demand as accurately as they can based on demand forecasting

estimates (Vaze and Barnhart, 2012). Therefore, less displaced passengers may signify a better satisfaction of passenger demand. Following the definition of the comparison metrics that will be used,  $\Delta_{Z_i}(\tilde{x}, \hat{x}) = Z_i(\tilde{x}) - Z_i(\hat{x}) \forall i = 1, \dots, 7$  denotes the difference between quality metric  $Z_i$  of the no-TFI and the TFI schedule. The results of this high-level comparison are illustrated in Figure 2-6.

An initial observation is that both schedules resulted in no slot rejections. That is because the capacity of the airport during off-peak times can accommodate displaced requests from time periods that demand exceeds supply. Similar observations were reported by Ribeiro et al. (2018) regarding this objective. In addition, regarding the maximum displacement objective, the TFI schedule reports an improvement of 5.88% ( $Z_2(\hat{x}) = 16$ ) in comparison to the no-TFI schedule ( $Z_2(\tilde{x}) = 17$ ).



**Note:** \*increases with respect to this metric denote simultaneous improvements concerning the number of displaced requests, and the schedule displacement

**Figure 2-6:** Radar plot comparing the no-TFI and the TFI schedule

Similar observations are extracted for all the remaining comparison metrics since the TFI schedule reports reduced total displacement (5.5%), number of

displaced slot requests (19.1%) and passengers (24.5%) in comparison to the no-TFI schedule. From the passengers' perspective, one notes a significant improvement, since more than 21 thousand passengers will be allocated to the times requested.

However, based on the average displacement per displaced request ( $Z_5(x)$ ), the TFI schedule is worse by almost 8 x 15-minute time-intervals (20.4%) of total displacement per displaced request. That is because the rate of change in the number of displaced requests (a reduction exceeding 19%) is greater than the improvement (reduced by 6%) of the total displacement objective (the same observation holds for Figure 2-12). Finally, the average number of passengers displaced per displaced request dropped by an average of 6.6% (more than 13 passengers per displaced request).

### **2.7.2.2 Impact of scheduling flexibility preferences on slot priorities' objective values**

Another interesting analysis that can facilitate discussions among the interested stakeholders, is the presentation of the results for each priority level (see Table 2-6). The slot request priorities are essential to the slot coordination process and therefore the aforementioned objectives will have to be compared for each priority considered in  $Q$ . In this section, for simplicity  $Z_1(x)$  is omitted since its reported value is 0 (no rejected requests) and remained unchanged after the solution of the TFIM.

By comparing the two schedules at each priority level Table 2-6, one observes that the TFIM results in deteriorated allocations for priorities with historical usage rights, i.e.,  $H$  and  $CH$ , especially when the requests have an effective period greater than four weeks ( $\sigma_m = 1$ ). As reported in Table 2-6,  $PSO$ ,  $CH$  and  $H$  requests with  $\sigma_m = 1$  receive significant increases in terms of all reported

measures. On the other hand, requests considered as ad-hoc operations ( $h_m = 1$ ) receive more favourable slot allocations. The improvement reported at the airport-wide level, is mainly attributed to the significant reduction of the reported metrics at the others' level. The improvements in terms of total displacement and displaced passengers experienced at the others' ( $O$ ) level, are by far greater than the deterioration of the metrics faced by the  $H$  and  $CH$  levels.

By considering that the total displacement of each airline at the TFI schedule is less than or equal to the one obtained by the no-TFI schedule (as per constraints (2.38)), it is concluded that airlines introducing their TFI preferences, may accept compromises at the allocation of their requests falling into the higher levels of the slot scheduling hierarchy and obtain a better overall slot scheduling outcome for their slot request portfolio.

Even though the objectives of the upper slot priorities are compromised after the solution of the TFIM, all airlines experience the same or even improved slot allocations with respect to the total displacement that they receive. However, the final decision regarding the acceptability of the TFI schedule depends on the preferences of each airline and the slot coordinators regarding the schedule quality metrics observed for each slot request priority. A more detailed analysis on the outcome of TFIM model for each airline is provided in the following section.

$q \in Q$		Comparison metrics						No. of Requests
Priority ( $p$ )	Series Yes/No	$Z_2(x)$	$Z_3(x)$	$Z_4(x)$	$Z_5(x)$	$Z_6(x)$	$Z_7(x)$	
CH	Yes	<b>4</b> , 15	<b>589</b> , 2633	<b>27</b> , 35	<b>21.8</b> , 75.28	<b>5559</b> , 6972	205.9, <b>199.2</b>	182
	No	4, <b>3</b>	<b>63</b> , 19	31, <b>9</b>	<b>2</b> , 2.1	8804, <b>1605</b>	284, <b>178.3</b>	53
H	Yes	<b>0</b> , 12	<b>0</b> , 1565	<b>0</b> , 12	<b>0</b> , 130.41	<b>0</b> , 2144	<b>0</b> , 178.7	129
	No	<b>6</b> , <b>6</b>	13, <b>11</b>	4, <b>2</b>	<b>3.2</b> , 5.5	802, <b>354</b>	200.5, <b>177</b>	10
NE	Yes	<b>2</b> , 3	<b>727</b> , 779	<b>9</b> , <b>9</b>	<b>80.8</b> , 86.6	<b>1510</b> , <b>1510</b>	<b>164.8</b> , 167.8	32
	No	<b>0</b> , <b>0</b>	<b>0</b> , <b>0</b>	<b>0</b> , <b>0</b>	<b>0</b> , <b>0</b>	<b>0</b> , <b>0</b>	<b>0</b> , <b>0</b>	6
O	Yes	17, <b>16</b>	15383, <b>10775</b>	223, <b>179</b>	69, <b>60.2</b>	40473, <b>31619</b>	181.8, <b>176.5</b>	299
	No	<b>13</b> , 16	394, <b>338</b>	145, <b>106</b>	2.7, <b>3.2</b>	28691, <b>20462</b>	197.9, <b>193</b>	336
PSO	Yes	<b>0</b> , 1	<b>0</b> , 150	<b>0</b> , 3	<b>0</b> , 50	<b>0</b> , 122	<b>0</b> , 40.67	10
	No	-	-	-	-	-	-	0
Notes	The content of each cell is tabulated based on the following format: $Z_{q,i}(\tilde{x})$ , $Z_{q,i}(\hat{x})$ ; the metrics that outperform their counterparts are highlighted in <b>bold</b> ; Maximum displacement: $Z_2(x)$ ; Total displacement: $Z_3(x)$ ; Number of displaced slot requests: $Z_4(x)$ ; Average displacement per displaced request: $Z_5(x)$ ; Number of displaced passengers: $Z_6(x)$ ; Average number of displaced passengers per displaced request: $Z_7(x)$ .							

**Table 2-6:** Comparison of the no-TFI and TFI schedules for each slot priority

### 2.7.2.3 Impact of timing flexibility preferences on airlines' objectives

Despite compromising the objectives of the upper slot scheduling hierarchies, the TFIM results in improved or unchanged total displacement for all airlines, thus providing substantial incentives for considering TFI preferences during the initial slot allocation. Out of the 80 airlines that submitted slot requests, the schedules of 33 of them were altered after the solution of the TFIM. The schedules of 47 airlines remained unchanged after the provision of the TFI schedule.

To provide more insights on the influence of the TFI considerations to the slot schedules of these 33 airlines, the section includes a combined bar chart – data table (Figure 2-7) which explores the distribution of the gains and losses of each airline after the solution of the TFIM with respect to various schedule quality metrics. For each airline ( $a$ ) tabulates as a row, the columns of Figure 2-7 contain the difference between the observed values of each quality metric ( $Z_i$ ) of the no-TFI ( $\tilde{x}$ ) and the TFI schedule ( $\hat{x}$ ) such that  $\Delta_{Z_{\alpha,i}}(\tilde{x}, \hat{x}) = Z_{\alpha,i}(\tilde{x}) - Z_{\alpha,i}(\hat{x}) \forall i = 3, \dots, 7$ . Therefore, positive observations (blue bars) signify improvements (decreases) after the solution of the TFIM. Respectively, negative observations (red bars) denote deteriorations (increases) after the solution of the TFIM.

The requests of the airlines that are influenced by the disclosure of the TFI correspond to the 76.7% of the total requests submitted to the airport. On average, the only tabulated measure that increased after the disclosure of the TFI preferences is the maximum displacement. On the other hand, for all other measures, the TFIM yields improved values. As expected, due to the design of the TFIM, the total displacement of each airline  $Z_{a,3}(\hat{x})$  remains equal or improves compared to the no-TFI schedule  $Z_{a,3}(\tilde{x})$ . Interestingly, the airlines that are influenced by the TFIM are airlines whose requests fall into multiple slot request



priorities. In particular, most airlines have submitted requests both of higher (*PSO*, *H* or *CH*) and lower priorities (*O* or ad-hoc requests).

<i>A</i>	<i>M</i>	Comparison metrics					
		Maximum Displacement	Total Displacement	Displaced Requests	Number of displaced passengers	Average displacement per displaced request	Average number of passengers per displaced
A10	28	0	4	-2	-388	3.38	5.57
A11	4	0	4	2	324	-0.34	0.47
A14	98	-1	1	11	2464	-3.00	0.00
A17	6	1	35	4	1078	-28.48	21.47
A18	32	2	16	12	1476	1.33	123.00
A19	132	1	8	2	290	-5.16	0.00
A24	48	-2	26	38	11760	-10.63	39.10
A29	2	-1	18	-1	-167	16.58	0.00
A31	8	-1	74	-2	-360	40.33	0.00
A32	2	-1	68	4	720	-12.88	0.00
A33	20	-1	0	1	148	-1.16	0.00
A34	12	1	55	2	322	-3.40	0.00
A36	4	-2	0	2	378	-7.17	0.00
A37	16	-2	25	-2	-360	40.71	0.00
A39	36	0	42	-3	-558	18.88	0.00
A4	32	-3	12	2	360	-5.00	0.00
A43	6	1	18	2	296	9.00	148.00
A48	28	-4	0	0	18	0.00	1.13
A49	2	0	12	-2	-470	2.55	0.07
A50	2	-7	27	2	424	-7.77	10.67
A51	12	0	0	-2	-336	7.43	0.00
A53	18	1	43	-1	-189	89.33	-13.67
A58	6	-4	2	12	2532	-25.00	0.00
A59	2	0	30	-3	-26	20.94	23.78
A6	2	0	21	-1	-144	21.50	2.67
A60	2	-2	2	0	0	1.00	0.00
A61	50	-1	8	0	0	1.14	0.00
A62	62	-2	0	0	90	0.00	6.58
A63	30	0	28	6	806	-2.11	-12.22
A64	22	1	104	0	0	52.00	0.00
A66	120	-7	12	-3	-369	8.04	7.56
A72	4	1	202	4	932	3.75	0.00
A8	6	-4	2	0	0	0.14	0.00
<b>Mean</b>	<b>25.88</b>	<b>-1.09</b>	<b>27.24</b>	<b>2.55</b>	<b>637.91</b>	<b>6.85</b>	<b>11.04</b>

**Figure 2-7:** *Distribution of the gains/losses per airline and objective*

The remaining 47 airlines whose schedules remained unchanged after the TFIM, are airlines that submitted requests which fell into a single priority, e.g., only *H* requests characterised as series-of-slots. This observation is justified by the fact that when an airline submits requests falling into a single slot request priority,

the trade-offs among its requests are constrained by the TFIM and become less intense.

Regarding the reported metrics, the total displacement improves by more than 27 units per airline on average. This is justified by the design of the mechanism which does not allow deteriorations regarding this metric. The only reported metric that deteriorated was the maximum displacement, which increased by one unit per airline on average. However, only two airlines (*A50* and *A66*) received increases surpassing the one hour (4 x 15-minute time intervals) and 15 out of the 33 airlines received better or equal maximum displacement to the no-TFI schedule. On the contrary, the number of displaced requests is improved or remained unchanged for most airlines (22 out of 33). The maximum gain observed for this metric is for airline *A24* who received 38 less displaced requests. The largest reported loss across all airlines is just 3 displaced requests and is received by 3 airlines (*A66*, *A59*, *A39*).

Similar trends are reported for the number of displaced passengers ( $Z_{a,6}(x)$ ) where maximum gain is reported for *A24* receiving 11760 fewer displaced passengers. The largest loss is disproportionally smaller resulting in an increase of just 558 passengers for *A39*. In addition, one observes that the average displacement per displaced request is on average improved by almost 6.85 15-minute intervals per airline. 13 airlines experience deteriorations regarding this metric. However, for these 13 airlines the reduction in terms of the number of displaced requests was disproportionally larger than the reduction in terms of total displacement and therefore more displacement is allocated to each displaced request. Concerning the average number of passengers per displaced request, only two airlines received increases (*A53*, *A63*), while on average each airline receive a reduction of 11 passengers per displaced request.

As suggested by Zografos and Jiang (2019), the discussion on individual airlines' schedules enables to study the effect of the TFIM on each airline's request portfolio. For example, airline *A50* received a large deterioration with respect to its maximum displacement since two *H* (historic) requests carrying less passengers received greater displacements so as to accommodate *O* requests of the same airline which concerned more passengers. Similar observations are extracted for *A66* which also received a deterioration of 7x15-minute time-intervals to its maximum displacement. In particular, the *O* requests submitted as series of slots received improved allocations at the expense of *H* and ad-hoc *O* requests. Interestingly, airlines that received deteriorations at their number of displaced requests (e.g., *A51, A10, A66, A48, A39*) have also submitted ad-hoc requests. Comparisons of higher resolution can be obtained by Figure 2-8 and Figure 2-9 which illustrate the trade-offs among the requests submitted by the same airline.

Up to this point, there is no discussion regarding the displacement allocated to each airline in the no-TFI schedule, and how this is internalised and reallocated in the TFI schedule. The disclosure of the TFI from airlines submitting multiple requests that fall into different priorities in *Q*, may result in compromises on the objectives of some of the airlines' requests to favour their overall request portfolio. Such compromises are mainly attributed to requests that fall into the upper hierarchies of the slot scheduling hierarchy (*Q*). The presented figures (Figure 2-8 and Figure 2-9) shed light on the compromises and the gains experienced by the requests of each airline within each slot hierarchy and allows the study of the influence of the TFI on the request portfolio submitted by each airline. In both figures, data points on the right hand side of the *x-axis* are the ones who benefit in terms of total and maximum displacement (Figure 2-8 and Figure 2-9) respectively, while the left hand side includes airlines' requests in slot priorities whose objectives

became worse. On both occasions it is observed that the TFIM benefits requests of priority  $O$  ('others' priority) at the expense of the  $H$  and  $CH$  levels.

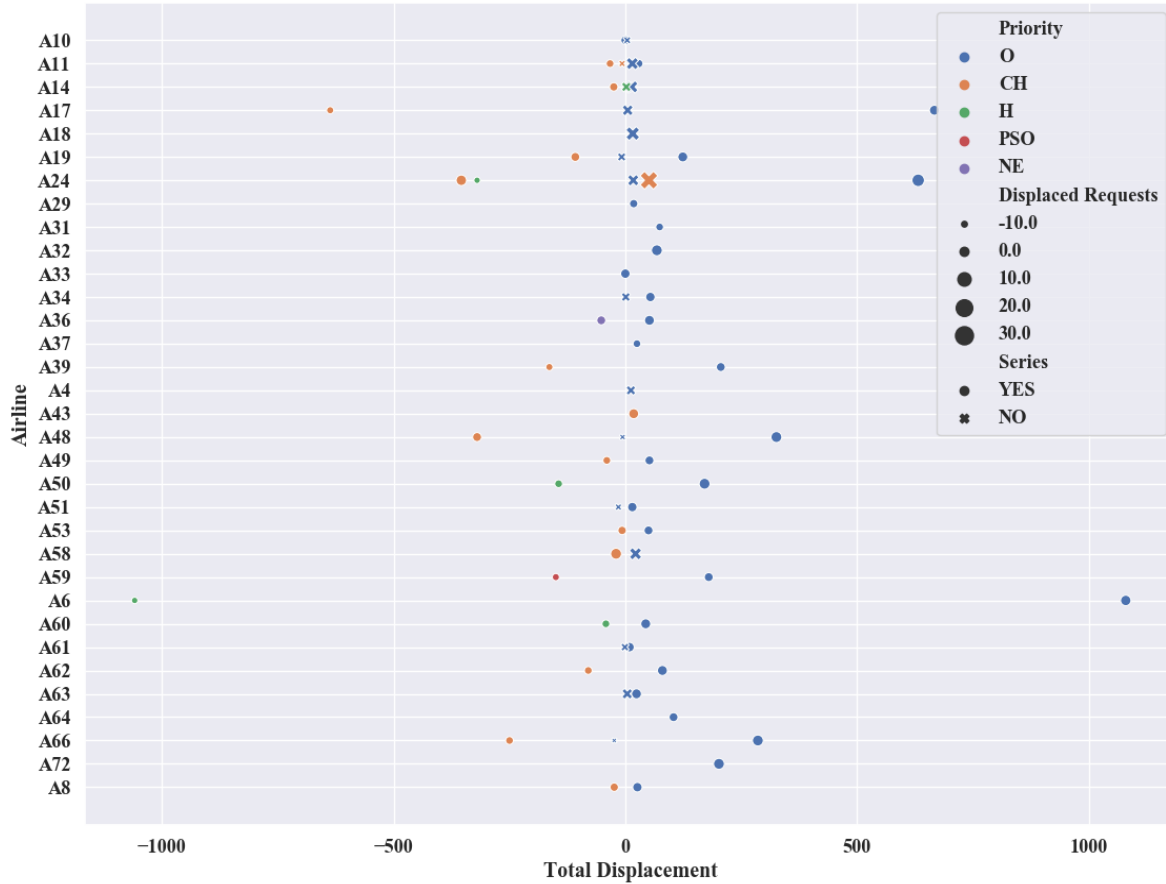


**Figure 2-8:** *Distribution of total displacement and the number of displaced requests per airline and request priority*

In particular, the total displacement of each airline is re-allocated by reducing the number of displaced requests and passengers at the expense of increased maximum displacement for their requests with historical rights and public service obligations. However, most airlines (28 out of 33) do not receive deteriorations of maximum displacement which are larger than 5 time-intervals. Airlines submitting only  $O$  requests (e.g., A66, A64) received improved allocations for all their requests with respect to all discussed metrics. This is explained by the fact that within the slot request portfolio of each airline there is a transfer of

benefits from requests falling into the upper hierarchy levels ( $H$  and  $CH$  levels) to requests that are submitted under the lower echelons of the slot scheduling hierarchy ( $O$  level). In past studies, benefits to the lower slot scheduling hierarchies implied the introduction of sacrifices for some airlines (Zografos and Jiang, 2019). However, in this case such sacrifices are endogenized by the request portfolio of each airline, thus resulting in weakly-dominated slot allocations for all airlines.

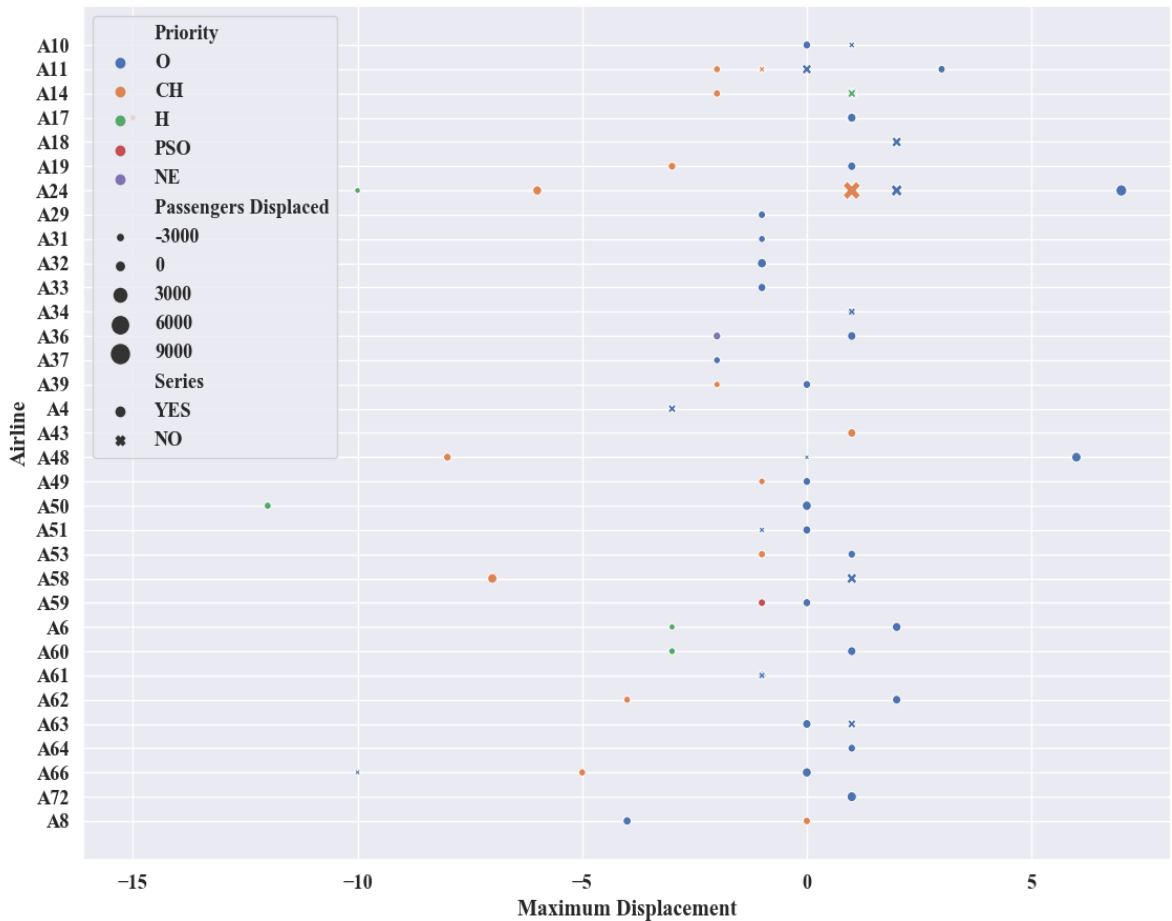


**Figure 2-9:** *Distribution of maximum displacement and displaced passengers per airline and priority*

Based on the TFIM and the analysis included in this section, airport slot coordinators may provide alternative slot allocations to airlines whose requests can't be allocated to their requested times. Through Figure 2-8 and Figure 2-9 one can observe that such alternative slot timings introduce compromises to the

allocations of certain requests of the airlines and improve the overall slot scheduling outcome. In doing so, the presented figures can be used to compare the outcome of the initial slot allocation without considering airlines' flexibility preferences and the impact of the amended schedule after the disclosure of airlines' TFI. The presentation of the results for each airline and slot priority provides in-depth decision support to all interested stakeholders, thus minimising conflicts and easing negotiations and discussions during the slot coordination process.

A key observation that is extracted from the disaggregate presentation of the results, is that the TFI schedule ( $\hat{x}$ ) is airline-non dominated, in the sense that none of the 33 airlines (whose objectives are changed in the TFI schedule) experienced deteriorations (increases) to its objectives ( $Z_{\alpha,i}(\tilde{x}) \leq Z_{\alpha,i}(\hat{x}) \forall i = 1, \dots, 7$ ) without receiving improvements (decreases) to at least one of them. This result is important for the acceptability of  $\hat{x}$ , since in schedules which are airline-dominated, the participants of the system, i.e., the airlines, receive unnecessary deteriorations to their objectives, thus rendering the airport schedules less acceptable for them. Based on the TFIM, each airline's total displacement ( $Z_{\alpha,3}(x)$ ) is less than or equal to the one reported by the no-TFI schedule. Therefore, the TFI schedule will not be airline-dominated since each airline will have at least one of the considered metrics less or equal to the ones given by the TFI schedule.

From a decision-making standpoint, the acceptability of the TFI schedule depends on the preferences of the airlines regarding the schedule quality metrics. For instance, *A50* and *A66* received worse (higher) maximum displacement in the TFI schedule, while all other reported metrics were improved. If these airlines perceive maximum displacement as a significantly more important metric, they will not accept the allocations of the TFI schedule despite the improvements regarding multiple schedule quality metrics. Therefore, the acceptability of the TFI schedule

requires airlines' preferences regarding the reported quality metrics. In response to this, the airlines may use the TFIM, and the analysis presented in this section to examine different scenarios of TFI and review the effect of their stated scheduling flexibility on their request portfolio.

From a policy-making standpoint, the proposed TFIM is important since it allows policy-makers to examine the implications of the TFI's disclosure on the efficiency of the airport slot allocation. Additionally, by using the TFIM, the implications of making the TFI mandatory can be studied and hence be anticipated and communicated to all the interested parties. These properties render the proposed modelling and solution methodology a tool that can support the ongoing review of the slot request prioritisation of IATA.

#### **2.7.2.4 Impact of the dynamic capacity constraints on airport slot scheduling decisions**

Having analysed the impact of the TFI considerations on the ASA decision-making, the discussion that follows focuses on the impact of the dynamic capacity constraints introduced in section 2.4.3 and the synergetic benefits obtained by their integration with the TFI. Before presenting the computational results and comparisons, an analytical visualisation that demonstrates the two alternative capacity considerations is provided.

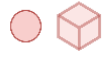



Subplot (a) of Figure 2-10 demonstrates that the dynamic capacity constraints increase the apron capacity of the studied airport by adding 27 feasible cases of capacity utilisation (points lying on the arcs defined by edges  $(\iota, \kappa)$ ,  $(\iota, \mu)$ ,  $(\kappa, \lambda)$  and  $(\lambda, \mu)$ ). The superiority of the dynamic capacity constraints is further highlighted by the fact that the three-dimensional capacity envelope (representing the static capacity constraints) is completely dominated by the envelope created by the dynamic capacity constraints. In addition, subplot (b) of Figure 2-10

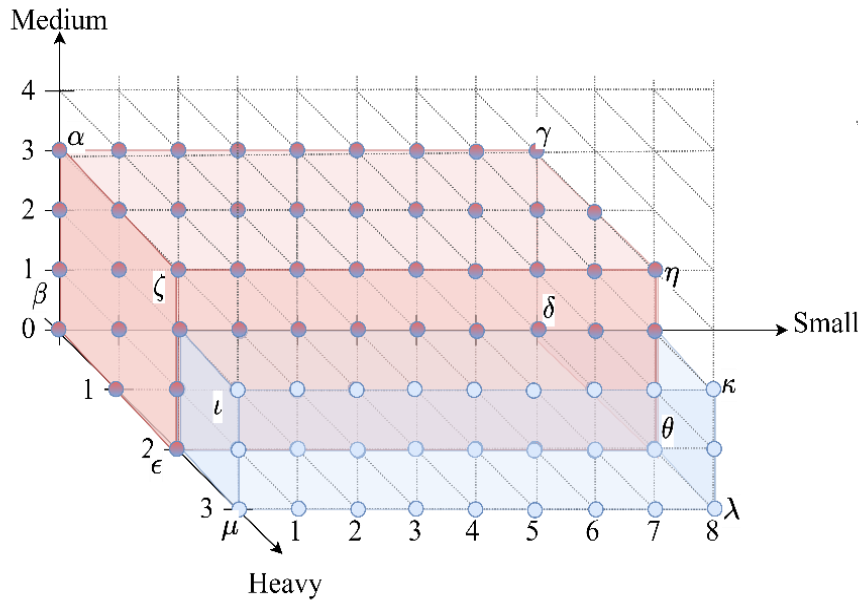
illustrates that in the absence of multiple passenger types, the dynamic passenger terminal constraints allow the accommodation of additional passengers of a certain type, i.e., Schengen/Non-Schengen.

As a result, the capacity for arriving (departing) passengers coming from (travelling to) Schengen and non-Schengen areas can reach the operational limits of the terminal per movement type (arrival or departure) which is 2300 passengers. The observations stemming from the analytical presentation of the airport's capacity, are validated by other studies recognising that flexible airport declared capacity definitions result in a better exploitation of the resources of the airport (Mirković and Tošić, 2014). Therefore, the better utilisation in terms of apron and passenger capacity achieved by the demand-based and dynamic allocation of capacity, makes more extensive use of the airport's infrastructure, hence allowing the accommodation of additional passengers, resulting in the reduction of the numbers of displaced requests and passengers (Odoni, 2020). This is computationally validated by the following experiments. In order to study the impact of the dynamic capacity constraints, a comparative analysis that considers four alternative passenger demand scenarios *ceteris paribus* is conducted.

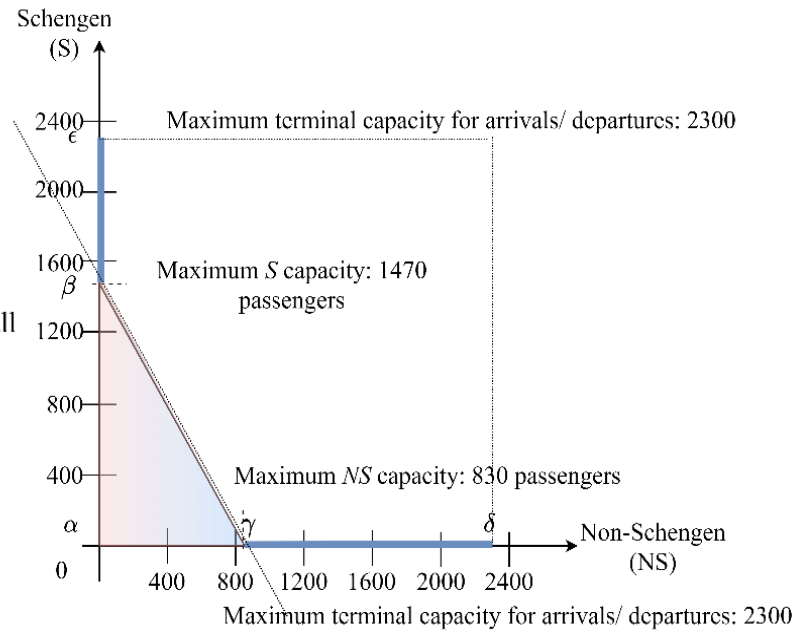
The scenarios selected for this analysis (i) enable us to conduct a sensitivity analysis with respect to the benefit of the dynamic capacity constraints; and (ii) take advantage of the dynamic capabilities of the airport's infrastructure (see subplot (b) of Figure 2-10) with respect to potential increases of passenger demand. All scenarios are compared under the static and the dynamic capacity constraint settings, i.e., having the dynamic apron and passenger terminal constraints inactive/active.



<b>Legend</b>		
Capacity with static apron configurations represented by paralleloepipedon $A$ defined by edges $\alpha, \beta, \gamma, \delta, \epsilon, \zeta, \eta, \theta$		} <b>Apron capacity</b>
Capacity with dynamic apron configurations represented by paralleloepipedon $B$ defined by the edges of $A$ and additional edges $\iota, \kappa, \lambda, \mu$		
Capacity with static terminal capacity configurations represented by the area defined by edges: $\alpha, \beta, \gamma$		} <b>Terminal capacity</b>
Capacity with dynamic terminal capacity configurations represented by the area defined by edges: $\alpha, \beta, \gamma, \delta, \epsilon$		



Subplot (a) - Apron capacity envelope



Subplot (b) - Passenger capacity envelope

**Figure 2-10:** Comparison of the airport's capacity under the static and dynamic apron/passenger terminal constraints

This analysis provides an empirical validation on the influence of the dynamic capacity constraints and the benefits that they provide in comparison to the static capacity constraints. All scenarios are built using the experimental setup that is described in section 2.7.1. The only difference among the scenarios is that the passenger demand is modified by altering the load factor parameter ( $\xi_m$ ).

As a result, the considered scenarios are:

Scenario 1: The baseline scenario where the load factor is equal to 80% ( $\xi_m = 0.8 \forall m \in M$ ).

Scenario 2: The increased passenger demand scenario where the load factor is equal to 85% ( $\xi_m = 0.85 \forall m \in M$ )

Scenario 3: The increased passenger demand scenario where the load factor is equal to 90% ( $\xi_m = 0.9 \forall m \in M$ )

Scenario 4: The increased non-Schengen passenger demand scenario, where the load factor for movements concerning the Schengen area is equal to 90% ( $\xi_m = 0.9 \forall m \in M_{Non-Schengen}$ ) and the load factor of domestic and Schengen flights is set to 80% ( $\xi_m = 0.8 \forall m \in M_{Schengen \cup Domestic}$ )

Scenarios (1)-(4) are solved under the dynamic and the static capacity constraints and compared based on multiple performance metrics (subplots (a)-(f) of Figure 2-13). The discussion of the results is presented and organised based on each individual scenario.

**Scenario 1:** This is the base scenario where the load factor is considered as stated in the declared capacity parameters of the studied airport. Under this scenario the benefit of dynamic capacity constraints appears to be insignificant. In particular, the maximum displacement is the same under both capacity constraint settings (17

x 15-minute intervals). At the same time, both constraint considerations resulted in no request rejections and a total displacement of about 17000 x 15-minute intervals (the dynamic capacity constraints' improvement is only 20 units of total displacement. Similar observations hold for the numbers of displaced passengers

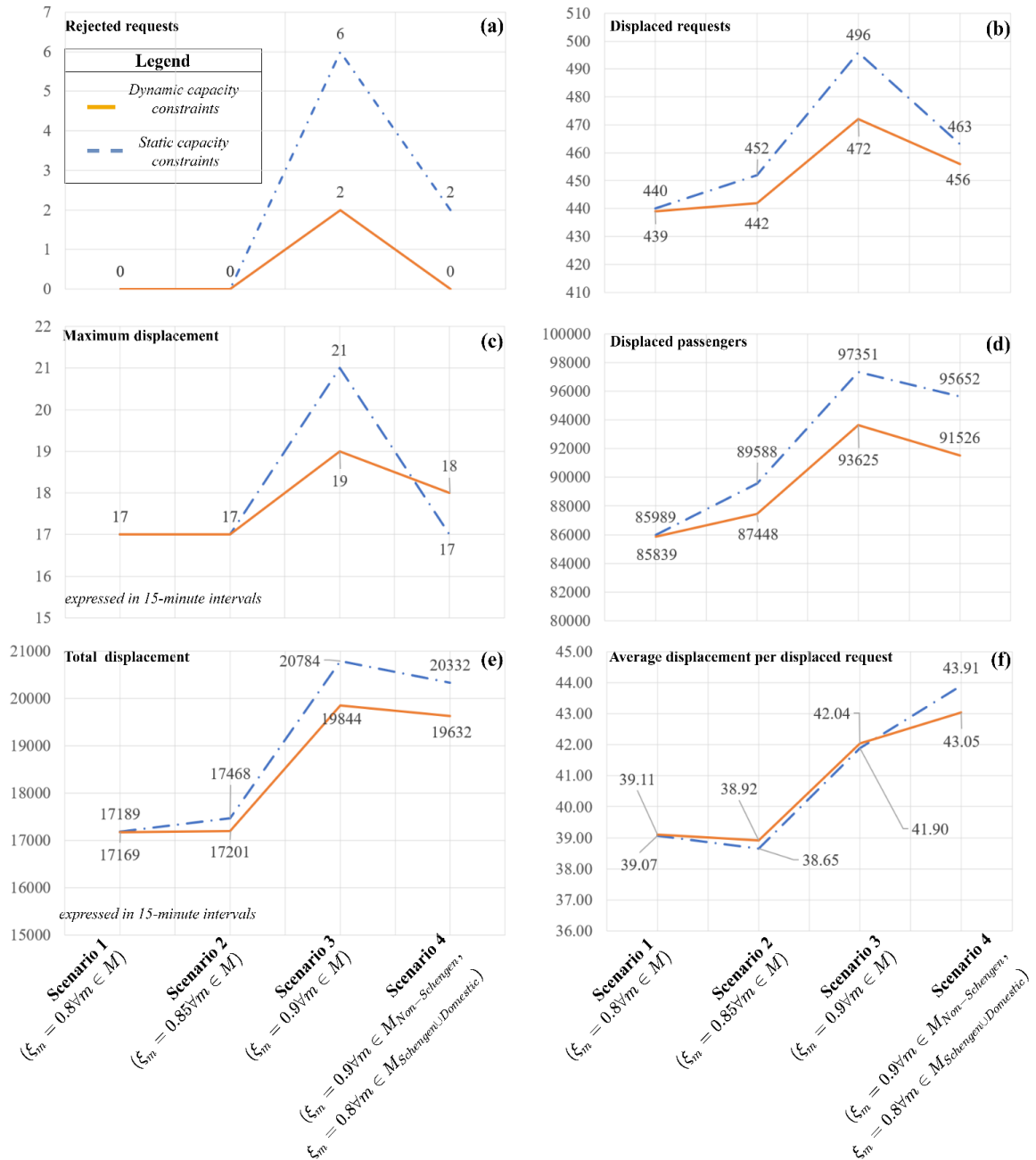


**Figure 2-11:** Comparison of the dynamic and static capacity constraints under alternative scenarios

and displaced requests where the improvements given by the dynamic capacity constraints are subtle (below 0.24%). This set of computational results shows that the airport's landside is not severely constrained as compared to its runway capacity.

**Scenario 2:** This scenario represents a case where the aircraft load factor is increased by 5% in comparison to the base scenario, i.e., from 80% to 85%. In this scenario, the benefits of the dynamic capacity constraints increase significantly. Again, the number of rejected requests is the same under both settings (0 rejected requests and 17 x 15-minute intervals of maximum displacement). However, the improvement given by the dynamic capacity constraints in terms of total displacement is increased from 0.12% (20 x 15-minute intervals) to over 1.5% (267 x 15-minute intervals), i.e., the impact is increased by more than 12 times. The same holds for the number of displaced requests and passengers that are improved by 2.26% (reduction of 10 displaced requests) and 2.45% (reduction of 2140 displaced passengers) respectively under the dynamic capacity setting. The increase in the benefit of the dynamic capacity constraints with respect to these metrics in relation to *Scenario 1*, is 10 times for the number of displaced requests (from 1 less displaced request in *Scenario 1* to 10 less displaced requests in *Scenario 2*) and more than 14 times for the number of displaced passengers (from 150 less displaced passengers in *Scenario 1* to 2140 less displaced passengers in *Scenario 2*). This finding reveals that the dynamic capacity constraints make a better use of the airport capacity and absorb the congestion caused by the increased aircraft utilisation. As a result, the consideration of dynamic capacity configurations does not transfer the displacement to the airlines' schedules. This observation becomes more important when considering that an increase of 5% in terms of passenger

demand results in increased benefits that are 10 times more significant than the benefits observed in the base scenario (*Scenario 1*).

**Scenario 3:** By further increasing the load factor (to 90% for all requests), the benefits of dynamic capacity become rather important. Most importantly, this significant increase leads to the rejection of some slot requests, since the turnaround time constraints of some requests could not be satisfied under this increased load factor setting. However, in this case, the dynamic capacity constraints could accommodate 4 additional requests in comparison to their static counterparts. In particular, under the dynamic capacity setting, only one paired request is rejected (an arrival and departure request), whereas under the static capacity setting there are 3 paired requests that are rejected (6 since they concern pairs of requests). The maximum displacement is also increased for both capacity settings. However, the dynamic capacity constraints outpace their static counterparts by 10%, since they report a maximum displacement of 19 x 15-minute intervals, as compared to 21 x 15-minute intervals. The observations with respect to this dyad of objectives reveal that dynamic capacity constraints are more resilient towards significant demand surges, hence reinforcing the capabilities of airports to continue operating in a sustainable manner. On another note, the values of the remaining objectives improve by about 5% as compared to the static capacity setting, i.e., total displacement improves by 4.74% (from 20784 to 19844 x 15-minute intervals), the number of displaced requests is reduced by 5.08% (from 496 to 472) and the number of displaced passengers is decreased by 4% (from 97351 to 93625). The results concerning this increased-demand scenario show that the capacity limits of the airport are approached, the benefit of dynamic capacity considerations is augmented and improves the resilience of the airport's infrastructure.

**Scenario 4:** *Scenario 3* introduced a significant increase (10%) to the load factor of all requests. However, it is worth studying the effect of non-homogeneous increases to the load factor of different types of requests, i.e., requests serving Schengen/ Domestic and Non-Schengen airports, since passengers on board Schengen/ Domestic flights require less service times while in the passenger terminal than passenger on board Non-Schengen flights (due to passport control and security). This is also reflected in the declared capacity of the airport where the number of Schengen and Domestic passengers is allowed to reach 1470 passengers as opposed to the limit of 830 passengers for Non-Schengen passengers. Under this scenario the dynamic capacity constraints result in significant benefits. In particular, the inability of the static capacity constraints to adapt to the change based on the present passenger types, resulted in the rejection of 1 paired request. On the other hand, the dynamic capacity constraints were capable to accommodate all requests at the expense of 1 unit of maximum displacement. This is justified by the fact that the dynamic passenger terminal capabilities of the airport allow the Non-Schengen passengers to use additional terminal resources when there are no other passenger types. Since the number of rejected requests is the most significant objective function (as per expression (2.6), this observation suggests that the schedule given by the dynamic capacity constraints dominates the one given by the static capacity configuration. This is further validated by the fact that all other performance metrics are improved when considering the dynamic capacity configurations, i.e., total displaced is improved by 3.57% (from 20332 to 19632 x 15-minute intervals), the number of displaced requests is reduced by 1.54% (from 463 to 456 displaced requests) and the number of displaced passengers is diminished by 4.51% (from 95622 to 91526 displaced passengers).

Through the comparative analyses included in this section, it is shown that the dynamic capacity constraints lead to a more resilient expression of airport capacity that can adapt to and absorb potential surges in traffic and passenger demand. The most significant observation is that under all considered scenarios the dynamic capacity constraints improve on all key performance metrics simultaneously. From a combinatorial optimisation perspective, this result is rather significant since the objectives that are improved are conflicting with each other (e.g. the maximum and the total displacement, the number of displaced requests) (Ribeiro et al., 2018) and their values cannot be reduced simultaneously.

Consequently, the dynamic configuration of airport capacity sets new boundaries on the allocations that are achievable by an airport. This is validated by operational studies which report similar benefits when airport capacity adapts dynamically to the demand characteristics (Mirković and Tošić, 2014, 2017). Finally, the considered scenarios reveal that airline demand reaches the limits of airport infrastructure, the benefits given by the dynamic capacity constraints increase in a non-commensurable and more significant manner. From an airport operations perspective, the introduction of the dynamic capacity constraints allows airport authorities to study the implications of increased airline and passenger demand on the ability of the airport to absorb delays and accommodate requests.

#### **2.7.2.5 Impact of the joint consideration of the TFI and the dynamic capacity constraints**

This section discusses the joint benefit of the TFI and the dynamic capacity constraints, and the synergetic benefits obtained by their integration. To achieve this, the section comprises several comparisons among schedules obtained from different modelling variants by pivoting around the constraints enabling the static/dynamic capacity allocation, and the TFI considerations. The comparisons

are clustered based on the modelling setting that is considered. The results reported are extracted from Figure 2-12.

**Comparison between  $\tilde{\mathbf{x}}_S$  and  $\hat{\mathbf{x}}_S$  (TFI under static capacity constraints):**

In order to assess the performance on the TFI *ceteris paribus* without the presence of the dynamic capacity constraints, a schedule obtained by a model that considers the TFI ( $\hat{\mathbf{x}}_S$  identified by orange in Figure 2-12) and a schedule that does not consider the TFI ( $\tilde{\mathbf{x}}_S$  identified by red in Figure 2-12) are compared. Both schedules include static capacity constraints. When TFI is considered without the presence of dynamic capacity constraints, an improvement of 619 units of total displacement (from 17189 to 16570), i.e., a reduction of 3.6%, is observed. In addition, the number of displaced requests is reduced by 61 (from 440 to 379), which corresponds to a reduction of 13.86%. The number of displaced passengers is also reduced by 17272 (from 85989 to 68717), i.e., an improvement exceeding 20%. Overall, the computational experiments suggest that the TFI reduces all main metrics of interest simultaneously (except for maximum displacement which remains the same, i.e., 17 x 15-minute intervals). Regarding the average number of displaced passengers per displaced request, one observes that the TFI led to a reduction of the average size of displaced aircraft by 14.1 seats (from 195.4 to 181.3), i.e., an improvement of 7.22%. The only metric that increases is the average displacement per displaced request which increased by about 12% (from 39.1 to 43.72). However, this increase is expected since the average displacement per displaced request is a relative metric that is calculated as the ratio between the total displacement and the number of displaced requests. Therefore, this increase signifies that the reduction in the number of displaced requests that was provided by  $\hat{\mathbf{x}}_S$  outpaces the reduction in terms of total displacement (it is almost 4 times larger).



**Comparison between  $\tilde{\mathbf{x}}_D$  and  $\hat{\mathbf{x}}_D$ :** A comparison that is useful for understanding the combined benefit of the TFI and the dynamic capacity considerations would be to assess the impact of the TFI when the dynamic capacity constraints are active. Therefore, the base schedule with dynamic capacity allocation considerations ( $\tilde{\mathbf{x}}_D$ ) (identified by red in Figure 2-12) and the TFI schedule with dynamic capacity allocation considerations ( $\hat{\mathbf{x}}_D$ ) (identified by blue in Figure 2-12) are compared. This analysis allows us to study the benefit of the TFI when the dynamic capacity allocation constraints are active. This comparison exhibits that the joint consideration of the TFI and the dynamic capacity constraints results in significant improvements for all schedule quality metrics. For the case of the average displacement per displaced request, it appears that there are significant increases. However, this is justified by the improvement of the number of displaced requests in  $\hat{\mathbf{x}}_D$ , which is more significant (greater by 3.6 times) than the improvement reported for total displacement. Furthermore, the maximum displacement is improved by one 15-minute interval and the total displacement is reduced by more than 5.2% (899 x 15-minute intervals). In addition, in the TFI model with dynamic capacity allocation, there are 84 less displaced requests (19.13% improvement) and more than 21051 less displaced passengers (24.53% improvement). Finally, the combined consideration of dynamic terminal capacity allocation and the TFI (identified by blue in Figure 2-12) enabled a reduction to the average size of the displaced aircraft by 6.6% (more than 13 passenger seats per displaced request).

By observing the two comparisons presented above (between  $\tilde{\mathbf{x}}_S$  and  $\hat{\mathbf{x}}_S$ , and  $\tilde{\mathbf{x}}_D$  and  $\hat{\mathbf{x}}_D$ ) one concludes that the consideration of dynamic capacity constraints amplifies the benefits of the TFI. When the TFI and the dynamic capacity constraints are jointly considered, maximum displacement is reduced by 15 minutes. On the other hand, under the static capacity constraint setting, maximum displacement could not be improved. Furthermore, with respect to the total

displacement objective, when the dynamic capacity constraints are active the benefit of the TFI is increased by 45.2% (when the TFI is considered with the static capacity constraints, total displacement is improved by 619 units, whereas when the TFI is considered in conjunction with the dynamic capacity constraints this improvement raises to 899 units).

Similarly, the benefit with respect to the number of displaced requests is increased by 37.7% (the improvement given by the TFI under the static capacity constraint setting translates to 61 less displaced requests, whereas the joint consideration of the TFI and the dynamic capacity constraints resulted in 84 less displaced requests).

In addition, the influence of TFI with respect to the number of displaced passengers is further amplified when dynamic capacity constraints are active. This argument is supported by reporting an increased reduction exceeding 21.8% (from 17272 less displaced passengers when there are no dynamic capacity constraints to 21051 less displaced passengers when the TFI is considered in conjunction with the proposed dynamic capacity constraints). The following remark summarises the conclusions from this dyad of comparative analyses.

**Remark 2.3** The benefits that are provided by the consideration of the TFI are augmented when the dynamic capacity constraints are active.

In what follows, the section comprises two additional comparative analyses which aim to assess whether the benefits of the dynamic capacity constraints are increased when TFI considerations are present or not.

**Comparison between  $\tilde{\mathbf{x}}_s$  and  $\tilde{\mathbf{x}}_D$ :** In comparing the base schedules obtained under the dynamic and the static capacity constraints *ceteris paribus* (all other parameters and expressions of the experimental setup are identical between the two

variants), there is need to assess the impact of the dynamic capacity constraints when the TFI considerations are inactive. Under this setting, minor gains with regard to major quality metrics simultaneously (see Figure 2-12) are observed. In particular, the total displacement in the schedule with dynamic capacity allocation constraints is decreased by 0.1% in comparison to the schedule with static capacity considerations (a reduction of 20 x 15-minute time intervals). The dynamic capacity constraints reduced the number of displaced requests by only 0.2% (from 379 to 355 displaced requests). A minor improvement is also reported for  $\mathbf{Z}_6(\mathbf{x})$ , where the benefit of the dynamic capacity allocation is translated to almost 150 less displaced passengers (a reduction of 0.17% in comparison to the model with the static constraints). Such results indicate that in the studied airport instance the dynamic capacity constraints do not yield significant benefits when considered on their own. However, in the following analysis, it is demonstrated that the benefits of dynamic capacity constraints are amplified when considered in conjunction with the TFI.

**Comparison between  $\hat{\mathbf{x}}_S$  and  $\hat{\mathbf{x}}_D$ :** In comparing the schedules obtained by the TFIM under the dynamic and the static capacity constraints *ceteris paribus* (all other parameters and expressions of the experimental setup are identical between the two variants), one can assess the impact of the dynamic capacity constraints when the TFI considerations are active. Under this setting, simultaneous gains for all major quality metrics are reported (see Figure 2-12).

In particular, the maximum displacement in the TFI schedule with dynamic capacity allocation constraints ( $\hat{\mathbf{x}}_D$ ) is decreased by 5.8% in comparison to the TFI schedule with static capacity considerations ( $\hat{\mathbf{x}}_S$ ) (from 17 to 16 15-minute time intervals). This result indicates that the TFI considerations in the model with the static capacity constraints could not improve the maximum displacement objective (in comparison to the no-TFI schedule). In addition, improved capacity utilisation

enabled by the dynamic capacity allocation constraints reduced schedule displacement by 300 x 15-minute time intervals less in comparison to  $\hat{x}_S$  (improvement of 1.8%). This simultaneous reduction is of importance, since the maximum and total displacement are two conflicting objectives that are characterised by significant trade-offs, i.e. the minimisation of total displacement requires sacrifices in terms of maximum displacement (Zografos et al., 2017a; Ribeiro et al., 2018).

In addition to the improvements to the total and maximum displacement metrics, the dynamic capacity constraints reduced the number of displaced requests by more than 6.3% (from 379 to 355 displaced requests). An improvement is also reported for  $Z_6(\mathbf{x})$ , where the benefit of the dynamic capacity allocation is translated to almost 4000 less displaced passengers (a reduction of 5.7% in comparison to the model with the static constraints). Interestingly, the average number of displaced passengers and the average displacement per displaced request are increased by the dynamic capacity constraints. This is justified by the fact that in  $\hat{x}_D$  the improvement in terms of displaced requests exceeds the difference from  $\hat{x}_S$  in terms of schedule displacement (similarly the difference between the schedules in terms of passengers is relatively bigger than the number of displaced requests).

The comparisons between  $\tilde{x}_S$  and  $\tilde{x}_D$ , and  $\hat{x}_S$  and  $\hat{x}_D$  prove that the TFI has a multiplicative effect on the benefits given by the dynamic capacity constraints. For instance, when TFI considerations are active, the reduction in terms of total displacement is increased by 15 times (when the dynamic capacity constraints are applied on their own, it is observed that total displacement reduces by 20 x 15-minute intervals, whereas the joint consideration of the dynamic capacity constraints led to 300 x 15 minutes of reduced total displacement).

Same observations are given for the number of displaced requests where the combined consideration of the TFI and the dynamic capacity constraints increased the benefits of the latter by 24 times (from 1 less displaced request to 24 less displaced requests when the dynamic capacity constraints and the TFI are jointly considered). The reduction in the number of displaced passengers is also increased significantly (from 150 when the dynamic capacity constraints are applied on their own, to about 4000 less displaced passengers when combined with the TFI). Therefore, the two comparative analyses given above allow us to conclude that the TFI has a multiplicative effect on the benefits of the dynamic capacity constraints. This is formalised in the following remark.

**Remark 2.4** The benefits that are provided by the consideration of the dynamic capacity constraints are augmented when the TFI considerations are active.

Based on Remark 2.3 and Remark 2.4 one concludes that the joint consideration of the TFI and the dynamic capacity constraints results in significant synergies and significant improvements in terms of slot allocation decision-making.

Overall, the joint consideration of the TFI and the dynamic capacity constraints that is proposed in this chapter, results in synergies yielding significant improvements with respect to all key metrics previously proposed in the literature, i.e., the maximum (improvement of 5.88%) and schedule displacement (improvement of 5.24%), and the numbers of displaced passengers (improvement of 24.66%) and requests (improvement of 19.32%). These allocations dominate those produced by the static capacity considerations with respect to all main schedule quality metrics (the TFI schedule with the dynamic capacity constraints lies closer to the centre of Figure 2-12).

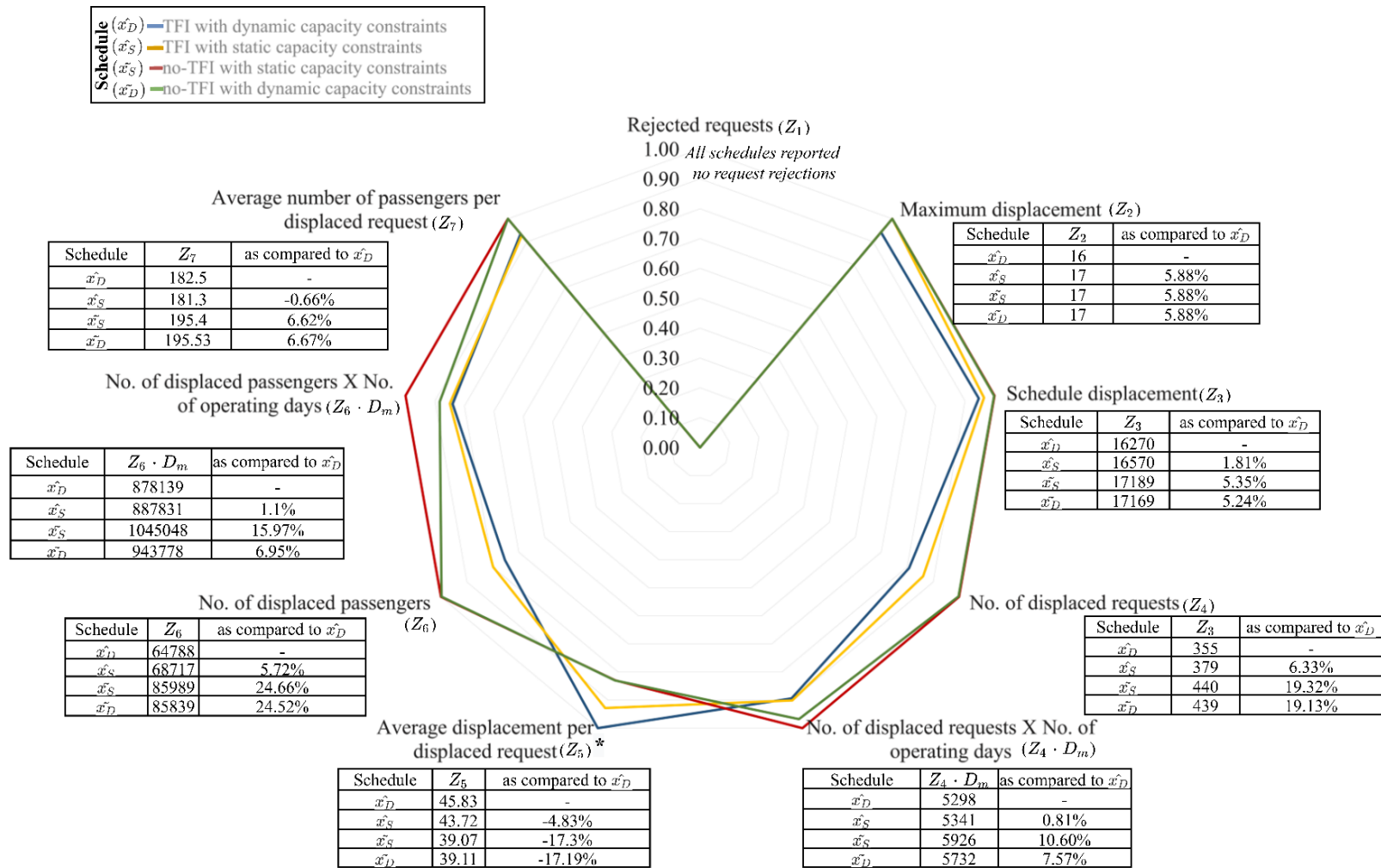


**Figure 2-12:** Radar chart comparing the performance of the capacity constraints and the TFI

### 2.7.2.6 Assessment of the influence of the introduced policy constraints

In assessing the importance of the primary policy rules that are introduced in this work, a comparison of 3 alternative slot prioritisation scenarios enables the study of the impact that alternative slot prioritisation regimes have on the objectives of the requests falling into each slot scheduling priority. These schedules are:

- The base schedule ( $\tilde{x}_D$ ) solved based on sequence  $Q$ , which corresponds to the consideration of all primary priority rules that are active in the considered airport (see the experimental setup in section 2.7.1).
- The base schedule ( $\tilde{x}'_D$ ) solved based on sequence  $Q = \{PSO_{SP}^\sigma, H_{SP}, CH_{SP}, NE_{SP}, O_{SP}\}$ . This schedule recognises the existence of PSO routes but does not differentiate between ad-hoc and series of slot requests.
- The base schedule ( $\tilde{x}''_D$ ) solved based on sequence  $Q = \{H_{SP}, CH_{SP}, NE_{SP}, O_{SP}\}$ . This schedule does not recognise the existence of PSO routes and does not differentiate between ad-hoc and series of slot requests.

The three schedules described above are compared on a *ceteris paribus* basis meaning that the only differentiating element is the priority structure used for their solution. This analysis allows us to observe the influence of the alternative policy considerations on the slot scheduling performance of each priority. The discussion that follows is organised based on each slot prioritisation scenario. The objective values reported are tabulated on Figure 2-13.

**Differentiating between ad-hoc and series of requests:** The comparison between  $\tilde{x}_D$  and  $\tilde{x}'_D$  exhibits the effect of a schedule that differentiates between ad-hoc requests and request series ( $\tilde{x}_D$ ) and its relative performance to a schedule ( $\tilde{x}'_D$ ) that assigns the same priority to series and ad-hoc requests.

An initial observation is that the introduction of the additional priority rules results in significant changes to the slot scheduling outcome, i.e., increases with respect to maximum displacement and the number of displaced requests and passengers for ad-hoc requests; and improvements with respect to metrics that consider each request’s effective period. In particular, the overall maximum displacement remains unchanged, yet the maximum displacement of ad-hoc requests is reduced when the ad-hoc requests receive the same priority as request

Schedules compared		Priority	Maximum displacement	Schedule Displacement	No. of displaced requests	No. of displaced requests x No. of operating days	No. of displaced passengers	No. of displaced passengers x No. of operating days
$\tilde{x}_D$ and $\tilde{x}'_D$	H	Series	0	0	0	0	0	0
		Ad-hoc	-6	-13	-4	-4	-802	-802
	CH	Series	-1	-5	-2	13	-169	892
		Ad-hoc	-2	-25	-11	-3	-3270	1486
	NE	Series	0	0	0	0	0	0
		Ad-hoc	0	0	0	0	0	0
	O	Series	0	728	6	581	-1	67130
		Ad-hoc	-4	-26	-9	19	-571	4543
	PSO	Series	0	0	0	0	0	0
		Ad-hoc	0	0	0	0	0	0
<b>Overall/Total</b>			<b>0 (0.00%)</b>	<b>659 (3.84%)</b>	<b>-20 (-4.56%)</b>	<b>606 (10.57%)</b>	<b>-4813 (-5.61%)</b>	<b>73249 (7.76%)</b>
$\tilde{x}_D$ and $\tilde{x}''_D$	H	Series	0	0	0	0	0	0
		Ad-hoc	-6	-13	-4	-4	-802	-802
	CH	Series	-1	20	1	28	477	4122
		Ad-hoc	-3	-50	-18	-18	-5135	-2067
	NE	Series	0	0	0	0	2	1100
		Ad-hoc	0	0	0	0	0	0
	O	Series	0	738	14	581	1689	65362
		Ad-hoc	-4	-78	-19	-23	-2463	-3401
	PSO	Series	0	0	0	0	0	0
		Ad-hoc	0	0	0	0	0	0
<b>Overall/Total</b>			<b>0 (0.00%)</b>	<b>617 (3.47%)</b>	<b>-26 (-6.30%)</b>	<b>564 (8.96%)</b>	<b>-6232 (-7.83%)</b>	<b>64314 (6.38%)</b>
$\tilde{x}'_D$ and $\tilde{x}''_D$	H	Series	0	0	0	0	0	0
		Ad-hoc	0	0	0	0	0	0
	CH	Series	0	-25	-3	-15	-646	-3230
		Ad-hoc	1	25	7	15	1865	3553
	NE	Series	0	0	0	0	-2	-1100
		Ad-hoc	0	0	0	0	0	0
	O	Series	0	-10	-8	0	-1690	1768
		Ad-hoc	0	52	10	42	1892	7944
	PSO	Series	0	0	0	0	0	0
		Ad-hoc	0	0	0	0	0	0
<b>Overall/Total</b>			<b>0 (0.00%)</b>	<b>42 (0.24%)</b>	<b>6 (1.43%)</b>	<b>42 (0.66%)</b>	<b>1419 (1.75%)</b>	<b>8935 (0.88%)</b>

**Notes:**  $\tilde{x}_D$  is the base schedule with dynamic capacity constraints solved based on the setup of section 7.1.  
 $\tilde{x}'_D$  is the schedule with dynamic capacity constraints solved based on  $Q = \{PSO, H, CH, NE, O\}$  (without differentiating between ad-hoc and series of requests)  
 $\tilde{x}''_D$  is the schedule with dynamic capacity constraints solved based on  $Q = \{H, CH, NE, O\}$  (without differentiating between ad-hoc and series of requests and considering the existence of PSO routes)

**Figure 2-13:** Comparison between the base schedules given under alternative policy considerations



series. For instance, *H* ad-hoc requests, i.e., historic requests with an effective period of less than 5 weeks, have received 6 additional units (6 x 15-minute intervals) of maximum displacement in  $\tilde{x}_D$  as compared to  $\tilde{x}'_D$ . Similarly, ad-hoc requests falling into the *CH* and *O* priorities, have received increased maximum displacement (2 and 5 x 15-minute intervals respectively). Similar results are reported for the number of displaced passengers and requests, where the metrics appear to be increased for ad-hoc requests of *H*, *CH* and *O* priorities. Most importantly, the number of displaced ad-hoc *CH* requests is increased by 35% (11 requests) while the number of displaced passengers is increased by 37% (3270 passengers). This set of results stems from the fact that by neglecting the prioritisation of request series over ad-hoc operations ( $\tilde{x}'_D$ ), ad-hoc historic (*H*) and changes to historic (*CH*) requests are allocated before request series falling into the others (*O*) priority, therefore having additional slots at their disposal. Yet, this prioritisation setting contradicts the requirements of IATA WSG and reduces the compatibility of the proposed model with the ASA decision-making process, which requires requests with larger effective periods to receive improved allocations over ad-hoc requests.

This policy requirement is active in  $\tilde{x}_D$  and its benefit on request series is reflected by the metrics that consider the effective period of each request. For instance, schedule displacement is reduced by 3.84% (659 x 15-minute intervals) when request series are prioritised over ad-hoc requests. This improvement is caused by the additional capacity that is available for request series of *O* priority, which leads to a reduction of 4.7% (728 x 15-minute intervals) in comparison to  $\tilde{x}'_D$ . In addition, significant improvements (10.57%) are reported when considering the requests that are displaced throughout the scheduling season (a reduction of 606 displaced requests).

With respect to this metric, it is observed that the prioritisation of request series over ad-hoc requests results in improved allocations for requests of larger effective periods. The benefit becomes more significant for *O* requests where an improvement of more than 12% (600 less displaced requests throughout the scheduling season) is reported. Similar findings are reported for the number of passengers that are displaced throughout the scheduling season (aggregate improvement of 73249 passengers (7.76%)). This improvement is mainly distributed to *O* request series (67130 less displaced passengers) but also results in minor improvements for *CH* requests. This set of findings reveals that the prioritisation scheme of IATA WSG results in improved allocations for requests with a longer effective period. In contrast, the allocation scheme that did not consider the prioritisation of request series over ad-hoc requests, resulted in improved allocations for ad-hoc requests but larger displacements for requests series with larger effective periods and aircraft.

**Considering PSO as a distinct priority:** By comparing  $\tilde{x}_D$ ,  $\tilde{x}'_D$  and  $\tilde{x}''_D$  one observes that the effect of PSO routes is imperceptible (less than 1% for most metrics). This is justified by the fact that public service obligations (PSO) represent less than 5% of the individual slot requests submitted to the airport. In addition, in the airport under consideration all PSO requests had already a historic status. As a result, the consideration of the PSO as a distinct priority does not affect the allocation of the concerned requests, since in both cases they receive no displacement. However, in other airport instances that the PSO requests are characterised as other request priorities, there may be significant differences when considering them in a distinct priority level. At this point it is worth noting that the PSO rule is a requirement rather than an option, since the slot coordination process has to abide by European regulations (Council Regulation (EEC) No 95/93,

1993; European Commission, 2018). Finally, PSO routes have to be considered explicitly because in the case of severe capacity changes (e.g., capacity reductions due to maintenance or public safety and health purposes), the PSO routes should receive the slots that they request so as to continue serving the remote areas that they concern.

Overall, the prioritisation of request series over ad-hoc requests, improves the slot allocation outcome for request series since it results in significant improvements with respect to schedule displacement and displaced passengers and requests throughout the slot scheduling season. This finding aligns with the aims of IATA WSG which seek to improve service continuity and schedule consistency (IATA, 2019a). On the other hand, when ad-hoc requests receive the same priority as request series, the quality of the allocations of request series is undermined and the allocations of ad-hoc requests are improved.

## 2.8 Concluding remarks

This chapter proposed an integrated modelling and solution framework that optimises slot scheduling decisions in slot coordinated airports. The proposed framework comprises a Timing Flexibility Identifier Model (TFIM) that considers airlines' operational flexibility for each submitted request; and constraints that enable the dynamic allocation of the airport's apron and passenger terminal resources. The proposed approach integrates all primary criteria and several secondary rules of IATA WSG, hence complying with the regulatory requirements applied in practice. The model is tightened by valid inequalities that reduce the computational times required for its solution. Using data from a slot-coordinated airport, computational results illustrate that the joint impact of the timing flexibility and the dynamic capacity allocation considerations improve airport capacity utilisation and airport slot allocations by simultaneously reducing all

schedule quality metrics previously considered in the literature (improvements ranging between 5.5% and 24%). Furthermore, the consideration of the dynamic capacity allocation requirements of the airport results in improvements for all schedule quality metrics without requiring additional infrastructure investments. The proposed approach enables to study the trade-offs among requests of different slot priorities submitted by the same airline, provides insights that inform the airlines on the impact of their disclosed flexibility and support slot coordinators in making alternative slot suggestions. The proposed framework can hence provide improved airport capacity utilisation and more efficient and acceptable slot allocations, which adhere to the operational needs of the airlines operating at the airport. Its value becomes more prominent in regional slot coordinated airports with limited infrastructure as it improves their ability to accommodate additional flights and passengers, hence improving their connectivity potential.

The proposed formulations can be used in other airport slot scheduling contexts that are not necessarily related to coordinated airports. For instance, the expressions enabling the dynamic allocation of the airport's terminal and apron capacity can be used in cases that external factors impose restrictions on the resources of an airport (e.g., reduced terminal utilisation due to social distancing rules and health-related concerns). The proposed model is solved based on an *a-priori* articulation of stakeholders' preferences. Therefore, future research may use the proposed methodology under different preference and objective prioritisation scenarios to provide decision support that studies the impact of stakeholders' preferences on airport slot schedules. The proposed model considers additional decision-making and regulatory requirements but requires significant computational times for the solution of small and medium airport instances, hence hindering the use of this model for large hub airports. To this effect, the development of suitable

heuristic algorithms that will enable the solution of larger airport instances, is a promising area for future research



# Chapter 3:

## Multi-objective airport slot scheduling incorporating operational delays and multi-stakeholder preferences

### 3.1 Introduction

The Airport Slot Allocation (ASA) process described in the World Airport Scheduling Guidelines (WASG) has been the main blueprint for managing and allocating saturated airport capacity (IATA/ACI/WWACG, 2020). WASG considers a set of rules that is overseen by airlines, airports, coordinators, and air navigation service providers (hereafter referred to as ASA stakeholders)<sup>6</sup> that acknowledge and prioritise multiple scheduling performance metrics (e.g., efficiency, fairness). The primary goal of WASG is to alleviate the undesirable outcomes of delays and congestion which are expressed in terms of uneconomic airport and airline operations as well as excessive CO<sub>2</sub> emissions. The ASA process defined in WASG, is a multi-objective, multi-stakeholder decision-making process which requires the consideration of stakeholders' preferences with respect to multiple performance metrics of both strategic and operational nature.

Aiming to optimise ASA decisions, researchers have proposed ever more accurate formulations so as to consider the real-world problem characteristics that arise in ASA problems, i.e., introduction of multiple objectives, consideration of the rules prioritising airlines' requests, proposition of detailed capacity constraints (see an analysis on previous studies in section 3.1.2). Despite the modelling effort put to addressing various problem characteristics, there are two crucial ASA decision-

---

<sup>6</sup> In the context of this study the terms stakeholder(s)/expert(s) are used interchangeably so as to refer to professionals that work in organisations that are part of the coordination committees (see (a) – (d) in page 2) of the studied or of other airports. The terms stake-holding organisation/expert are hence used to reflect organisations/experts that could participate in coordination committees of the studied or of other airports.

making components that are omnipresent in the real-world ASA process and are currently untapped by the ASA literature. Namely, the estimation and consideration of the operational delays associated with strategic airport slot scheduling decisions, and the consideration of the diverging views of the ASA stakeholders with respect to multiple airport slot scheduling objectives and performance metrics.

The consideration of operational delays in strategic airport slot allocation decisions is of utmost importance since it constitutes a fundamental objective of airport demand management (Swaroop et al., 2012). The importance of expected delays associated with airport slot schedules has been well established (Gillen et al., 2016, pp. 1, 2, 14; Cavusoglu and Macário, 2021, p. 7), yet operational delays have solely been considered in tactical re-timing models that introduce scheduling interventions a few days prior to operations (Jacquillat and Odoni, 2015; Jacquillat and Vaze, 2018).

In addition, there are no studies to consider holistically the needs of stakeholders that are relevant to the ASA with respect to multiple objectives and their implications on the airport slot scheduling alternatives that will be considered for operations. This issue becomes rather significant when considering the diverging views of airlines, airports, air navigation service providers and coordinators (hereafter referred to as ASA stakeholders), as well as the recent policy amendments to the WASG which seek to modernise the ASA process through increased collaboration among the interested parties. The dearth of models considering the above issues, limits the decision-support capabilities of the literature and hinders the potential for adopting ASA models in practice (Cavusoglu and Macário, 2021). Besides, the concurrent consideration of operational delays and stakeholders' preferences may aid in the quantification of the benefits of capacity expansions at congested airports from a multi-stakeholder perspective (Adler and Yazhemsky, 2018).



This paper contributes to the literature through the introduction of an ASA solution methodology that (a) considers the operational delays associated with airport slot scheduling decisions; and (b) provides an explicit and systematic approach for modelling of the preferences of the multiple groups of ASA stakeholders in determining the most preferable non-dominated airport schedules. In addressing (a) and (b), this paper proposes an exact multi-objective solution method that guarantees the completeness of the tri-objective non-dominated set for each priority level of the ASA decision-making process. Furthermore, to reduce the inherent decision-making complexity associated with the cardinality of the non-dominated set, the paper proposes a methodology that aids in the identification of high quality (in relation to the complete non-dominated set) representative sets of non-dominated solutions. A multi-criteria schedule evaluation and selection method is introduced which considers simultaneously strategic scheduling and operational delay performance metrics. Furthermore, this hybrid method incorporates stakeholder preference weights and schedules' performance with respect to individual airline's objectives, for selecting a commonly agreed schedule.

Before elaborating further on the contributions of this paper (section 3.1.3), the remainder of this section provides a background on the main concepts of the ASA decision-making process (section 3.1.1) as well as a concise literature review (section 3.1.2).

### **3.1.1 Background**

ASA is an administrative process for managing airline access to congested airports. The ASA defined by WASG (IATA/ACI/WWACG, 2020) is the dominant airport demand management mechanism and is currently applied consistently in 190-207 airports (depending on the season) which concern approximately 40% of global air-travel demand (Odoni, 2020). As per WASG, each calendar year is divided into two scheduling seasons. During each scheduling season there is a series of activities where multiple parties engage and determine the airport slot schedule of each

airport. In what follows we provide a brief description of the main activities of the ASA process defined by WASG.

### 3.1.1.1 Pre-season activity

As per the WASG, each airport is responsible for carrying an annual capacity assessment. This capacity assessment aims to determine on whether an airport will face a capacity shortage or not. In cases where the capacity is not adequate to serve airline demand, then the airport may be characterised as either a *Level 2* or a *Level 3* airport. Level 2 airports are also referred to as *schedule facilitated* and may experience occasional congestion during some days of operations (e.g., weekends). In schedule facilitated airports scheduling conflicts may be resolved by mutual schedule adjustments that are agreed between the airlines and the appointed schedule facilitator. In Level 3 airports (also referred to as *schedule coordinated*) such mutual adjustments and resolution attempts are not possible. That is because the capacity of a Level 3 airport is systematically insufficient to satisfy airline demand.

For a schedule coordinated airport, the national aviation authority is responsible for the appointment of a slot/schedule coordinator that will enact independently, neutrally, and transparently. The main duty of the coordinator is to allocate slots to carriers based on the scheduling parameters defined during the airport's capacity assessment (e.g., load factors per flight type, maximum number of movements, passengers, parked aircraft). Once the status and the scheduling parameters of the airport are determined, the appointed coordinator defines the initial slot pool (number of airport slots available after the allocation of historic requests) and informs airlines about the available capacity. Respectively, airlines wishing to access the airport submit their requests for the next scheduling season/period. Airline requests are submitted bi-annually before the summer and winter Schedule Coordination Conference (SCC) using the *Standard Schedules Information Manual (SSIM)* format.

### 3.1.1.2 Initial slot allocation

Once all requests are received by the coordinator, the *initial slot allocation* is carried out and airport capacity is distributed to airlines in the form of slots. A slot represents the right to access the airport's infrastructure during a specific time of the day. During the initial slot allocation process coordinators consider a complex set of rules and priorities comprising general priorities, local guidelines, and primary and secondary criteria, which are further detailed below.

As per the main principles of WASG, requests for series-of-slots pre-empt ad-hoc requests. Based on their effective period, requests can be classified as requests for a series-of-slots and individual or ad-hoc operations. A request for a series-of-slots is a request for more than 5 weeks of operations. On the contrary, ad-hoc requests concern less than 5 weeks of operations and may be submitted a few days prior operations.

Furthermore, the primary criteria of WASG define the request priorities. According to the primary criteria, the first requests to be allocated by the coordinator, are requests for pre-existing operations. These requests are referred to as historic and normally, if there are no capacity adjustments due to maintenance or expansion works, they receive their requested times. Historic (*H*) requests are determined based on the *use-it-or-lose-it* rule which states that historic status is solely granted to requests operated for at least 80% of the planned/requested days (this rate has been reduced to 50% during the COVID-19 pandemic so as to adjust to the reduced passenger demand and allow airlines to retain the historic statuses of their flights).

As per the rules of WASG, the remaining capacity after the allocation of *H* requests is referred to as the *slot pool*. Up to 50% of the slot pool is reserved for new entrant (*NE*) requests which concern requests submitted by airlines with less than 3 requests per day. *NE* requests receiving slots that are at most one hour

earlier or later from their requested times, should accept the allocation or lose their *NE* status. The remainder of the slot pool is allocated to requests for amending historic operations (also referred to as *Changes to Historic (CH)*) and *Other (O)* requests. Please note that before the revision of the policy framework defining the ASA process, the slot pool was defined after the allocation of both *H* and *CH* requests. Additional primary criteria differentiate between two types of *CH* requests, i.e., requests willing to accept offers between the requested and the historic times and requests that will either accept the historic or the requested time slot.

Within each of the *H, NE, CH* and *O* priorities, requests wishing to extend operations from/to other seasons receive increased priority in relation to requests concerning a single season of operations (referred to as year-round requests). In addition to this set of primary criteria, coordinators should consider local or regional guidelines. An example drawn from European airports is the prioritisation for routes with *Public Service Obligations (PSO)*. As per the PSO rule, operations that are essential for the connectivity and development of remote areas receive an increased priority (Bråthen and Eriksen, 2018; European Commission, 2018). In cases where there is no capacity to allocate a request to the desired slot, airlines should disclose their timing flexibility preferences and coordinators should make alternative offers without placing the carriers in a disadvantageous position. Through the disclosure of their timing flexibility preferences, airlines may communicate their willingness to accept counter offers if a requested time is unavailable.

The consideration of the primary criteria and airlines' timing flexibility preferences determines which requests will receive slots during times that there is no adequate capacity. However, there are secondary criteria which are used for tie-breaking purposes in order to determine requests' prioritisation within each of the main request priorities (*H, NE, CH, O*). These secondary criteria suggest among others the consideration of competition, curfews, connectivity, passengers' needs and the frequency of operations.

### 3.1.1.3 Conference and post conference activities

Following the initial allocation, the airlines and the coordinators engage in a series of discussions to resolve potential conflicts before the SCC. During the SCCs the interested stakeholders (airlines, coordinators, airport, and air-traffic authorities) meet and discuss adjustments to the coordinators' initial allocation so as to resolve timing discrepancies between the times allocated in different airports. Following the SCC, air carriers should decide on whether they will retain, return, or modify each of the slots that they received.

The studies discussed in the following section concern the initial slot allocation process since it defines – to a great extent – the basis of the schedules that will be operated during the scheduling seasons. The framework proposed in this work provides an integrated modelling of the activities and processes of the initial slot allocation and considers all main policy criteria.

## 3.1.2 Previous related work

In this section, we support the contributions made by our work by identifying literature gaps with respect to the consideration of operational delays and multi-stakeholder preferences. Whenever applicable, we make references to the solution methods and the objectives considered by previous related studies. For an inclusive review on the components of the existing ASA models, the interested reader is referred to the recent papers of Jorge et al. (2021) and Katsigiannis and Zografos (2021a).

### 3.1.2.1 Multi-objective airport slot allocation models

The majority of existing ASA studies considers multiple objectives (with the exception of the formative model in Zografos et al., 2012 and the heuristic of Ribeiro et al., 2019a). Existing multi-objective ASA models can be broadly divided into *a-priori* and *a-posteriori* approaches (Cohon, 1978; Marler and Arora, 2004).

A-priori multi-objective optimisation solution methods require the articulation of the stakeholders' preferences in the absence of information regarding the trade-offs between the objectives incorporated in the multi-objective formulation. These preferences can be articulated as goals, limits, and objective coefficients, or through the lexicographic ordering of the objectives. The use of lexicographic optimisation produces a single solution to the multi-objective problem reflecting the associated priority structure of the objectives. In the ASA literature, current studies (Ribeiro et al., 2018, 2019b; Katsigiannis and Zografos, 2021a) use a single lexicographic ordering of the objectives considered in their corresponding multi-objective formulations to generate a single schedule. The generation of a single solution determined by the a-priori selection of the importance of the objectives does not provide the capability to investigate trade-offs among the considered objectives.

A-posteriori multi-objective solution methods first generate the non-dominated set (also referred to as efficient frontier) expressing the trade-offs among the objectives considered, and then in the light of this information require the expression of the preferences of the stakeholders in order to select, among the generated efficient schedules, the most preferred schedule. ASA bi-objective and multi-objective models using a-posteriori solution methods (Zografos et al., 2017a; Zografos and Jiang, 2019; Fairbrother et al., 2019; Androutsopoulos et al., 2019; Jiang and Zografos, 2021; Zeng et al., 2021) have mainly employed the  $\varepsilon$ -constraint solution approach (Haimes, 1971) which guarantees the generation of all non-dominated points for up to two objectives (Cohon, 1978). Existing ASA studies employing this method, reformulate the models by maintaining a single objective formulation and express the remaining objectives as constraints.

A modified version of the  $\varepsilon$ -constraint method reflecting the hierarchical optimisation structure of the ASA problem following the IATA WSG (IATA, 2019a) for setting the priorities for the satisfaction of the slot requests was used in

(Zografos et al., 2017a; Fairbrother et al., 2019; Androutsopoulos et al., 2019; Zografos and Jiang, 2019; Jiang and Zografos, 2021). Katsigiannis et al. (2021) provided a hybrid, lexicographic-based variant of the  $\epsilon$ -constraint method which may produce a large, yet incomplete, subset of weakly-dominated and non-dominated schedules for three objectives, by considering the multiple priority levels of the ASA process. Following this principle, Jorge et al. (2021) considered additional objective functions and generated a subset of efficient solutions that considers secondary policy rules and criteria.

Despite the multiple alternatives offered by existing ASA studies that employ a-posteriori solution methods, the literature faces complications in considering the preferences of the multiple ASA stakeholder groups when indicating the schedules that will be considered for operations. In particular, existing a-posteriori methods may elicit airport slot schedules through mechanisms that consider fairness in conjunction with airlines' preferences with respect to total displacement (Fairbrother et al., 2019); frameworks that consider airlines' timing flexibility (Katsigiannis and Zografos, 2021a) or select the most preferable fairness objective and subsequent frontier using a voting mechanism that considers airlines' and coordinators' views (Jiang and Zografos, 2021); and ranking mechanisms using arbitrary sets of weights so as to assess alternative airport slot schedules without considering stakeholders' views (Jorge et al., 2021).

As a result, existing studies eliciting schedules from the set of non-dominated alternatives cannot grasp the interactions between the preferences of the different groups of ASA stakeholders, while they consider the preferences of airlines and coordinators in isolation without taking into account the views of airport and air-traffic authorities. This observation suggests that existing research is not capable of proposing solutions that balance the diverging preferences of the ASA stakeholder groups, thus hindering the applicability of ASA in practice and its acceptability by the ASA stakeholders. This argument is motivated by the fact that

WASG require the proposed airport schedules to take into account the needs of all interested stakeholders (IATA/ACI/WWACG, 2020). Furthermore, in considering the preferences of airlines and coordinators, current studies are limited to the use of synthetic data or sensitivity analyses so as to examine how alternative preference considerations impact airport slot scheduling decisions.

Regarding the objectives considered by existing multi-objective ASA models (Ribeiro et al., 2018; Jorge et al., 2021; Katsigiannis and Zografos, 2021a; Katsigiannis et al., 2021), we note that the solution algorithms that are currently employed are not capable of producing the complete set of non-dominated points for more than two objectives. From a research standpoint, the need for generating the complete efficient frontier for more objectives has been acknowledged by previous multi-objective ASA studies (Ribeiro et al., 2018, Katsigiannis et al., 2021) as an important research gap, since it may improve the decision-support offered by mathematical ASA models. The need for generating the complete set of trade-off solutions for more objectives is also highlighted from a decision-making perspective, since the ASA process involves multiple stakeholders with different objectives.

Hence, the generation of the complete spectrum of trade-off solutions among multiple objectives can inform the decision-making process and lead to more acceptable airport slot schedules. With respect to this research gap and decision-making need, we note that the proposition of a model that is capable of generating the complete set of non-dominated points and characterising the trade-offs for three objective functions is an issue that has not been addressed by the ASA literature.

### **3.1.2.2 Airport slot allocation studies considering expected delays**

The estimation of expected delays is one of the primary determinants of airport efficiency (Swaroop et al., 2012) since it provides insights on the trade-off between operational delays and scheduling efficiency and contributes to the determination of the ‘socially-optimal’ level of operations at an airport (Swaroop et al., 2012).



This fundamental trade-off between schedule displacement and operational delays not only provides a lookahead on the operational implications of the proposed airport slot schedules but also enables the interested parties to assess the capacity utilisation and the ability of the airport to satisfy airline demand under a certain declared capacity setting (Zografos et al., 2017b). In addition, the consideration of operational delays in conjunction with stakeholders' preferences allows one to examine the impact of their preferences and the resulting slot allocation decisions on the delays and the use of the airport's capacity during operations.

The importance of estimating the expected delays of schedules has been established by existing tactical models (Jacquillat and Odoni, 2015; Jacquillat and Vaze, 2018) which optimise queue lengths or employ service rate constraints by considering runway service times. However, strategic ASA models and algorithms have not considered the interrelation between the operational delays and the proposed airport slot schedules, and the importance that ASA stakeholders assign to the expected delay performance metrics.

Zeng et al. (2021) minimised the total displacement weighted by the probability to operate each allocated time slot. The probabilities/weights were estimated based on historical data regarding the slots operated during previous seasons, however this approach does not capture the interdependencies between airlines' requests (demand) and the airport capacity (supply) for the current scheduling season. The model of Zeng et al. (2021) considers series of slots during a whole scheduling season, however does not incorporate the prioritisation rules of WASG for the satisfaction of slot requests.

As a result, there are no strategic ASA models to provide estimates on the flight delays associated with the schedules generated by the ASA optimisation models and consider the preferences of the ASA stakeholders with respect to the delays of each schedule.

### 3.1.3 Contributions

This paper introduces a unified framework that provides a lookahead on the operational implications of multiple non-dominated airport schedules and considers multi-stakeholder preferences for the assessment and selection of airport slot scheduling solutions. In considering these two problem attributes, our framework appropriately integrates and implements a series of techniques and methodologies (as detailed in section 3.2) that address the following research questions:

- How to evaluate the peak operational delays associated with strategic airport slot scheduling?
- How to reduce decision complexity without compromising the quality and diversity of the schedules presented to the decision-makers?
- How do the different ASA stakeholder groups prioritise the performance metrics proposed in the literature?
- How to consolidate the ASA stakeholder views and produce schedules that balance their interests?
- What are the implications of multi-stakeholder preferences on airport slot scheduling decisions?

In addressing the above questions, the algorithmic aspects of our work achieve the following contributions.

*Multi-level extension of the Quadrant Shrinking Method (QSM):* We propose an application of QSM which considers the request priorities of the ASA process to generate the complete non-dominated set for the different ASA priority levels. This enables the generation of the full set of non-dominated points for each ASA priority level. The proposed implementation benefits from warm start solutions and variable reduction techniques which allow the efficient generation of the non-dominated set.

*Selection of representative sets of non-dominated solutions/schedules:* To address the complexity associated with the large cardinality of the non-dominated

set, we propose a method that adapts dynamically to the shape of the provided non-dominated set and balances the trade-off between decision complexity (number of points presented to the decision makers) and convergence in relation to the complete non-dominated set (measured using the hypervolume indicator (Zitzler et al., 2003; Cao et al., 2015)).

*Assessment of schedules using empirical data and a hybrid multicriteria assessment methodology:* Using preference data from domain experts, we integrate an Analytical Hierarchy Process (AHP) model with the Technique of Preference by Similarity to the Ideal Solution (TOPSIS). The proposed AHP/TOPSIS variant can assess schedules' operational and strategic performance by incorporating stakeholder preference weights and schedules' relative performance with respect to individual airline's objectives.

The remainder of this paper is organised as follows. Section 3.2 provides a summary of the proposed framework, which is further detailed in section 3.3. Section 3.4 presents the application of the framework using request and capacity data from a coordinated airport and preference data from an empirical study with industry experts. Finally, section 3.5 concludes this chapter's findings and provides suggestions for future research.

## 3.2 Overview of the proposed framework

The framework proposed in this paper (Figure 3-1) consists of five main steps that are repeated for each request priority level identified in the WASG. A high-level visualisation of the proposed framework is provided in Figure 3-1, where each algorithmic component is represented by a rectangle and is annotated by the current paper's section that details it.

Firstly, an objective function considering the number of rejected requests is minimised (*Step 1*). Step 1 serves as a feasibility step for the general case that there may be inadequate capacity to accommodate all requests. *Step 2* generates the

complete set of non-dominated points<sup>7</sup> for any three linear objectives (e.g., total displacement, maximum displacement, displaced slot requests) subject to the minimum number of rejected requests reported by *Step 1*. *Step 2* can be performed regardless of the objective functions that are considered. Hence, by configuring the model of *Step 2* using alternative sets of objective functions, the framework can be calibrated/modified based on the needs of the stakeholders that are pertinent to each airport. For the purpose of generating the complete set of non-dominated points for any triplet of linear objective functions, we implement the Quadrant Shrinking Method (QSM) (Boland et al., 2017) and solve it for each level of the ASA hierarchy.

Furthermore, based on the ASA problem requirements, we apply the QSM for each priority level and introduce a multi-level adaptation of the method. That is because the frontier of the non-dominated schedules generated for the Other, New Entrant and Changes to Historic requests, depends on the schedule selected by the stakeholders' preferences with respect to Historic requests. To the best of our knowledge, this is an original application of the QSM in a multi-level decision-making setting. During the application of the method, the proposed variant benefits from problem specific integer programming exploits (see section 3.3.2) which reduce computational times and speed up the generation of non-dominated schedules. *Steps 1* and *2* constitute the schedule generation module of our approach.

Having produced the full set of non-dominated alternatives, an operational delay estimation module based on the  $M(t)/E_k(t)/1$  queue is used so as to provide macroscopic estimates on the operational delays of each generated schedule experienced during the peak days of operations (*Step 2.b*) (see section 3.3.4.1). The purpose of this step is to estimate the operational delays associated with the

---

<sup>7</sup> Hereafter, the terms points, solutions, and schedules are used interchangeably to signify a non-dominated airport slot schedule produced by the proposed framework.

potentially large number of non-dominated points. This enables the subtractive clustering algorithm that follows to propose representative schedules through the joint consideration of strategic performance and operational delays without requiring significant computational times for estimating the latter. The operational delays associated with the peak days of the schedules that are presented to the decision-making process (the representative schedules) are estimated by considering the entire airfield's operations using the strategic analytical module outlined in section 3.3.4.2.

Having full information on the available alternatives, their strategic and operational performance, the proposed framework integrates a subtractive clustering algorithm (*Step 3*) that reduces the decision-complexity arising from the multiple non-dominated schedules and indicates a subset of representative solutions without compromising the information offered to the decision-making process. The clustering algorithm considers both operational and strategic performance metrics and proposes a small subset of points without significantly compromising the variety of slot scheduling alternatives offered to the decision-makers.

This step reduces the decision-complexity from the decision-makers perspective, since it does not require coordinators to examine multiple schedules comprising multiple days, requests, and thousands of flights. The need for reducing the number of points presented to the ASA stakeholders and decision makers is further motivated by the fact that human beings do not have the capacity to process multiple complex alternatives.

In fact, formative studies in the field of psychology indicate that human decision making is limited to judgements and decisions of no more than  $7\pm 2$  alternatives (Miller, 1956). To the best of our knowledge our framework is the first to integrate a solution space reduction technique that provides guarantees on the quality of the resulting subset in relation to the complete non-dominated set. *Step*

3 may be conditional to the number of solutions generated at *Step 2* or can be tuned (following a parameter optimisation routine detailed in section 3.4.3.1) based on the complete non-dominated set so as to propose a subset of points without compromising the representativeness of the complete non-dominated set. The algorithm used in *Step 3* constitutes the clustering (or solution reduction) module of the framework.

Having determined the schedules that will be presented to the stakeholders, a strategic analytical module for estimating the expected delays (*Step 4*) provides a lookahead view on the delays of each representative schedule during the most congested days of the scheduling season by considering the whole airfield. In addition to *Step 2.b* that provided macroscopic estimates on the operational delays caused by runway congestion, the analytical delay estimation module implemented in *Step 4* refines those estimates and provides improved decision-making support by considering the entire airfield operations by assessing the delays of all representative schedules. Hence, the proposed framework can provide operational performance estimates on the proposed schedules and inform the ASA stakeholders.

Finally, a schedule selection module (*Step 5*) (*steps 5.a.* and *5.b.*) ranks the generated schedules based on both expected delays and displacement related performance criteria. *Step 5* provides a holistic schedule elicitation mechanism that considers the preferences of all ASA stakeholder groups and provides the best compromise solution by balancing the views of the stakeholders with respect to multiple displacement and delay related metrics.

In contrast to previous studies with preference considerations (Fairbrother et al., 2019; Jiang and Zografos, 2021; Katsigiannis et al., 2021) that consider airlines and coordinators' views, our framework supports the multi-stakeholder nature of WASG through the consolidation of the preferences of all stakeholder groups, assesses the generated non-dominated schedules and proposes the best compromise solution. Steps 1-5 are repeated for all schedule priorities.

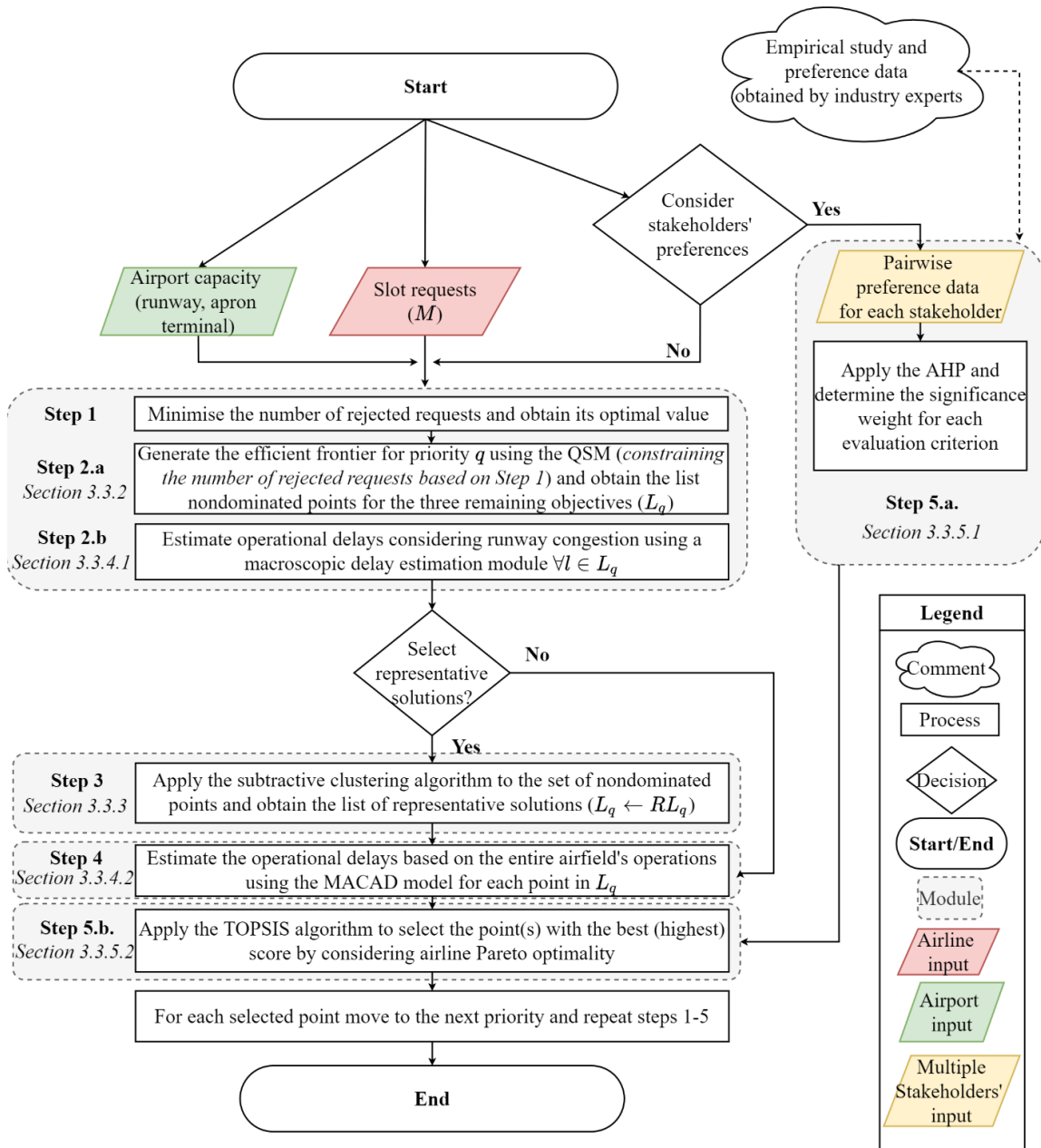


Figure 3-1: Overview of the proposed framework

### 3.3 A multi-objective, multi-stakeholder airport slot allocation framework

In this section, we discuss the framework that we propose for solving the multi-objective ASA problem under WASG by considering the operational delays of each generated schedule and the stakeholders' preferences.

### **3.3.1 A multi-objective airport slot allocation model for constructing airport slot schedules**

Before providing a description of the functionalities of the framework (sections 3.3.2-3.3.5), for the sake of completeness, we make a concise reference to the model that is used to in the schedule generation module of the framework so as to construct airport slot schedules (Katsigiannis and Zografos, 2021a). The model presented below, extends the modelling variant presented in Katsigiannis and Zografos (2021a) by considering turnaround constraint expressions modelling request rejections for both paired and unpaired requests, and priority constraints that consider the request prioritisation defined by WASG.

The considered schedule generation module is a Quadr-Objective Airport Slot Allocation Model (QOSAM) that can be used either as part of the proposed framework or independently. Like most ASA studies, QOSAM takes as input the airlines' requests submitted to the airport as well as the airport's capacity parameters and specifications. Based on this input, a data analysis procedure is conducted in order to extract additional parameters.

The input and the decision variables required to formulate QOSAM are provided in Table 3-1.

After the provision of the model's input, the following subsection analyses the policy amendments introduces by WASG and provides the base modelling components (decision variables, constraint, and objective expressions) (subsection 3.3.1.1) and the main slot prioritisation constraints (subsection 3.3.1.2).



Input sets	
$F$	Set of terminals available at the airport indexed by $f$
$Q$	Sequence of slot priorities indexed by $q$
$K$	Set of movement types indexed by $k$
$A$	Set of airlines submitting requests indexed by $a$
$M$	Set of slot requests indexed by $m$ . In differentiating between the legs of a request, $ma$ and $md$ are used for arrival and departures respectively ( $M_a$ : by airline $a$ , $M_q$ : by priority $q$ , $M^k$ : movement $k$ )
$D$	Set of days in the scheduling season indexed by $d$ ( $D_m$ denotes the days that $m$ operates)
$C$	Set of capacity time interval lengths indexed by $c$ and $\tilde{c}$
$T_c$	Set of time intervals per day calculated based on interval length $c$ indexed by $t$
$\check{A}$	Multiset of origin/destination airports (denoted by $\check{a}$ ) served by the focal airport with $\omega(i) =  \{\check{a} \in \check{A}   \check{a} = i\}  = \sum_{\check{a} \in \check{A}} 1_i(\check{a})$ being the multiplicity of element $i$
Input parameters	
$t_m(\overline{t_m})$	Requested (historic) time for request $m$
$T_{\max(\min),m}$	Turnaround time parameters of slot request $m$
$sep$	Separation parameter used in the unpaired turnaround expressions
$u_{d,t,c}^k$	Runway capacity for movement $k$ for period $[t, t+c)$ on day $d$ based on time scale $c$
$a_{d,m}$	1, if request $m$ is requested on day $d$ ; 0, otherwise
$v_m$	1 if $a_{d,md} = a_{d,ma} + 1$ ; 0, if $a_{d,md} = a_{d,ma}$ (overnight indicator parameter)
$\psi_{t,m}$	Displacement of request $m$ calculated as $t - t_m$
$b_m$	1, if request $m$ is requested on day $d$ ; 0, if the request is an auxiliary unpaired movement
Decision variables and expressions	
$x_{t,m}^f$	1, if request $m$ is allocated to time $t$ on terminal $f$ ; 0, otherwise
$\Psi$	Auxiliary variable defining the maximum displacement objective
$Z$	Set of objectives ( $Z_q$ of priority $q$ , $Z^a$ of airline $a$ )

**Table 3-1:** *Input data and decision variables for the base model*

### 3.3.1.1 Constraints and objective function

Given the above notation, QOSAM is defined by expressions (3.1)-(3.6).

$$\sum_{f \in F} \sum_{t \in T_{\tilde{c}}} x_{t,m}^f \leq 1 \quad \forall m \in M_q \quad (3.1)$$

$$\sum_{f \in F} \sum_{m \in M_q^k} \sum_{t' \in [t, t+c-1]} a_m^d x_{t',m}^f b_m \leq u_{d,t,c}^k \quad \begin{array}{l} \forall d \in D, c \\ \in C, k \in K, t \\ \in [0, |T_{\tilde{c}}| \\ - c] \end{array} \quad (3.2)$$

$$\begin{aligned}
T_{\min,m} - \left(1 - \sum_{f \in F} \sum_{t \in T_{\tilde{c}}} x_{t,md}^f\right) (|T_{\tilde{c}}| + T_{\min,m})(1 + v_m) \\
\leq \sum_{f \in F} \sum_{t \in T_{\tilde{c}}} [x_{t,md}^f(t + v_m|T_{\tilde{c}}|)] - \sum_{f \in F} \sum_{t \in T_{\tilde{c}}} x_{t,ma}^f t \quad \forall m \in M_q: b_{md} = 1 = b_{ma} \\
\leq T_{\max,m} + \left(1 - \sum_{f \in F} \sum_{t \in T_{\tilde{c}}} x_{t,ma}^f\right) |T_{\tilde{c}}|(1 + v_m)
\end{aligned} \tag{3.3}$$

$$\begin{aligned}
\lfloor sep/\tilde{c} \rfloor \sum_{f \in F} \sum_{t \in T_{\tilde{c}}} x_{t,ma}^f - \left(1 - \sum_{f \in F} \sum_{t \in T_{\tilde{c}}} x_{t,md}^f\right) (|T_{\tilde{c}}| + \lfloor sep/\tilde{c} \rfloor) \\
\leq \sum_{f \in F} \sum_{t \in T_{\tilde{c}}} [x_{t,md}^f(t + v_m|T_{\tilde{c}}|)] - \sum_{f \in F} \sum_{t \in T_{\tilde{c}}} x_{t,ma}^f t \quad \forall m \in M_q: b_{md} = 1 - b_{ma}
\end{aligned} \tag{3.4}$$

$$\sum_{t \in T_{\tilde{c}}} x_{t,m}^f |\psi_{t,m}| \leq \Psi \quad \forall m \in M_q \tag{3.5}$$

$$Z_q = \min \left\{ \begin{array}{l} \sum_{m \in M_q} \frac{|\check{A}|}{\omega(AP_m)} \left(1 - \sum_{f \in F} \sum_{t \in T_{\tilde{c}}} x_{t,m}^f\right) |D_m| \\ \max_{\forall m \in M_q} \{|\psi_{t,m}| x_{t,m}^f\} = \Psi \\ \sum_{m \in M_q} \sum_{f \in F} \sum_{t \in T_{\tilde{c}}: t \neq t_m} x_{t,m}^f |D_m| \\ \sum_{f \in F} \sum_{m \in M_q} |D_m| \sum_{t \in T_c} (x_{t,m}^f |\psi_{t,m}|) \end{array} \right. \tag{3.6}$$

Expressions (3.1) state that each request may receive at most one time slot or be rejected. Expressions (3.2) are rolling runway capacity constraints. Please note in (3.2) that with the aid of parameter  $b_m$  auxiliary movements of unpaired requests do not consume runway capacity. Expressions (3.3) define the turnaround time of each paired request. Unlike previous formulations of the turnaround time constraints, expressions (3.3) allow one or both legs of a request to be rejected (see Proposition 3.1). Similarly, expressions (3.4) and (3.5) define the turnaround time constraints of unpaired requests, which are required to have a minimum turnaround time defined based on parameter  $sep$  (minutes of separation). Expressions (3.5) are auxiliary expressions defining the maximum displacement across all requests.

Finally, expression (3.6) defines the objective of the base formulation which consists of (from the top to the bottom) the number of rejected requests ( $Z_1$ ), maximum displacement ( $Z_2$ ), the number of the displaced requests ( $Z_3$ ) and the total displacement ( $Z_4$ ) objectives. In minimising the number of rejected requests, for each request leg, we introduce weights which are inversely proportional to the number of requests that serve the concerned airport. In doing so, we take into account the competition and connectivity (Burghouwt and Redondi, 2013) of each slot request (IATA/ACI/WWACG, 2020).

In addition to expressions (3.1)-(3.6), QOSAM integrates apron and passenger capacity constraints identical to those proposed in Katsigiannis and Zografos (2021a). For the sake of brevity the mathematical formulation of the passenger terminal and apron constraints is not included in this paper, yet the interested reader may refer to the paper of Katsigiannis and Zografos (2021a) (Chapter 2 of the current thesis) which includes detailed descriptions and formulations.

QOSAM minimises the number of rejected requests, the maximum and total schedule displacement, and the number of displaced requests. These objectives are considered since they comply with the requirements of WASG as follows:

- *Minimisation of rejected requests* is herein considered before the solution of the tri-objective model and solution algorithm; and provides an initial incumbent that acts as a basis to construct the non-dominated schedules based on the following objectives. The minimisation of this objective introduces a hard constraint on the number of rejected requests reported in the schedules generated by the solution generation module of the proposed framework.
- *Minimisation of the maximum displacement* acts as a measure of fairness and a guarantee of the schedules' quality of service (Zografos et al., 2017a;

Jacquillat and Vaze, 2018; Katsigiannis and Zografos, 2021a). When considered in conjunction with other objectives, the minimisation of maximum displacement can be used to address additional policy rules and secondary criteria of WASG (Jorge et al., 2021).

- *Minimisation of the total displacement* represents a commonly accepted measure of scheduling efficiency which is used by coordinators to measure the displacement throughout the whole set of slot requests. This metric is often used to consider the needs of the travelling public and the carriers (Jorge et al., 2021).
- *Minimisation of the number of displaced requests* is often used by coordinators as a performance metric to indicate the number of requests that will belong to the list of unsatisfied slot requests (pending list). This metric can be combined with total displacement and calculate the average displacement per displaced request to consider the requirements of the travelling public (Katsigiannis and Zografos, 2021a).

**Proposition 3.1** Expressions (3.3) hold for both individual and paired rejections of request legs.

*Proof.* In order to prove this, there is need to examine that (3.3) holds under all potential cases of request rejections. These are as follows:

- I.  $\sum_{f \in F} \sum_{t \in T_{\bar{c}}} x_{t,ma}^f = 1, \sum_{f \in F} \sum_{t \in T_{\bar{c}}} x_{t,md}^f = 0$   
(arrival scheduled; departure rejected)
- II.  $\sum_{f \in F} \sum_{t \in T_{\bar{c}}} x_{t,ma}^f = 0, \sum_{f \in F} \sum_{t \in T_{\bar{c}}} x_{t,md}^f = 1$   
(arrival rejected; departure scheduled)
- III.  $\sum_{f \in F} \sum_{t \in T_{\bar{c}}} x_{t,ma}^f = 0, \sum_{f \in F} \sum_{t \in T_{\bar{c}}} x_{t,md}^f = 0$   
(arrival and departure rejected)
- IV.  $\sum_{f \in F} \sum_{t \in T_{\bar{c}}} x_{t,ma}^f = 1, \sum_{f \in F} \sum_{t \in T_{\bar{c}}} x_{t,md}^f = 1$   
(arrival and departure scheduled)

In I,  $\exists t' \in T_{\bar{c}}: x_{t',ma}^f = 1$ . Then (3.3) becomes equal to  $T_{\min,m} - (|T_{\bar{c}}| + T_{\min,m})(1 + v_m) \leq -t' \leq T_{\max,m}$ .  $-t' \leq T_{\max,m}$  holds  $\forall t' \in T_{\bar{c}}, v_m \in \{0,1\}$ . When  $v_m = 0$ ,  $-t' \leq -|T_{\bar{c}}|$  which is true  $\forall t' \in T_{\bar{c}}$ . Similarly, when  $v_m = 0$ ,  $-t' \geq -2|T_{\bar{c}}| - T_{\min,m}$  which also holds  $\forall t' \in T_{\bar{c}}$ . In II,  $\exists t' \in T_{\bar{c}}: x_{t',md}^f = 1$ . Then (3.3) is  $T_{\min,m} \leq t' + v_m|T_{\bar{c}}| \leq T_{\max,m} + |T_{\bar{c}}|(1 + v_m)$ .  $T_{\min,m} \leq t' + v_m|T_{\bar{c}}|$  holds  $\forall t' \in T_{\bar{c}}, v_m \in \{0,1\}$ . When  $v_m = 0$ ,  $t' \leq T_{\max,m} + |T_{\bar{c}}|$ , which holds  $\forall t' \in T_{\bar{c}}$  (same expression is given when  $v_m = 1$ ). Case III is trivially satisfied, since  $T_{\min,m} - (|T_{\bar{c}}| + T_{\min,m})(1 + v_m) \leq 0 \leq T_{\max,m} + |T_{\bar{c}}|(1 + v_m)$  which is true for  $v_m \in \{0,1\}$ . In case IV, expression (3.3) reduces to the turnaround times proposed in Katsigiannis and Zografos (2021a) and Katsigiannis et al. (2021).

### 3.3.1.2 Priority constraints

The ASA process for the majority of the world's congested airports was previously defined by the World Schedule Guidelines of IATA (IATA, 2019a) (hereafter referred to as IATA WSG). However, under the newly proposed WASG (IATA/ACI/WWACG, 2020) there are some significant changes that require considerable modelling amendments. This section provides a brief description of the main slot request priorities and the policy amendments introduced by the newly proposed WASG and introduces priority constraints that reflect the recent policy amendments.

Both IATA's WSG and WASG recognise four main slot request priorities, i.e., requests for historic operations (hereafter referred to as *historic* denoted by  $H$ ), amendments to historic operations (herein referred to as *changes to historic* denoted by  $CH$ ), new entrants' requests (hereafter referred to as *new entrants* denoted by  $NE$ ) and other requests (hereafter referred to as *others* denoted by  $O$ ). These request classes are the main request prioritisation criteria, however additional criteria exist, which for the sake of brevity are not included in the analysis that follows.

**Request prioritisation as per IATA WSG:** As per the previous version of IATA WSG (IATA, 2019a), the first class of requests to be considered by the coordinators is  $H$ . When there are no capacity reductions,  $H$  requests should receive the historic time of operations. Following  $H$  requests,  $CH$  requests were allocated based on two subclasses, i.e.,  $CH$  requests that accept allocations between the requested/amended and historic times (denoted by  $CR$ ), and  $CH$  requests that will either accept the historic or the requested/amended time (denoted by  $CL$ ). The slots remaining after the allocation of  $H$  and  $CH$  requests compose the *slot pool*, of whom up to 50% is allocated to  $NE$  requests and the remaining to  $O$  requests. Note that within each class, excluding  $H$ , IATA's WSG prioritise requests that extend operations to a year-round basis over requests for a single period of operations.

**Current prioritisation as per WASG:** The revised WASG does not affect  $H$ 's prioritisation but alters the definition of the slot pool to be the remaining slots after the allocation of  $H$  requests. As a result, in the revised version, the slot pool is shared by  $NE$ ,  $CH$  and  $O$ . As in previous versions,  $NE$  may receive up to 50% of the slot pool, however, as per the WASG the remainder of the slot pool (after the allocation of  $NE$ ) is distributed to  $CH$  and  $O$  requests. WASG does not alter the classification of  $CH$  requests into  $CR$  and  $CL$  and the prioritisation of year-round over single period requests remains unchanged.

The framework proposed in this study considers the WASG. In what follows, the remainder of this chapter will refer to the priorities of  $H$  and  $NE$ ,  $CH$ ,  $O$  as ASA priorities or ASA hierarchy.

Below, we provide priority constraints which model the newly proposed WASG. In doing so, we introduce variables  $HM_{d,t,c}^k, NEM_{d,t,c}^k \forall d \in D, c \in C, k \in K, t \in [0, |T_{\hat{c}}| - c]$  which represent historic and new entrants' movements respectively.

$$\sum_{t \in [t_m + \min\{0, \bar{t}_m - t_m\}, t_m + \max\{0, \bar{t}_m - t_m\}]} x_{t,m}^f = \sum_{t \in T_{\bar{c}}} x_{t,m}^f \quad \forall m \in M_{CR \cup H}, f \in F \quad (3.7)$$

$$x_{\bar{t}_m, m}^f = 1 - x_{t_m, m}^f \quad \forall m \in M_{CL}, f \in F \quad (3.8)$$

$$HM_{d,t,c} = \sum_{f \in F} \sum_{m \in M_H} \sum_{t' \in [t, t+c-1]} a_{m_k}^d x_{t',m}^f b_m \quad \forall d \in D, c \in C, t \in [0, |T_{\bar{c}}| - c] \quad (3.9)$$

$$NEM_{d,t,c} = \sum_{f \in F} \sum_{m \in M_{NE}} \sum_{t' \in [t, t+c-1]} a_m^d x_{t',m}^f b_m \quad \forall d \in D, c \in C, t \in [0, |T_{\bar{c}}| - c] \quad (3.10)$$

$$\sum_{d \in D} \sum_{t \in T_{\bar{c}}} NEM_{d,t,c} \leq \left\lfloor \frac{\sum_{d \in D} \sum_{t \in T_{\bar{c}}} (u_{d,t,c}^k - HM_{d,t,c}^k)}{2} \right\rfloor \quad \forall c \in C \quad (3.11)$$

Constraints (3.7) state that historic requests ( $H$ ) should receive their historic time ( $\bar{t}_{m_k}$ ), i.e., the time that they received in the previous season. In addition, constraints (3.7) ensure that each  $CR$  request will receive a time between its historic and requested times. Constraints (3.8) respect the rules for ( $CL$ ) requests by allocating either the historic or the requested time. Constraints (3.11) define the slot pool, i.e. the available slots after the allocation of historic requests (defined as per expression (3.9)), of whom up to 50% is allocated to requests of new entrants (defined as per expression (3.10)) with the remaining being given to  $CH$  and  $O$  requests according to WASG. During the pre-processing of the request data, if the total number of offered slots minus the number of the requested historic movements divided by two is greater than the number of new entrants' movements, then constraints (3.9), (3.10) and (3.11) can be dropped, since the capacity remaining after the allocation of historic requests trivially satisfies the slot pool's allocation to new entrants.

### 3.3.2 Schedule generation module

This section details the schedule generation module of this framework (identified by steps 1 and 2 in Figure 3-1).

The technique used for solving multi-objective optimisation problems, depends on the problem structure, the number of objectives and the stakeholders of the concerned decision process. In the context of the ASA defined by WASG, we note the presence of multiple stakeholders with different (or even conflicting) objectives. For instance, airport authorities wish to extend the airport's connectivity by scheduling as many slots as possible, while airlines may tolerate a displaced request if it leads to substantial improvements of the positioning of their other requests. However, since airlines are not eager to disclose their valuation for each of their requests, if the generation of all non-dominated solutions is possible, then it should be preferred over a-priori methods. Given several non-dominated points, the stakeholders can convene and choose the solution that best expresses their needs without revealing their detailed preferences.

The objective set proposed in QOSAM (see section 3.3.1) consists of four objectives that are optimised for each slot request priority  $q \in Q$ . Firstly, we minimise the number of rejected requests and provide an initial incumbent solution that acts as a feasibility step and reduces the solution times required by the tri-objective solution approach detailed below.

Secondly, we generate an efficient frontier that considers the trade-offs among maximum displacement ( $Z_2$ ), the number of displaced requests ( $Z_3$ ) and total/schedule displacement ( $Z_4$ ). However, we note that the framework may incorporate any ASA model regardless of its linear objective functions. Among the available algorithms that guarantee the generation of all non-dominated points for three objectives (Kirlik and Sayın, 2014; Dächert and Klamroth, 2015; Boland et al., 2016, 2017), the most efficient is the Quadrant Shrinking Method (QSM) (Boland et al., 2017) which decomposes the tri-objective problem and reduces the number of Mixed Integer Programming (MIP) instances needed to generate the complete non-dominated set. A QSM variant adapted to the ASA problem is detailed in Algorithm 3-1.



At the core of the QSM (see Algorithm 3-1) lies a two-dimensional non-dominated search (2D-NDS). A quadrant in the 2-dimensional space is defined by  $\mathbf{u} = (u_1, u_2)$ , thus limiting maximum displacement ( $Z_2$ ) by  $u_1$  and the number of displaced requests ( $Z_3$ ) by  $u_2$ . Therefore, in the context of the ASA problem, in the first step of the 2D-NDS the proposed adaptation minimises total displacement ( $Z_4$ ) subject to (3.1)-(3.11) combined with the passenger and apron constraints of Katsigiannis and Zografos (2021a) and constraint maximum displacement ( $Z_2$ ) and the number of displaced requests ( $Z_3$ ) by  $\mathbf{u}$ . The solution to this MIP yields a weakly dominated solution (WD).

The second phase of the 2D-NDS minimises the summation of the three objectives ( $Z_2 + Z_3 + Z_4$ ) subject to (3.1)-(3.11) combined with the passenger and apron constraints of Katsigiannis and Zografos (2021a) and additional constraints that limit the values of the objectives based on the first step of the 2D-NDS (see Notes of Algorithm 3-1), resulting in a non-dominated solution (ND). The algorithm keeps track of the unexplored quadrants and parses them iteratively using the following logic. At the outset, a double ended list ( $DL$ ) is initialised with a non-binding value (e.g.  $(+\infty, +\infty)$ ) (see line3 of Algorithm 3-1).

The list keeps track of how the algorithm explores each quadrant containing potential non-dominated solutions. This is done by searching the right (lines 6-19 of Algorithm 3-1) and the top (lines 21-34 of Algorithm 3-1) boundaries of the quadrant. The right boundary of each quadrant is provided based on the front element of  $DL$ . In the case that it yields a non-dominated solution ( $ND$ ),  $(Z_2(ND) - \varepsilon_{z_2}, u_2)$  and  $(u_1, Z_3(ND) - \varepsilon_{z_3})$  are added to the front of  $DL$  (with  $\varepsilon_{z_2}, \varepsilon_{z_3}$  being the search steps of objectives  $Z_2$  and  $Z_3$  during the 2D-NDS). If there are no non-dominated solutions, the algorithm moves to the exploration of the top boundary, which resembles to the process described for the right boundary.

<b>Input</b>	Requests of priority class $q$ ( $M_q$ ), Search steps for objectives $Z_2$ and $Z_3$ ( $\varepsilon_{z_2}, \varepsilon_{z_3}$ ), Optimal value of the number of rejected requests' objective ( $Z_1^*$ )
<b>Output</b>	List of efficient solutions of priority $q$ ( $L_q$ )

---

```

1  Initialise the list of efficient solutions  $L_q$  to be empty
2  Initialise the number of rejected requests to be equal to  $Z_1^*$ 
3  Initialise the double-ended linked list  $DL$  with  $(+\infty, +\infty)$ 
4  while  $DL$  is not empty do
5      Right_boundary_not_treated  $\leftarrow$  True
6      while Right_boundary_not_treated = True do
7          Pop the front element of  $DL$  and denote it by  $u = (u_1, u_2)$ 
8           $WD \leftarrow$  QOSAM ( $obj = Z_4, Z_1 = Z_1^*, Z_2 = u_1, Z_3 = u_2$ )
9           $ND \leftarrow$  QOSAM ( $obj = Z_2 + Z_3 + Z_4, Z_1 = Z_1^*, Z_2 = Z_2(WD), Z_3 = Z_3(WD), Z_4 =$ 
10              $Z_4(WD)$ )
11          if  $ND = \text{Null}$  then
12              | Right_boundary_not_treated  $\leftarrow$  False
13          else
14              | Add  $ND$  to  $L_q$ 
15              | if  $u_1 < Z_2(ND)$  or  $DL$  is empty then
16                  | Add  $(Z_2(ND) - \varepsilon_{z_2}, u_2)$  to the front of  $DL$ 
17              | end if
18              | Add  $(u_1, Z_3(ND) - \varepsilon_{z_3})$  to the front of  $DL$ 
19          end if
20      end while
21      Top_boundary_not_treated  $\leftarrow$  True
22      while Top_boundary_not_treated = True do
23          Pop the back element of  $DL$  and denote it by  $u = (u_1, u_2)$ 
24           $WD \leftarrow$  QOSAM ( $obj = Z_4, Z_1 = Z_1^*, Z_2 = u_1, Z_3 = u_2$ )
25           $ND \leftarrow$  QOSAM ( $obj = Z_2 + Z_3 + Z_4, Z_1 = Z_1^*, Z_2 = Z_2(WD), Z_3 = Z_3(WD), Z_4 =$ 
26              $Z_4(WD)$ )
27          if  $ND = \text{Null}$  then
28              | Top_boundary_not_treated  $\leftarrow$  False
29          else
30              | Add  $ND$  to  $L_q$ 
31              | if  $u_2 < Z_3(ND)$  or  $DL$  is empty then
32                  | Add  $(u_1, Z_3(ND) - \varepsilon_{z_3})$  to the back of  $DL$ 
33              | end if
34              | Add  $(Z_2(ND) - \varepsilon_{z_2}, u_2)$  to the back of  $DL$ 
35          end if
36      end while
37  end while
38  return  $L_q$ 

```

**Notes:** Solution of the quadr-objective ASA model (expressions (3.1)-(3.11) combined with the passenger and apron constraints of Katsigiannis and Zografos (2021a)) with objective  $Z_i$  and constraints for the other objectives  $Z_j \forall j \in \{1,2,3,4\}/i$  (e.g. QOSAM ( $obj = Z_4, Z_1 = Z_1^*, Z_2 = u_1, Z_3 = u_2$ ) minimises  $Z_4$  constraining  $Z_1, Z_2$  and  $Z_3$  by  $Z_1^*, u_1$  and  $u_2$  respectively)

**Algorithm 3-1:** *The Quadrant Shrinking Method (QSM) adapted to the ASA problem*

The only exception is that when an  $ND$  is found,  $(u_1, Z_3(ND) - \varepsilon_{z_3})$  and  $(Z_2(ND) - \varepsilon_{z_2}, u_2)$  are added to the back of  $DL$ . As shown in Boland et al. (2017), for frontiers with a cardinality of  $|L_q|$  the QSM will solve no more than  $3|L_q| + 1$  MIPs.

At this point, it is important to note that the implementation of the QSM variant detailed in Algorithm 3-1 benefits from two efficient components. First is the utilisation of warm-start solutions, where the weakly-dominated (*WD*) solution generated in line 23 of Algorithm 3-1 is used as an initial incumbent for the generation of the non-dominated solution in line 24 of Algorithm 3-1, hence resulting in the significant reduction of the required computational times. Second is the elimination of decision variables that concern allocations that lie outside the threshold defined by the maximum displacement reported by the *WD* solution.

To provide a glance on the computational impact of this exploit, we provide the following example. Assume an airport slot allocation problem that concerns a single day of operations comprising a single request. The day concerned is discretised based on 5-minute time intervals, hence having  $288 \times 5$ -minute time intervals. During the generation of the weakly dominated solution as per Algorithm 3-1, we assume that line 23 (or line 8) resulted in a maximum displacement of  $30 \times 5$ -minute intervals ( $Z_2 = 30$ ).

Hence, by considering that the maximum displacement ( $Z_2$ ) of the non-dominated solution (line 24 of Algorithm 3-1) will be less than or equal to the maximum displacement of the weakly-dominated solution, the number of decision variables that are used in line 24 (or line 8) of Algorithm 3-1 reduces to just  $2 \times 30$  (a reduction of almost 80% in the number of variables, since in the case that there is not such a consideration, the number of variables would be 288).

### **3.3.3 Clustering module: selecting a subset of representative solutions**

Since the proposed framework integrates a solution generation module (see Steps 1, 2 in Figure 3-1 and section 3.2) that reports the complete set of non-dominated solutions, it provides full information on the properties of the non-dominated schedules that can be obtained. However, as the number of objectives increases, the

cardinality of the non-dominated set tends to increase significantly (Brunsch et al., 2014). This observation renders the decision-making process rather difficult since the stakeholders cannot fully assess the characteristics of each point. The incurred decision-making complexity is further exacerbated in the context of ASA, where each non-dominated point represents an airport slot schedule comprising of multiple airlines requests for operations spanning across multiple days. This complexity is further exacerbated by the fact that stakeholders may have diverging views with respect to both strategic and operational delay performance metrics.

On the other hand, the generation of the complete set of non-dominated points provides information on the trade-offs among the considered objectives and provides an exact mapping of the non-dominated solution space. Hence, in balancing the cardinality/complexity and the quality of the resulting set of non-dominated schedules, there is need to select a subset of non-dominated points that provide information on the diversity and the trade-offs among the multiple solutions of the non-dominated set. The selected subset of non-dominated solutions should hence be representative of the non-dominated set and should provide a comparable mapping of the solution space and information on the trade-offs among the considered operational and strategic objectives and performance metrics.

To indicate a high-quality subset of representative non-dominated schedules we employ a clustering method that allows the selection of a subset of solutions that are representative of the characteristics of the non-dominated set (see step 3 in Figure 3-1). The parameters of the clustering algorithm are optimised so as to generate representative sets of small cardinalities while maintaining a good coverage in relation to the complete non-dominated set. The algorithm that we integrate for the selection of representative solutions, is the subtractive clustering algorithm detailed in Chiu (1994).

This clustering technique is preferred over alternative methods (e.g., k-means clustering), since the cluster centres that it produces (centroids) are members of the non-dominated set and hence can be righteously presented to the stakeholders as representative solutions. Another property of the implemented technique is its consistency, since the initial cluster centres (candidate centroids) that it generates are independent of random factors (as opposed to the k-medoids algorithm, i.e., a variant of the k-means clustering selecting existing rather than artificial points). In addition, in contrast to the k-means and the k-medoids clustering algorithms, which are both NP-hard problems (Hsu and Nemhauser, 1979; Aloise et al., 2009), the selected algorithm does not require the solution to a minimisation problem (Zio and Bazzo, 2011), therefore being a tractable approach even for non-dominated sets of larger cardinalities. For the sake of brevity, we are not providing a description of the selected subtractive clustering algorithm. For a detailed description and an application of the algorithm for reducing the solution space of a tri-objective frontier, the interested reader is referred to Zio and Bazzo (2011).

In all computational results (see section 3.4.1 for the computational setup and section 3.4.3.1 for the resulting representative frontiers), the parameters (squash, radius and step) of the clustering algorithm are selected so as to propose a representative set of non-dominated solutions that has low cardinality but comparable quality to the complete non-dominated set. In order to determine the values of the parameters, we assess all possible combinations of the parameter set (*squash* ranging between 0 and 3 with an increment 0.05, *radius* ranging between 0 and 1 with an increment of 0.05 and *step size* between 0 and 1 with an increment of 0.05) and propose representative sets of different cardinalities. Then, for each set of representative points we assess the maximum quality/coverage that can be offered in relation to the complete non-dominated set.

In assessing the quality of the non-dominated and the representative sets we use the hypervolume indicator, which is a widely used metric for comparing sets of non-dominated solutions (Zitzler et al., 2003; Cao et al., 2015)<sup>8</sup>. The hypervolume indicator is a set indicator that facilitates the evaluation process of non-dominated sets by considering the cardinality, the dispersion, and the coverage of the solution space with respect to the considered objectives. In this case that the complete frontier of non-dominated points is known (since it is generated by the schedule generation module of the proposed framework), the hypervolume indicator provides a comparative assessment metric between the size, diversity and dispersion of the non-dominated space covered by the representative set, in comparison to the complete non-dominated set. Hence, the larger is the hypervolume of the representative set, the more the largest is the coverage and convergence of the representative set in relation to the complete non-dominated set.

Finally, from the multiple sets of representative points, we select the parameter set that balances the trade-off between the number of representative solutions and the coverage in relation to the complete non-dominated set. That is because by increasing the number of points in the representative set, after a certain point, the contribution of each additional representative point becomes insignificant. Hence, given that the purpose of the clustering module is to provide a meaningful reduction of the solutions offered to the decision-making process, in the computational experiments that follow the number of representative points is determined based on the following logic.

First, the full set of combinations between the *radius*, *squash* and *step size* parameters is determined and representative sets for each combination are created.

---

<sup>8</sup> Please note that in calculating the hypervolume of the complete and the representative frontiers we use as reference their common nadir point (artificial point exhibiting the maximum objective values observed in the complete non-dominated set)(Zitzler et al., 2003).

Then, the representative sets are grouped based on their cardinality and for each cardinality level, the representative set with the best hypervolume in relation to the non-dominated set is selected. Following this step, by iterating over the unique cardinality values (starting from the set with the least number of points), the parameter tuning routine, examines the marginal increase for each additional representative point. Once, the increase in terms given by a unitary increase of the cardinality of the representative set drops below 1%, the routine terminates and returns the selected number of representative points and the corresponding representative set.

Computational results determining the number of representative points and the optimal values of the clustering parameters are provided in section 3.4.3.1.

### **3.3.4 Delay estimation modules: estimation of the expected delays associated with the non-dominated and the representative schedules**

The estimation of expected delays contributes to the proposition of schedules that consider the fundamental trade-off between operational delays and scheduling efficiency, thus aiding the determination of the ‘socially-optimal’ level of operations at an airport (Swaroop et al., 2012). The consideration of operational delays provides a lookahead on the implications of the proposed ASA solutions and enables the interested parties to assess the capacity utilisation and the ability of the airport to satisfy airline demand under a certain declared capacity setting (Zografos et al., 2017b). The importance of considering operational delays has been established in tactical ASA models (Pyrgiotis and Odoni, 2015; Jacquillat and Odoni, 2015; Jacquillat and Vaze, 2018) that consider a single or a few days of airport operations (as opposed to this study that considers the airport operations during the scheduling season).

The proposed framework provides a modelling and estimation of operational delays for each non-dominated and representative schedule that is presented to the decision-makers.

#### **3.3.4.1 Estimation of operational delays for the complete non-dominated set**

Since the number of non-dominated points comprising the solution space of the tri-objective ASA problem is large, the simulation and estimation of the operational performance of each schedule that considers landside and airside operations appears to be intractable. Hence, for estimating the operational delays of the schedules composing the complete non-dominated set, the framework proposed in this work employs a tractable macroscopic operational delay estimation module.

The estimation of the operational delays associated with all non-dominated schedules (see step 2.b in Figure 3-1), before the application of the subtractive clustering algorithm presented in section 3.3.3, allows the determination of representative schedules through the explicit consideration of the operational delays associated with each non-dominated schedule. Hence, in pruning non-dominated points and presenting representative solutions to the decision makers, the proposed framework considers explicitly the operational and the strategic performance of each generated schedule.

In order to assess the benefits of the produced airport slot schedules on the congestion of the airport, there is need to have a tractable model that can provide an assessment of the generated schedules with respect to the expected delays during days of severe congestion. The main algorithm used in the literature that utilises the  $M(t)/E_k(t)/1$  model is the DELAYS model (Kivestu, 1976), which constructs epochs based on the expected service completion times of customers. The runway delay estimation module applied in step 2.b in Figure 3-1 considers runway service



times based on the  $M(t)/E_k(t)/1$  (the runway system is modelled as a single server accommodating both arrival and departure movements) and considers a queueing engine where aircraft are sequenced on a first come first served basis. An overview of the delay estimation module that is used to provide operational delay estimates for each non-dominated schedule, is provided in Figure 3-2

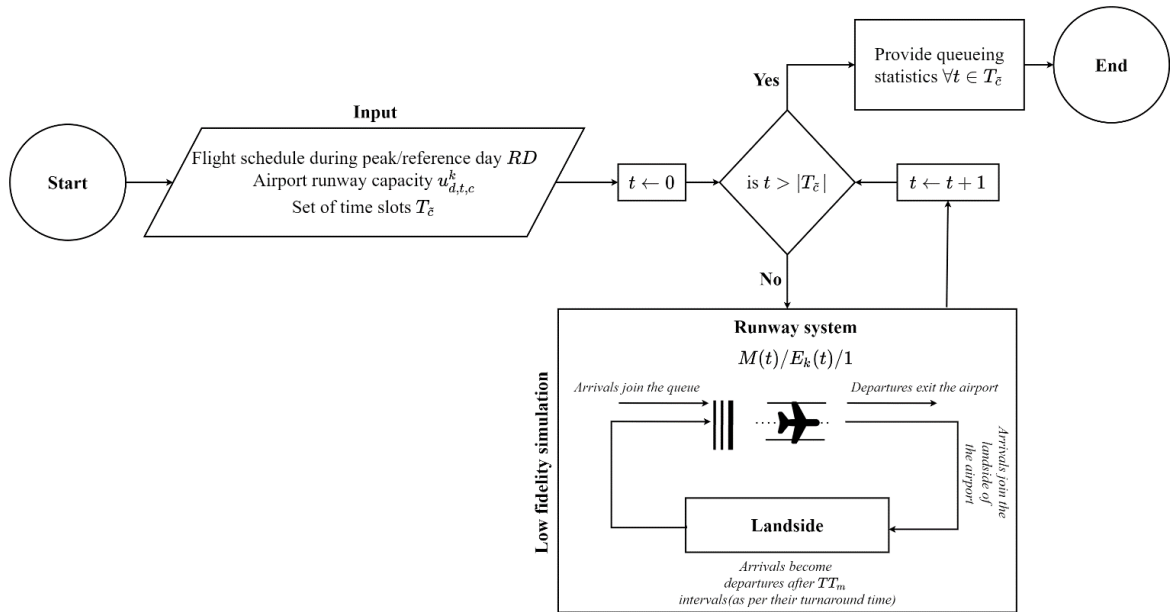


**Figure 3-2:** Schematic overview of the macroscopic operational delay estimation module

At the outset, the module requires the flight schedule obtained during a reference day of operations ( $RD$ ), the airport's runway capacity ( $u_{d,t,c}^k$ ) and the set of time slots that comprise the reference day ( $T_{\epsilon}$ ). At this point it is worth noting that the reference day is the most congested day of the scheduling season based on the number of request series that it concerns. The proposed module allows stakeholders to specify alternative reference days so as to examine the operational delays expected under less congested periods of the scheduling season.

Following the specification of the input parameters, the proposed module iterates over the time slots that compose the reference day and calculates

operational delay metrics for each time slot  $t \in T_{\mathcal{E}}$  based on the following logic. The arrival/departure movement rate per time slot is determined based on the number of aircraft that request to arrive/depart as per the flight schedule during the reference day. Similarly, the service rate of the runway system is determined by the airport's runway capacity constraints at each time slot ( $u_{d,t,c}^k$ ). Hence, the proposed approach may provide estimates on the waiting times for each time slot of the reference day without requiring heavy input and computations. The proposed macroscopic delay estimation module resembles to the airport delay estimation module proposed in the operational study of Pyrgiotis et al. (2013) which examines delay propagation across a network of airports.

Parameter  $k$  of the time-dependent  $k^{\text{th}}$ -order Erlang service-time distribution is determined so as to attain values that are equivalent to the analytical module that is used for estimating the operational delays of the representative schedules that is detailed in section 3.3.4.2. Hence, in all computational experiments, for the considered airport data, the considered parameter for the Erlang distribution is set to 2, since we observe that the estimated delays are not significantly different (less than 1.5 minutes) from the estimation module used for assessing the delays of the representative schedules.

### **3.3.4.2 Estimation of operational delays for the representative non-dominated points**

The macroscopic delay estimation module detailed in the previous section enables the subtractive clustering algorithm to prune non-dominated solutions by considering both operational and strategic delay metrics. After, the selection of the representative points, the framework employs an analytical delay estimation module that considers the operations at the entire airfield (see step 4 in Figure 3-1) and provides estimates on the delays expected during days of severe congestion.

The strategic analytical tool that we integrate at Step 4 (see Figure 3-1) of our framework (MACAD model) (Stamatopoulos et al., 2004) provides strategic decision support (Zografos et al., 2013) and models the entire airfield as opposed to other aggregate expected delay estimation models (Jacquillat and Odoni, 2015; Pyrgiotis and Odoni, 2015) that are used in the context of ASA. Indicatively, the tool considers the runway occupancy times associated with different aircraft types, the inter-arrival/inter-departure separations, the runway layout of the airport and the apron buffer capacity, hence holistically modelling the arrival/departure runway system, the arrival/departure taxiway system and the apron area (Stamatopoulos et al., 2004). MACAD provides queuing statistics (average and maximum waiting times for both arrivals and departures during the whole day) for each schedule (Stamatopoulos et al., 2004).

A particularity of the ASA problem defined by WASG, is that in order to provide expected delay estimates, there is need to consider a reference day (among the days composing the scheduling season) based on which the MACAD software will produce queuing statistics and expected delay estimates. Hence, similar to the macroscopic runway delay estimation module that is used to assess the operational delays of the complete non-dominated set, at the outset of the expected delay estimation module described hereafter, the days of the scheduling season are ordered in terms of daily congestion (number request series operating each day weighted by the number of days that each request concerns). Then the estimation of the expected delays can be conducted based on the reference day that is used to define congestion/delays or declared capacity (reference day). The literature mentions that the declared capacity is usually set based on the 65%-100% of the maximum throughput of the airport, depending on local regulations and ad-hoc analyses (Kumar and Sherry, 2009; de Neufville and Odoni, 2013; Dray, 2020). If the reference day is available or provided by the stakeholders, then the expected

delay estimation module will consider this day for estimating the expected delays, however in the event that the reference day is not available or known, the day with the most and lengthiest series can be used as a sensible proxy (ranked using  $\sum_{m \in M} a_m^d |D_m| \forall d \in D$  as per the notation in section 3.3.2) (Swaroop et al., 2012).

That is because the peak day provides a day with operations that extend to multiple other days (since it has the most series of slots) of the scheduling season. In addition to the provision of queuing statistics, MACAD may be used under different capacity or demand scenarios so as to estimate the expected delays of the selected airport slot schedule and provide insights regarding its operational feasibility and robustness (Stamatopoulos et al., 2004). The process for estimating the expected delays of each representative airport slot schedule is provided in Algorithm 3-2 (delay estimation module).

---

<b>Input</b>	List of efficient solutions or selected representatives of priority $q$ ( $L_q$ ) Reference day ( $RD$ ) Capacity scenario ( <i>scenario</i> )
<b>Output</b>	Expected delay estimates $OD_l, \forall l \in L_q$

---

```

1  for  $l \in L_q$  do
2       $DAYS_l \leftarrow$  list of days in the scheduling season ranked based on the series that
      operate on each day
3  end for
4  for  $l \in L_q$  do
5      if  $RD$  is None then
6           $RD \leftarrow DAYS_l[1]$ 
7      else
8           $RD \leftarrow DAYS_l[RD]$ 
9      end if
10     if scenario is None then
11         Use runway declared capacity parameters
12     end if
13      $OD_l \leftarrow$  Estimate delays based on scenario and  $RD$  using MACAD
14     return  $OD_l$ 
15 end for

```

---

**Algorithm 3-2:** *Expected delay estimation module*

At the outset of the delay estimation module, for each non-dominated solution  $l$  in  $L_q$  Algorithm 3-2 orders the days that the schedule concerns based on

the number of slot requests multiplied by the days that each request operates (lines 1-3 of Algorithm 3-2). Hence, the first day of the list  $DAYS_l$  is the day that maximises the number of the lengthiest slot requests that schedule  $l$  applies to (similarly the  $i^{\text{th}}$  day in  $DAYS_l$  is the  $i^{\text{th}}$  most congested in terms of daily operations). Then, a reference day is selected (RD) (lines 5-9 of Algorithm 3-2). The reference day may be selected by stakeholders based on the local regulations and parameters for measuring air traffic delays (e.g., the day that is more or equally congested than 90% of the days in the season).

Alternatively, in the absence of preferences with respect to the reference day (similar to the experiments and computational results), the consideration of the day that concerns most request series ( $DAYS_l$  [1]) may provide a suitable reference day since it considers requests that span across multiple days. Please note that the user may supply a runway capacity scenario, based on which the expected delays will be estimated. This capability allows the provision of expected delay estimates under limited, i.e., bad weather or reduced visibility, or decreased capacity conditions, i.e., capacity expansions or maintenance.

In addition, the users may supply alternative declared capacity scenarios so as to study the relationship between the slot scheduling solutions provided by the preferences of the stakeholders and the declared capacity of the airport. However, if the user does not wish to include alternative capacity scenarios, the proposed module will operate by default based on the declared capacity parameters of the airport (see lines 10-12 of Algorithm 3-2) and provide a lookahead estimate on the delays associated with each schedule. That is because the declared capacity provides a representative estimate of the runway capabilities of the airport (Morisset and Odoni, 2011) and constitutes a crucial input for the ASA process. Once the capacity scenario and the representative day are selected, the MACAD model is used to

simulate the delays of the arrivals and departures of the airport system (line 14 of Algorithm 3-2) during the reference day.

The expected delay estimates obtained using the described estimation module on data from a real-world coordinated airport are provided in section 3.4.3.4.

### **3.3.5 Schedule elicitation module**

Once the set of non-dominated solutions is generated and the representative solutions are selected, there is need to assess the performance of each point so as to select the schedule that will be finally applied. The schedule selection module (see steps 5.a and 5.b in Figure 3-1) of the proposed framework is analysed in this subsection. The schedule selection module considers: (i) the preferences of the stakeholders with respect to multiple metrics (see section 3.3.5.1); (ii) the fitness of each representative point in relation to the other points of the representative set; and (iii) the comparative efficiency of each schedule with respect to the objectives of each airline. Points (ii) and (iii) are detailed in section 3.3.5.2.

#### **3.3.5.1 Objective's prioritisation based on the Analytical Hierarchy Process (AHP)**

In order to determine the significance of each schedule with respect to multiple objectives and the preferences of the ASA stakeholders, we propose an *Analytical Hierarchy Process* (AHP) model. The AHP is a widely used (Behzadian et al., 2012) multi-criteria solution approach that decomposes complex problems into pairwise comparisons between the criteria that are significant with respect to a certain goal (Saaty, 2008).

An interesting aspect of the AHP is that it may consider both qualitative and quantitative criteria and construct weights and priorities based on the knowledge, experience and preferences of multiple stakeholders/experts (Saaty,

1989). AHP is compatible with the multi-criteria method used to assess the schedules' relative performance (see section 3.3.5.2) since it provides normalised weights that are commensurate regardless of the objective. Furthermore, the AHP has been proposed as a suitable tool for resource allocation (Ramanathan and Ganesh, 1995a) and air traffic management problems (Castelli and Pellegrini, 2011; Sidiropoulos et al., 2018), yet we observe its limited application in ASA. The only application of AHP relating to ASA is the work of Madas and Zografos (2010) that employs the technique so as to select suitable slot allocation strategies for different types of airports. Therefore, the current paper is the first to integrate the AHP to an administrative ASA solution approach. The AHP paradigm proposed in this paper is illustrated in Figure 3-3 and is further detailed below.

*The first step* of the AHP is to define the goal of the decision process. For the current study, the objective is to provide weights (prioritise) the objectives and schedule quality criteria that will be used so as to assess the performance of each airport slot schedule. *The second step* is to analyse the objective of the decision process into simpler elements which can be assessed by the participants. *The third step* organises the elements (defined in the second step) into a hierarchical structure (see Figure 3-3). The nodes of the AHP model represent the criteria, i.e., objectives and quality metrics, and the arcs/links illustrate the relationships within the hierarchy.

The highest level of the hierarchy (see Level 1 of Figure 3-3) represents the goal of the study which is to determine the importance of each objective concerning the quality of an airport slot schedule. The second level is the opinion aggregation level (see Level 2 of Figure 3-3) that is used to combine the opinions of the participants of the study. The bottom level of the hierarchy consists of the objectives and the schedule quality criteria (see Level 3 of Figure 3-3). The metrics

used at this level of the AHP model are widely used slot scheduling performance metrics (grouped under the pseudo-nodes ‘Expected delays’ and ‘Displacement related metrics’) that are used in administrative ASA models existing in the literature, i.e., maximum/total displacement, rejected/displaced slot requests, expected delays. Furthermore, regarding the expected delay metrics, additional sub-criteria are considered, i.e., the type of metric (average/maximum delay) and the type of movement (arrivals/departures). That is because the average or maximum delay associated with different types of movements may be receive different importance by the participants.

Based on this hierarchical structure, a questionnaire is built so as to extract the pairwise preferences of each expert participating in the study. Using this questionnaire, the opinions of the participating experts are expressed through the questionnaire in the form of pairwise comparisons that are used to build a square (if there are  $|J|$  criteria then the matrix is of size  $|J| \times |J|$ ) pairwise comparison matrix (let it be denoted by  $\mathcal{C}$ ). The set of the matrices for all experts is denoted by  $\mathcal{CS}$ , while the stake-holding groups of organisations are denoted by  $NG$ . The elements lying on the diagonal of each matrix represent the comparison of each criterion with itself, hence receiving values equal to one. The remaining elements of the matrix receive values ranging between  $1/9$  and  $9$ . In the case that the value of a cell  $(i, j)$  is greater than one (less than one), then the criterion of the  $i^{th}$  row is more important (less important) than the criterion of the  $j^{th}$  column. A value of one indicates equal importance. Following the extraction of the pairwise preference data, the AHP processes the pairwise comparison matrix in order to compute the vector of the objectives’ weights.



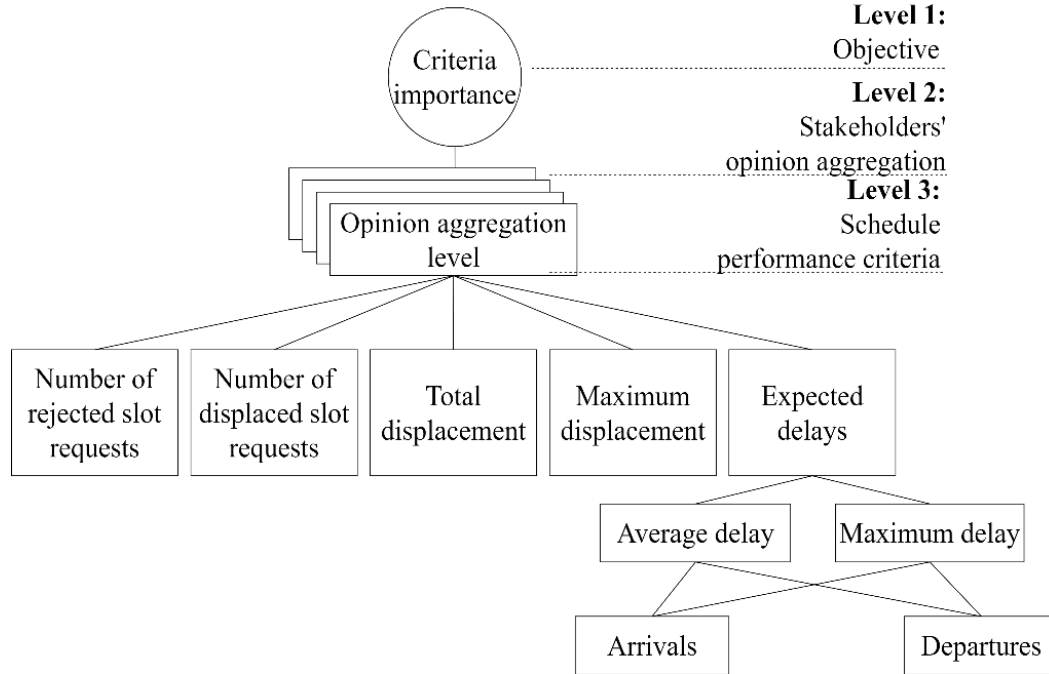


**Figure 3-3:** Illustration of the proposed AHP model

The AHP process starts by normalising the content of each pairwise preference matrix ( $s$ ) by dividing each element in  $s$ , i.e.,  $c_{jk}^s$ , by the sum of the corresponding column ( $\sum_{j'=1}^{|J|} c_{j'k}^s$ ). Then an eigenvector ( $\beta_j^s$ ) for each examined criterion ( $j \in J$ ) is calculated based on the eigenvalue approach which is given by dividing the normalised cells of the preference matrix ( $\overline{c}_{jk}^s$ ) with the number of the considered criteria  $|J|$ . Following this step, the judgements included in each pairwise preference matrix ( $s \in CS$ ) are evaluated for their consistency. This is done using the Consistency Index ( $CI$ ) and the Consistency Ratio ( $CR$ ) proposed by Saaty (1989). The  $CI$  of each participant ( $s$ ) is calculated using an estimate of the eigenvalue of the preference matrix of each participant ( $l_{max}^s$ ) using  $\sum_{j'=1}^{|J|} \left( \sum_{k'=1}^{|J|} \beta_{j'}^s c_{j'k'}^s / \beta_{j'}^s \right) / |J|$ . The consistency of the judgements of each expert ( $CI_s$ ) is calculated using  $(l_{max}^s - |J|) / (|J| - 1)$ .

Having calculated the  $CI$  for each participant, the second element that is required for the calculation of the consistency ratio is  $RI_{|J|}$ , which represents a

Random Index built based on large samples of matrices (of size  $|J|$ ) with random elements. Then the  $CR_s$  of each participant is given as the ratio between  $CI_s$  and  $RI_{|J|}$ . Based on Saaty (1989), the judgements of each participant are consistent if the  $CR$  is less than 0.1. In the opposite case, the expert that provided matrix  $C$  should be invited to revisit his/her judgements. The process described so far is repeated for all participants.

The final priorities of each criterion are calculated by aggregating the weights calculated for each expert ( $s \in CS$ ) and stakeholder group ( $g \in NG$ ). For the aggregation of the weights, we use of a simple arithmetic mean with equal scaling weights. The selection of this opinion aggregation function over the weighted geometric mean is justified by the fact that it is proved to be more appropriate in achieving consensus among the participants (Ramanathan and Ganesh, 1994, 1995b), since it satisfies the Pareto optimality axiom.

In the context of airport slot allocation, the interested stakeholder groups are the airport slot coordinating bodies, the airlines that submit requests, the airport authorities and the Air Navigation Service providers (ANS) (IATA, 2020). Hence, the number of stakeholder groups considered in this study can be set equal to 4 ( $NG = 4$ ). For the aggregation of the experts' preferences within each group ( $g \in N$ ) with respect to criterion  $j$  ( $\beta_j^g$ ), the arithmetic mean is the summation of all  $\beta_j^s$  divided by the number of stakeholders within group  $g$  ( $|CS_g|$ ). Similarly, in order to derive the weights of the schedule assessment criteria ( $\beta_j$ ,  $j = 1, 2, 3, 4, \dots, |J|$ ), there is need to aggregate the preferences across all stakeholder groups ( $g \in NG$ ). The opinion aggregation function for each criterion is the sum of all  $\beta_j^g$  ( $g \in NG$ ) divided by the number of groups considered in the study ( $NG$ ).

$\beta_j^g$  and  $\beta_j$  are calculated by considering that all stakeholders with each stakeholder group have the same influence (weight) on the determination of the priorities of each group ( $\beta_j^g$ ) and that all stakeholder groups have the same influence on the determination of the weights of the criteria ( $\beta_j$ ). This setting suggests that all stakeholder groups' have similar contributions to the ASA process while the weights of the criteria  $\beta_j$  will produce ASA scheduling solutions that satisfy the interests (expressed through the declared preferences) of the stakeholders without making discriminations between them. However, in the case that one wishes to assign different weights to each stakeholder group we may need to get additional information on the involvement and the role of the relevant experts and expert groups. In this case, one should consult the work of Hanowsky and Sussman (2008) and Hanowsky (2008) which study the appropriate selection and incorporation of stakeholders' views for the design of an Air Traffic Management Ground Holding mechanism.

The proposed hierarchy provides a generic AHP slot allocation model for the ASA problem that organises the considered schedule assessment criteria in a single level. However, alternative AHP models may organise the assessment criteria differently (e.g., by differentiating between movement types, i.e., charter vs. scheduled flights or by considering the expected delays and the displacement related metrics as distinct nodes of the hierarchy). An empirical application of the proposed AHP process, leveraging preference data from industry experts is presented in section 3.4.2. The application presented in section 3.4.2. can be used *per se* in future ASA models so as to rank automatically the non-dominated/alternative schedules, i.e., by using the objectives' weights provided in section 3.4.2. Alternatively, the proposed AHP architecture can be used so as to provide airport-specific weights, therefore allowing stakeholders in different airports to define different schedule

assessment criteria and weights based on their needs (e.g., airport strategy, national guidelines). In cases that pairwise preference data are inexistent or difficult to procure, this step can be replaced by a simple application of the schedule selection module described in the following section.

### **3.3.5.2 Schedule selection based on stakeholder preferences and each solution's performance**

Multi-criteria decision-making techniques allow the evaluation of a set of alternatives with respect to certain attributes of interest. In the context of the proposed ASA solution framework, the alternatives under evaluation are the airport slot schedules included in the non-dominated set or the set of representative solutions. Among the various multi-criteria decision-making techniques, we chose to implement a variant of the *Technique for Order Preference by Similarity to Ideal Solution* (TOPSIS) (Hwang and Yoon, 1981; Lai et al., 1994).

TOPSIS is a widely used multi-criteria technique, with logistics and transportation being among the most common areas of application (Behzadian et al., 2012). The only application of this multi-criteria approach on ASA is the work of Jorge et al. (2021) which was applied without integrating preference data for weighting the objectives. TOPSIS is selected in this study due to: (a) its scalability (suitable for treating large numbers of attributes and alternative schedules); (b) its ability to operate under limited or no preference data (Marler and Arora, 2004; Yadav et al., 2019); (c) its ability to integrate multi-objective optimisation problems (Lai et al., 1994); and (d) its compatibility with the AHP (the objectives' weighting mechanism presented in section 3.3.5.1).

These properties render TOPSIS an effective tool that can be adjusted to the presence or absence of preference data (line 1-3 of Algorithm 3-3). Regarding (d), apart from being frequently combined in hybrid AHP-TOPSIS methods

(Behzadian et al., 2012), AHP and TOPSIS are highly-compatible since the weights provided by the AHP ( $\beta_j, j = 1, 2, 3, 4, \dots, |J|$ ) are already normalised such that  $\sum_{j \in J} \beta_j = 1$ . For an intuitive presentation of the TOPSIS algorithm we refer the reader to the work of Yadav et al. (2019). The algorithm that is developed and used in this study for assessing each solution's performance is detailed in Algorithm 3-3.

---

	Non-dominated representative solutions $q$ ( $L_q$ ) indexed by $l$
<b>Input</b>	Evaluation criteria $J$
	Preference weights ( $\beta_j, j = 1, 2, 3, 4, \dots,  J  \mid \sum_{j \in J} \beta_j = 1$ )
<b>Output</b>	Ranked list of efficient solutions of priority $q$ ( $RL_q$ )

---

1	<b>if</b> $\beta_j, j = 1, 2, 3, 4, \dots,  J $ <b>is None</b> <b>then</b>
2	$\beta_j \leftarrow 1/ J , j = 1, 2, 3, 4, \dots,  J $
3	<b>end if</b>
4	Calculate the TOPSIS index for each $l \in L_q$
5	Initialise $dom_l$ for each $l \in L_q$ to be equal to one ( $dom_l \leftarrow 1$ )
6	<b>for</b> $a \in A, l \in L_q, l' \in L_q/l$ <b>do</b>
7	<b>if</b> $Z_j^a(l) > Z_j^a(l'), j = 1, 2, 3, 4, \dots,  J $ <b>then</b>
8	$dom_l \leftarrow dom_l + 100 \times ( M_a   M ^{-1})$
9	<b>end if</b>
10	<b>end for</b>
11	$RL_q \leftarrow$ ranked solutions in $L_q$ using the division of the TOPSIS index by $dom_l$
12	<b>return</b> $RL_q$

---

**Algorithm 3-3:** *TOPSIS considering other schedules that dominated airlines' objectives*

The algorithm is initiated by applying the TOPSIS using as input all representative solutions of priority  $q$  (see line 4 of Algorithm 3-3) and the stakeholders' preferences with respect to each evaluation criterion  $j$ . The preferences of the stakeholders are expressed as weights ( $\beta_j, j = 1, 2, 3, 4, \dots, |J| \mid \sum_{j \in J} \beta_j = 1$ ) and are calculated by the AHP model of section 3.3.5.1. The TOPSIS variant developed and used in this study extends the TOPSIS algorithm by considering whether an airline in a solution  $l \in L_q$  receives simultaneous deteriorations for all its objectives in relation to all other non-

dominated points in  $L_q/l$ . This is done by proposing a *dominance counter* ( $dom_l$ ) that considers the schedules in  $L_q$  where all objectives of an airline ( $a \in A$ ) are worse than those reported in  $l$  (see lines 5-10 of Algorithm 3-3).

In particular, the index is calculated for each solution ( $l$ ) by iterating over all airlines that submitted requests and counting the schedules ( $l' \in L_q/l$ ) that dominate the current solution with respect to each airlines' objectives (total/maximum displacement, displaced/rejected request, share of expected delays). If there is a schedule  $l' \in L_q/l$  where all the objectives of airline  $a$  are better (lower) than the ones reported in  $l$ , i.e.,  $Z_j^a(l) > Z_j^a(l'), j = 1, 2, 3, 4, \dots, |J|$ , then the dominance index of  $l$  ( $dom_l$ ) is increased by the share of the airline's requests in relation to the total number of submitted requests ( $100|M_a||M|^{-1}$ ). Hence, for each schedule  $l' \in L_q/l$  that dominates  $l$  with respect to the objectives of an airline, the dominance index is augmented by values in the interval (0,100) (see line 8 of Algorithm 3-3).

In this study we extend the *TOPSIS* index by dividing the fitness of each solution by the dominance counter (hereafter we will refer to this compound index as *d-TOPSIS*). The *d-TOPSIS* index captures cases where there are trade-offs between the overall schedule performance (from the viewpoint of all ASA stakeholders) and ranks solutions by balancing the relative performance of the schedule-wide and the individual airlines' objectives. As a result, a schedule ( $l$ ) that is not dominated by other schedules with respect to the objectives of the airlines, will have a dominance index value that is equal to 1, hence having a *TOPSIS* index that is equal to its *d-TOPSIS* index. On the contrary for a schedule where there are airlines whose objectives are dominated in other schedules, the value of the *d-TOPSIS* will be decreased in relation to the value of the *TOPSIS* index, hence reducing the performance of the dominated schedule in relation to the other

representative schedules. The routine terminates after sorting and returning (in a descending order) the representative solutions' list based on the  $d - TOPSIS$  index (see lines 11, 12 of Algorithm 3-3).

In this study we extend the  $TOPSIS$  index by dividing the fitness of each solution by the dominance counter (hereafter we will refer to this compound index as  $d - TOPSIS$ ). The  $d - TOPSIS$  index captures cases where there are trade-offs between the overall schedule performance (from the viewpoint of all ASA stakeholders) and ranks solutions by balancing the relative performance of the schedule-wide and the individual airlines' objectives.

As a result, a schedule ( $I$ ) that is not dominated by other schedules with respect to the objectives of the airlines, will have a dominance index value that is equal to 1, hence having a  $TOPSIS$  index that is equal to its  $d - TOPSIS$  index. On the contrary for a schedule where there are airlines whose objectives are dominated in other schedules, the value of the  $d - TOPSIS$  will be decreased in relation to the value of the  $TOPSIS$  index, hence reducing the performance of the dominated schedule in relation to the other representative schedules. The routine terminates after sorting and returning (in a descending order) the representative solutions' list based on the  $d - TOPSIS$  index (see lines 11, 12 of Algorithm 3-3).

### 3.4 Application

In order to test the applicability and the performance of the proposed framework, we use request and declared capacity data from a slot coordinated airport. In addition, we conducted an empirical study so as to leverage pairwise preference data from industry experts that work for all types of ASA stake-holding organisations. This section comprises four subsections. The first section summarises the input data (requests, capacity parameters) and the modelling parameters (section 3.4.1).

In section 3.4.2 we discuss the results of the AHP study and interpret the objectives' prioritisation provided by the different groups of experts and the consolidation of their views. In the same section, we conduct a sensitivity analysis regarding the ordering of the objectives and discuss the consistency of the solution. Section 3.4.3 comprises a thorough presentation of the results of the application of the proposed framework on the considered airport instance.

### 3.4.1 Data and experimental setup

The proposed framework is tested on data obtained from a slot coordinated airport with seasonal demand that is located in a touristic area (solely coordinated during the summer scheduling season). The considered airport instance is representative of European coordinated airports since we observe that about 20% of European airport have similar or less passenger movements per year (Odoni, 2020). The declared capacity parameters of the airport are presented in Table 3-2 and the request data is summarised in Table 3-3. The declared capacity parameters are expressed only for the 15-minute and 60-minute rolling horizons. Regarding the passenger and apron constraints and the time separation between the utilisation of the different resources of the airport we consider the set up described in Katsigiannis and Zografos (2021a).

The distribution of the submitted requests per priority type and action code is presented in Table 3-3. For instance, more than 5% of the submitted requests concern new entrants' operations. In addition, we observe 449 requests demand more than 15,000 flights (individual slots) concerning about 1,400,000 passengers. On another note, we observe that the airport has no unpaired requests. This is motivated by the fact that the airport is not used as an operational base by any of the airlines that request access to its resources (a common characteristic of most regional airports).



Resource (model parameter)	Movement ( $k$ ) and/or Type( $r, o$ )	Capacity time intervals ( $C$ )			
		15 min	30 min	60 min	180 min
Runways ( $u_{d,t,c}^k$ )	Arrivals	-	-	4(5)	-
	Departures	-	-	6	-
	Total	3	-	10(11)	-
Passenger Terminal ( $E_{d,t,c,o}^{f,k}$ )	Arrivals	-	-	1110	-
	Departures (S/NS)	-	-	1140	-
	Total	-	-	(820/820)	-
	Total	-	-	2250	-
Aprons ( $\pi_{t,d,f,r}$ )	Light	8	-	-	-
	Medium	4	-	-	-
	Heavy	3	-	-	-
	Total	-	-	-	-

**Notes:** S: Schengen and Domestic; NS: Non-Schengen; Apron capacity is expressed based on IATA's aircraft wake category (*Light (H)/ Medium (M)/ Heavy (H)*). The runway capacity during Friday and weekends is included in parentheses.

**Table 3-2:** Declared capacity parameters

The performance of the proposed framework is tested using the data from the described airport instance. In all computational results presented in section 3.4.3, we use Gurobi 9.0 (Gurobi Optimization, LLC, 2021) as the selected integer-programming solver. The model and the proposed solution algorithm are implemented in Python 3.7 programming language (Rossum, 1995) using the Anaconda distribution.

Priority	Action Code	Request series		Individual requests	
		#	%	#	%
Historic	F	126	28.1%	4304	28.0%
Other	N	222	49.5%	7412	48.1%
Changes to historic	R	55	12.2%	2264	14.7%
	L	22	4.9%	748	4.9%
New entrant	B	24	5.3%	660	4.3%
<b>All</b>	<b>Total</b>	<b>449</b>	<b>100%</b>	<b>15388</b>	<b>100%</b>

**Notes:** Changes to historic requests that accept slot times between the historic or the requested time (R), changes to historic requests that will only accept the historic slot if the requested time is not available (L), percentage (%), number (#).

**Table 3-3:** Requests' distribution and priority code

The reported computational experiments were conducted on a computer having a 1.9-GHz Intel® i7-8650U central processing unit and 31.8 GB of RAM,

running on Windows 10 pro edition. For each iteration and Mixed Integer Program (MIP) solved during the schedule generation phase of the proposed framework, we are seeking exact solutions (optimality gap less than  $1e-4$ ). In generating the set of non-dominated points for the historic's ( $H$ ) priority, we set  $\varepsilon_{z_2} = 1$  (1 x 5 minute intervals of maximum displacement) and  $\varepsilon_{z_3} = 1$  (1 displaced slot request considering the number of operating days) (see Algorithm 3-1), while for the  $CH, NE, O$  priority we set  $\varepsilon_{z_2} = 2$  (2 x 5 minute intervals of maximum displacement) and  $\varepsilon_{z_3} = 150$  (150 displaced slot requests considering the number of operating days). The values of  $\varepsilon_{z_2}$  and  $\varepsilon_{z_3}$  for the  $H$  level are the finest that could have been selected and hence result in the complete non-dominated set. Regarding the  $CH, NE, O$  level, the values of  $\varepsilon_{z_2}$  and  $\varepsilon_{z_3}$  are selected so as to provide a dense frontier without iterating over solutions where the trade-offs are negligible.

Under the selected values of  $\varepsilon_{z_2}$ , for an increase/decrease of 2 x 5-minute intervals in the value of maximum displacement, the number of displaced requests is decreased/increased by 0.5% on average and the total displacement changes by an average of 1.2%. Similarly, for the selected value of  $\varepsilon_{z_3}$ , an increase/decrease of 150 displaced requests results in an average decrease/increase of 1.7% to the value of maximum displacement and a mean change of 0.24% to the value of total displacement. Hence, the selection  $\varepsilon_{z_2}$  and  $\varepsilon_{z_3}$  for the  $CH, NE, O$  level appears to be appropriate since it results in a dense frontier while providing an accurate mapping of the trade-offs among the considered objectives (average changes to the values of the considered objectives do not exceed 1.7%).

After the generation of the schedules, we apply the subtractive clustering algorithm (see section 3.3.3). The parameters used for selecting the representative schedules, are optimised by balancing the cardinality of the representative set and its quality (expressed in terms of hypervolume in relation to the complete non-

dominated set). Extensive computational results on the selection of the clustering parameters are presented in 3.4.3.1. Furthermore, section 3.4.3.1 compares the representative with the complete non-dominated set and demonstrate that the selected clustering parameters result in a representative set that exhibits significantly smaller cardinality but disproportionately milder reductions in terms of hypervolume.

<p><b>Runway configuration parameters</b></p> <ul style="list-style-type: none"> <li>• <u>Runway set</u>: A single runway operating both arrivals and departures (as per the layout of the airport)</li> <li>• <u>Average taxi time</u>: 2 minutes and a taxi deviation of 0.75 minutes (same for both arrivals and departures)</li> <li>• <u>Apron buffer capacity</u>: 3 aircraft</li> </ul> <p><b>Runway set properties</b></p> <ul style="list-style-type: none"> <li>• <u>Arrival-Departure separations</u>: 2 minutes</li> <li>• <u>Runway set operations</u>: 0 for all time periods</li> <li>• <u>Interarrival separations</u>: ‘Loose Separations’ (option included in the software)</li> <li>• <u>Interdeparture separations</u>: ‘Strict Separations’ (option included in the software)</li> <li>• Runway set attributes: Position uncertainty (0.25), Approach Path Length (4), Wind speed deviation (0)</li> <li>• <u>Approach speeds</u>: 110 km/h (small aircraft), 135 km/h (medium aircraft), 140 km/h (medium aircraft) with a standard deviation of 5 km/h for all aircraft types</li> <li>• <u>Occupancy times(mins)</u>: Standard deviation = 0.08 <ul style="list-style-type: none"> <li>○ <i>Arrivals</i>: 0.67 (small aircraft), 0.45 (medium aircraft), 0.83 (large aircraft)</li> <li>○ <i>Departures</i>: 0.83 (small aircraft), 0.92 (medium aircraft), 1 (large aircraft)</li> </ul> </li> </ul> <p><b>Apron attributes</b></p> <ul style="list-style-type: none"> <li>• <u>Stand vacation time</u>: 20 minutes</li> <li>• <u>Stand preparation time</u>: 7 minutes (standard deviation of 1 minute) [only remote stands available in the considered airport]</li> <li>• <u>Apron stands</u>: Input as per the declared capacity parameters (8 for light, 4 for medium and 3 for large aircraft)</li> <li>• <u>Turnaround times (mins)</u>: 30 (small aircraft), 40 (medium aircraft), 42 (large aircraft) and a standard deviation of 10 minutes for all aircraft.</li> </ul>
---

**Table 3-4:** *Parameters used in the MACAD model*

Finally, in order to provide detailed estimates and statistics on the expected delays associated with each representative schedule (see section 3.4.3.4), we refine the macroscopic delay estimates provided by the queueing engine detailed in section 3.3.4.1 through the use of the MACAD model and its implementation (Stamatopoulos et al., 2004). The parameters used in MACAD are detailed in the following table (Table 3-4).

### **3.4.2 Results from the application of the AHP model**

The application of the AHP model described in section 3.3.5.1, is presented so as to derive the objectives' weights that will be used in Algorithm 3-3 so as to rank and elicit the non-dominated schedules generated by Algorithm 3-1. The pairwise comparisons submitted by each study participant are checked for their consistency with each of them having a consistency ratio below 10%.

The consistency of the aggregated preferences (for each stakeholder group and the total number of participants) is also checked. The average consistency ratio of the aggregate results is just 3.2%, which is by far less than the 10% that is required for having consistent judgements. The resulting priority weights for the ASA assessment metrics presented in Figure 3-3 are presented in Figure 3-5.

The AHP model proposed in this paper is developed based on the multi-objective ASA literature and is validated by 7 ASA experts (1 airport operator, 3 slot coordinators, 2 airline scheduling executives and 1 air navigation service executive) and completed by 15 experts representing all four identified stakeholder groups. The validation process was based on semi-structured 1-1 discussions and interviews with each expert.

During these discussions, an initial list of schedule assessment criteria was presented to the experts. The experts were then asked to assess the list of the criteria based on its completeness and the extent that it represents the current

decision-making process. This process allowed the elimination of redundant criteria and the addition of other metrics that are important for airport operations (e.g., expected delays and differentiation between arrivals and departures). After the validation, a wider pool of 15 experts (6 airport slot coordinators, 4 airline experts, 3 experts working for air navigation service providers and 2 professionals working on airport operations) completed the questionnaire and provided their pairwise preference data.

The questionnaire that the respondents were asked to complete was built using the Qualtrics Survey Software (2020). A figure exemplifying the structure of the questionnaire is provided in Figure 3-4.

How much more does the minimisation of criterion **[a]** contributes to defining the quality of an airport slot schedule in comparison to the minimisation of criterion **[b]** ?

	Which criterion contributes more to defining the quality of an airport slot schedule?	Significance of the selected metric over the alternative (1 stands for equal importance - 9 states that the selected criterion is extremely more important)								
		1	2	3	4	5	6	7	8	9
Total displacement <b>[a]</b> vs. Maximum displacement <b>[b]</b>	<b>[a]</b> ▼	○	○	○	○	●	○	○	○	○
Total displacement <b>[a]</b> vs. No. of rejected requests <b>[b]</b>	<b>[a]</b> ▼	○	○	○	●	○	○	○	○	○
Total displacement <b>[a]</b> vs. No. displaced requests <b>[b]</b>	<b>[b]</b> ▼	○	○	○	○	○	●	○	○	○
Total displacement <b>[a]</b> vs. Expected Operational delays <b>[b]</b>	<b>[a]</b> ▼	○	○	○	○	●	○	○	○	○
Maximum displacement <b>[a]</b> vs. No. of rejected requests <b>[b]</b>	<b>[b]</b> ▼	○	○	○	○	○	○	○	●	○
Maximum displacement <b>[a]</b> vs. No. of displaced requests <b>[b]</b>	<b>[b]</b> ▼	○	○	●	○	○	○	○	○	○
Maximum displacement <b>[a]</b> vs. Expected Operational Delays <b>[b]</b>	<b>[a]</b> ▼	○	○	○	○	○	●	○	○	○
No. of rejected requests <b>[a]</b> vs. No. of displaced requests <b>[b]</b>	<b>[a]</b> ▼	○	○	○	○	●	○	○	○	○
No. of rejected requests <b>[a]</b> vs. Expected Operational Delays <b>[b]</b>	<b>[b]</b> ▼	○	○	○	●	○	○	○	○	○
No. of displaced requests <b>[a]</b> vs. Expected Operational Delays <b>[b]</b>	<b>[b]</b> ▼	○	○	○	○	○	○	○	●	○

Figure 3-4: Example of the structure of the AHP questionnaire (artificial response)

### 3.4.2.1 Objective priorities' interpretation and implications

Herein we will discuss and analyse the weights obtained by the application of the proposed AHP model. In doing so, we will cluster the discussion based on the weights derived from each group of study participants, i.e., individuals working for airport slot coordinators, airlines, air navigation service providers, airport operators, as well as the consolidated/aggregate weights that are used to indicate the best compromise solution.

All discussions included below are based on Figure 3-5. For convenience and presentation purposes, we identify each criterion (a total of 8) of the proposed AHP hierarchy using an identification number (*ID*) (as in Figure 3-5).

**Aggregate objective prioritisation:** Maximum displacement appears to be the most important metric when considering the aggregate objective weights (weight equal to 0.251). The relative importance of maximum displacement is not significantly larger than the one received by the total displacement objective (weight equal to 0.241). Unexpectedly, the number of rejected requests is ranked 3<sup>rd</sup> across all stakeholder groups receiving a weight of 0.208. Most importantly, it seems that the metrics associated with expected delays received higher priority than the number of displaced requests (0.204 against 0.099). This finding underlines the importance of considering operational delay-related metrics during the initial slot allocation. Regarding the relative importance between average and maximum expected delay, it seems that the average metric is more important as per the consolidated weights. However, at the lower decision level (that concerns the movement types associated with each delay metric), the consolidated views as well as all stakeholder groups' independent views agree that the most important movement type are the arrivals. This is justified by the increased costs associated with delayed arriving aircraft, i.e., fuel consumption, and use of airspace resources.

**Coordinators' objective prioritisation:** From the coordinators' perspective the most important metric is by far total displacement (0.397) followed by the number of rejected requests (0.267) and the maximum displacement (0.172). However, it appears that the expected delays received less importance than the number of displaced requests (0.066 versus 0.098). This suggests that the coordinators assign increased importance to the displacement-related assessment criteria that are already present in the literature, i.e., number of displaced requests, total displacement, and maximum displacement. The observations regarding the lower echelons of the AHP hierarchy are similar to the consolidated results that we discussed above.

**Airlines' objective prioritisation:** Airlines' preference weights appear to be different from the views of the coordinators, further validating the existence of diverging views and the need for multiple stakeholder considerations. This stakeholder group assigns the most priority to maximum displacement (an increase of more than 47% in comparison to the aggregate importance of maximum displacement). This is justified by the fact that airlines submitting requests draft a complex schedule that tries to address the needs of passengers. Hence, minimising the maximum deviation from the requested time appears as an objective of utmost importance for airlines. The second most important objective is the number of rejected requests (importance equal to 0.25) suggesting that airlines are intolerant to potential request rejections and the incurred revenue losses.

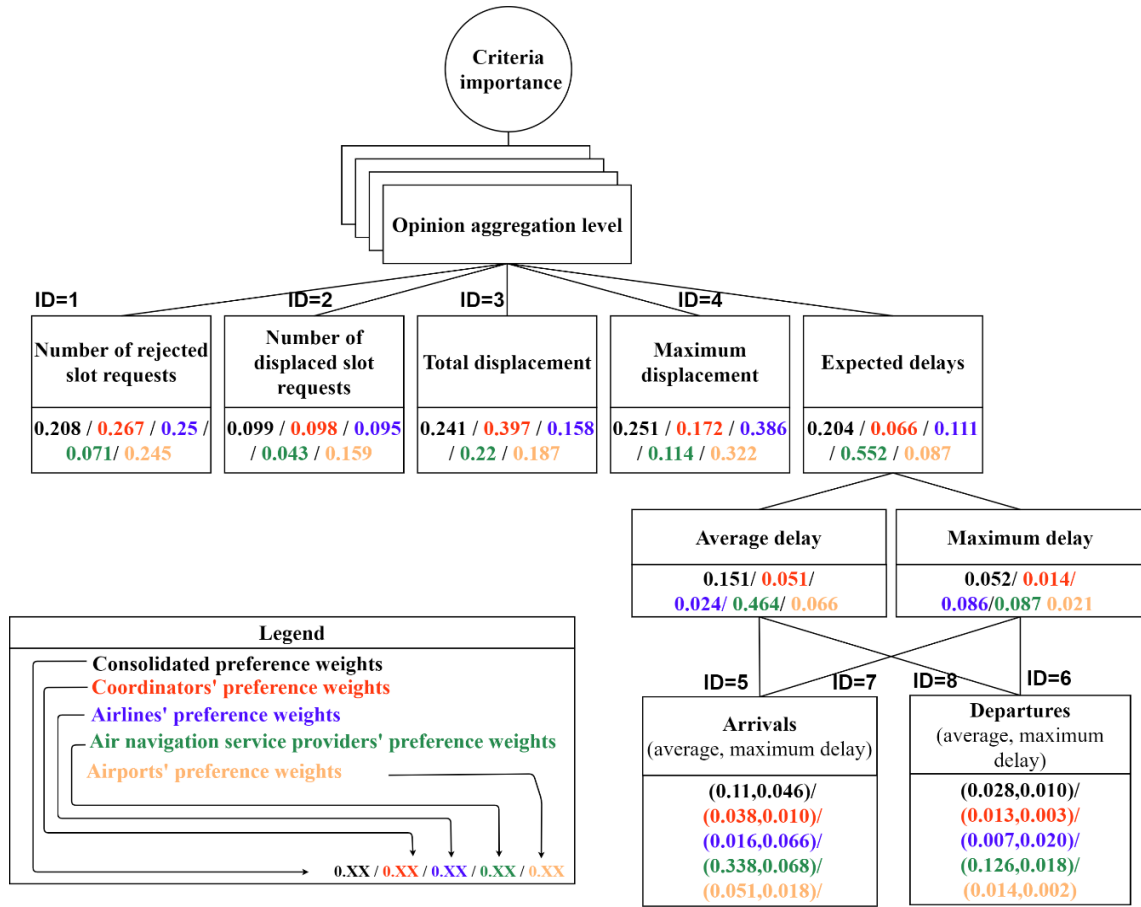


**Figure 3-5:** Objectives' priorities derived by the application of the AHP

Consequently, the total displacement objective was ranked as 3<sup>rd</sup> with a weight of 0.158. Interestingly, the expected delays appear to be of importance for airlines with a weight of 0.111. In conjunction with the above observation, the reduced importance reported for the number of displaced requests (0.095) suggests that airlines prefer to have more displaced slots if that leads to reduced maximum displacement and improved performance with respect to expected delays. Regarding the relative importance between the maximum and the average delays, study results suggest that airlines are the only stakeholder group to assign more importance to the maximum expected delay. This suggests that airlines seek to avoid cases of larger expected delays that would require them to internalise delays by paying additional man-hours and fuel costs. This observation becomes more evident when



considering that the maximum expected delays for arriving flights receive a weight that is almost 4 times larger than the importance attributed to the average delays of the same movement type.

**Air navigation service (ANS) providers' objective prioritisation:** The most eminent observation regarding this stakeholder group is the increased importance attributed to expected delays (0.55). This observation is in accordance with the nature of ANSs' services and duties. Following this metric, is the total displacement (0.22) and the maximum displacement (0.114). The number of rejected and displaced requests appear to be of lesser importance (0.071 and 0.043 respectively), thus indicating the ANS providers are willing to accept a sacrifice of a few rejected or displaced requests if that improves the performance of the schedule.

**Airport operators' objective prioritisation:** Airport operators assigned an increased importance to the maximum displacement objective (0.322) since this metric enacts as a guarantee of the airports' level of service (in the sense that there will be no requests with more displacement than a specified value). The second most important metric is the number of rejected requests (0.245) which acts as a proxy of the airport's capacity saturation. This metric is also important for airports since it determines their profitability and connectivity. The total displacement was ranked as the third objective (0.187), followed by the number of displaced requests (0.159) and the expected delays (0.087).

#### **3.4.2.2 Sensitivity analysis of the AHP weights**

Having discussed the results of the AHP study, there is need to analyse the issues that may arise during its application (Saaty, 2015; Schoner and Wedley, 1989; Stan Schenkerman, 1994). First is the uncertainty associated with the ambiguity of each criterion's relative importance. Second is the possibility of having rank reversals.

Regarding the possible ambiguity on the relative importance of each criterion, the AHP proposed in this paper does not require a scaling factor as proposed in Schoner and Wedley (1989). This is justified by the fact that during the schedule elicitation process presented in section 3.3.5.2, the relative measurement of each objective is normalised based on two crisp numeric values, i.e., the distance from the nadir and the utopia points. As a result, the value of a direct/final solution and the relative measurement of each objective are expressed based on the same scale (each criterion does not depend on its unit of measurement), thus eliminating the need for scaling.

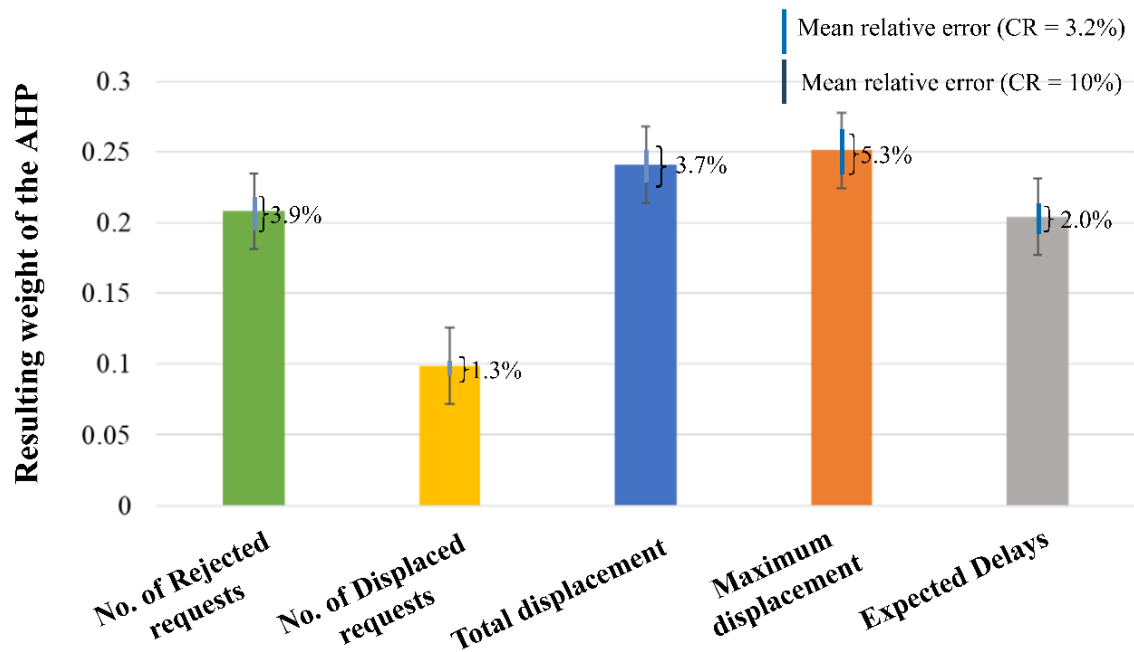


**Figure 3-6:** *Sensitivity analysis – Mean relative error of the objectives' priority weights*

Concerning rank reversals, it is important to underline that the main reasons behind this phenomenon is uncertainty regarding (i) the values of the objectives; and (ii) the judgements of the respondents (Sidiropoulos et al., 2018). Regarding the latter, the reported consistency ratio (3.2%) implies a high consistency of respondent's judgement and hence a reduced error of judgement (see Figure 3-6).

The high consistency is further justified by the large number (15 study participants) of respondents (Aull-Hyde et al., 2006) that are enabled by the multi-stakeholder design of the proposed AHP model. As for (ii), the uncertainty associated with the values of the objectives is an issue that is exogenous to the decision-making context of the ASA process, which is a strategic problem. Hence, the actual values of the objectives, i.e., displacement on the day of operations, cannot be foreseen accurately during the time of the initial slot allocation (several months prior to the day of operations). In hedging against this uncertainty, the robustness of the proposed approach is reinforced by the inclusion expected assessment metrics (e.g., maximum delays of arriving aircraft). Finally, it is important to stress that rather than being the definitive criterion for ranking and selecting the generated airport schedules, the resulting priority weights are used in conjunction with the  $d - TOPSIS$  index which anchors the ranking of each schedule to its objectives' similarity to a reference point.

By calculating the mean relative error proposed by Tomashevskii (2015) (see Figure 3-6), we may conduct a sensitivity analysis and shed light on the potential rank reversals that can occur. From Figure 3-6 it becomes evident that a high-priority objective, i.e., total/maximum displacement, cannot be reversed with an objective that received lower priority weights, i.e., no. of displaced requests or the expected delays. The occurrence of a rank reversal could only occur in cases of high inconsistencies, as those are quantitatively measured by the consistency ratio (which in this case is  $3.2\% \ll 10\%$ ).

In fact, by considering a consistency ratio that is equal to the one reported by the application of the proposed AHP model, we may have a single reversal between the total displacement and the maximum displacement objectives. However, even at this case a reversal would occur after the simultaneous

misjudgement for both objectives (given the small number of alternatives and pairwise comparisons considered in the proposed AHP model, this event is quite unlikely (Miller, 1956)).

### **3.4.3 Computational results and analysis of the schedules obtained from the proposed framework**

The purpose of this section is to discuss the results of the framework proposed in this study. This section is organised based on five subsections. At the outset, section 3.4.3.1 discusses the tuning of the clustering algorithm and its parameters and presents the resulting set of representative points for each priority level and conducts comparisons between the scheduling decisions made by the ASA stakeholders under the subtractive and complete non-dominated set. Section 3.4.3.2 conducts a comparative analysis between the schedules selected by the alternative preference scenarios. Section 3.4.3.3 compares the schedules that were selected after the alternative stakeholder preference considerations and compares their aggregate performance with the other representative schedules generated by the framework. Furthermore, we discuss the  $d - TOPSIS$  index and the factors that affect the elicitation of a schedule. A discussion on the impact of the framework on the expected delays of the selected schedules is presented in section 3.4.3.4. Section 3.4.3.5 visualises the effect of the consolidated preferences of the stakeholders and each representative solution on the objectives and allocations of each airline. Finally, section 3.4.3.6 presents a series of interactive decision support visualisations that allow stakeholders to examine each reported schedule in a disaggregate manner.

Being at the outset of the section, it is useful to define the different objective prioritisation scenarios (expressed as weights  $\beta_j$  in Algorithm 3-3) that will be used in the analyses that follow. We will denote each set of preference weights by  $\beta^g$ ,

which is superscripted by the stakeholder group ( $g$ ) or preference scenario that it concerns. In addition, given that the proposed AHP model consists of 8 assessment metrics, each  $\beta^g$  will be a set of weights of the following structure (using the *IDs* of Figure 3-5)  $\beta^g = \{\beta_1^g, \dots, \beta_8^g \mid \sum_{i=1..8} \beta_i^g = 1\}$ . Hence,  $\beta^g \forall g \in \{\text{Equally weighted (NONE), Consolidated (CONS), Coordinators (COORD), Airlines (AIR), ANS, Airports (AIP)}\}$  are defined as per Figure 3-5 as follows (each numeric value is rounded to three decimals):

- $\beta^{NONE} = \{0.125, 0.125, 0.125, 0.125, 0.125, 0.125, 0.125, 0.125\}$
- $\beta^{CONS} = \{0.208, 0.099, 0.241, 0.251, 0.111, 0.046, 0.040, 0.0107\}$
- $\beta^{COORD} = \{0.267, 0.098, 0.397, 0.172, 0.038, 0.013, 0.010, 0.003\}$
- $\beta^{AIR} = \{0.25, 0.095, 0.158, 0.386, 0.016, 0.007, 0.066, 0.020\}$
- $\beta^{ANS} = \{0.071, 0.043, 0.22, 0.114, 0.338, 0.126, 0.068, 0.018\}$
- $\beta^{AIP} = \{0.245, 0.159, 0.187, 0.322, 0.051, 0.014, 0.018, 0.002\}$

### 3.4.3.1 Selection of representative solutions and tuning of the clustering algorithm

The application of the solution generation algorithm presented in section 3.3.2 resulted in 32 non-dominated points for the historic's priority ( $H$ ). Based on the selected point for the  $H$  priority, the algorithm generated between 73-78 non-dominated points for the  $CH, NE$  and  $O$  requests (these are the two decision levels as per WASG's requirements). The computational cost required to produce the frontiers was approximately 1.9 hours for the  $H$  and 13.2 hours on average for each frontier of the  $CH, NE$  and  $O$  requests. The presentation of all non-dominated schedules to the relevant stakeholders, is a cumbersome task that introduces additional complexity to the decision-making process. As a result, there is need to select a number of representative solutions that offer comparable quality to the complete non-dominated set. The clustering algorithm integrated with our framework is tuned for each priority level ( $H$  and  $CH, NE, O$ ) so as to select a

representative set that balances the trade-off between the cardinality of the representative set and the quality of the resulting set of representative points in relation to the complete non-dominated set (expressed in terms of hypervolume). Having the complete frontier as input, we select the clustering parameters based on the following process.

During the parameter tuning routine, we generate the representative sets for all combinations of the clustering parameters (squash ranging between 0 and 3 with an increment 0.05, radius ranging between 0 and 1 with an increment of 0.05 and step size between 0 and 1 with an increment of 0.05). During the application of this step, we observed that the step size parameter does not affect the outcome of the clustering procedure. As a result, in the analyses that follow the step size parameter is omitted and we focus our discussion on the squash and the radius parameters. Second, we group the representative sets based on the number of representative points that they have and observe the maximum coverage for each number of representative points regardless of the parameter combination. This second step allows us to determine the best possible coverage given by representative sets of different cardinalities and obtain the performance curve of the clustering algorithm for different numbers of representative solutions. As a result, for each decision level of the WASG priorities, we are able to reduce the number of generated points and the decision complexity associated with their presentation to the decision-making process.

**Results relating to the historic's ( $H$ ) level:** In subplot (a) of Figure 3-7, we observe that by using 5 representative solutions, the subtractive clustering algorithm is able to achieve a coverage of 76.3% in relation to the complete non-dominated set (exhibiting a hypervolume of 377,532). After this point, each additional representative point improves the hypervolume by less than 1.5% for up

to the 15 representatives and less than 1% on the overall average, thus implying that the benefits in terms of coverage are outpaced by the complexity incurred by the added solutions. The parameters that resulted in the representative set are provided in subplot (b) of Figure 3-7, i.e.,  $H$  level. Under this parameter set, the subtractive clustering reduces the number of points from 32 (as reported in the complete non-dominated set) to just 5 points in the representative set. Concurrently, the hypervolume of the representative set covers 76.3% of the complete set's hypervolume.

Given, the fact that the hypervolume indicator assesses the dispersion, cardinality, and convergence of the representative set in comparison to the complete non-dominated set, the quality achieved by the five points of the representative set, stands as proof of its representativeness and the ability of the subtractive clustering algorithm to reduce decision-complexity. The resulting representative and complete non-dominated sets for the  $H$  priority are provided in Figure 3-8. In both cases, all alternative preference considerations converged to the same schedule. Hence, under the two settings (the complete and the representative sets), the schedule selected for the  $H$  level is not affected by the stakeholders' preferences. The reason behind the convergence to a single point, is that in contrast to the general case where  $H$  requests receive no displacement, the current airport instance has reduced runway capacity in comparison to the previous scheduling season and introduces mild displacements for a few request series. Hence, despite the multiple non-dominated points, the variability in terms of objectives is not significant. In fact, there are no more than 12 request series which receive different allocations amongst the schedules comprising the complete frontier.

In comparing the schedules selected under the two alternative frontier settings, we observe insignificant changes with respect to the various performance

metrics. With respect to the location of the selected schedules in the solution space, we observe that they lie in proximity and hence the performance metric values that they report are not significantly different. Table 3-5 provides a comparative analysis between the values of the performance metrics of interest.

First, the maximum displacement of the two objectives is identical, i.e., 6 x 5-minute intervals, while there are slight differences with respect to the number of displaced requests (from 141 displaced requests in the schedule selected when considering the complete non-dominated set, to 140 displaced requests in the schedule selected when considering the representative frontier) and the value of the total displacement objective (from 554 x 5-min intervals in the schedule selected when considering the complete non-dominated set, to 632 x 5-min intervals in the schedule selected when considering the representative frontier).



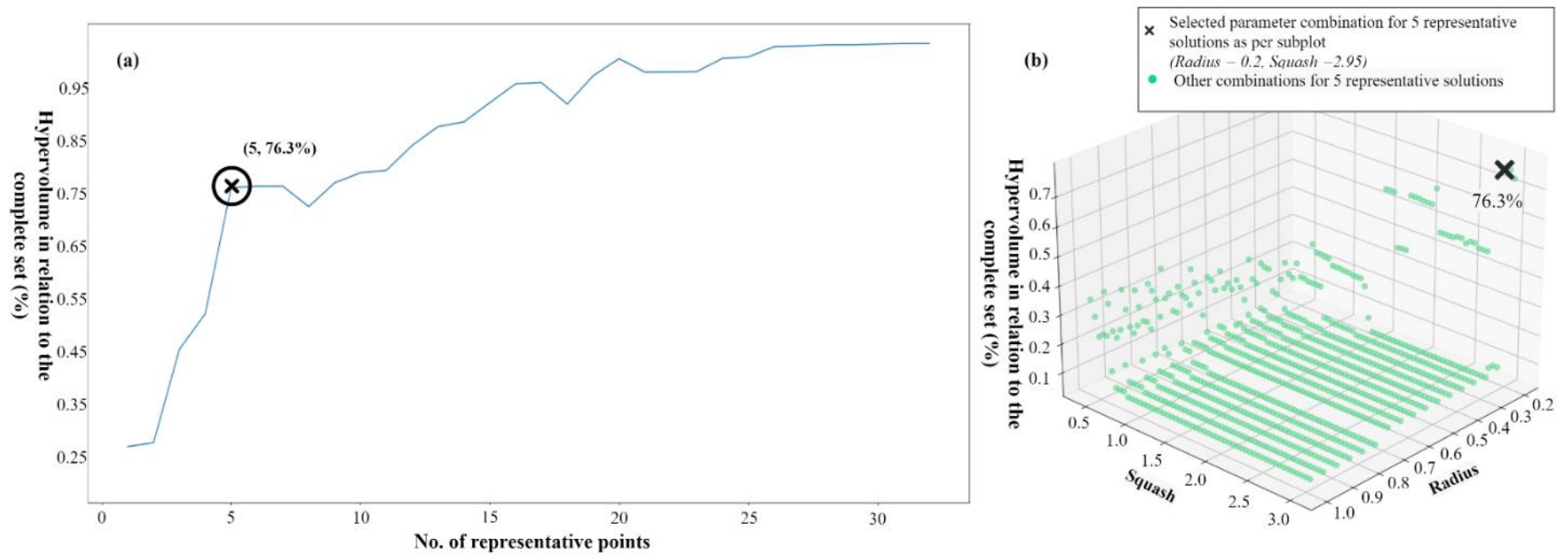


**Figure 3-7:** Determination of the representative points and the clustering parameters for the H level

The increase in terms of total displacement in the schedule selected under the representative schedule is compensated with improvements with respect to all operational performance metrics. However, due to the fact that the differences between the two schedules are limited to 7 request series, we observe that the differences with respect to the two schedules' operational performance are mild (do not exceed 0.16 minutes for maximum delays and 0.11 minutes for departures).

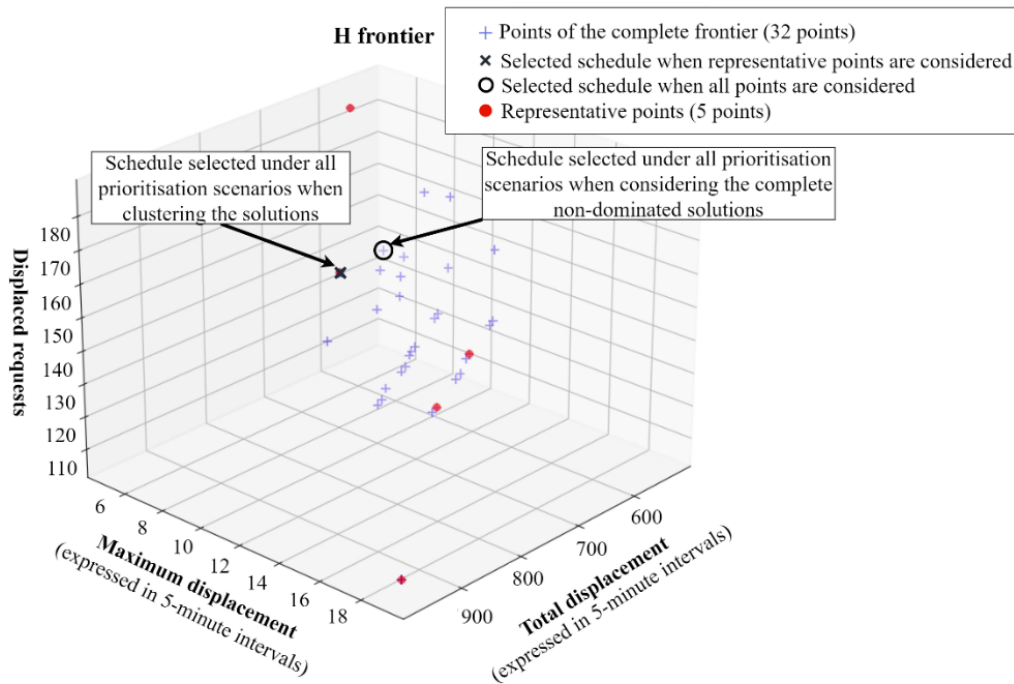


**Figure 3-8:** Demonstration of the complete and the representative frontiers for each stakeholder group (*H* priority)

This comparative analysis validates that the subtractive clustering algorithm does not compromise the quality of the scheduling alternatives that are provided to the decision-makers. The neutrality of the schedule pruning procedure is supported by the fact that the schedules selected when considering the complete and the representative sets exhibit similar values for all considered metrics and lie in proximity in the solution space. To conclude, for the *H* priority level, the subtractive clustering algorithm elicits a representative set with 84% less schedules

in comparison to the complete set of non-dominated schedules but has a hypervolume that is reduced by 23.7%. For the sake of completeness, a similar comparative analysis is provided for the *CH, NE, O* level in the remainder of this section.

**Results relating to the *CH, NE, O* level:** Since the solution generation module is solved for each priority level defined in WASG, the frontier generated for the historic's level constraints the capacity for the level of the other requests' level and thus determines the generated non-dominated set. Hence, for the two schedules selected for the historic's requests (as demonstrated in Figure 3-7 and Table 3-5), there is need to generate two distinct frontiers for all other requests. Figure 3-9 provides a concise visualisation of the frontiers generated by the consideration of the representative and complete non-dominated sets, and the corresponding schedules (as presented in Figure 3-8 and Table 3-5) for the *H* level. The two frontiers have different cardinalities (the frontier generated by considering the representative points comprises 78 non-dominated schedules, while the frontier generated by considering the complete non-dominated set comprises 72 points) and hypervolumes (1,076,351,892 for the frontier in subplot b.1 of Figure 3-9; and 1,045,878,632 frontier in subplot b.2 of Figure 3-9).

In addition, we observe that when clustering the non-dominated points of the *CH, NE, and O* level (based on the clustering routine's results presented in Figure 3-10 the resulting representative set (see subplot b.1. of Figure 3-9) is composed by 10 non-dominated points (as opposed to the complete non-dominated set that comprises 78 points), which are able to cover over 70% of the hypervolume of the complete non-dominated set presented in subplot b.1 of Figure 3-9. Similar to the *H* level, the proposed approach for selecting representative schedules results in a significant reduction with respect to the number of points that are presented

to the decision-makers and does not introduce significant compromises with respect to the hypervolume of the complete non-dominated set.

Performance metrics		Schedule set – selected schedule	
		Complete	Representative
Displaced requests		141	140
Maximum displacement (5-min intervals)		6	6
Total displacement (5-min intervals)		554	632
Max operational delays (minutes)	Arrivals	7.29	7.13
	Departures	8.37	8.22
Mean operational delays (minutes)	Arrivals	3.68	3.60
	Departures	3.98	3.87

**Table 3-5:** Comparison of the  $H$  schedules selected by considering the complete and the representative schedule sets

In subplots b.1 and b.2 of Figure 3-9 we observe that the consideration of stakeholders' preferences results in different airport slot scheduling solutions. In subplot b.1 (schedule selected by considering the representative schedules), we note that stakeholders' preferences converge to the selection of two schedules. In particular, the airports and the airlines' preferences indicate the same schedule that the no preference and the consolidated preference scenarios selected. Air navigation service providers and coordinators' preferences resulted in another scheduling alternative. On the other hand, when considering the complete non-dominated sets, there are three different schedules that are selected by the alternative stakeholder preference considerations. The airports' preferences result in a schedule that is different from the schedules selected by the other preference scenarios. Furthermore, the airlines', the no preference and the consolidated scenarios converge to the same schedule, while air navigation service providers agree with the slot coordinators on a different schedule.

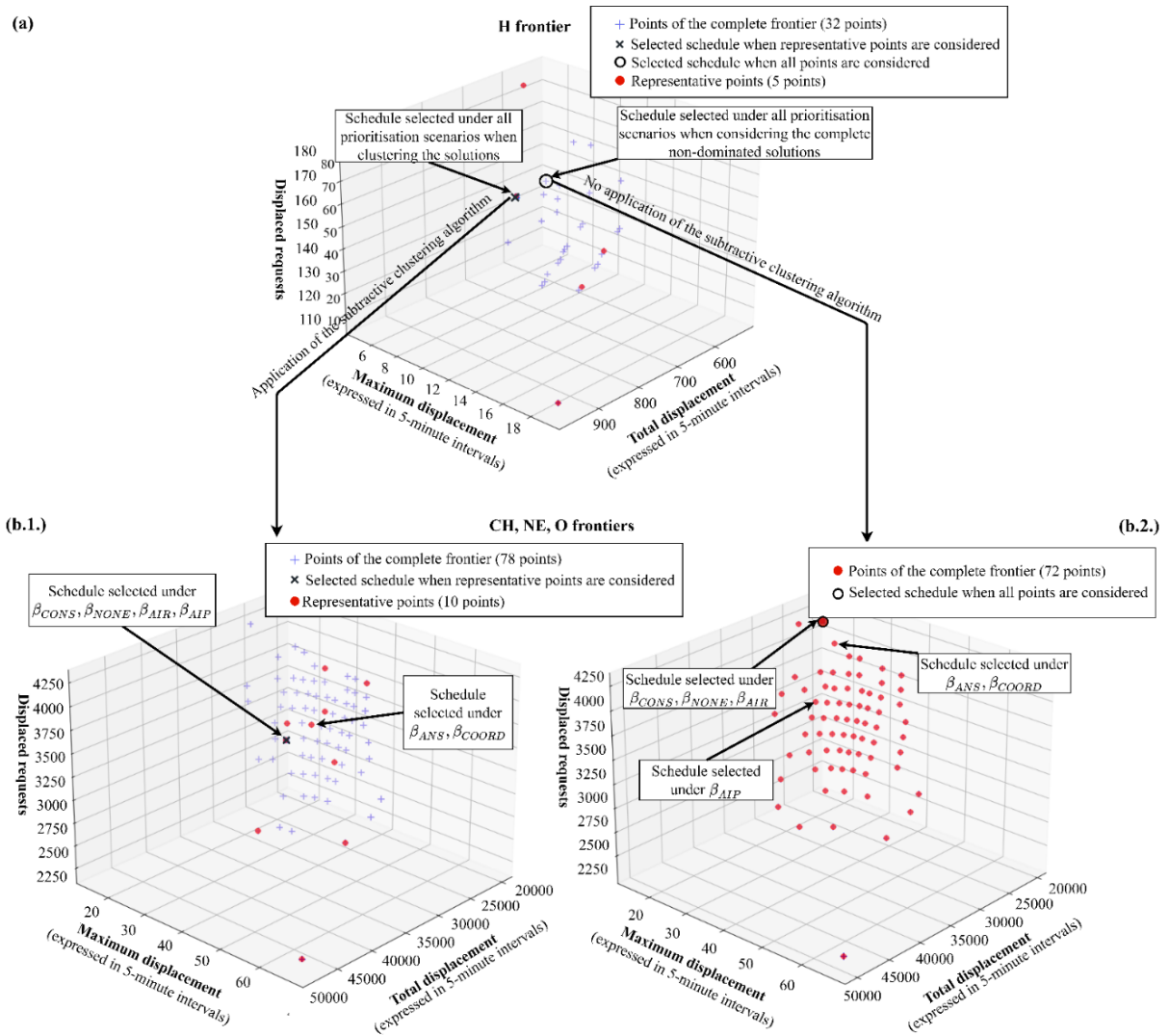


**Figure 3-9:** Diagrammatic representation of the frontiers generated from the selected *H* schedules

To facilitate comparative analyses and discussions on the schedules selected by the alternative stakeholder considerations under the representative and the complete sets (as per subplots b.1 and b.2 of Figure 3-9), Table 3-6 provides the values of the operational and strategic performance metrics of interest associated with each schedule. In both sets of non-dominated points (the representative and the complete), the coordinators and the air navigation service providers' preferences result in schedules of less displaced requests and total displacement as compared to

the schedules selected by the other preference scenarios. This reduction is at the expense of maximum displacement (which increases by 2 x 5-min intervals when considering the complete frontier, and 3 x 5-min intervals when considering the representative frontier) but also leads to lower levels of maximum and average expected delays.

Furthermore, we observe that the schedules provided by the consideration of the representative sets exhibit improved values for all operational delay metrics but increased values for maximum displacement. In addition, the number of displaced requests reported in the schedules selected when considering the representative set, dominates the number of displaced requests reported by the schedules that are selected when considering the complete non-dominated set.

This set of findings confirms that the reduction of decision complexity achieved by the representative set, results in different airport slot scheduling solutions without significantly compromising the quality of the decisions made by the ASA stakeholders. This statement is motivated by the fact that despite the reduced points presented to the decision-makers (the representative set in subplot b.1, Figure 3-9 has a cardinality that is 87% smaller than the cardinality of the complete non-dominated set in subplot b.2, Figure 3-9), the schedules reported when considering the representative set of schedules are not dominated by the schedules selected when the full frontier is made available to the ASA stakeholders.

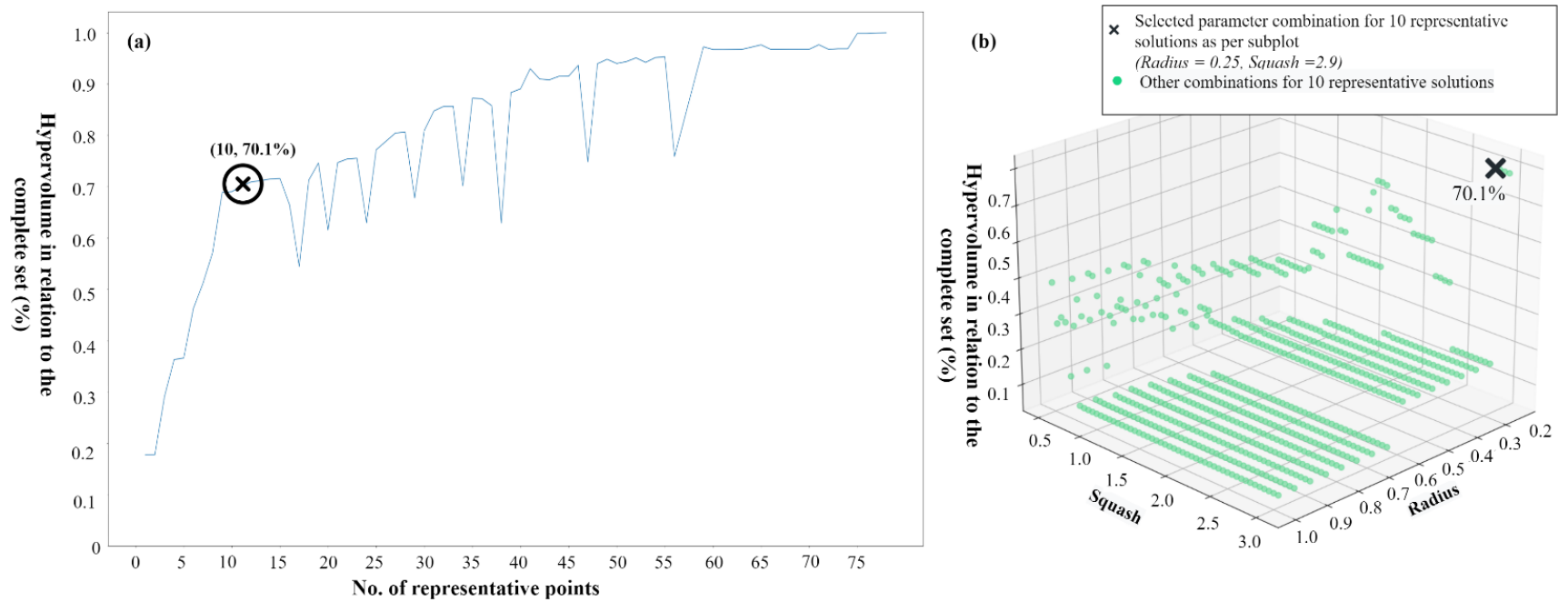


**Figure 3-10:** Determination of the representative points and the clustering parameters for the CH, NE, and O level

Performance metrics		Schedule set – selected schedule				
		Complete frontier (as per subplot b.2 of Figure 3-9)			Representative (as per subplot b.1 of Figure 3-9)	
		AIP	AIR, CONS, NONE	ANS, COORD	AIP, AIR, CONS, NONE	ANS, COORD
Displaced slots		3401.00	4229.00	3999.00	2981.00	3131.00
Maximum displacement (5-min intervals)		18.00	18.00	20.00	21.00	24.00
Total displacement (5-min intervals)		23697.00	22523.00	21737.00	24194.00	21907.00
Maximum operational delays (minutes)	Arrivals	22.13	21.73	21.61	20.92	19.18
	Departures	26.07	26.91	27.34	26.46	26.29
Mean operational delays(minutes)	Arrivals	11.55	11.37	10.78	11.58	11.25
	Departures	15.77	14.22	14.47	15.51	14.69

**Table 3-6:** Comparison of the CH, NE, O schedules selected under the complete and the representative schedule sets



**Implications of the clustering algorithm and the parameter tuning procedure for decision-making:** Since the parameters of the clustering algorithm are optimised and are not considered as static input, the proposed tuning routine can be used by practitioners, regardless of the airport instance, the number of objectives (herein the algorithm's parameters are optimised based on 7 objectives/performance metrics) and the solution generation module, so as to determine the number of alternative airport slot schedules that will be considered for application. The optimisation of the clustering parameters results in representative sets that balance the trade-off between the number of representative solutions and the coverage of the representative set in relation to the hypervolume of the complete non-dominated set. For the considered airport instance, the proposed parameter tuning routine suggested that by using only 13%-15% of the generated airport slot schedules as representative schedules we receive a frontier of comparable quality to the complete non-dominated set (the hypervolume was more than 70%-76% of the hypervolume offered by the complete non-dominated set).

With respect to the decisions made by the different groups of ASA stakeholders, we observe that the representative set leads to schedules that are non-dominated when considering the points of the frontier generated by considering the complete spectrum of slot scheduling alternatives. Interestingly, if one would like to select a representative set that is different from the one suggested by the parameter tuning routine, the proposed clustering and parameter tuning procedure allow the interested parties to explore, for alternative numbers of representative schedules, the maximum hypervolume that can be achieved (see subplot (b) of Figure 3-7 and Figure 3-10). This functionality facilitates the selection of the appropriate number of representative points based on the requirements of the decision-making process in different airports. On another note, since the

alternative/representative schedules composing the representative set comprise of alternative allocations, the proposed methodology provides to the coordinators and the other stakeholders a set of alternative allocations that can be negotiated before and during the bi-annual slot scheduling conferences. In addition, the representative sets proposed by the proposed clustering algorithm and the parameter tuning routine can be righteously presented to the stakeholders without needing adjustments. This is due to the fact that the representative solutions are non-dominated airport schedules that are generated by the solution generation module of our framework. Ultimately, the selected clustering algorithm selects representative solutions based on a deterministic process and hence can provide consistent results and support airport slot coordinators in proposing alternative allocations to requests that could not receive their requested timings. This observation is in line with the requirements of the ASA decision environment which requires consistency during the initial slot allocation process (IATA/ACI/WWACG, 2020). After validating the ability of the proposed clustering algorithm to reduce decision-complexity through the selection of high-quality airport slot schedules, the discussions included in the sections that follow, focus on the points of the representative set, and provide in depth analyses on the decision-making implications of the representative schedules.

#### **3.4.3.2 Selected schedule under alternative preference considerations**

In this section, we present the representative schedules relating to the considered airport instance. In doing so, we will compare the schedules that were selected through the consolidation of the stakeholders' preferences and the schedules that would be selected based on the consideration of the preferences of each stakeholder group *per se*.

With respect to the stakeholders' preferences, for the  $H$  (historics') level all objectives' prioritisation scenarios resulted in the same point. This outcome is justified by the fact that among the representative schedules belonging to the  $H$  frontier (5 points as per Figure 3-8), all alternative preference scenarios result in a point with a  $D - TOPSIS$  index that is greater than the indexes of the other representative solutions. Out of the multiple non-dominated schedules generated for the  $H$  level (32 in total), the five representative solutions (denoted by red points in Figure 3-8) provide a good coverage of the frontier and exhibit significantly different objective values, thus providing a set of alternatives with non-homogeneous properties (see section 3.4.3.1). At the lower decision level which consists of the  $CH, NE$  and  $O$  requests, different prioritisation scenarios result in different non-dominated points and airport slot schedules. In particular,  $\beta^{ANS}$  and  $\beta^{COORD}$ , resulted in a point that is different from the point indicated by the other preference scenarios. The cardinality of the non-dominated set for this lower decision level is 78 schedules (of whom we selected 10 points as representatives as per section 3.4.3.1). The selected schedule at the  $H$  level is combined with the 10 points at the  $CH, NE$  and  $O$  level so as to provide 10 alternative aggregate airport slot schedules.

By observing Figure 3-9 and Figure 3-11 we note that the prioritisation scenarios  $\beta^{AIP}$ ,  $\beta^{AIR}$ ,  $\beta^{CONS}$ ,  $\beta^{NONE}$  resulted in the same schedule (identified in Figure 3-11 as Group 1). Furthermore,  $\beta^{ANS}$  and  $\beta^{COORD}$  resulted in a different schedule (identified in Figure 3-11 as Group 2). In order to construct the schedule of Group 1 we combine the representative point selected at the  $H$  level and the representative point selected by  $\beta^{AIP}$ ,  $\beta^{AIR}$ ,  $\beta^{CONS}$ ,  $\beta^{NONE}$  at the  $CH, NE$  and  $O$  level. Similarly, to construct the Group 2 schedule we combine the representative point selected at the  $H$  level and the representative point selected by  $\beta^{ANS}$  and  $\beta^{COORD}$  at

the *CH,NE* and *O* level. Figure 3-11 provides a visual comparison of the two aggregate schedules that were selected by the alternative preference considerations. For the sake of clarity, the discussion is organised as per the objectives concerned.

**Displacement-based assessment metrics (Maximum/Total displacement, Displaced requests):** Regarding the maximum displacement objective, we observe that the schedule selected by Group 1 received a maximum displacement of 21 x 5-minute intervals, i.e., 105 minutes. In contrast, the preferences of ANS and COORD resulted in a schedule of increased maximum displacement, i.e., 24 x 5-minute intervals. This is justified by the fact that Group 1 concerns stakeholder groups which expressed significant aversion towards high values of maximum displacement. In contrast, coordinators prioritised total displacement over maximum displacement and air navigation service providers considered the operational delays as their most significant set of performance metrics.

In addition, we observe that the schedule selected by Group 1 provides a good trade-off between the maximum displacement and the other two objectives that were used for the generation of the frontier, i.e., total displacement, and displaced requests, which also received increased significance by airlines and coordinators. The best total displacement objective value among the two selected schedules is reported by Group 2 (22,539 x 5-minute intervals), while Group 1 preferences converged to a schedule with an increased total displacement (an increase of 9.3% in comparison to Group 2).

Regarding the number of displaced requests, we observe that Group 1 received the best objective value (3121 displaced requests) at the expense of total displacement and the operational delay metrics. Group 2 received the maximum of the two schedules concerning the displaced requests' objective (3271 displaced

requests). One can observe the trade-offs among the considered displacement-related objectives and the preferences of the stakeholders.

**Expected delay assessment metrics:** With respect to the expected delays, we observe that the intensity of the trade-offs is milder. First is that the expected delay metrics are approximated without being optimised explicitly and second is that the expected delay metrics are measured for a single day of operations (the metrics do not span across the whole scheduling season since they concern a single day of operations).

However, we observe that the schedule of Group 1 reports higher values for all expected delay metrics, i.e., average/maximum expected delays for arriving/departing movements, while Group 2 reported the best values. Between these two schedules, we observe a trade-off between the displacement-related performance metrics and the expected delay metrics. Group 1 schedule exhibits lower maximum displacement and displaced requests but increased expected delays and total displacement in comparison to Group 2.

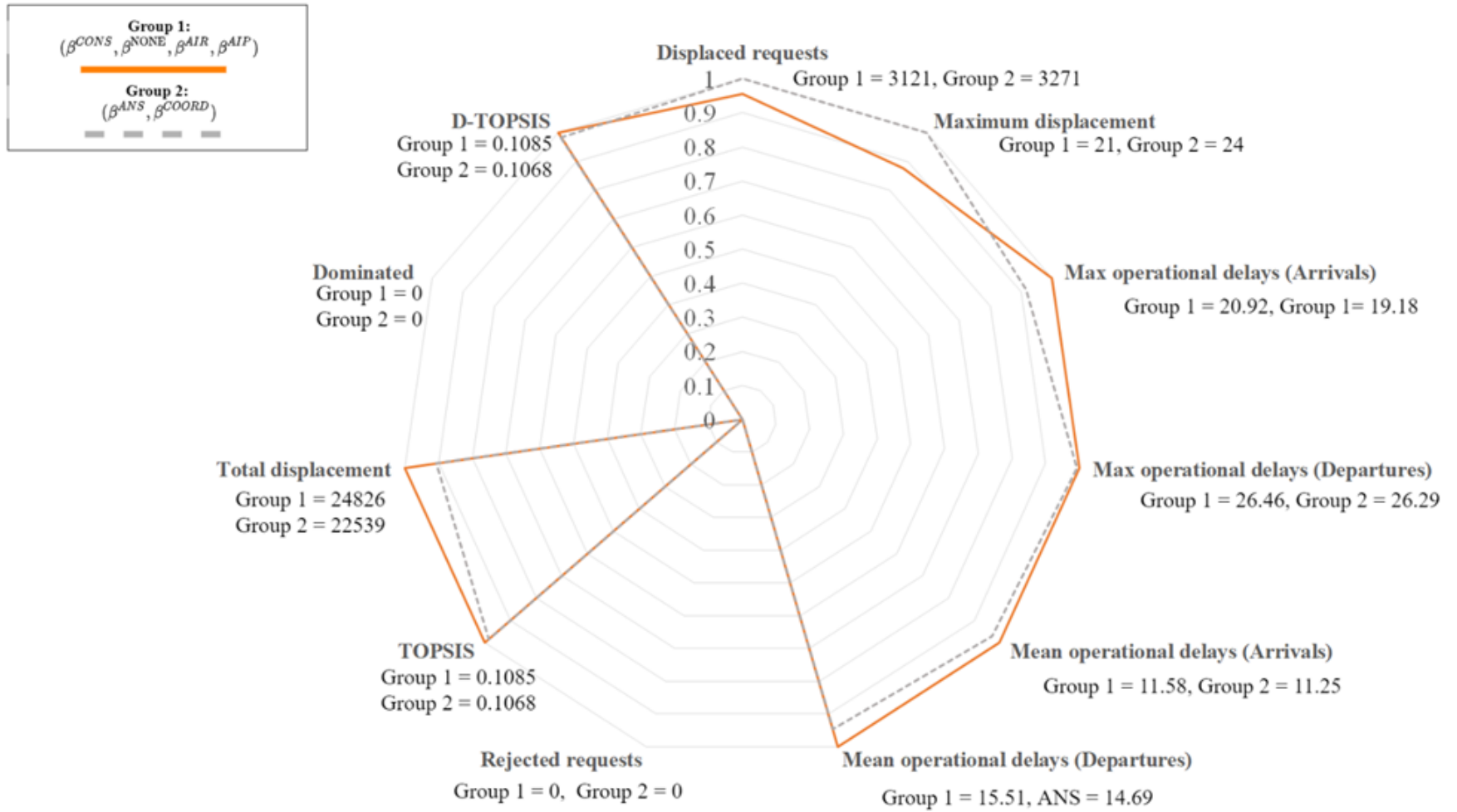


Figure 3-11: Comparisons between the selected schedules of the different stakeholder groups

### 3.4.3.3 Comparison of the selected schedules and the non-dominated representative points

A useful functionality of the proposed framework is that in addition to the schedules selected by the alternative preference considerations, it reports the non-dominated representative solutions that are provided by the clustering module.

This allows the pertinent stakeholders to examine the alternatives that they have at hand, their objective values, and their performance with respect to their preferences. In this section we provide *value path diagrams* (see subplots (a) and (b) of Figure 3-12) which aid ASA stakeholders in understanding the trade-offs between the objectives under consideration (Dal Sasso et al., 2019). The diagrams facilitate comparisons between the schedules indicated by the stakeholders' preferences (Group 1 and Group 2) and the remaining representative non-dominated solutions (Rep 1 – Rep 6). The weighting scenario considered for reporting the  $d - TOPSIS$  index is  $\beta^{CONS}$ . The values reported on the vertical axis of the subplots (ranging between 0 and 1) are normalised using the percentage difference between each solution and the minimum value of the corresponding performance metric (Dal Sasso et al., 2019; Katsigiannis et al., 2021).

Figure 3-12 comprises two subplots. Subplot (a) contains value paths representing the trade-offs among the expected delay metrics, while subplot (b) presents value paths concerning the displacement-related and the performance indices ( $d - TOPSIS$  and  $TOPSIS$ ). For the sake of clarity, each subplot is discussed independently.

#### **Discussion on the expected delay metrics (subplot (a) of Figure 3-12):**

The solution selected by  $\beta^{AIP}$ ,  $\beta^{AIR}$ ,  $\beta^{CONS}$ ,  $\beta^{NONE}$  (identified in Figure 3-12 as Group 1) exhibits increased values for all expected delay metrics. On the other hand, the solution reported by the Group 2 weighting considerations, the best values for all

expected delay metrics. A common observation for all reported schedules is that there are significant trade-offs between the maximum and the average (mean) expected delay performance metrics, i.e., low values at the maximum delays of arrivals (departures) result in high values for mean delays for the same movement type and *vice versa*.

**Discussion on the displacement-related metrics (subplot (b) of Figure 3-12):** The trade-offs among the displacement-related performance metrics are more intense. Hence, the representative points are alternatives that are diverse with respect to the objectives used to generate the frontier. Among the representative solutions we observe intense trade-offs which indicate that the considered objectives are conflicting. Each reported solution appears to yield different trade-offs among the objectives, but we are able to make some general remarks that are particularly useful for ASA stakeholders. First is that there is a strong trade-off between total and maximum displacement for all solutions, i.e., low (better) values for the maximum displacement objective, imply increased (worse) values for the total displacement objective. A strong trade-off relationship is reported between the number of displaced requests versus the maximum displacement, while we observe milder trade-offs between the number of displaced requests versus the total displacement. In this case, all solutions receive lower total or maximum displacements at the expense (increase) of displaced requests and *vice versa*.

**Discussion on the schedule performance indices (subplot (b) of Figure 3-12):** Regarding the schedule performance indices reported in this work, we observe that for four points (Rep 3, Rep 4, Rep 5 and Rep 6) the dominance counter suggests that the airlines' objectives are dominated by other representative solutions since  $d - TOPSIS < TOPSIS$ . An interesting observation is that the schedule denoted by Rep 3 reports the best value for the TOPSIS index among the



representative points but performs poorly when observing the  $d - TOPSIS$  index. This finding suggests that there exist schedules that compromise individual airlines' objectives (as per the metrics of Figure 3-12) so as to achieve improved overall scheduling performance (measured by  $TOPSIS$ ). In the case that a schedule is to be selected on the basis of all stakeholders, then all representative solutions are admissible, and the airline-dominated solutions may not be filtered out, however if the stakeholders do not wish to examine airline dominated solutions, Rep 3 - Rep 6 may trivially be filtered out. Fortunately, the  $d - TOPSIS$  index proposed in this work hedges against this phenomenon by prioritising schedules that are airline non-dominated. The schedules selected by the alternative preference considerations of the stakeholders, i.e., Group 1, Group 2, are airline non-dominated. Please note that the schedule Group 1 (selected by the consolidated preference scenario) reported the second-best for  $TOPSIS$  and the best values for  $d - TOPSIS$ . In addition, we note that as per the  $\beta^{CONS}$  ranking presented in subplot (b) of Figure 3-12 ranked the Group 2 schedule second based on the  $d - TOPSIS$  index.

A finding that relates to both displacement-related and expected delay objectives, is that there appears to be a negative correlation between the maximum displacement and the expected delay metrics, i.e., the more we increase maximum displacement the more we reduce the maximum delays for arrivals and departures. This is justified because increased maximum displacement leads to a wider spread of the requests throughout their day of operations and hence results in reduced expected delays. In the next section, we provide further insights on the expected delays of the selected schedules.

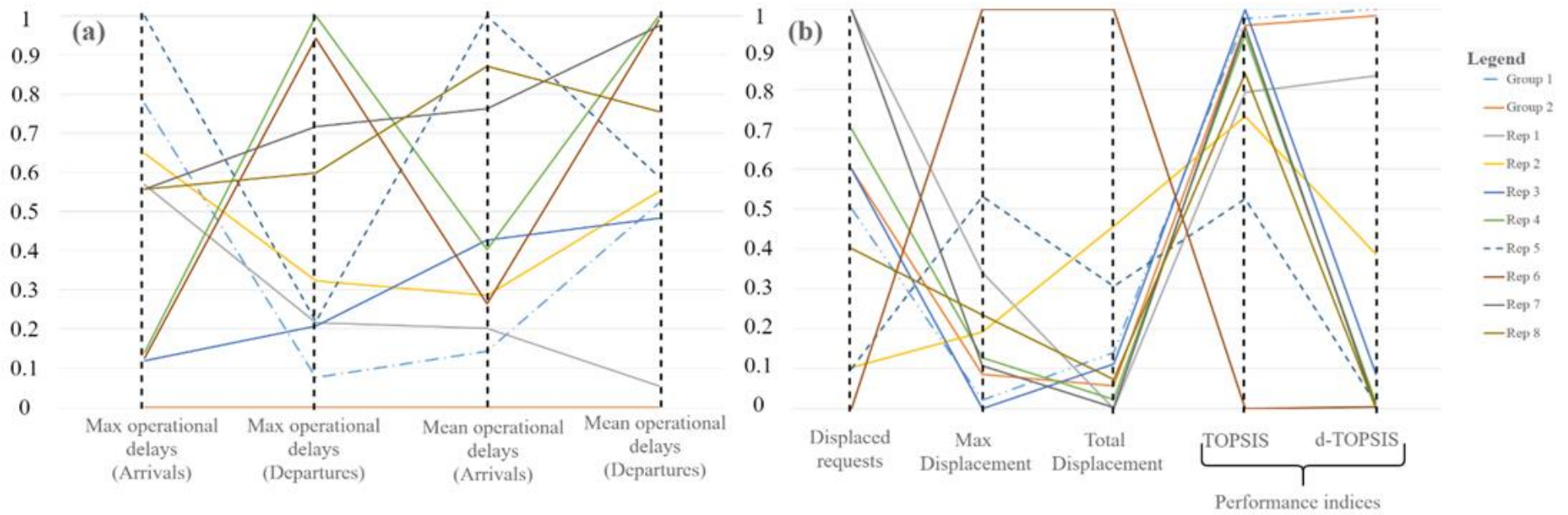


**Figure 3-12:** Value path diagrams displaying the trade-offs between the reported solutions

#### 3.4.3.4 Assessment of the schedules' expected delays

Through an analytical delay estimation module (detailed in section 3.3.4) one can assess the impact of the framework's allocations on the expected delays of the airport under consideration. In Figure 3-13, we compare the estimated delays of the allocations produced by the framework (under Group 1 and Group 2 schedules) and the delays that would be expected under a hypothetical schedule where the requested slots would operate as submitted by airlines. In doing so, we use as a reference the 'peak day' of operations of each airport, i.e., the day with the largest number of request series weighted by the number of days that each request operates, and the declared capacity of the airport.

Figure 3-13 shows that there are two periods of significant congestion which result in important waiting times for both arriving and departing flights. For arriving movements, we observe the morning peak period from 09:00 to 11:00 and the evening peak period spanning from 16:00 to 20:00. The corresponding peak periods for departing movements span from 10:00 to 13:00 (morning peak) and 18:00 to 23:00 (evening peak). These periods of increased movement activity can be observed in the schedules of both arrivals and departures, and result in significant delays (relative to size of the airport).

In particular, by considering the allocations produced by our framework, we observe that during the morning peak period arriving movements experience delays of less than 21 minutes and departing movements may experience delays of up to 26.5 minutes. The evening peak periods appear to be less congested and result in maximum delays of approximately 20 and 22 minutes for arrivals and departures respectively. Outside these two peak periods, the maximum expected delays fall to approximately 8-11 and 12-14 minutes for arrivals and departures accordingly.

The expected delays associated with the selected schedules validate the purpose of the declared capacity of the airport, without which we would experience significant delays for both arrival and departure movements during the morning peak (a maximum of 61 minutes for arriving and 54.7 minutes for departing movements). In contrast, by respecting the declared capacity of the airport, the allocations composing the selected schedules result in maximum delays that were below 26.5 minutes throughout the day.

An important observation stems from the fact that in the peak times of the coordinated schedules (Group 1 and Group 2), there are at most 5 departure movements that experience a maximum delay of 26.5 minutes and 5 arrival movements that experience a delay of 19.2-20.9 minutes (see Figure 3-13). In contrast, in considering the hypothetical schedule where flights operate as requested, we count 10 departure movements that experience delays of 54.7 minutes and 7 arrival movements that experience delays of 60.9 minutes. Hence, through this analysis we are able to quantify the benefits of schedule coordination under the declared capacity of the airport. The average reported benefits offered by the Group 2 and the Group 1 schedules translate to an improvement of about 414 minutes of departure delays (from 547 to 132.5 minutes) and 321.5 of less arrival delays (from 426.3 to 104.5 minutes of delays).

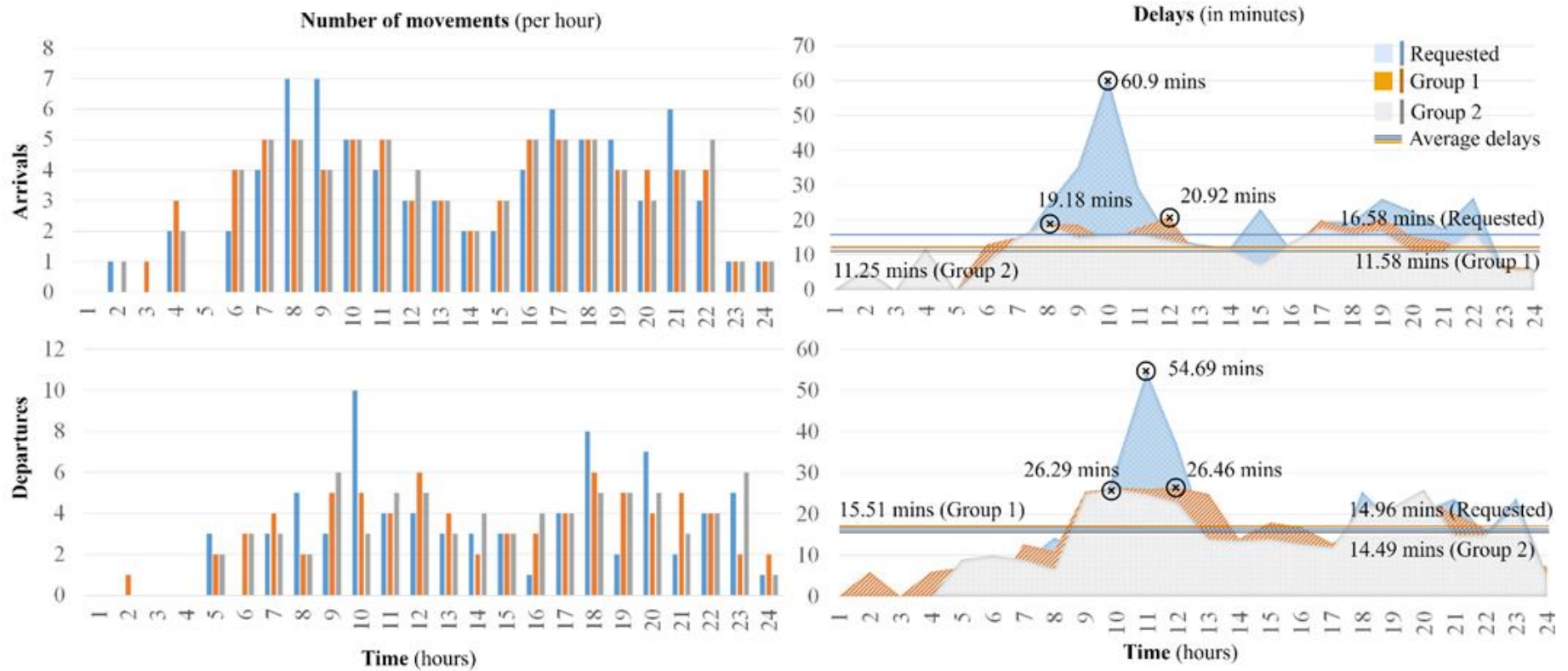


Figure 3-13: Comparison of the estimated delays of the requested and the allocated slots during the peak day

In comparing the expected delays of the Group 1 and the Group 2 schedules we observe no significant differences regarding the average and maximum delays of both arrivals and departures. During the arrivals' morning peak, the maximum expected delays reported by Group 1 are 9.1% larger than the ones reported by the Group 2 schedule (see Figure 3-13). For the departures' morning peak period we observe that the Group 2 schedule reports operational delays that are reduced by less than 1% in comparison to Group 1. During the evening peak period that is less congested, we observe that Group 2 decreases the maximum expected delays by 20.8% in comparison to Group 1 (from 20.54 in Group 1 to 17.01 minutes in the Group 2 schedules) for arrivals. The delays of departing movements during the evening peak reported by Group 2 appear to be increased by 5.1% in comparison to Group 1 (from 22.95 minutes in Group 1 to 21.84 minutes in Group 2 schedule).

This observation suggests that the improved maximum delays reported by the Group 2 schedule are the result of displacing requests to the evening. This finding is also supported by the fact that the Group 2 schedule had an increased maximum and total displacement in comparison to the Group 1 schedule (see section 3.4.3.2) signifying that there is a trade-off between the maximum displacement and the expected delay metrics. This finding coupled by the increased number of displaced requests reported by the Group 2 schedule (3271 displaced requests) in comparison to the Group 1 schedule (3121 displaced requests) suggests that the benefits in terms of expected delays are given by assigning larger displacements and displacing more requests.

The delay profiles presented above provide a macroscopic estimate on the delays that are expected during the days with the most request series and allow the interested parties to examine the impact of their preferences on the expected delays of the proposed schedule. In addition, from the examination of the delay profiles

one can observe the intensity of the trade-offs between maximum displacement and the expected delays. Overall, we observe that the allocations of the schedules proposed by the proposed framework (under alternative preference considerations) consider the declared capacity of the airport and result in operational delays that do not exceed the 26.5-minute threshold.

#### **3.4.3.5 Influence of stakeholders' preferences on airlines' objectives**

An implication of the proposed decision framework for decision-making is that each stakeholder group can assess the impact of their preferences on the allocations concerning each airline. Hence, this feature contributes to the improvement of the acceptability of the proposed schedules since it allows the airlines to study the implications of each schedule on their request portfolio. In addition, the interested parties can review the performance of the selected schedule in relationship to the other non-dominated representative schedules and determine which schedule makes the most preferable use of the airport's capacity. Such an analysis is presented in Figure 3-14.

The figure presents the objective values for each airline that received displacements in at least one of the eight schedules (identified by Group 1, Group 2, and Reps 1-8). In the considered airport there is a total of 44 airlines, while 35 of them experienced displacements for one or more of their requests in one of the eight alternative schedules (airlines A2, A11, A14, A17, A20, A25, A31, A38, A41, A44 did not receive displacements in any of the considered schedules). In Figure 3-14, the colour of each bar is shaded based on the maximum displacement, while the ticker of each bar indicates the number of displaced requests. Please note that for scaling and visualisation purposes, the reported number of displaced requests does not consider the number of operating days ( $D_m$ ). Figure 3-14 ranks the airlines (horizontal axis) by considering the number of requests that they submitted, thus

allowing the extraction of arguments relating to the proportionality between the received displacements and the number of submitted requests.

The first observation is that there are significant changes with respect to the maximum displacement and the number of displaced requests for the airlines that submit multiple requests. This insight can be identified by observing that the colour (representing the maximum displacement) and the ticker (representing the number of displaced requests) of some airlines differ based on the schedule. For instance, airline A36 receives 20 displaced requests in schedule Rep 2 and 27 requests in schedule Rep 1.

The same holds for maximum displacement since we observe significant changes in each schedule. Airlines A01, A36, A09 and A30 received significantly different values for this objective in each schedule. The most profound example is schedule Rep 6 where airline A01 received a maximum displacement of 67 x 5-minute intervals. On the contrary, in all other schedules the same airline received a maximum displacement ranging between 5 and 10 x 5-minute intervals. Another interesting finding with respect to the maximum displacement objective that is common for all schedules with increased maximum displacement (Rep 5 and Rep 6), is that there are only a few airlines that experience large displacements. However, we observe that the  $d - TOPSIS$  index that is used to assess and select the schedules, hedged against this phenomenon (since the schedules of the airlines that received additional displacement, are dominated by the other schedules), and attributed a lower rank to schedules with large values of the dominance counter or schedules that perform worse than the others with respect to significant objectives.

Regarding the total displacement objective, we observe that the relative length of the bars (each schedule has its own scale for the total displacement objective) remain the same for most airlines that report large values of maximum



displacement. In addition, we observe that the airlines with the largest total displacements, i.e. A36, A09, A30 etc, receive large (worse) total displacements regardless of the objectives' prioritisation scenario.

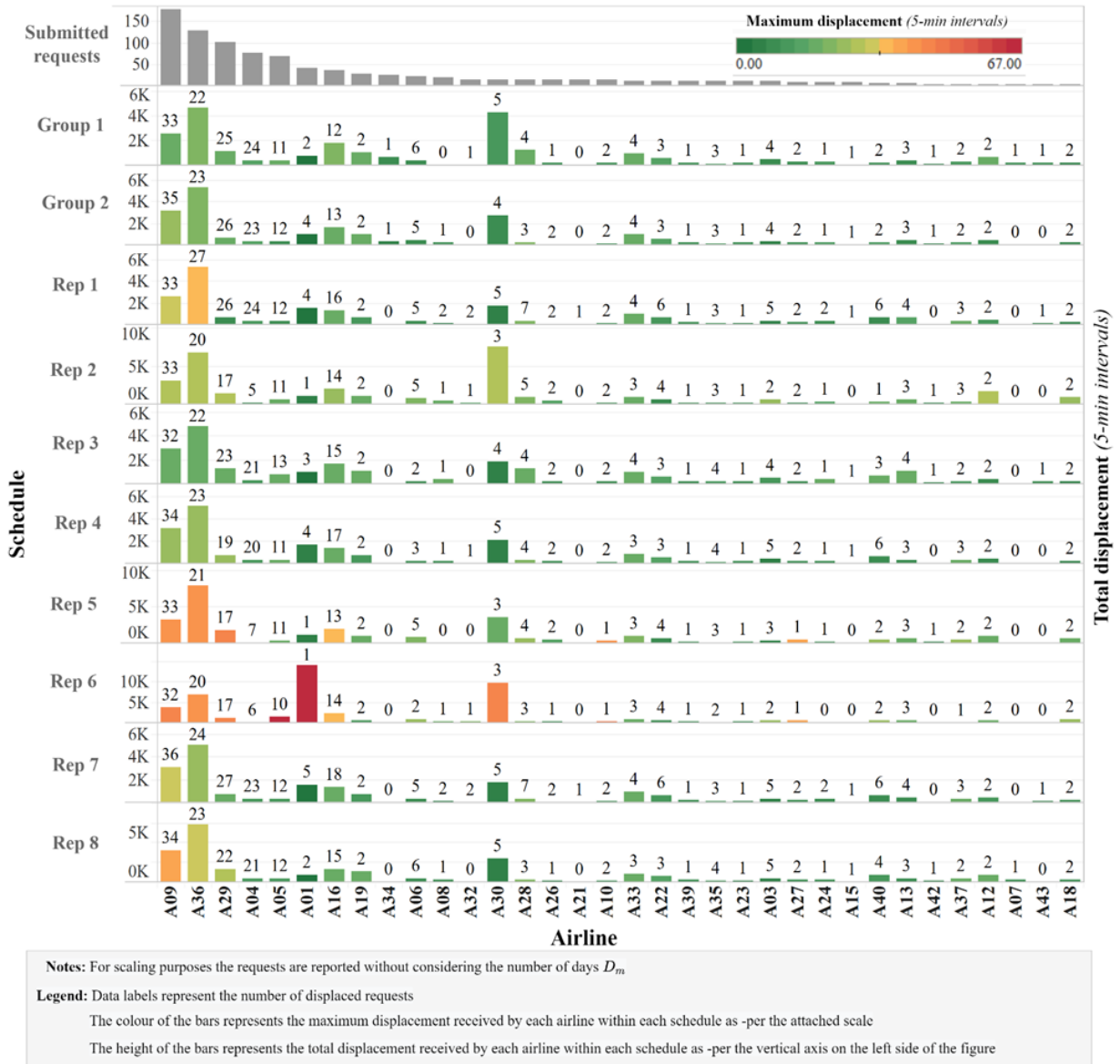


**Figure 3-14:** Comparative analysis of airlines' objectives under the different representative schedules

Hence, we observe that airlines whose requests result in the saturation of the airport's capacity will receive large displacements regardless of the preference considerations of the stakeholders. Another insight stems from the fact that the

airlines with the largest displacements are charter airlines or airlines that submit requests falling into the  $O$  priority level (A36, A09). Hence, they experience displacements that are caused because the requested slots are already allocated to requests with historic rights.

For instance, A01 received a total displacement of 14000 x 5-minute intervals in the Rep 6 schedule, but no more than 1500 x 5-minute time intervals in the other schedules. That is because airline A01 has submitted multiple requests falling into the changes to historic's and the others' priority. Similar observations can be extracted for all airlines requesting access to the airport.

Based on the results of Figure 3-14, all interested stakeholder groups, especially the airlines, can convene and compare the schedules generated under the different objective prioritisation scenarios and the other representative schedules. Through, the comparison of the schedule selected under the  $\beta^{CONS}$  prioritisation (Group 1) with different representative schedules that received high scores based on the TOPSIS and the d-TOPIS indexes, the stakeholders can review their strategies and assess the potential gains of each schedule.

The plot presented in Figure 3-14 is built using the academic version of a widely used analytics platform ("Tableau," 2021) and comes at an interactive format. The interested parties may use the interactive plot as a decision-support tool to explore seamlessly the objective values of each airline in each of the reported schedules. The interactive tool described in this work is made available to researchers and practitioners for download.

The interested reader may access it through the following link: <https://1drv.ms/u/s!Ak7YlQ06SzDigcEMR61aAps2VZ81IA?e=S1p918> (in the case that the link is not working please copy it as text and paste it in your browser).

Our findings suggest that the impact of alternative preference scenarios on the airlines' objectives, differ based on the particularities concerning the demand and capacity characteristics. In any case, the proposed methodology allows all pertinent parties to review the impact of their preferences with respect to multiple objectives. This decision support capability facilitates a more collaborative decision-making that allows stakeholders to exchange information and convene to a commonly acceptable solution. This solution can be used as a basis of negotiation before and during the bi-annual slot scheduling conferences, thus enabling the improved utilisation of airport capacity.

#### **3.4.3.6 Disaggregate and interactive visualisations for each schedule**

The ASA literature has acknowledged the value of suitable visualisations for their ability to quantify the benefits of the proposed schedules for different airlines and support ASA decision-making (Zografos and Jiang, 2019; Jorge et al., 2021; Katsigiannis and Zografos, 2021a). However, we note the absence of interactive tools that can be used by the interested parties without requiring programming skills or non-standard software. As a response, we have developed a series of interactive visualisation tools that distil the rich information generated by the proposed framework and can be used by individuals with little or no programming skills so as to inspect each of the proposed schedules.

**Inspecting the allocations for each airline's request portfolio:** Section 3.4.3.5 presented an interactive visualisation template that enables one to examine the slot scheduling objectives of each airline for each representative schedule on a '*drag and drop*' basis. The tool can be saved as a template, receive the data of different airport schedules coming from different airport instances, and plot them side by side, thus allowing each airline to inspect the quality of the allocations for their request portfolio. The developed template is available for download and can

be used by the interested reader, researcher, or practitioner so as to input their own data or conduct their own analyses independently. An illustrative screenshot of the tool is provided in the following figure.

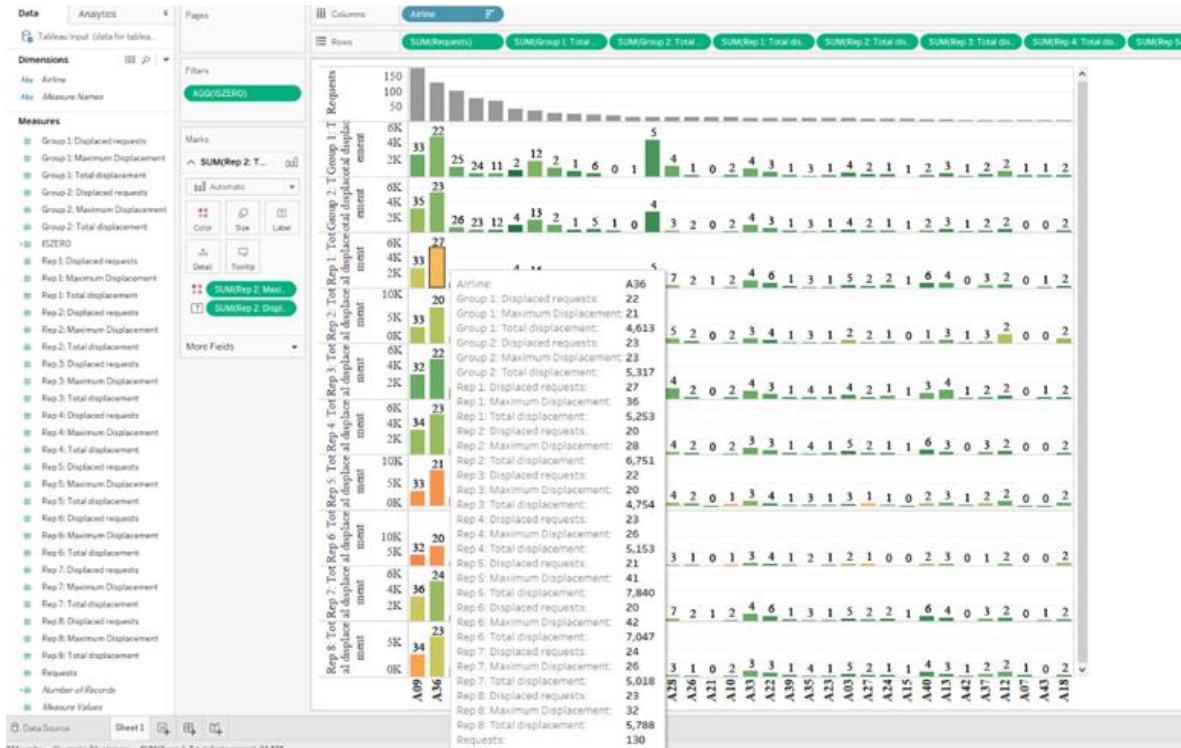


**Figure 3-15:** Screenshot illustrating the use of the interactive tool for comparing schedules

Figure 3-15 showcases that the user may select a specific airline (airline A36 in this case) and observe the values of the slot scheduling objectives that the airline received in the selected and the alternative schedules. In addition, the user may select alternative metrics (using the list on the left side of the screenshot) and plot them as per their own preferences. Using this tool, the relevant parties (airlines, coordinators) may receive information on the quality of the alternative allocations that are available and agree on the schedule that will be applied during the slot scheduling season. For instance, if the coordinator chose Rep 4 as the most preferable schedule, then airline A36 would most probably object to the allocations concerning its requests. That is because the objectives of A36 reported in schedule

Rep 4 are dominated by other schedules. This decision-making characteristic is captured by the proposed framework through the D-TOPSIS index. By considering the preferences of all pertinent parties with respect to multiple slot scheduling objectives, we observe that extremely non-beneficial allocations (having large displacements without benefits for the other objectives) received lower rankings (observe the  $d - TOPSIS$  index and the value path of the Rep 4 schedule in Figure 3-12).

**Disaggregate and interactive comparison of airport slot schedules:** The majority of existing ASA studies focus on analysing the aggregate values of each schedule's objectives. Recent studies have provided static disaggregate visualisations that exhibit the impact of the proposed airport slot scheduling solutions for each airline (Jiang and Zografos, 2021; Katsigiannis and Zografos, 2021a), or static visualisations which compare the allocations received by certain requests under alternative schedules (Jorge et al., 2021). Herein we introduce an interactive tool that allows one to view the whole airport schedule of the considered airport and study the allocations of each request individually. The proposed visualisation provides an intuitive representation of the allocated arrival and departure slots and their deviation from the requested times. In doing so, the user may display all details associated with each request and produce, with a single mouse click, graphs for each airline and movement type. The proposed visualisation tool solely requires the user to use their computer's mouse and does not require any technical knowledge or programming skills. The provided tools do not require commercial software and can be displayed and operated using any internet browser. The next series of screenshots highlight the functionalities of the described tool (see Figure 3-16, Figure 3-17 and Figure 3-18).

The main advantage of the tool presented in below is that each request is represented by a ‘bubble’, hence providing an intuitive representation of the displacements received by each request. The location of the bubble is determined by plotting the deviation between the allocated (vertical axis) and the requested slots (horizontal axis). Hence, the more a bubble deviates from the diagonal between the two axes, the larger is the displacement of the request. The size of the bubble is determined by the number of passengers and the number of days that each request concerns, i.e., as the bubble of each request increases, the larger becomes the size of the aircraft and the number of days that the request is to operate. The colour of the bubble is determined by the airline that submits the request.

In subplot (a) of Figure 3-16 we attach a screenshot of the output of the tool for a given schedule (Group 1 schedule in this case). The user may select the type of movement that they wish to plot, i.e., arrivals or departures (arrivals in this case). Next, the tool will present all arriving requests that received displacements of more than or equal to 5 minutes (requests that received no displacements are omitted since they would simply lie on the diagonal of the horizontal and vertical axes).

The plot allows the user to observe seamlessly the peak periods of the schedule, since the existence of bubbles during a time period implies the lack of airport capacity during that time and hence the displacement of the slot requests requiring the relevant time slots. As observed in subplot (a), the user may hover the cursor of the mouse above each bubble and receive all the information regarding the request, i.e., requested/allocated time, number of passengers, effective period, airline, request priority. For instance, in subplot (a) we see that the user has selected a request of airline A1 with 112 passengers, an effective duration of 210

days, falling into the ‘Others’ priority. The requested time of the request was at 10:20 but the allocated time was at 10:05 (a displacement of 15 minutes or 3 x 5-minute intervals).

In addition, the user may click on the name of an airline on the legend (right side of subplot (a)) and display only the requests of the selected airline (see subplot (b) where the user has selected to display the arrival requests of airline A19). Furthermore, the user may zoom in the graph using their mouse and focus on a specific period of the day. For instance, in subplot (c) of Figure 3-16 the user zoomed in so as to review the morning period from 5:00 to 13:00 (where they can observe in more detail the multiple requests that appear to be displaced). In the case that the user wishes to omit one or multiple airlines from their analyses, they may filter out the desired airlines by double-clicking on their names as they appear on the legend. For example, subplot (d) of Figure 3-16 excludes airlines A01 and A36.

Similar graphs and analyses can be produced for both arrivals and departures. Users may inspect, for a single schedule, the allocated/requested slots for both arrivals and departures (see Figure 3-17 where we plot all arrivals and departures for the Group 1 schedule) or compare the allocations that one or multiple airlines received in different schedules (see Figure 3-18 where we compare the allocations of airline A35 under two different schedules, i.e. Group 1 and Group 2 ). For instance, in Figure 3-17 one can see that the arrivals’ allocations deviate more from the diagonal line of the axes and hence conclude that the requests for arrivals tend to concentrate on a time period, thus causing additional displacement.

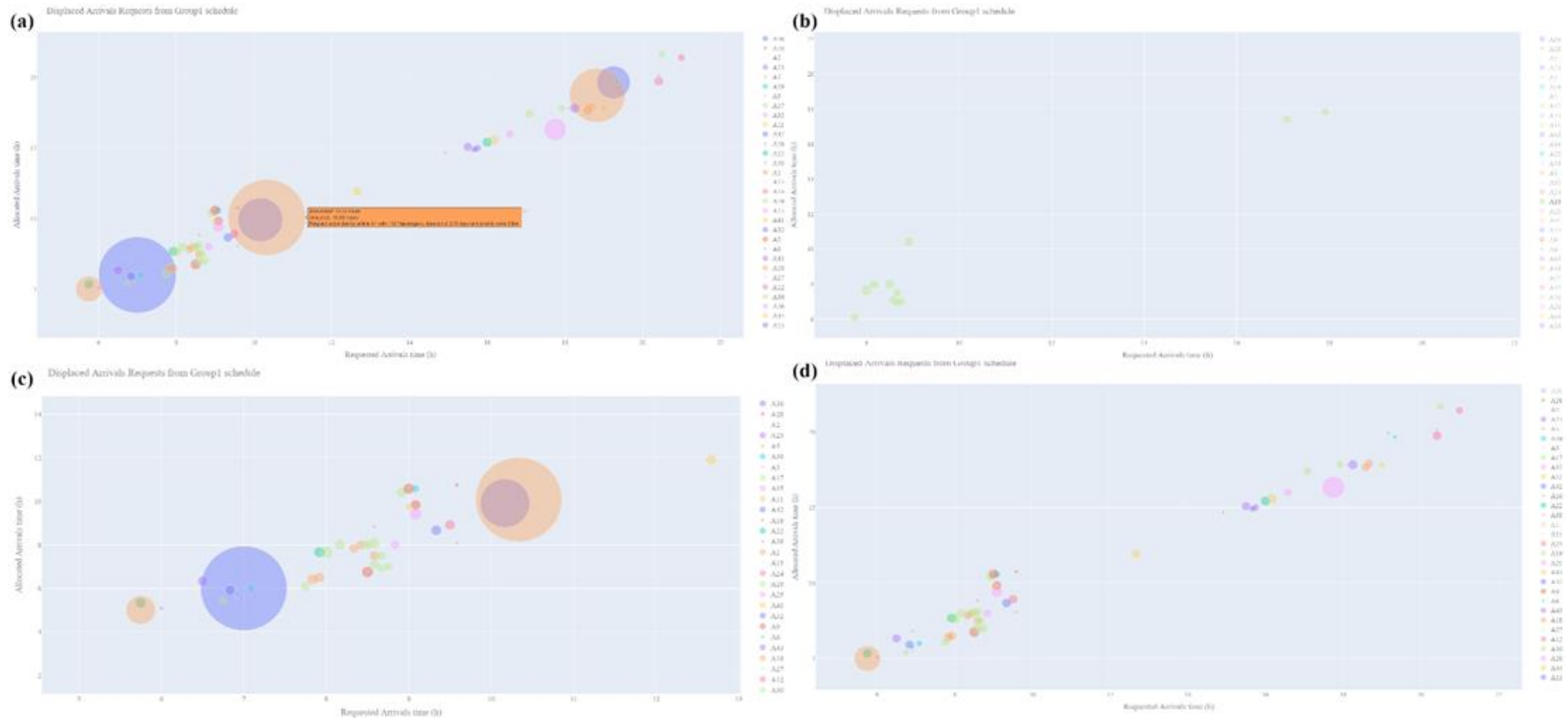


**Figure 3-16:** Screenshots showcasing the functionalities of the interactive visualisation tool



On the contrary, we observe that the displaced departure movements lie closer to the diagonal. In Figure 3-18 where we showcase how each airline (airline A35 in this case) may use the proposed tool and observe at a single glance its displaced requests in multiple schedules. The airline may then specify on whether it prefers 3 displaced requests with a smaller displacement (as per the allocation it received in Group 2 schedule) or 2 displaced requests that receive larger displacements (as per the allocations it received by Group 1).

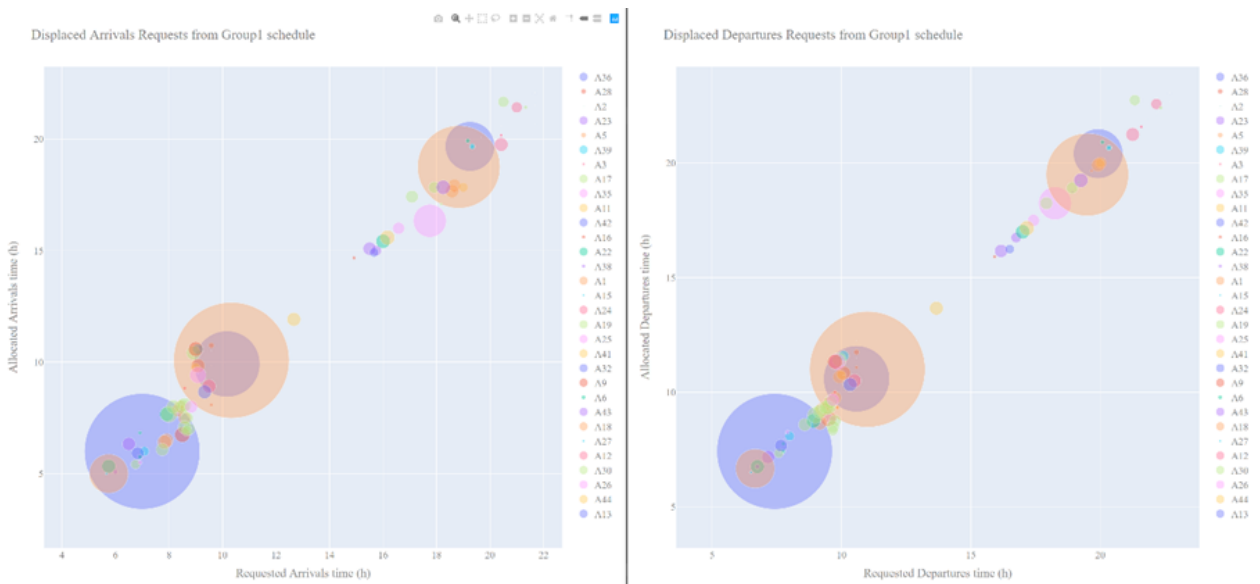


**Figure 3-17:** *Inspecting the arrivals and the corresponding departures for a single schedule*

The disaggregate visualisation tools used in this section are made openly available and can be downloaded through the following link:

- <https://1drv.ms/u/s!Ak7YlQ06SzDigaZO7iqPAF3foUMg1A?e=WrtV7k7>  
(in the case that the link is not working please copy the text and paste it in your browser).

The tools proposed in this section can be used without requiring programming skills by the user and hence can be used by the ASA stakeholders and other

practitioners. Finally, the disaggregate visualisations presented in Figure 3-16, Figure 3-17 and Figure 3-18 where may be exported using an HTML format (the standard protocol for building webpages) and can be used as standalone tools or can be embedded in integrated web applications and more advanced software.

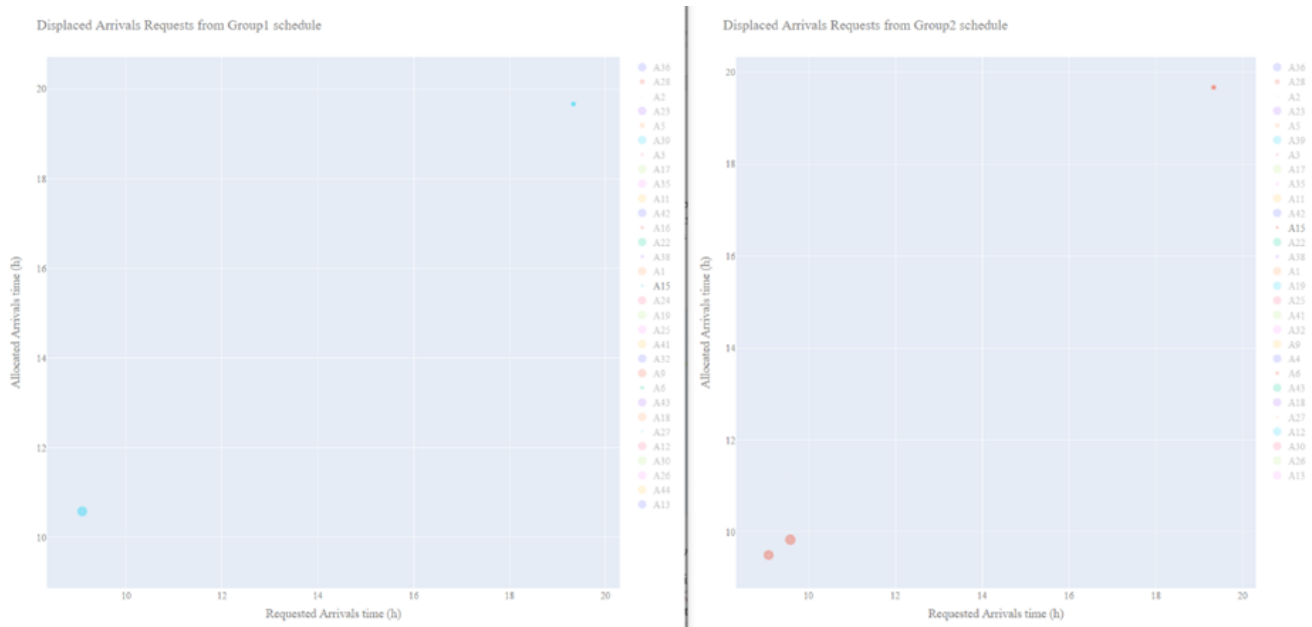


**Figure 3-18:** Comparing the arrival requests/allocations of multiple schedules for one or multiple airlines

### 3.5 Concluding remarks

In this paper, we have proposed and implemented an ASA modelling and solution approach which considers operational delays and multi-stakeholder preferences for assessing and selecting airport slot schedules. Our work determines the most preferable non-dominated schedules through the elicitation and incorporation of the preferences of all pertinent ASA stakeholders. Key contributions of the proposed methodological approach include:

**Generation of the non-dominated set and solution space reduction:** The framework guarantees the generation of the complete set of non-dominated points.

Our results suggest significant trade-offs among the considered objectives. The resulting sets of non-dominated points exhibit cardinalities that are multiple times larger than previous tri-objective, a-posteriori ASA studies and provide a wide spectrum of alternatives that allows the mapping of the solution space and the selection of representative solutions. The decision-making complexity that results from the rich information provided by the multiple non-dominated schedules is tamed by our framework through the integration of a subtractive clustering and parameter tuning procedure. Our computational results suggest that the proposed solution space reduction algorithm provides representative sets that do not compromise the information offered to the decision-making process despite being multiple times smaller (in terms of cardinality) than the complete non-dominated set. This functionality mitigates decision complexity and provides guarantees on the quality of the representative set.

**Consideration of the operational delays in making the choice of the most preferable schedule:** Our computational results suggest that schedules obtained under alternative preference considerations result in comparable levels of expected delays but improve significantly on the delays that would be experienced without the airport slot coordination process. Hence, the consideration of expected delays not only allows stakeholders to review the impact of their preferences but also enables the quantification of the impact associated with the airport's current declared capacity setting. For the considered airport instance, we observe from our results that the operational delays associated with the declared capacity of the airport are consistently below 27 minutes for both arrival and departure movements. This fact validates the performance of the proposed framework and underlines the role of the setting of the declared capacity in ensuring reasonable operational delays.

**Incorporation of multi-stakeholder preferences and use of empirical data from a survey with industry experts:** The proposed framework facilitates a more collaborative ASA decision-making process through the consideration of ASA stakeholders' preferences and provides more acceptable schedules with beneficial implications on airport capacity utilisation. The design of the proposed framework allows the proposition of airport slot schedules by consolidating the preferences of the stakeholders or by considering each stakeholder group's preferences independently. As a result, ASA stakeholders may experiment with alternative preference considerations and study their implications on the efficiency of the proposed airport slot schedules. Hence, the proposed framework may improve the potential for adopting mathematical ASA models and algorithms in practice. All computational results and analyses are based on preference data obtained through an empirical study with industry experts. The preference data validate that the interests of the ASA stakeholder groups are different (e.g., air-traffic authorities have increased preference towards reduced operational delay, while coordinators seek to optimise total and maximum displacement). Regarding the schedules selected under alternative preference considerations, we report commonly-agreed schedules reflecting the views of the relevant stakeholders.

The work proposed in this paper could be extended as follows. Regarding the consideration of stakeholders' preferences, future studies could extend the proposed hierarchical model by integrating additional criteria or altering its structure so as to reflect the decision-making needs in different airports. Another possible extension would entail the organisation of surveys with multiple industry-experts and ASA stakeholders in order to provide a set of commonly acceptable weights or priorities that could be used in multiple airport instances. In this study, we have demonstrated how the disaggregate analysis of the slot scheduling

---

outcomes for each individual airline may improve decision-making and the decision-support capabilities of the current ASA mathematical models. Hence, a potential pathway for future research would be to introduce airline-centric objectives. With regards to this research direction, the proposition of airline specific objectives that consider airlines' preferences regarding the slot scheduling objectives, i.e., the minimisation of the maximum number of displaced requests per airline, the average maximum displacement per airline, would enhance the capabilities of future mathematical models. The proposed solution methodology generates the complete solution space but requires significant computational times that hinder its application in large hub airports. The solution of larger airport instances, through the proposition of multi-objective heuristics that consider significant problem characteristics and policy criteria and can reduce the computational times required to obtain the non-dominated sets, is a promising area for future research. Work underway relates to the modelling of expected delays as an explicit optimisation objective and the proposition of solution methods where operational and scheduling delays are jointly optimised.



# Chapter 4:

## On the stable allocation of airport slots

### 4.1 Introduction

Airport Slot Allocation (ASA) decision-making comprises multiple processes. At the core of the ASA, airport slot coordinators receive airlines' requests for accessing airport resources and carry out the *initial airport slot allocation* by assigning time slots to each request. In doing so, requests are prioritised by a series of rules and criteria defined by the World Airport Scheduling Guidelines (WASG) (IATA/ACI/WWACG, 2020). However, due to the physical limitations imposed by airport capacity, some requests are displaced to later or earlier time intervals than the ones desired. At this point, coordinators decide which requests will be displaced by considering the airlines' preferences, their experience from previous scheduling seasons, and the rules of WASG which aim to make best possible use of airport capacity supply by considering passengers' needs, competition, and connectivity (IATA, 2021). The slot schedule provided by the airport slot coordinators during the initial slot allocation constitutes the basis of the airport slot coordination process and defines (at least to a great extent) the schedule that will be considered during the bi-annual slot coordination conferences and eventually the schedule that will be considered for operations.

Existing ASA studies (see section 4.1.1) model the ASA as a single-sided problem. However, ASA is a two-sided process where coordinators prioritise airlines' requests based on rules and regulations rather than economic criteria. In this context, a *stable schedule* is a schedule that provides no incentives to airlines and coordinators to alter or reject any of its allocations. The concept of *stability*, in non-monetary resource allocation systems, has been recognised as a desirable property (Roth et al., 1993) that can improve system's welfare for the participating

actors/agents. In the context of ASA, a stable schedule maximises the preferences' satisfaction across all slot-request-pairs, rather than myopically considering preferences of individual pairs. We further elaborate on the property of stability in section 4.3.2.

The *Stable Airport Slot Allocation Problem* (SASAP) variant introduced in this paper, considers the ASA problem as a two-sided matching game. The benefit of SASAP is that it enables the modelling of each submitted airline request and each available airport slot as heterogeneous agents and results in airport slot schedules where the utility achieved for each request cannot be improved without compromising the allocation of a more important request. Hence, the resulting airport slot schedules are Pareto optimal from each requests' perspective and guarantee that airlines and coordinators have no incentives to reject or alter the proposed allocations. Hereafter, such schedules are referred to as *stable*<sup>9</sup>. In the context of ASA, the term *stable* becomes a synonym of acceptable, since a schedule comprising Pareto optimal request-to-slot assignments is acceptable by both airlines and coordinators.

The issue of acceptability in the context of ASA is of particular importance, since besides being a decision-making requirement (IATA/ACI/WWACG, 2020), an acceptable schedule may lead to more consistent operations within the scheduling season of interest but also to improved continuity and inter-season scheduling consistency. That is because allocations that are acceptable by airlines in one season are more likely to be acceptable in the following scheduling seasons.

---

<sup>9</sup> In the Economics literature, the term *stable* and the property of *stability* are used so as to express demand-to-resource assignments where participating actors have no incentive to disturb the proposed assignment, since the welfare achieved for each agent cannot be improved (Roth et al., 1993).



In this paper, we address SASAP through the proposition of a *Stable Airport Slot Allocation Model* (SASAM) and a *Deferred Acceptance* (DA) solution algorithm.

Besides, in modelling airlines' preferences, current studies (Zografos et al., 2017a; Jacquillat and Vaze, 2018; Fairbrother et al., 2019; Katsigiannis and Zografos, 2021a) propose time-dependent functions without holistically capturing the factors associated with the importance of each request. The functions integrated in SASAM and the DA algorithm (hereafter referred to as *airlines' functions* or *airlines' side*), provide a more comprehensive representation of airlines' preferences since in addition to time-dependent preferences, they explicitly consider each request's operational characteristics (as expressed by the available seat kilometres of each request) as well as the inter-airline competition faced by each request. Furthermore, this paper provides an explicit modelling of each request's policy-based prioritisation by the coordinators (hereafter referred to as *coordinators' functions* or *coordinators' side*). The proposed functions translate the verbal rules (both primary and secondary) of WASG, while simultaneously incorporating surrogate indexes on the preferences of airlines, and the connectivity and competition relating to each request. The compliance of the proposed functions' properties with the policy rules and priorities of WASG is further supported by mathematical proof and comprehensive examples. The proposed airline and coordinator functions ensure a replicable and consistent slot allocation decision-making process. From a data availability perspective, the proposed methodology can be readily applied in practice, since it leverages data that are made available during the current ASA process and does not require the disclosure of sensitive commercial information.

In a nutshell, this paper contributes to the state-of-the-art by formulating the Airport Slot Allocation problem as a two-sided matching game. In doing so, a

stable Mixed Integer Programming (MIP) model is developed (SASAM), integrating inequalities that prune the formation of allocations that are not acceptable by airlines and coordinators. SASAM considers surrogate importance functions that integrate several operational and policy characteristics, competition, and connectivity, and model the preferences of airlines and the policy-based prioritisation of airlines' requests by the coordinators so as to propose acceptable request-to-slot assignments. A fast DA algorithm addresses the computational complexity of SASAM and generates multiple airport slot schedules by considering the trade-off between the efficiency of the schedule (expressed in terms of displacement-related metrics) and the spilled passenger/airline demand (flights/requests that could not be accommodated).

Before elaborating on the contributions of this work (section 4.1.2), the following section (section 4.1.1) discusses existing related studies and elaborates on the gaps addressed by this paper.

### 4.1.1 Previous related work

Research on airport demand management comprises (Zografos et al., 2017b): (a) administrative studies that consider non-monetary prioritisation schemes for managing airlines' access to congested airports; (b) market-based mechanisms that provide pricing and monetary mechanisms for allocating airport capacity; and c) hybrid approaches that consider both monetary and non-monetary demand management mechanisms. The research reported in this paper appertains to (a), since WASG allocate airport slots to airline requests using a prioritisation scheme that is based on historic usage rights and competition. The most relevant administrative studies are those considering airlines' preferences (Zografos et al., 2017a; Jacquillat and Vaze, 2018; Fairbrother et al., 2019; Jiang and Zografos, 2021; Katsigiannis and Zografos, 2021a), where we note that interactions between

airlines' preferences and the coordinators roles with regards to scheduling stability/acceptability have not been previously considered. However, it is worth noting that in market based mechanisms, the acceptable trading of airport slots was modelled by considering interactions between slot pricing and budget limitations (Bichler et al., 2021). Administrative ASA studies considering the policy rules of WASG, have grown from formative formulations (Zografos et al., 2012) that considered the main policy rules of WASG in conjunction to turnaround and runway capacity constraints, to formulations that consider multiple-objectives, expressions of airlines' preferences, policy rules and other ASA problem aspects. This section provides a concise summary of the administrative ASA literature by placing special emphasis on studies with preference considerations.

Zografos et al. (2017) formulated the WASG-based ASA process using two bi-objective formulations that optimised the maximum/total displacement and the total displacement in conjunction to the number of violated slot assignments. The latter formulation constitutes an initial attempt to improve the acceptability of airport slot scheduling solutions, since it allows the consideration of airlines' displacement preferences. Ribeiro et al. (2018) provided an explicit modelling of the policy rules relating to requests that amend pre-existing operations. Fairbrother et al. (2019) proposed a two-stage budget mechanism that does not require the disclosure of sensitive data. The proposed budget mechanism re-allocates displacement as per the expressed airline preferences but does not consider the views of the coordinator and the policy rules of WASG.

Jiang and Zografos (2021) incorporated preferences through the use of a voting mechanism where coordinators and airlines engage so as to select the most preferable efficiency-fairness trade-off. Ribeiro et al. (2019b) conducted a comprehensive study that examines the impact of alternative policy rules on

scheduling efficiency. Fairbrother and Zografos (2020) provided policy-making support by examining the effect of segmenting the scheduling season into subperiods and altering the length of requests for series-of-slots. Katsigiannis et al. (2021) proposed a multi-level, multi-objective modelling and solution methodology that considers maximum and total displacement in conjunction to the demand-based fairness objective of Fairbrother et al. (2019). Zeng et al. (2021) proposed a data-driven model that considers historic data so as to minimise the expected displacement. Katsigiannis and Zografos (2021a) considered airlines' timing flexibility preferences by modelling the policy concept of the Timing Flexibility Indicator (TFI). Jorge et al. (2021) augmented the formulation of Ribeiro et al. (2019b) by associating alternative scheduling objectives with the policy requirements of WASG. Katsigiannis and Zografos (2021b) proposed a unified framework that assesses the performance of non-dominated schedules by considering multi-stakeholder preferences and operational delay estimates.

At this point it is worth mentioning administrative ASA studies that consider the allocation of slots at a tactical level. This research stream has evolved in parallel to WASG-based ASA studies and exhibits several commonalities in terms of the considered objectives and capacity constraints. Jacquillat and Odoni, (2015) considered a single day of airport operations and minimises pre-tactical total and maximum displacement and the operational delays at the tactical decision horizon. Jacquillat and Vaze (2018) proposed a tactical model that considers airline equity and queuing constraints, and results in schedules that are Pareto<sup>10</sup> optimal with respect to airlines' total and maximum displacement. The proposed

---

<sup>10</sup> The term Pareto optimal/efficient is used throughout the document to define an allocation of resources to agents, where there are no other resource-to-agent assignments that make the interests of an agent better off without compromising the interests of another agent.

formulation integrates random weights for each request allowing airlines to express their preferences.

The compact literature review highlights that there are currently no ASA models to consider the ASA as a two-sided problem and guarantee the stability of the generated schedules. In this paper, the issue of schedule stability is addressed by a modelling and solution methodology that considers concurrently airline and coordinator functions so as to propose schedules where each request-to-slot assignment is Pareto optimal. Furthermore, despite the existence of models that consider airlines' timing preferences (Zografos et al., 2017a; Jacquillat and Vaze, 2018; Fairbrother et al., 2019; Katsigiannis and Zografos, 2021a), there is a dearth of models that holistically consider the factors relating to the importance of each request and their interrelationship with the coordinators' policy-based prioritisation. This paper considers airline and coordinator functions that consider problem aspects. Further details on the contributions that are brought upon by this paper, are provided in the following section.

### 4.1.2 Contributions

This study proposes a new ASA problem variant which considers the ASA as a two-sided matching game. One side of the game represents airlines' demand for the airport's resources, while the other side considers the policy rules and the coordinators' role for allocating requests to slots. Using the proposed methodology one can generate schedules that provide no incentives to airlines and coordinators to alter or reject the proposed request-to-slot assignments (such schedules are hereafter referred to as *stable*), consequently being more acceptable. We will refer to this problem variant as the *Stable Airport Slot Allocation Problem* (SASAP). In addressing SASAP our paper makes the following contributions:

- *It develops functions that approximate airlines' preferences and model the rules and priorities considered by the coordinators:* We propose functions that leverage available data sources and provide a consistent methodology that can approximate the value of each request and airport slot. The proposed functions consider airlines' preferences and model the policy rules and priorities that are applied by airport slot coordinators. In particular the proposed functions consider the distance covered by each request, route competition and connectivity, the available passenger kilometres, and other currently unconsidered request characteristics. The compliance of the proposed functions with the requirements of WASG is mathematically supported, while statistical analyses verify their robustness with respect to load factor data input unavailability.
- *It provides an MIP formulation that considers interactions between airline preferences and the priority assigned by coordinators based on the policy rules of WASG and leads to stable airport slot schedules:* To address SASAP, we propose a *Stable Airport Slot Allocation Model (SASAM)* that guarantees the generation of schedules comprising acceptable, Pareto optimal request-to-slot assignments. The formulation captures the interactions between airline demand and the priority assigned to each request by the coordinators based on the policy rules of WASG when allocating airport slots. From a combinatorial perspective, SASAM incorporates valid inequalities that prune request-to-slot assignments that block the formation of stable schedules.
- *It proposes a multi-objective, Deferred Acceptance (DA) algorithm that can generate stable airport schedules within tractable computational times:* To efficiently generate stable airport slot schedules, the paper introduces a DA

algorithm that can be used on its own or in conjunction to MIP formulations. The proposed DA algorithm can generate multiple stable, non-dominated points and provide insights on the trade-offs between spilled passenger/airline demand (expressed in terms of rejected requests or passengers) and the utilisation of the airports' resources.

- *It demonstrates the performance of the proposed DA algorithm and its applicability in real-world ASA decision-making:* Comparisons between alternative ASA schemes suggest that the consideration of the dynamics between the airlines' side and the coordinators' side enable the study of the trade-offs between the spilled airline/passenger and demand and airport capacity utilisation. Furthermore, the implementation of the proposed DA algorithm provides information on the trade-offs among multiple ASA performance metrics and has no commercial software dependencies, thus posing less barriers for adopting mathematical ASA models and algorithms in practice.

The following section provides a concise overview of the methodology that is proposed so as to address SASAP.

## **4.2 Summary of the proposed approach**

The methodology proposed in this paper considers the interactions between the airline demand and the coordinators' prioritisation subject to the policy rules defining the ASA process. An overview of the methodology developed in this paper is provided in Figure 4-1. Figure 4-1 identifies the two sides of ASA decision-making (airline demand and the coordinators' role in allocating airport capacity) and situates the proposed methodology's components.

At the outset, the proposed methodology requires three input sets, i.e., airlines' requests, airport capacity parameters and the policy rules and priorities that are considered for allocating slots. The first step of the proposed methodology is to provide importance functions that approximate the value assigned by the airlines to each of their submitted requests (demand), and functions that model the priority assigned by the coordinator to each request with respect to each time slot based on the policy rules of WASG. The proposed importance functions are detailed in section 4.3.2.1. An intrinsic aspect of the proposed functions is that their design is supported by mathematical proof that guarantees their compliance with the decision-making requirements of ASA. Concurrently, their properties in modelling the interactions between the airline and the coordinators' side, and their robustness concerning load factor data uncertainty are supported by a series of statistical analyses (see section 4.5.2). Once the prioritisation functions are constructed, an MIP Stable Airport Slot Allocation Model (SASAM) is built by incorporating inequalities that consider the policy rules of WASG and to the proposition of stable airport slot schedules. SASAM guarantees that the proposed schedules provide no incentives to airlines and coordinators to reject or alter to suggested request-to-slot assignments. This step concludes the pre-processing and the model-building phases of the proposed methodology.

Given SASAM, the paper proposes two alternative solution approaches that can solve SASAM and result in stable airport slot schedules. The first is an MIP row-generation solution approach, while the second is a DA algorithm that can generate multiple stable schedules by considering the trade-off between spilled airline/passenger demand and airport capacity utilisation. The DA algorithm is a more tractable solution method, which guarantees Pareto optimality and can be used for more challenging airport instances.



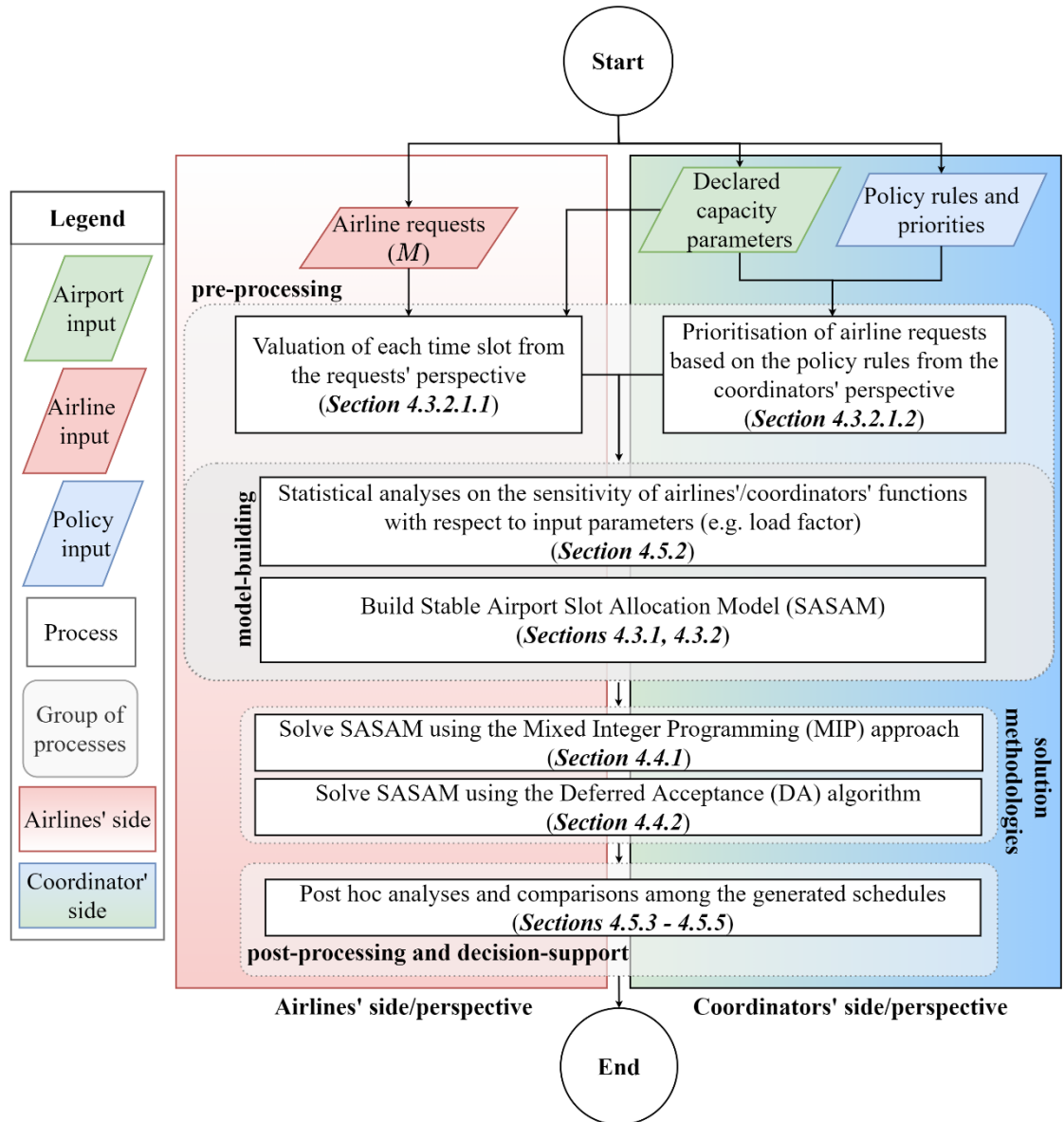


**Figure 4-1:** Overview of the proposed approach

The proposed MIP row-generation method is an exact algorithm that can be used for smaller airports and for benchmarking the DA algorithm (or other algorithms that will be developed in the future). Comparative analyses between the proposed DA and row-generation solution methods under different ASA schemes are provided in sections 4.5.3 and 4.5.4. The proposed methodology and its implementation provide output that can be used in comparative analyses that

quantify the price of stability and the airlines/requests that have to be displaced/rejected so as to achieve a stable schedule.

The remainder of this paper is organised as follows. Section 4.3 details the airlines and the coordinators' functions and the inequalities that compose the Stable Airport Slot Allocation Model. Section 4.4 discusses an MIP solution approach for solving SASAM and the Deferred Acceptance algorithm that are used to address the stable ASA problem. In section 4.5, we present comprehensive statistical analyses on the components of the proposed prioritisation functions and present an application of SASAM, and DA based on data obtained from a coordinated airport. Finally, section 4.6 concludes this paper and provides directions for future research.

## **4.3 The stable Airport slot Allocation Model (SASAM)**

Herein, we define the base modelling components (decision variables, constraint, and objective expressions) that are relevant to the formulation of the stable airport slot allocation model. In section 4.3.1 we present a base ASA model that will be the backbone of the Stable Airport Slot Allocation Model (SASAM). Section 4.3.2 presents the inequalities that prune allocations who block the formation of stable matchings. Subsection 4.3.2.1 details the prioritisation functions for each airline request and airport slot considering airlines' preferences and the priorities assigned by the coordinators based on WASG. Section 4.3.2.2 formalises the stability enforcing inequalities and provide their adaptations for specific cases of slot request priorities, i.e., new entrants' requests.

### **4.3.1 Modelling foundations**

The foundation of SASAM is based on the seminal model of Zografos et al. (2012), which introduces tight expressions (precedence constraints) for the turnaround

times of paired arrival-departure requests. The components of the modelling foundation of SASAM are provided below.

### Input sets

$Q$ : set of request priority classes, such as historic (H), changes to historic (CH), new entrants (NE), others (O), indexed by  $q$

$K: \{Arr, Dep, Total\}$  set of movement types indexed by  $k$

$A$ : set of airlines submitting requests indexed by  $a$  ( $a_m$  being the airline that submits request  $m$ )

$M$ : set of request series indexed by  $m$

$M_a$ : is the set of requests submitted by airline  $a$

$M_q$ : set of request series of slot priority  $q$

$M^k$ : set of request series  $m$  of movement type  $k$ , i.e.,  $M^{Arr(Dep)}$ :  $M^{Arr} \cup M^{Dep} = M^{Total} = M$ , set of arrival (departure) series

$\Omega = M \times M$ : set of paired requests indexed by  $(ma, md)$  which are the paired arrival and departure movements accordingly

$D$ : set of days in scheduling season indexed by  $d$

$D_m$ : being the set of days that movement  $k$  of slot  $m$  is to operate

$W$ : set of weeks in scheduling season indexed by  $w$  where  $|W| = (D \text{ div } 7) + 1$

$W_m: \{w_{n_m}, \dots, w_{N_m}\}$  set of weeks in scheduling season that slot  $m$  is to operate with  $W_m \subseteq W$  and  $n_m$  being the starting week of operation  $m$  and  $N_m$  being the index of the last week that slot  $m$  will operate such that  $n_m \leq N_m \leq |W|$ .

$W_m = \{w_{n_m + \rho \omega_m} : w \in W, \rho \in [0, \frac{N_m - n_m}{\omega_m}]\}$ , where  $\omega_m$  the frequency of operations of slot  $m$ . Note that an arrival and a departure can't be requested for different durations ( $W_{m_{Arr}} = W_{m_{Dep}} = W_m$ ). If  $N_m = n_m$ , then  $|W_m| = 1$

$\mathcal{C}$ : set of capacity time interval lengths indexed by  $c$ , where  $\tilde{c}$  is the selected coordination interval

$T_{\tilde{c}} = \{0, \dots, |T_{\tilde{c}}|\}$ : set of time intervals per day calculated based on interval length  $c$  indexed by  $t/t'$  with cardinality  $|T_{\tilde{c}}|$

$\check{A}$  = set of origin/destination airports (indexed by  $\check{a}$ ) served by the focal airport, with  $\check{a}_m$  denoting the airport served by request  $m$

### Parameters

$t_m/\bar{t}_m$ : requested/historic time for request series  $m$

$v_m = \begin{cases} 1, & \text{if } a_{d,ma} = a_{d,ma} + 1 \\ 0, & \text{if } a_{d,md} = a_{d,md} \end{cases}$  : is the overnight indicator of each pair of requests, stating whether the departure of request  $m$  is requested to be scheduled a day after the arrival

$TT_m$ : turnaround time of paired request  $m$

$u_{d,t,c}^k$ : capacity for movement type  $k$  for period  $[t, t + c)$  on day  $d$  based on interval length  $c$

$a_m^d = \begin{cases} 1, & \text{if } m \text{ is requested on day } d \\ 0, & \text{otherwise} \end{cases}$

$AP_{md}, AP_{ma} \in \check{A}$ : next airport destination, previous airport of origin of request  $m$ .

### Decision variables and expressions

$x_{t,m} = \begin{cases} 1, & \text{if request series } m \text{ is allocated to time } t \\ 0, & \text{otherwise} \end{cases}$

$\psi_{t,m} = t - t_m$ : the displacement of movement  $k$  of slot  $m$

$\Psi$ : auxiliary variable defining the maximum displacement objective as a set of linear constraints

### Base model

$$\sum_{t \in T_{\tilde{c}}} x_{t,m} \leq 1 \quad \forall m \in M \quad (4.1)$$

$$\sum_{m \in M^k} \sum_{t' \in [t, t+c-1]} a_m^d x_{t',m} \leq u_{d,t,c}^k \quad \forall c \in C, d \in D, k \in K, t \in [0, |T_{\bar{c}}| - c] \quad (4.2)$$

$$\sum_{t \in [0, \kappa)} x_{md,t} + \sum_{t \in [\kappa - TT_m, |T_{\bar{c}}|]} x_{ma,t} \leq 1 \quad \forall (ma, md) \in M \times M: v_m = 0, \kappa \in [TT_m, |T_{\bar{c}}|) \quad (4.3)$$

$$\sum_{t \in [0, \kappa)} x_{md,t} + \sum_{t \in [\kappa - TT_m + |T_{\bar{c}}|, |T_{\bar{c}}|]} x_{ma,t} \leq 1 \quad \forall (ma, md) \in M \times M: v_m = 1, \kappa \in [0, TT_m) \quad (4.4)$$

$$\sum_{t \in T_{\bar{c}}} x_{t,m} |\psi_{t,m}| \leq \Psi \quad \forall m \in M \quad (4.5)$$

$$Z_1 = \sum_{m \in M} \left( 1 - \sum_{t \in T_{\bar{c}}} x_{t,m} \right) |D_m| \quad (4.6)$$

$$Z_2 = \Psi \quad (4.7)$$

$$Z_3 = \sum_{m \in M} |D_m| \sum_{t \in T_{\bar{c}}: t \neq t_m} x_{t,m} \quad (4.8)$$

$$Z_4 = \sum_{m \in M} |D_m| \sum_{t \in T_{\bar{c}}} (x_{t,m} |\psi_{t,m}|) \quad (4.9)$$

$$\min Z = \beta_1 \frac{Z_1}{|M||D|} + \beta_2 \frac{Z_2}{|T_{\bar{c}}|} + \beta_3 \frac{Z_3}{|M||D|} + \beta_4 \frac{Z_4}{|M||T_{\bar{c}}||D|} \quad (4.10)$$

Expressions (4.1) state that each request may receive at most one time slot or be rejected. Expressions (4.2) are runway capacity constraints. Expressions (4.3) and (4.4) are precedence constraints defining the turnaround time of paired requests with overnight indicators ( $v_m$ ) equal to 0 and 1 correspondingly. In the case that a request does not have a paired movement then (4.3) are trivially satisfied for all time intervals regardless of the movement type of the unpaired request. Inequalities (4.5) are auxiliary expressions defining the maximum displacement across all requests. Expressions (4.6)-(4.9) define the objectives of the model which are (from the top to the bottom) the number of rejected requests ( $Z_1$ ), maximum displacement ( $Z_2$ ), the number of the displaced requests ( $Z_3$ ) and the total displacement ( $Z_4$ ) objectives. Ultimately, expression (4.10) corresponds to the

objective function of this initial formulation, which is a normalised scalarisation of objectives  $Z_1$  to  $Z_4$ . The objective set comprises of the main efficiency request criteria used in existing ASA studies. Weights  $\beta_j, j = 1,2,3,4$  represent the relative importance that the stakeholders of the ASA process attribute to each objective. Such weights can be obtained a-priori (Ribeiro et al., 2018) or through empirical surveys which provide an explicit modelling of stakeholders' preferences (Katsigiannis and Zografos, 2021b).

### 4.3.2 Enforcing stability in ASA decisions

Before presenting the definition of the preference functions, there is a need to provide some preliminary definitions that will facilitate the understanding of the formulations that follow. An instantiation of the interactions between the airlines' preferences and the coordinators' side given in Table 4-1. In the example presented in Table 4-1, there are three requests and three available slots. From this toy example one understands that airlines have preferences over slots (for each of their requests) and coordinators prioritise requests for each of the available slots based on WASG. For instance, request  $r_1$  prefers slot  $s_2$  to slot  $s_3$  and slot  $s_3$  to slot  $s_1$ . However, as per each request's coordinators' function, slot  $s_2$  would rather accommodate request  $r_2$ . A stable matching to this toy instance is  $\{(s_1, r_3), (s_3, r_1), (s_2, r_2)\}$ . This matching is stable since there are no slots that can be matched with another available request without compromising a more important allocation, while concurrently none of the requests can be allocated to another available slot (other than the one that they have received), since the slots are matched with requests that are more preferable for them. Therefore, a stable matching maximises the preferences' satisfaction across all slot-request-pairs, rather than myopically considering preferences of individual pairs.

In this toy example, one could find an acceptable set of matches between slots and requests, however it becomes evident - even for small and simplistic problem instances - that finding an acceptable matching is not trivial. In reality, finding a stable matching to the ASA problem, which comprises multiple constraints as per expressions (4.1)-(4.4) (turnaround time, assignment, multi-movement rolling runway capacity constraints), requests and slots, becomes a challenging problem.

As per the example discussed above, a schedule  $s$  can be expressed as a subset of  $M \times T_c$  where  $(m, t)$  denotes that request  $m$  is allocated to time slot  $t$ . Then, in a schedule one could say that a time slot  $t$  is fully occupied when the number of scheduled requests consume all available capacity, i.e.,  $\sum_{m \in M^k} \sum_{t' \in [t, t+c-1]} a_{m_k}^d x_{t', m} = u_{d, t, c}^k$ , for at least one day ( $d$ ) and capacity time interval length ( $c$ ). Given the above concepts, the following definition formalises the conditions that render an assignment of a request  $m$  to a time slot  $t$  a blocking pair, i.e., a request-to-slot assignment that blocks the formation of an acceptable schedule.

Airlines' preferences	Coordinators' prioritisation based on WASG
$r_1: s_2, s_3, s_1$	$s_1: r_3, r_1, r_2$
$r_2: s_1, s_2, s_3$	$s_2: r_2, r_1, r_3$
$r_3: s_1, s_2, s_3$	$s_3: r_3, r_1, r_2$

For simplicity assume that  $s_1, s_2, s_3$  are slots with capacity of 1 request.

**Table 4-1:** A toy instance of the preferences of the airlines and the priority assigned by the coordinator based on WASG

**Definition 4.1.** Given a feasible schedule provided by the solution of expressions (4.1)-(4.5) and (4.10) we may say that a feasible (as per the capacity and turnaround time constraints) allocation  $(m, t)$  is blocking the formation of a stable schedule if the following conditions hold as follows:

1. Either  $m$  is not allocated in  $s$  or it would rather be allocated to another available time slot different from  $t$ ; or
2. The slot  $t$  is not fully occupied and it would better accommodate requests of higher importance.

The above definition is adapted to the ASA context using the many-to-many matching definition of Gale and Shapley (1962) and its adaptation in other resource allocation problems (Diebold and Bichler, 2017; Delorme et al., 2019; Pettersson et al., 2021). As per the above definition, if allocations of type (1) were to occur, the airline that submits request  $m$  has no incentive to accept the allocation. In the case of type (2) allocations, the coordinator could use the capacity of time slot  $t$  so as to accommodate requests of higher priority/importance. Allocations (1) and (2) are hereafter referred to as a *blocking allocations/pairs* since they block the formation of a stable airport schedule. Therefore, a schedule that has at least one blocking pair (un-stable schedule) is not acceptable (either by the airlines or the coordinators). In what follows this section is organised in two subsections which detail the building blocks of the Stable Airport Slot Allocation Model (SASAM). Section 4.3.2.1 discusses the time-dependent prioritisation functions. Subsection 4.3.2.2 presents the stability enforcing inequalities and provides mathematical proof on the ability to produce acceptable airport slot schedules.

#### 4.3.2.1 Prioritisation functions

In modelling the ASA process as a two-sided game there is need to consider functions that model (a) the airlines' side; and (b) the coordinators' side.

In constructing (a) and (b), one would ideally use revenue/cost data associated with each submitted request. However, such data constitute commercially sensitive information and hence is not disclosed by airlines. As a result, there is need to use surrogate metrics that model the importance of each



request/slot from the airlines/coordinators' perspective. In the absence of cost/revenue information, in modelling (a), previous research has considered surrogate expressions of airlines' preferences by proposing a uniform threshold of maximum acceptable displacement (Zografos et al., 2017a), random priority weights (Jacquillat and Vaze, 2018), time-dependent preference functions considering the passengers served and the effective period of each request (Fairbrother et al., 2019) and timing-flexibility functions that consider earliness/tardiness in conjunction with the number of passengers served throughout the scheduling season (Katsigiannis and Zografos, 2021a). With regards to (b) we note that previous studies have considered airlines preferences in isolation without explicitly considering the coordinators' side.

In this work, we propose prioritisation functions for each airline request and airport slot. The proposed functions exploit data that are made available by airlines during the initial slot allocation and provide an approximation of (a) and model (b) for the first time. Concerning (a), our work augments previous attempts in modelling airline preferences, since it considers the seat kilometres associated with each request (considering the distance of the requested movement(s), the passengers, and the effective frequency of the request) and the competition dynamics associated with the concerned route. Furthermore, our work is the first to provide an explicit modelling of (b). Both the airlines and the coordinators' functions consist of a time-dependent delay-discounting base that is capable of considering airlines' earliness/tardiness preferences, and a tie-breaking exponent that is used to differentiate between airline requests/airport slots concerning the same time-period. The time-dependent base in (a) reflects airlines' timing preferences (expressed using the timing flexibility indicator (TFI)) (Katsigiannis and Zografos, 2021a), while in (b) its adaptation is guaranteed to comply with the main policy rules and priorities of WASG (consideration of historic/changes to

historic/new entrant and year-round prioritization criteria). Decisions on the modelling of (a) and (b) have been made so as to approximate airlines' preferences and guarantee the compliance of the proposed prioritisation functions with WASG's requirements. The suitability of the importance functions is further supported in sections 4.5.2.1 and 4.5.2.2 accordingly.

The majority of the main modelling components composing (a) and (b) are made available during the initial slot allocation process. The only complexity that arises concerns the load factor of each request. Ideally, the proposed functions would incorporate load factor estimates for each submitted request. However, such data is not made available by airlines during the initial slot allocation process since it constitutes data of utmost commercial importance that is used to shape airline scheduling decisions (Barnhart and Cohn, 2004). Based on current practice, coordinators use aggregate load factor estimates that differentiate between scheduled/charter and domestic/international requests. An indicative set of examples of the load factor parameters that are made available and used by coordinators is provided in the coordination parameters of major coordinated airports, which can be obtained through the following link: <https://www.acl-uk.org/latest-airport-info/>. In this study, in accordance with current practice, all computational experiments are based on load factor assumptions which differentiate between charter and scheduled operations. The modelling of the prioritisation functions is supported by a series of statistical analyses and sensitivity results with respect to the influence of alternative load factor assumptions (see section 4.5.2) and the ability of (a) and (b) to differentiate among requests sharing similar characteristics. The analyses suggest that the values of (a) and (b) are not significantly changed when altering the value of the load factor parameters.

The integration of (a) and (b) in the combinatorial Stable-ASA-Model (SASAM) (section 4.3.2.2) and solution approach (section 4.4.1), and the Deferred Acceptance (DA) algorithm (section 4.4.2) that we propose, allows us to consider the interactions between airline demand and the priorities assigned by coordinators when allocating airport slots and generate stable schedules that provide no incentive for amending or rejecting the proposed allocations.

#### ***4.3.2.1.1 Prioritisation from the airlines' perspective***

To prioritise slots for each request submitted to the airport, there is need to consider the characteristics that are valued by airlines when drafting their schedules. A frequent metric that is used for considering the importance of alternative routes and airline operations is the *available seat kilometres/miles* metric. The available seat kilometres metric is often used on its own right to assess the performance of airline operations (Feng and Wang, 2000), or combined with cost/revenue data to measure airline efficiency and support airline scheduling or airline fleet decisions (Baltagi et al., 1995; Wei and Hansen, 2003).

However, due to the fact that cost and revenue data are not disclosed by airlines, the *season-wide available seat kilometres* can be used to approximate the value of each request without requiring cost/revenue input. This argument is supported by empirical analyses that suggest that the most significant determinants of airfares and airline revenues are travel distance, passengers and aircraft load factors (Vowles, 2006). That is because requests concerning more passengers and longer distances are more difficult to implement for airlines since they require more resources. Hence, the season-wide available seat kilometres metric augments previous research that approximates airlines preferences by considering additional operational characteristics that are valued by airlines (distance covered, load factor,

passenger seats). The season-wide available seat kilometres metric constitutes the first component of the airlines' prioritisation function.

In addition, to the season-wide available kilometres, another determinant of airfares and airlines' revenues is the competition faced by the airline for the route concerning each submitted request ( $m \in M$ ). Competition is a significant element that is considered by airlines when planning their scheduling decisions since it determines the aircraft size that will be used for a route and the frequency of services concerning the route (Vaze and Barnhart, 2012). Furthermore, since route competition affects airfares and airline frequency (Morrison and Winston, 1990) in deregulated markets, the consideration of route-specific competition dynamics enables a better modelling of airlines' scheduling preferences. Consequently, the second element of the proposed airlines' prioritisation functions is the route-specific competition faced by each request. Given these two modelling components, the exponent of the airlines' prioritisation function is calculated using the following formula.

$$\xi_m = \frac{\overbrace{\Delta(O_m, D_m) sen_m l f_m |D_m|}^{\text{season-wide available seat kilometres/miles}}}{\max_{m' \in M_{am}} \{\Delta(O_{m'}, D_{m'}) sen_{m'} l f_{m'} |D_{m'}|\}} p_m \Bigg\} \begin{array}{l} \text{competition} \\ \text{index} \end{array} \quad (4.11)$$

The data required to construct  $\xi_m$  can be inferred by the information disclosed by airlines when submitting their slot requests. In particular, in expression (4.11), the origin-destination distance is calculated in our work using the following formula:

$$\Delta_m(O, D) = R \oplus \times \cos^{-1}[\sin(\varphi_O) \sin(\varphi_D) + \cos(\varphi_O) \cos(\varphi_D) \cos(\lambda_D - \lambda_O)] \quad (4.12)$$

$\Delta_m(O, D)$  is the distance covered by request  $m$  that connects an origin ( $O$ ) and destination ( $D$ ) airport with given latitude and longitude coordinates  $(\varphi_O, \lambda_O)$  and  $(\varphi_D, \lambda_D)$  (in decimal degrees) based on the great circle distance formula (see expression (4.12)) which considers earth's radius ( $R_\oplus$ ) and curvature (Hickley, 2004). In the case that  $m$  is an arrival,  $\Delta_m(AP_{ma}, AIP)$  is calculated as the distance of the studied airport ( $AIP$ ) from the previous airport of origin ( $AP_{ma}$ ), while if  $m$  departs from the studied airport, the covered distance is calculated as the distance between the studied airport and the next destination airport  $\Delta_m(AIP, AP_{md})$ .

Furthermore, the number of seats requested by  $m$  ( $sen_m$ ) is disclosed by airlines as per the Standard Schedules Information Manual (SSIM) format.  $lf_m$  is the load factor associated with request  $m$ , however, since it is rarely known in advance, for the purposes of the initial slot allocation, coordinators consider aggregate load factor estimates (calculated using historic data) that differentiate between different types of operations (charter, scheduled) and markets (domestic, international). Finally,  $|D_m|$  is the number of days that request  $m$  is to operate and is calculated through the joint consideration of the frequency of operations and the number of weekdays that request  $m$  concerns.

$p_m$  is the competition index relating to request  $m$  that is defined as:

$$p_m = \left( \frac{|\{a \in A | \exists \mu \in M_a : \ddot{a}_m = \ddot{a}_\mu\}|}{\max_{m' \in M_{a_{m'}}} |\{a \in A | \exists \mu \in M_a : \ddot{a}_{m'} = \ddot{a}_\mu\}|} \right) \quad (4.13)$$

(4.13) accounts for the number of carriers that serve a route and counts the number of unique airlines flying to the airport concerning request  $m$  ( $|\{a \in A | \exists \mu \in M_a : \ddot{a}_m = \ddot{a}_\mu\}|$ ) and the number of airlines that serve the route/airport in an airline's request portfolio with the largest competition (largest number of airlines serving the route). This index models route-specific competition

by considering the number of carriers serving each route. This intuitive modelling choice is supported by the fact that in competitive markets, the average number of carriers per route is higher than those experienced in regulated markets with less competition (Kahn, 1988). The index excludes from the counts airlines that belong to the same alliance as airline  $a_m$ . Hence, the greater the number of airlines serving the route, there is more competition and hence the value of the competition index increases. Furthermore, the index may be adjusted so as to filter out requests that request to operate at significantly different time intervals, i.e., during times that are more than  $\tau$  intervals away from the requested time of  $m$  ( $t_m$ ). This would alter the definition of (4.13) as follows.

$$p_m^\tau = \left( \frac{|\{a \in A | \exists \mu \in M_a: \ddot{a}_m = \ddot{a}_\mu \cap t_\mu \in [t_m - \tau, t_m + \tau]\}|}{\max_{m' \in M_{a_{m'}}} |\{a \in A | \exists \mu \in M_a: \ddot{a}_{m'} = \ddot{a}_\mu \cap t_\mu \in [t_m - \tau, t_m + \tau]\}|} \right) \quad (4.13')$$

(4.11) may consider different load factor parameters for each request. However, as argued in section 4.3.2.1, since load factor data are not disclosed by airlines, current practice considers aggregate load factor estimates per movement type, i.e., charter/scheduled, based on the coordination parameters of the airport. For instance, the current study assumes a load factor of 85% (as per the declared capacity parameters of the airport under consideration) and 100% (common operational assumption) for scheduled and charter operations respectively. This is in accordance with current practice which considers similar aggregate load factor values.

To provide insights on the influence of the load factor on the value of the demand prioritisation's functions exponent, section 4.5.2 provides a series of statistical analyses that suggest that there is no statistical evidence that the load factor affects the value of the proposed exponent (both for the coordinators

and airlines functions). Again, if one wishes to consider load factor estimates of higher fidelity in (4.11), they may consider load factor data for each request, which can be procured through independent commercial sources. Expressions (4.11) can be used as a sensible proxy to model the importance that each airline assigns to each request in relation to the other requests that the same airline submits. Expressions (4.11) may be transformed so as to express the relative importance of request  $m$  in relation to the other request(s) submitted by airline  $a$  (airline submitting request  $m$ ). Using the following transformation, the value of each request is anchored to the request portfolio of each airline.

$$\xi'_m = \frac{\xi_m}{\max_{m' \in M_{a_m}} \xi_{m'}} \quad (4.14)$$

Up to this point, this section has discussed how the exponent of the demand prioritisation function depends on the characteristics of the request. In considering that different time slots are valued differently for each submitted request, expression (4.14) is incorporated in a time-dependent delay discount utility function (see expression (4.15)).

$$E_m(t) = [\mu_m^{t_m}(t)]^{2-\xi'_m} \quad (4.15)$$

Expression (4.15) considers airlines' timing flexibility preferences as expressed by the Timing Flexibility Indicator (Katsigiannis and Zografos, 2021a) and determines how the importance that an airline assigns to each of its requests is depreciated as the allocated slot deviates from the requested times.

Hence, the proposed time-dependent functions, not only consider each request's importance in relation to the other requests belonging to an airline's portfolio, but also considers the timing flexibility preferences of airlines for each of the requests that they submit. This flexibility can be determined by airlines'

internal operational criteria and constraints and hence does not require airlines to reveal sensitive commercial information (Katsigiannis and Zografos, 2021a) regarding their scheduling behaviour. Interestingly, since the introduction of the TFI, the concept of airline timing flexibility has become increasingly important and it's currently transitioning from being a voluntary option to being a requirement. The importance of airlines' timing flexibility preferences is manifested in the following excerpt from the World Airport Scheduling Guidelines (WASG) (IATA/ACI/WWACG, 2020, p. 34): '*airlines and other aircraft operators should clearly indicate the range of flexibility they are prepared to accept (if any) using the appropriate industry codes and format in their submission*'.

In (4.15)  $\mu_m^{tm}(t)$  is the TFI membership function provided in Katsigiannis and Zografos (2021a) and considers an airline's earliness ( $\varphi_m^l$ )/tardiness( $\varphi_m^u$ ) flexibility preferences for request  $m$  as per expression (4.16).

$$\mu_m^{t'}(t) = \begin{cases} \frac{t' - t}{\varphi_m^l - 1} + 1, & \text{if } t \leq t' \text{ and } t - t' > \varphi_m^l - 1 \\ \frac{t' - t}{\varphi_m^u + 1} + 1, & \text{if } t - t' > 0 \text{ and } t - t' < \varphi_m^u + 1 \\ 0, & \text{if } t - t' \leq \varphi_m^l - 1 \text{ or } t - t' \geq \varphi_m^u + 1 \end{cases} \quad (4.16)$$

As per expression (4.16), in the function denoted by (4.15), the maximum utility of each request (a value of 1) is observed when the request receives its requested time ( $t_m$ ). This is a realistic assumption since the '*requested slot time presumably reflects the top preference of the carrier*' (Odoni, 2020, p. 57). Meanwhile, function (4.15) captures airlines upper/lower flexibility bounds, since for time slots lying outside the  $[\varphi_m^l + t_m, \varphi_m^u + t_m]$  interval, the reported utility becomes 0. The exponent of function (4.15) takes values between (1,2] hence being a super-additive expression that penalises larger displacements (Androutsopoulos et al., 2019; Castelli et al., 2011; Fairbrother et al., 2019). The fact that the



exponent of (4.15) depends on the characteristics of the requests, shapes the delay-discount behaviour between the requested time and the lower and upper flexibility bounds provided by the airlines  $(\varphi_m^{l(u)})$ .

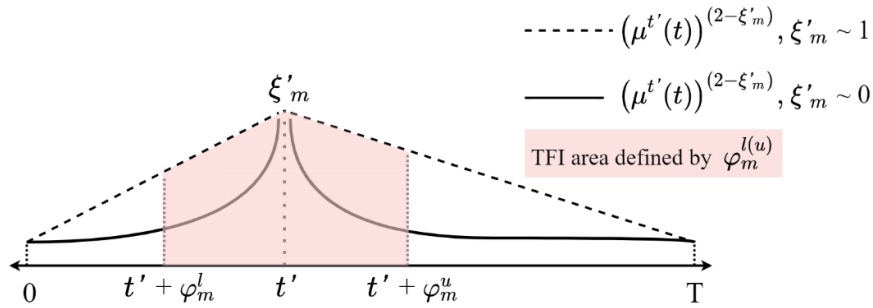


**Figure 4-2:** Graphical representation of each request’s function

For instance (see Figure 4-2), a request with a larger number of available seat kilometres facing increased competition, would receive a value for  $\xi'_m$  that is closer to 1, hence reducing the rate of discount in (4.15). Similarly, a request that does not face a similar level of competition or concerns a smaller number of available seat kilometres, would receive a value for  $\xi'_m$  that is closer to 0, thus receiving more drastic discounts to the utility of a request. According to this observation, an important property of (4.15) is that more important requests (based on (4.14)) will pre-empt *ceteris paribus* other requests. This observation is further formalised in the following proposition.

**Proposition 4.1** The utility of more important requests (as per (4.15)) that cannot be accommodated to their requested times, will always be greater than the utility of less significant requests *ceteris paribus*.

*Proof.* Assume two requests  $(m_1, m_2)$ . Then, to prove that the utility of  $m_1$  will always be greater than the utility of  $m_2$ , it would suffice to prove that:

$$\mathcal{E}_{m_1}(t) > \mathcal{E}_{m_2}(t) \stackrel{(4.15)}{\iff} \left[ \mu_{m_1}^{t_{m_1}}(t) \right]^{2-\xi'_{m_1}} > \left[ \mu_{m_2}^{t_{m_2}}(t) \right]^{2-\xi'_{m_2}} \quad \forall t \neq t_{m_1}, t_{m_2}$$

Since all other factors are equal ( $t_{m_1} = t_{m_2}, \varphi_{m_1}^{l(u)} = \varphi_{m_2}^{l(u)}$ ), the only difference between the two parts of the above inequalities is the exponent. As a result, we know by (4.16) that  $\mu_{m_1}^{t_{m_1}}(t) = \mu_{m_2}^{t_{m_2}}(t) \in (0,1) \quad \forall t \in T_{\bar{c}}$ . For simplicity let us denote  $a = \mu_{m_1}^{t_{m_1}}(t) = \mu_{m_2}^{t_{m_2}}$  and transform the above inequalities using logarithms.

$$(2 - \xi'_{m_1}) \log a > (2 - \xi'_{m_2}) \log a \stackrel{\text{since } \log a < 0}{\iff} 2 - \xi'_{m_1} < 2 - \xi'_{m_2} \iff \xi'_{m_1} > \xi'_{m_2}$$

Hence, we prove that  $\mathcal{E}_{m_1}(t) > \mathcal{E}_{m_2}(t) \stackrel{\text{ceteris paribus}}{\iff} \xi'_{m_1} > \xi'_{m_2}$ . This holds for each time interval  $t$  that falls into the requests' tardiness/earliness bounds.

Based on Proposition 4.1, the following remark draws useful conclusions regarding the properties of (4.15).

**Remark 4.1** When displaced, more important requests will pre-empt less important requests *ceteris paribus*. In the case that none of the requests is displaced then the utility of each request (regardless of its importance) is equal to 1 (100% utility).

Figure 4-2 provides a graphical representation of how the shape of (4.15) changes for the extreme values of the exponent (4.14).

### ***Discussion on the airline demand prioritisation functions***

Despite the absence of cost/revenue data regarding airlines' requests, ASA studies have used surrogate metrics and functions so as to approximate airlines scheduling preferences. The approximation proposed in this paper enhances previous models considering airlines' preferences by taking into account additional operational characteristics and market dynamics. In addition to the factors previously

considered in the literature (passengers, effective operational period, time-dependent components), the demand prioritisation functions (as modelled in function (4.15)) proposed in this work provide an explicit modelling of route-specific competition and consider the number of seat kilometres offered by each request. Hence, expressions (4.15) consider the main determinants of airline revenues/costs, i.e., passengers, distance (Feng and Wang, 2000), competition (Morrison and Winston, 1990), load factors (Baltagi et al., 1995) and provide a meaningful approximation of the importance assigned by airlines to each of the submitted requests.

From a technical perspective, the proposed prioritisation functions guarantee that requests of higher importance will pre-empt requests of lower importance *ceteris paribus*. To further demonstrate the applicability of (4.15) we have conducted extensive statistical analyses that exhibit the robustness of the exponent of (4.15) with respect to alternative load factor scenarios and the ability of (4.11) to distinguish between requests with similar operational characteristics. Our analyses are appended in section 4.5.2.1.

#### ***4.3.2.1 Functions relating to the coordinators' side***

The exponent of the coordinators' function is different from the exponent of the airline demand prioritisation function and considers the secondary policy criteria defined by the World Airport Scheduling Guidelines (WASG). The exponent of the coordinators' prioritisation function for each request is denoted by  $\psi_m$  and is formulated as follows.

$$\psi_m = \xi_m'' \left( \overbrace{\left( 1 - \frac{|\{\mu \in M | \ddot{a}_m = \ddot{a}_\mu\}|}{\max_{m \in M} |\{\mu \in M | \ddot{a}_m = \ddot{a}_\mu\}|} \right)}^{\text{connectivity index}} \overbrace{\left( \frac{|\{a \in A | \exists \mu \in M_a : \ddot{a}_m = \ddot{a}_\mu\}|}{\max_{m \in M} |\{a \in A | \exists \mu \in M_a : \ddot{a}_m = \ddot{a}_\mu\}|} \right)}^{\text{competition index}} \right) \quad (4.17)$$

In (4.17)  $\xi_m''$  is calculated as  $\xi_m / \max_{m \in M} \xi_m$  and provides a proxy on the importance of a request in relation to all other requests submitted to the airport (in contrast to  $\xi_m'$  which provides the importance of requests in comparison to the other requests of the same airline).  $\xi_m''$  allows (4.17) to consider the needs of cargo/passenger airlines, the effective period and the frequency of operations associated with each request (since these are the components of  $\xi_m$  as per expression (4.14)). In addition, expression (4.17) integrates a connectivity index which considers the number of requests that serve a specific route (Burghouwt and Redondi, 2013). The connectivity index counts the number of requests ( $|\{\mu \in M | \ddot{a}_m = \ddot{a}_\mu\}|$ ) that serve the airport ( $\ddot{a}_m$ ) served by request  $m$ , divided by the requests of the most connected route  $\max_{m \in M} |\{\mu \in M | \ddot{a}_m = \ddot{a}_\mu\}|$ . Hence, as per the formulation of the index, the larger the number of requests serving a route, the less is the connectivity offered by the request ( $m$ ) and therefore the value of the connectivity index diminishes. This implies that a request that serves a route that is not served by other requests, will receive the maximum value of connectivity since it connects the airport to a completely new route.

The last component of  $\psi_m$  is the competition index, which accounts for the number of carriers that serve a route. The competition index counts the number of unique airlines flying to the airport concerning request  $m$  ( $|\{a \in A | \exists \mu \in M_a : \ddot{a}_m = \ddot{a}_\mu\}|$ ) and the number of airlines that serve the route/airport with the largest competition (largest number of airlines serving the route). Hence, the greater the number of airlines serving the route, there is more competition and hence the value of the competition index increases (the value of the competition index decreases). Given that the three components of (4.17) may receive values between 0 and 1, then  $\psi_m$  also takes values between 0 and 1. Once calculated for all requests,  $\psi_m$  can be rescaled so to express the relative priority (as

per the secondary criteria of WASG) of request  $m$  with respect to the other requests submitted at the airport. This is done through the following expression.

$$\psi'_m = \frac{\psi_m}{\max_{m \in \mathcal{M}} \psi_m} \quad (4.18)$$

Overall,  $\psi'_m$  considers: Competition; Connectivity; Passengers/Shippers needs; and the Effective period and frequency of operations. As a result, the proposed exponent models the majority of the secondary rules of WASG (see (IATA/ACI/WWACG, 2020, pp. 35–36)). The time-dependent base of the coordinators' function takes into account all main criteria of WASG since it considers historic's and changes to historic's rules as well as new entrants and year-round operations. The base of the function incorporates  $\psi'_m$  and is formulated as follows:

$$\Psi_m(t) = \left( \mu_m^{t_m}(t) + I_m \bar{\mu}_m^{t_m}(t) + y_m \right)^{(2-\psi'_m)} \quad (4.19)$$

In (4.19),  $I_m$  and  $y_m$  are binary parameters.  $I_m$  is equal to one if request  $m$  concerns operations with historical usage rights, i.e., historic ( $H$ ), changes to historic ( $CH$ ) requests, and 0 otherwise.  $y_m$  is equal to one if request  $m$  extends to a year-round set of operations. As a result, expression (4.19) provides a seamless modelling of several primary criteria of the administrative ASA regulatory framework. For new entrant requests, expression (4.19) becomes equal to  $\left( 2\mu_m^{t_m}(t) \right)^{(2-\psi'_m)}$  with  $\varphi_m^{u(t)}$  being equal to  $60/\tilde{c}$ , i.e., the 1-hour equivalent expressed in coordination intervals. This modification considers WASG's rules for new entrants which require carriers to accept slot offerings that are within one hour from the requested times, or lose the new entrant status. (IATA/ACI/WWACG, 2020). Similar to expressions (4.15), function (4.19) is a time-dependent, super additive function that may penalise large displacements (since the exponent is

greater or equal to 1), hence similar to Proposition 4.1 , the greater the value of  $\psi'_m$ , the larger is the tie-breaking priority assigned to request  $m$ . On another note, function (4.19) guarantees that requests with historic usage rights will receive the highest priorities for time slots that lie within their historical usage and their currently requested times (if different). This claim is formally proved in the following propositions (Proposition 4.2 and Proposition 4.3 ).

**Proposition 4.2**  $\mu^{t_m}(t) + \mu^{\bar{t}_m}(t)$  will receive its maximum value ( $\psi'_m, I_m$  and  $y_m$  *ceteris paribus*) for time slots between the requested ( $t_m$ ) and the historic ( $\bar{t}_m$ ) time slots.

*Proof.* Assume that  $0 \leq t_m \leq \bar{t}_m \leq |T_{\bar{c}}|$ . Let's assume the time-dependent function  $J(t)$ , which is equal to  $\mu^{t_m}(t) + \mu^{\bar{t}_m}(t)$  where  $\mu^{t_m}(t), \mu^{\bar{t}_m}(t)$  are given by expression (4.16).  $\forall t \in (t_m, |T_{\bar{c}}|)$  we have  $(\mu^{t_m}(t))' = -1/(|T_{\bar{c}}| - t + 1) < 0$ . Hence,  $\mu^{t_m}(t)$  is strictly decreasing in  $[t_m, |T_{\bar{c}}|]$ .  $\forall t \in (0, t_m)$  we have (4.16)  $(\mu^{t_m}(t))' = +1/(1 + t_m) > 0$ . Hence,  $\mu^{t_m}(t)$  is strictly increasing in  $[0, t_m]$ . As a result,  $\forall s \in [0, t_m]$  we have  $J(s) = \mu^{t_m}(s) + \mu^{\bar{t}_m}(s) \leq \mu^{t_m}(t_m) + \mu^{\bar{t}_m}(t_m) = J(t_m)$ , since  $J(s)$  is increasing in  $[0, t_m]$ .  $\forall s \in [\bar{t}_m, |T_{\bar{c}}|]$  we have  $J(s) = \mu^{t_m}(s) + \mu^{\bar{t}_m}(s) \leq \mu^{t_m}(\bar{t}_m) + \mu^{\bar{t}_m}(\bar{t}_m) = J(\bar{t}_m)$ , since  $J(s)$  is decreasing in  $[\bar{t}_m, |T_{\bar{c}}|]$ . Therefore,  $\max\{J(s): s \in [0, |T_{\bar{c}}|]\} = \max\{J(s): s \in [t_m, \bar{t}_m]\}$ . Similarly, we may prove that if  $0 \leq \bar{t}_m \leq t_m \leq |T_{\bar{c}}|$   $\max\{J(s): s \in [0, |T_{\bar{c}}|]\} = \max\{J(s): s \in [\bar{t}_m, t_m]\}$ .

**Proposition 4.3** In the case that the requested and the historic times coincide ( $\bar{t}_m = t_m$ ), the maximum of  $\Psi_m(t)$  is obtained for  $t_m$  and has a value  $\Psi_m(t_m)$ .

*Proof.*  $\Psi_m(t)$  is strictly increasing from time intervals between 0 and  $\bar{t}_m = t_m$  and strictly decreasing from  $\bar{t}_m = t_m$  to  $|T_{\bar{c}}|$ . Hence, its maximum value is exactly  $\Psi_m(t_m)$ .

In addition, we may further specify the conditions under which  $\Psi_m(t)$  will receive its maximum value exactly for the requested or the historic times ( $t = t_m$  or  $t = \bar{t}_m$ ).

**Proposition 4.4**  $\mu^{t_m}(t) + \mu^{\bar{t}_m}(t)$  ( $\psi'_m, I_m$  and  $y_m$  *ceteris paribus*) will receive its maximum value either during time slot  $t = t_m$  if  $\bar{t}_m \geq |T_{\bar{c}}| - t_m$  and  $t_m \leq \bar{t}_m$ , or  $t = \bar{t}_m$  if  $\bar{t}_m \leq |T_{\bar{c}}| - t_m$  and  $t_m \geq \bar{t}_m$ .

*Proof.* Since  $J(t) = \mu^{t_m}(t) + \mu^{\bar{t}_m}(t)$  comprises of two piecewise linear functions it follows that also  $J(t)$  is a piecewise linear function. Recall that every piecewise linear function obtains its maximum value at the points that it is not differentiable ( $t_m, \bar{t}_m$  in our case) or at the limits of its domain ( $0, |T_{\bar{c}}|$ ). However, based on Proposition 4.2 it suffices to check for the maximum of  $J(t)$  only at  $J(\bar{t}_m)$  and  $J(t_m)$ . Note that  $J(t_m) = 1 + \mu^{\bar{t}_m}(t_m)$  and  $J(\bar{t}_m) = \mu^{t_m}(\bar{t}_m) + 1$ . Hence, we may only compare  $\mu^{t_m}(\bar{t}_m)$  and  $\mu^{\bar{t}_m}(t_m)$ . If  $t_m \leq \bar{t}_m$ , from (4.16), we have that:  $\mu^{t_m}(\bar{t}_m) = 1 - (\bar{t}_m - t_m)/(|T_{\bar{c}}| - t_m + 1)$  and  $\mu^{\bar{t}_m}(t_m) = 1 - (\bar{t}_m - t_m)/(1 + \bar{t}_m)$ .

By comparing the two functions, we get:

$$\mu^{\bar{t}_m}(t_m) - \mu^{t_m}(\bar{t}_m) = \frac{(\bar{t}_m - t_m)(\bar{t}_m - |T_{\bar{c}}| + t_m)}{(|T_{\bar{c}}| - t_m + 1)(1 + \bar{t}_m)} \quad (4.20)$$

Both components of the denominator in (4.20) are positive and  $t_m \leq \bar{t}_m$ . Therefore,  $\mu^{\bar{t}_m}(t_m) - \mu^{t_m}(\bar{t}_m) \geq 0 \Leftrightarrow \bar{t}_m - |T_{\bar{c}}| + t_m \geq 0$ . Then  $\max\{J(s): s \in [0, |T_{\bar{c}}|]\} = J(t_m)$ . Similarly, if  $t_m \geq \bar{t}_m$ ,  $\mu^{\bar{t}_m}(t_m) - \mu^{t_m}(\bar{t}_m) \geq 0 \Leftrightarrow \bar{t}_m \leq |T_{\bar{c}}| - t_m \Leftrightarrow \max\{J(s): s \in [0, |T_{\bar{c}}|]\} = J(\bar{t}_m)$ .

An important aspect of (4.19) is that the requirements of (IATA/ACI/WWACG, 2020) are satisfied as soft constraints. For instance, a historic ( $H$ ) request will always pre-empt a request without historic rights *ceteris*

*paribus*. In addition, a year-round request will also pre-empt requests that are requested for a single period of operations. As a result, and in conjunction with Proposition 4.1 -Proposition 4.4 , may grasp all primary slot scheduling criteria of WASG. Finally, guarantee that more significant requests as per the exponent of the function will always pre-empt less significant requests (may be proved using Proposition 4.1 ).

### ***Discussion on the coordinators' functions***

Overall, the coordinators' functions provide an explicit modelling of the priorities assigned by the coordinator to each request (based on the WASG rules and the airlines preferences). In particular, the coordinator's functions consider all main policy rules and criteria defining the ASA process. For instance, the functions can be adapted to model the policy rules associated with historic and changes to historic requests, new entrants' requests, and year-round operations. Furthermore,  $\psi'_m$  considers competition, connectivity, and each request's operational characteristics (passengers, effective period of operations, distance covered) in relation to the other requests comprising the request set. To further support the design of the proposed prioritisation functions, in section 4.5.2.2, we provide statistical analyses that validate the robustness of  $\psi'_m$  with respect to load factor data uncertainty, and its ability to differentiate among requests sharing similar characteristics.

At this point, it is worth mentioning that the coordinators' functions can be calibrated based on the local decision-making context and the requirements of each airport. For instance, expressions (4.17) may be altered through the introduction of weights for  $\xi''_m$ , the connectivity and competition indexes and assign a higher relative importance to requests that face severe competition or contribute to the connectivity of the airport. The airport-specific adaptation of (4.17) and (4.19)



based on the discretion available to the coordinators for applying WASG, is a promising pathway for future research.

#### ***4.3.2.1.3 Demonstration of the proposed functions for different request priorities***

A demonstration of the functions for different types of request priorities is given in Figure 4-3, which demonstrates the shape of the time dependent functions both for the airlines (subplot (a)) and the coordinator (subplot (b)). The requests presented in Figure 4-3 belong to all main slot request priorities (i.e., Historic, Changes to Historic, New Entrant and Other requests). Subplot (a) exhibits how the preference functions of requests with identical requested times are shaped by the  $\xi'_m$  exponent (as defined in expressions (4.14)). For instance, subplot (a) exhibits how a more important request (since it has a larger value for  $\xi'_m$ ) falling into the *CH* slot request priority will pre-empt a *NE* request when displaced. The curve representing the preference function of the *CH* request lies above the line of the *NE* entrant request because the  $\xi'_m$  of the *CH* request is greater than the  $\xi'_m$  of the *NE* request (the *NE* request is to operate for 8 weeks, while the *CH* request concerns operations concerning 20 weeks. For the sake of completeness subplot (a) showcases how the arrival and departure movements of a historic request will pre-empt the corresponding movements of a request falling into the Others' priority.

Regarding the coordinators' functions (subplot (b)), we observe how the shape of the functions is determined by the priority class of each request. Notably, *H* requests pre-empt all other requests during their requested times, and since there is available capacity for all historic requests, the proposed functions ensure that they will not be pre-empted by requests of lower priority. In addition, the *CH* request appears to have reduced importance in comparison to the *NE* request during time slots that are within one hour from the requested times. Furthermore, one can distinguish how the prioritisation function of the *CH* request has a double top

between the historic and the requested times. Finally, in subplot (b) it is evident that the movements associated with the  $O$  request will be pre-empted by all other requests. An exception is the  $NE$  request, whose priority diminishes when displaced more than one hour from the requested time.

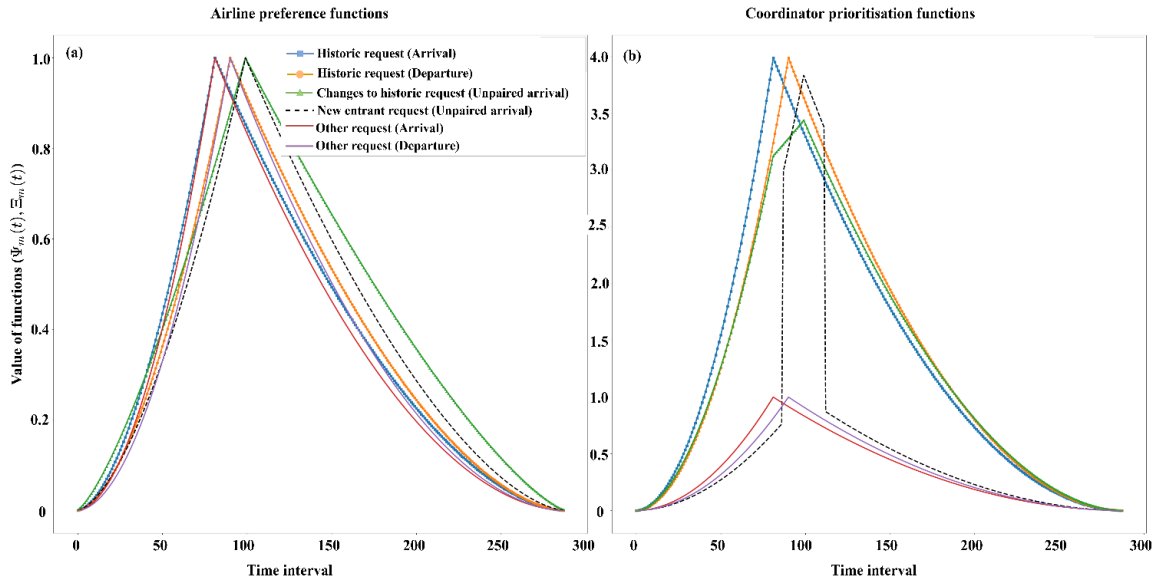


**Figure 4-3:** *Plots of the proposed functions for requests of different priorities*

### 4.3.2.2 Stability enforcing inequalities

We may now introduce the constraints that prune the creation of blocking allocations and lead to stable airport slot scheduling decisions. The inequalities that follow, extend the inequalities proposed by Baïou and Balinski (2000), which defined the polytope of the college admissions problem. According to the college admissions problem, multiple students are matched to multiple colleges. Students and colleges have preferences over each other, and colleges have a certain student capacity that cannot be exceeded. In the ASA problem the constraints that have to be considered are more complex and require additional modelling effort. Specifically, the inequalities that follow consider multiple capacity constraint dimensions, i.e., the runway capacities for arrivals, departures and total movements, turnaround/precedence constraints and problem specific policy rules

concerning new entrant movements. In what follows we provide the formulations of the inequalities and prove their ability to prune blocking allocations.

Let  $\omega_{d,t,\bar{c}}^{k,m}$  be a binary variable. Inequalities (4.21) define  $\omega_{d,t}^{k,m}$  as follows.  $\omega_{d,t}^{k,m} = 1$ , if the number of requests of movement type  $k$  that are scheduled on time  $t$  and day  $d$  and have higher priority over  $m$ , is less than the available capacity  $u_{d,t,c}^k$ ; and  $\omega_{d,t}^{k,m} = 0$ , if there is no available capacity left after the allocation of requests of higher priority than  $m$ .

$$\begin{aligned}
 u_{d,t,c}^k \omega_{d,t}^{k,m} &\geq u_{d,t,c}^k && \forall c \in C, k \in K, m \in \\
 - \sum_{\mu \in M^k: \psi_\mu(t) > \psi_m(t)} a_\mu^d \sum_{t' \in [t, t+c-1]} x_{t',\mu} &\geq 0 && M^k: d \in D_m, t \in [0, |T_{\bar{c}}| - c]
 \end{aligned} \tag{4.21}$$

In addition, since a request can be scheduled on time  $t$  if and only if there is available capacity both for the specific movement type and total movements, i.e., an arrival (departure) is scheduled if there is available capacity for arrivals (departures) and total movements, constraints (4.22) are added so as to keep track of the available capacity for both total movements and arrivals (departures).

$$\begin{aligned}
 \frac{\sum_{k' \in (k, Total)} \sum_{d \in D_m} \omega_{d,t}^{k',m}}{|D_m|} &\leq \frac{2|D_m| - 1}{|D_m|} + us_t^m && \forall c \in C, k \in \\
 &&& (Arr, Dep), m \in M^k / M_{NE}^k, t \in T_{\bar{c}}
 \end{aligned} \tag{4.22}$$

In (4.22) the left-hand side takes values between 0 and 2. If the left hand side has a value of 2, then time slot  $t$  is under-scheduled with respect to  $t$ . The right-hand side of the constraints comprises  $(2|D_m| - 1)/|D_m| < 2$  and variable  $us_t^m$ . Hence, as per (4.22),  $us_t^m$  is an auxiliary binary variable which is equal to 1 if there is available capacity both for  $k$  and *Total* movements across all days concerning request  $m$  and 0 otherwise. Please observe that in (4.22) we do not consider new entrants' requests. That is because we introduce adjusted inequalities

that consider the rules of WASG for this request priority in section 4.3.2.2.1. In addition,  $\delta_{t,m}$  is another auxiliary variable which is equal to 1 if assignment  $(m, t)$  violates the turnaround time constraints of  $m$  as per the following constraints.

$$\sum_{t \in [0, \kappa)} x_{md,t} + \sum_{t \in [\kappa - TT_m, |T_{\bar{c}}|]} x_{ma,t} \leq 1 + \delta_{t,m} \quad \forall (ma, md) \in M \times M: v_m = 0, \kappa \in [TT_m, |T_{\bar{c}}|] \quad (4.23)$$

$$\sum_{t \in [0, \kappa)} x_{md,t} + \sum_{t \in [\kappa - TT_m + |T_{\bar{c}}|, |T_{\bar{c}}|]} x_{ma,t} \leq 1 + \delta_{t,m} \quad \forall (ma, md) \in M \times M: v_m = 1, \kappa \in [0, TT_m) \quad (4.24)$$

Given expressions (4.21)-(4.24), the following constraints ensure that there will be no blocking allocations.

$$us_t^m \leq \left( \sum_{\tau \in T_{\bar{c}}: \mathcal{E}_m(\tau) > \mathcal{E}_m(t)} x_{m,\tau} \right) + \delta_{t,m} \quad m \in M, t \in T_{\bar{c}} \quad (4.25)$$

Therefore, the solution of expressions (4.1)-(4.5), (4.10) and (4.21)-(4.25) leads to stable airport slot allocation schedules, thus concluding the formulation of SASAM. This finding is formalised in the following proposition. Please note that the definition of  $us_t^m$  in (4.25) is different for new entrant requests. Instead of being defined as per (4.22), the auxiliary variable for new entrant requests is altered so as to account the slot pool definition of WASG. The adjusted definition of  $us_t^m$  is provided in the following subsection.

**Proposition 4.5** Expressions (4.1)-(4.5), (4.10) and (4.21)-(4.25) lead to schedules that are free of blocking allocations.

*Proof.* This will be a proof by contradiction. Assume a feasible allocation  $(m, \tau)$  of a schedule produced by solving expressions (4.1)-(4.5), (4.10) and (4.21)-(4.25). Since the allocation is feasible the turnaround time constraints are not violated and  $\delta_{\tau,m} = 0$ . Now suppose that the allocation blocks the formation of a stable schedule. Therefore, either the request  $(m)$  is assigned to a slot  $t$  that has  $\mathcal{E}_m(t) < \mathcal{E}_m(\tau)$  or

it is not assigned at all to a slot that belongs to its preference list. Hence,  $\sum_{t \in T_{\tilde{c}}: \varepsilon_m(t) \geq \varepsilon_m(\tau)} x_{m,\tau} = 0$ . In addition, since the allocation is blocking the formation of a stable schedule there should be available capacity during time interval  $t$  across all days that  $m$  operates, hence  $us_t^m = 1$ . This means that (4.25) is violated which is a contradiction to the initial assumption, the allocation is not feasible. As a result, expressions (4.25) prune unstable allocations.

**Proposition 4.6** The solution of the model described by expressions (4.1)-(4.5), (4.10) and (4.21)-(4.25) leads to a schedule that is feasible for the airport based on the model of section 4.3.1

*Proof.* This is proved by the fact that constraints (4.1)-(4.5) are maintained in the formulation of SASAM. Therefore, the solution of SASAM is feasible for the model defined by (4.1)-(4.5) and (4.10).

#### 4.3.2.2.1 Considering new entrants' rules

To consider the rules associated with the slot pool and the new entrants' requests we introduce the following constraints.

$$HM = \sum_{m \in M_H} \sum_{t \in T_{\tilde{c}}} x_{t,m} \quad (4.26)$$

$$NEM_m = \sum_{\mu \in M_{NE}/m: \Psi_{\mu}(t) > \Psi_m(t)} \sum_{t \in T_{\tilde{c}}} x_{t,\mu} \quad \forall m \in M_{NE} \quad (4.27)$$

$$NEM_m \leq 0.5 \left[ \sum_{d \in D} \sum_{t \in T_{\tilde{c}}} (u_{d,t,\tilde{c}}^{Total}) - HM \right] = SP \quad \forall m \in M_{NE} \quad (4.28)$$

Constraints (4.26)-(4.28) define the slot pool, i.e. the available slots after the allocation of historic requests (expression (4.26)) of whom up to 50% are allocated to requests of new entrants (defined in (4.27)) with the remaining being given to  $CH$  and  $O$  requests. Consequently, the stability constraints for new entrant requests

are modified by substituting (4.22) with (4.30). In (4.30),  $us_t^m=1$  where there is available runway capacity in both the slot pool and the runways during all days that  $m$  is requested to operate. Inequalities (4.30) are defined with the aid of the following inequalities.

$$\left( \sum_{d \in D} \sum_{t \in T_{\bar{c}}} u_{d,t,\bar{c}}^{Total} \right) \Omega_m \geq SP - NEM_m \quad \forall m \in M_{NE} \quad (4.29)$$

Expressions (4.29) are added so as to monitor the remaining capacity in the slot pool after the allocation of more important requests than  $m$ . Hence,  $\Omega_m$  is 1 if there is remaining capacity in the slot pool, and 0 otherwise.

$$\begin{aligned} \left( \frac{\sum_{k' \in (k, Total)} \sum_{d \in D_m} \omega_{d,t}^{k',m}}{|D_m|} \right) + \Omega_m & \quad \forall k \in (Arr, Dep), m \in \\ & \quad M_{NE}^k, t \in T_{\bar{c}} \\ & \leq \frac{2|D_m| - 1}{|D_m|} + 1 + us_t^m \end{aligned} \quad (4.30)$$

In (4.30),  $us_t^m$  takes the value of 1 if there is available runway capacity during all days that request  $m$  is to operate and there is available capacity in the slot pool. Hence, as per the requirements of WASG, if 50% of the remaining capacity of the slot pool does not suffice to allocate all new entrant requests, then the new entrant requests that will be prioritised over other requests, will be the ones that exhibit better performance with respect to the secondary criteria of WASG (as per  $\Psi_m(t)$  and expressions (4.21)). Given this updated set of expressions for new entrant requests, we may prove through a simple substitution, that expressions (4.25) hold and prune blocking allocations when  $us_t^m$  is defined by (4.30). After the addition of (4.30), the proposed formulation results in a slot allocation model that prunes unstable slot allocations (see Definition 4.1) and considers all primary slot allocation rules regarding series of slots, new entrants, requests with historic rights and year-round operations. Concurrently, as argued in

section 4.3.2.1 ,  $\Psi_m(t)$  and  $\mathcal{E}_m(t)$  consider additional criteria and policy rules, hence providing a holistic modelling of the ASA problem defined by WASG.

## 4.4 Solution methodology

This section discusses the solution methodologies that are developed so as to solve SASAM. Section 4.4.1 details a row generation technique that is used so as to improve the computational times required when introducing stability considerations, i.e. the model solved when considering expressions (4.1)-(4.5), (4.10) and (4.21)-(4.30). The row-generation procedure allows the solution of challenging airport instances but requires days so as to produce a single airport schedule. Consequently, Section 4.4.2 proposes a fast deferred acceptance algorithm that can generate multiple airport slot schedules with guaranteed stability.

### 4.4.1 MIP solution approach

As per the objective function of SASAM<sup>11</sup>, one can solve a single MIP problem by optimising expressions (4.10) subject to constraints (4.1)-(4.5) and the stability constraints (4.21)-(4.30). However, the introduction of stability constraints (4.21)-(4.30) introduces increased computational load and results in models that cannot be solved under the standard settings of commercial solvers. In fact, even for small test instances (considering more than a week of operations) SASAM faces memory errors that inhibit its solution to optimality. Row generation appears to be a suitable combinatorial optimisation technique for this problem since constraints are added dynamically as per the following logic.

First, the solution procedure is initiated by building and solving a variant of the base model which optimises expression (4.10) subject to constraints (4.1)-

---

<sup>11</sup> The objective function of SASAM is a scalar of four objectives (number of rejected/displaced requests, total/maximum displacement). The four objectives are converted to a scalar using relative importance weights obtained by ASA stakeholders (see Table 4-3 and Katsigiannis and Zografos (2021b)).

(4.5). The schedule that is given after the initial solution of the base model constitutes the initial incumbent of the proposed approach. Once the initial incumbent is generated, an iterative process determines whether the initial incumbent includes allocations  $(m, t)$  that block the formation of a stable schedule (as per Definition 4.1), or not. This process results in a list of unstable assignments (denoted by  $UA$ ). If the size of  $UA$  is greater than 0, then the incumbent under consideration contains at least one blocking pair and the respective stability constraints, i.e., expressions (4.21)-(4.30), are appended to the base model.

The solution to augmented version of the base model results in a new incumbent solution that is again checked for existing blocking pairs. The solution algorithm terminates when an incumbent has no blocking pairs, i.e., all stability constraints are satisfied, and a stable airport slot schedule is returned. The proposed row generation approach was able to improve on the computational times reported by the standard application of the selected solver (version 9.1 of Gurobi solver (Gurobi Optimization, LLC, 2021)). During our tests with different sizes of data instances, the standard solution approach solved only one instance to optimality (requiring over 17 hours of solution time) and generated stable, yet suboptimal solutions for the 5 and 10-week instances.

On the other hand, the row generation procedure generated stable schedules for all problem instances and was able to solve to optimality all instances up to 10 weeks. Despite the improvements introduced by the proposed row-generation technique, it appears that the model cannot be solved to optimality when considering the whole scheduling season. Hence, there is need to provide an alternative solution approach which proposes stable airport slot schedules without requiring significant computational times. A bi-objective deferred-acceptance



algorithm that can generate multiple non-dominated stable ASA schedules is detailed in the following section.

#### 4.4.2 Deferred acceptance algorithm

The Deferred Acceptance (DA) algorithm of Gale and Shapley (1962) is known to lead to Pareto optimal many-to-many assignments in linear time based on the number of submitted applications by the demand-side (Manlove, 2013). However, existing DA algorithms cannot be applied in ASA decision-making, since the ASA process has additional problem requirements.

In this section we detail a DA algorithm which considers the following problem specificities: (i) The capacity of each time interval is expressed in a multi-resource manner, i.e., rolling capacity constraints for arriving/departing and other movements (see expressions (4.2) in section 4.3.1); (ii) The capacity of each interval is checked for multiple periods, i.e., an assignment of a request to a time should be feasible for each day of the scheduling season; (iii) there are both paired and unpaired requests; (iv) for paired requests (comprising an arrival and departure movement), there is need to consider that the arrival movement should precede the departure (see expressions (4.3) and (4.4) in section 4.3.1). The above problem characteristics increase the computational difficulty associated with finding a stable airport slot schedule and render the proposition of a DA algorithm for the ASA problem a challenging task. In this paper, we propose a DA algorithm that addresses all aforementioned problem characteristics (Algorithm 4-1).

The algorithm requires as input the request set ( $M$ ) and the slots that are available during each day of the scheduling season ( $t \in T_{\mathcal{E}}$ ). For each request, expressions (4.15) and (4.19) may be used to construct the preference list of each request  $m$  with respect to each time slot  $t$  and the coordinators' functions. Hence, demand preference lists consider airlines' timing flexibility, lower and upper

flexibility bounds as well as several operational characteristics as per expressions (4.15). The size of the airlines' preference lists depends on the airlines' upper and lower timing flexibility bounds as per expression (4.16). In addition, the coordinators' functions (defined by expressions (4.19)) consider all main slot allocation rules and priorities, while incorporating competition and connectivity considerations.

Initially, the list of paired requests ( $PR$ ) and the list of request-to-slot ( $P$ ) pairs are empty (line 1), while the list of un-paired requests ( $UR$ ) is equal to the request set (line 2).  $UR$  is organised based on  $\psi'_m$  in a decreasing order (line 3). That is a pre-processing step which aims to allocate first requests of higher importance, which are less likely to be displaced in the following iterations. During each iteration the algorithm selects a request (line 5) and determines on whether the request has an empty preference list or not. In the case that the request list is empty (line 6), the request is rejected and receives no time slot (line 7).

Consequently, tuple  $(m, None)$  is added to  $P$ , request  $m$  is added to  $PR$  and removed from  $UR$ . In the case that the request list is non-empty, the algorithm determines the time slot that has the best ranking in the preference list of  $m$  (line 9). In continuation, the algorithm differentiates between paired and unpaired requests. For paired requests, the algorithm determines the type of the request. If the considered request is an arrival ( $m \in M^{Arr}$ ), the time that the departure movement applies to ( $td$ ) is determined based on the arrival time and turnaround time of the request ( $td = TT_m + ta - |T_{\epsilon}|v_m$ ) (line 11).

	<p><b>Input:</b> Request set (<math>M</math>); Set of available airport slots (<math>t \in T_c</math>); Airline preference list - <math>\mathcal{E}_m = \{\mathcal{E}_m(t)   \forall t \in T_c, \mathcal{E}_m(t) &gt; 0\}</math>; List of priorities as assigned by the coordinators based on WASG - <math>\Psi_m = \{\Psi_m(t)   \forall t \in T_c, \Psi_m(t) &gt; 0\}</math></p> <p><b>Output:</b> Set of stable allocations <math>P</math></p>
1	Initialise the list of paired requests and the list of pairs to be empty ( $PR = \{\}, P = \{\}$ )
2	Initialise the list of un-paired requests to be equal to the total number of requests ( $UR = M$ )
3	organise $UR$ on a descending order based on $\psi'_m$ defined in expression
4	<b>while</b> $ UR  > 0$ <b>do</b>
5	$m \leftarrow UR(0)$
6	<b>if</b> $ \mathcal{E}_m  = 0$ <b>then</b>
7	add $(m, None)$ to $P$ ; add $m$ to $PR$ ; remove $m$ from $UR$
8	<b>else do</b>
9	$t \leftarrow \operatorname{argmax}_{t \in T_c} \mathcal{E}_m(t)$
10	<b>if</b> $m$ is a paired request <b>then</b>
11	<b>if</b> $m \in M^{Arr}$ <b>then</b> $ta \leftarrow t, td \leftarrow TT_m + ta -  T_c v_m$
12	<b>if</b> $m \in M^{Dep}$ <b>then</b> $td \leftarrow t, ta \leftarrow td +  T_c v_m - TT_m$
13	<b>if</b> $td$ or $ta \notin T_c$ <b>then</b>
14	remove $\mathcal{E}_m(t)$ from $\mathcal{E}_m$ and go to line 6
15	<b>else do</b>
16	<b>if</b> $m \in M^{Arr}$ <b>then</b>
17	$ta \leftarrow t, td \leftarrow None$
18	<b>else do</b>
19	$ta \leftarrow None, td \leftarrow t$
20	<b>if</b> the allocations $(ma, ta), (md, td)$ are feasible <b>then</b>
21	add $(ma, ta), (md, td)$ to $P$ ; add $m$ to $PR$ ; remove $m$ from $UR$ and $\mathcal{E}_m(t)$ from $\mathcal{E}_m$
22	<b>else do</b>
23	$ca = \{\mu \in M   \Psi_{ma}(ta) > \Psi_\mu(ta) \wedge D_{ma} \cap D_\mu \neq \emptyset, ta \neq None\}$
24	$cd = \{\mu \in M   \Psi_{md}(td) > \Psi_\mu(td) \wedge D_{md} \cap D_\mu \neq \emptyset, td \neq None\}$
25	<b>if</b> $ca, cd = \emptyset$ <b>then</b>
26	remove $\mathcal{E}_m(t)$ from $\mathcal{E}_m$
27	<b>else do</b>
28	organise $ca, cd$ on an ascending order based on $\Psi_\mu(ta) \forall \mu \in ca$ and $\Psi_\mu(td) \forall \mu \in cd$ accordingly
29	<b>for</b> $\{\mu_a   \mu_a \in ca\} \cup \emptyset$ <b>do</b>
30	remove $\mu_a$ from $P$ ; remove $\mu_a$ from $PR$ ; add $\mu_a$ from $UR$
31	<b>if</b> the allocations $(ma, ta), (md, td)$ are feasible <b>then</b>
32	add $(ma, ta)$ and $(md, td)$ to $P$ ; add $m$ to $PR$ ; remove $m$ from $UR$ and $\mathcal{E}_m(t)$ from $\mathcal{E}_m$
33	<b>break</b>
34	<b>else do</b>
35	<b>for</b> $\{\mu_d   \mu_d \in cd\} \cup \emptyset$ <b>do</b>
36	remove $\mu_d$ from $P$ ; remove $\mu_d$ from $PR$ ; add $\mu_d$ from $UR$
37	<b>if</b> the allocations $(ma, ta), (md, td)$ are feasible <b>then</b>
38	add $(ma, ta)$ and $(md, td)$ to $P$ ; add $m$ to $PR$ ; remove $m$ from $UR$ and $\mathcal{E}_m(t)$ from $\mathcal{E}_m$
39	go to line 4
40	<b>else do</b>
41	add $(\mu_a, td)$ to $P$ ; add $\mu_d$ to $PR$ ; remove $\mu_d$ from $UR \forall \mu_d \in cd$
42	<b>else do</b>
43	add $(\mu_a, ta)$ to $P$ ; add $\mu_a$ to $PR$ ; remove $\mu_a$ from $UR \forall \mu_a \in ca$
44	remove $\mathcal{E}_m(t)$ from $\mathcal{E}_m$
45	<b>return</b> $P$

**Algorithm 4-1:** A deferred acceptance algorithm for ASA

In contrast, if the considered request is a departure ( $m \in M^{Dep}$ ), the arrival time is expressed as a function of the departure time and the turnaround time ( $ta = td + |T_{\bar{c}}|v_m - TT_m$ ) (line 12). Please note, that lines 11 and 12 consider the overnight indicator of paired requests and hence comply with all ASA requirements concerning turnaround times. In the case that any of the arrival and departure times do not abide with the turnaround time of the request, the infeasible slots are trivially removed from the preference list of the concerned requests (line 14). Hence, Algorithm 4-1 considers turnaround times that are equal to the initially requested time-difference of the arrival and the departure requests.

Following this step, the algorithm attempts to schedule the requests to times  $ta$  and  $td$ . If there is available capacity (as per expressions (4.2)) during  $ta$  and  $td$  the request is matched and  $UM, P$  and  $UR$  are updated accordingly. Please note that at this point, the auxiliary movements of unpaired requests (if the request is an arrival, the auxiliary movement is a departure and *vice versa*) receive a time slot indicated by *None* and trivially satisfy all capacity constraints (auxiliary movements do not consume airport capacity).

Hence, the ability to schedule an unpaired request is solely determined by the requested movement. In the case that there is not adequate capacity to schedule the request, there is need to determine whether there are requests of lower importance in comparison to request  $m$  or not. This is done by enumerating previously scheduled requests that have a lower priority than the arrival (line 23) or the departure (line 24) movement of  $m$ . During this step, the requests that are considered are the ones that have at least one common day of operations (since requests without common days of operations are not blocking pairs). In the case, that there are no such requests, the runway capacity is consumed by requests of higher priority, time slot  $t$  is infeasible for  $m$  and thus is removed from its preference

list  $(\mathcal{E}_m(t))$  (line 26). Alternatively, if there is at least one request of lower priority in comparison to  $m$ , the algorithm attempts to swap request  $m$  with each request that has a lower priority than  $m$ .

This process is detailed in lines 29-44 of Algorithm 4-1. The algorithm iteratively removes requests that have a lower priority than the arrival of movement of  $m$  (line 36) and then, through an inner loop (lines 35-39), attempts to remove requests that are pre-empted by the departure movement of  $m$ . Regardless of the existence of requests that are of lower priority than the arrival of  $m$ , the inner loop will be executed once (for every request that is pre-empted by the departure movement of  $m$ ). Once, the allocation of  $m$  becomes feasible,  $m$  is allocated to  $t$  (lines 32 or 38), both loops terminate (lines 33 or 39), and the  $UR, P$  and  $PR$  lists are updated.

The algorithm then proceeds to the next request in  $UR$ . Alternatively, if both loops terminate without being able to match request  $m$ , the algorithm re-matches the requests (since they do not block the allocation of  $m$ ) that were previously unmatched so as to accommodate  $m$  (lines 41 and 43) and time slot  $t$  is removed from the preference list of  $m$  (line 44). This signifies, that the allocation of  $m$  is not blocked by the requests that are allocated to  $t$  but from other requests that are matched to adjacent time slots. These requests are considered during other iterations. The process described above is repeated for all requests. The ASA-DA algorithm (Algorithm 4-1) terminates when either all requests are matched to a slot, or requests that remain unmatched have empty preference lists (the request has been rejected by all slots). Algorithm 4-1 generates stable schedules. This observation is formalised in the following proposition.

**Proposition 4.7** The schedule generated by Algorithm 4-1 is stable.

*Proof.* This will be a proof by contradiction (similar to Gale and Shapley (1962)). Assume that a schedule ( $s$ ) given by Algorithm 4-1 is not stable. Since  $s$  is not stable, there must exist a blocking pair  $(\mu, \tau)$ . Then, as per Definition 4.1:

- **Case 1:** either there is available capacity for a slot  $t$  that belongs in the preference list of  $\mu$  such that  $\Psi_\mu(t) > \Psi_\mu(\tau)$  ( $\tau$  may also be equal to *None* implying that  $\mu$  is not scheduled); or
- **Case 2:**  $\tau$  could accommodate request  $m$  that is more preferable than  $\mu$  such that  $\Psi_m(\tau) > \Psi_\mu(\tau)$ .

For each request the algorithm parses the time slots by sorting the preference list for each  $m \in M$  (as per  $\mathcal{E}_m$ ) and will only provide feasible request-to-slot matches (based on the turnaround and capacity parameters). Hence, request  $\mu$  will only be matched to a slot, either if all slots of higher importance ( $t \in T_{\bar{c}/\tau}: \mathcal{E}_\mu(\tau) > \mathcal{E}_\mu(t)$ ) are not feasible for  $\mu$  (either because the capacity of each slot is consumed by requests of higher priority, or because the slot is not feasible for  $\mu$ 's turnaround constraints). This suggests that there cannot exist a slot  $t$  that is feasible and more preferable than  $\tau$  for  $\mu$ . In addition, if  $m$  (that has a greater priority than  $\mu$  with respect to  $\tau$ ) is not matched to  $\tau$ ,  $\tau$  is infeasible for  $m$ . This is justified by the fact that the algorithm attempted to match  $m$  to  $\tau$  (by removing requests of lesser importance) and  $m$  could not be allocated to  $\tau$  (due to capacity or turnaround limitations). Hence, neither Case 1 nor Case 2 hold. This is a contradiction to the initial assumption and  $(\mu, \tau)$  is not a blocking pair. Hence, Algorithm 4-1 leads to schedules that are free of blocking pairs.

Furthermore, one can prove that the schedules ( $s$ ) provided by Algorithm 4-1 are Pareto optimal from the requests perspective, i.e. there is no other schedule

(other than  $s$ ) where a request ( $m$ ) may receive a time slot ( $t$ ) that is better than the slot received in schedule  $s$  (time slot  $\tau$ ) such that  $\mathcal{E}_m(t) > \mathcal{E}_m(\tau)$ .

**Proposition 4.8** The schedule generated by Algorithm 4-1 is Pareto optimal from the requests' perspective.

*Proof.* Assume a stable schedule where a request  $\mu$  is allocated to a slot  $t$ . Now, assume that there exists a time slot  $\tau$  that is more preferable for  $\mu$  such that  $\mathcal{E}_\mu(\tau) > \mathcal{E}_\mu(t)$ . Since the schedule is stable, the capacity of  $\tau$  has been used to accommodate requests ( $m \in M/\mu$ ) that are better than slot request  $\mu$  ( $\Psi_m(\tau) > \Psi_\mu(\tau) \forall m \in M/\mu$  allocated to  $\tau$ ). As per Algorithm 4-1, each  $m \in M/\mu$  prefers  $\tau$  to all other time slots that are in their preference lists. Hence,  $\tau$  is not feasible for  $\mu$  since the assignment  $(\mu, \tau)$  would constitute a blocking pair. Now assume a hypothetical schedule where  $\mu$  is matched to  $\tau$  and there are is at least one  $m \in M/\mu$  matched to another time slot that produces a stable allocation. Yet, in this case, there exists a request  $m$  (other than  $\mu$ ) that received a less desirable slot  $t$  such that  $\mathcal{E}_m(\tau) > \mathcal{E}_m(t)$ . Concurrently,  $\tau$  prefers  $m$  to  $\mu$ .

Hence, we conclude that Algorithm 4-1 will remove a slot from a request's list only in cases that a slot is unattainable. Consequently, there cannot be a schedule where a request can receive an allocation that is improved (regarding its preference list  $\mathcal{E}_m$ ) in comparison to the allocation provided by the stable schedule generated by Algorithm 4-1. The schedules resulting from Algorithm 4-1 are therefore Pareto optimal as per the requests' perspective and preferences.

Having provided support on the ability of Algorithm 4-1 to propose stable airport schedules, in the following section we discuss the decision-making implications that arise from storing and dynamically updating the requests' preference lists.

#### 4.4.2.1 Storing and updating requests' preferences:

##### The memory of the DA algorithm and its benefits for ASA

A crucial set of inputs that is required for the DA algorithm (proposed in Algorithm 4-1) concerns the preference lists of each request submitted to the airport ( $m \in M$ ). The preference lists are updated when the algorithm matches a request to a slot (lines 21, 32, 38 of Algorithm 4-1) or when a slot is infeasible for a request (lines 14, 26, 44 of Algorithm 4-1). When a request  $m$  is scheduled to a time slot  $t$ , its preference list contains all time slots in  $T_{\mathcal{E}}$  except for  $t$  and the time slots that are infeasible for  $m$  (time slots that rejected  $m$ ). The property of storing and dynamically updating the preference lists of each request (hereafter referred to as *memory property*) is a characteristic of the proposed DA algorithm that has significant decision-support and decision-making implications.

First is that the elements remaining in the preference lists of scheduled requests are alternative potential allocations. As a result, Algorithm 4-1 not only provides a stable schedule but also supplies to the decision-making process all alternative time slots that are worthy of examination. This functionality supports the role of airport slot coordinators in proposing alternative slot timings for each request and allows the real-time reallocation of requests when new requests arrive dynamically. This functionality is further clarified by the example detailed in Figure 4-4.

Assume that Algorithm 4-1 has allocated multiple requests, yet additional requests are submitted to the airport after this initial allocation. Pre-scheduled requests occupy time slots and new request's preference lists are updated based on the time slots that are infeasible for them. Occupied time slot capacity is denoted in Figure 4-4 by red squares, while available capacity for a time slot is represented by green squares. In subplot (a) of Figure 4-4 one can observe a sample request that is submitted (denoted by  $m_1$ ).  $m_1$  requests time slot  $t_{m_1}$ . The priority assigned



by the coordinator based on WASG is denoted by the triangular function delimited by  $\psi'_{m_1}$  and the extreme values of the time slot axis.

The algorithm attempts to schedule  $m_1$  and iteratively removes the entries from the preference list of  $m_1$  ( $\mathcal{E}_{m_1}$ ). Removed entries correspond to time slots that are infeasible for  $m_1$  (slot that are infeasible for  $m_1$  occupied by requests of higher importance). As per subplot (a) of Figure 4-4,  $m_1$  received time slot  $\tau_{m_1}$ , which was the first time slot that was feasible for  $m_1$ . Now assume that  $m_2$  is submitted to the airport and  $\Psi_{m_2}(\tau_{m_1}) > \Psi_{m_1}(\tau_{m_1})$  (see subplot (b) of Figure 4-4). In this case,  $m_1$  is unmatched from  $\tau_{m_1}$ ,  $m_2$  is allocated to  $\tau_{m_1}$  and  $\tau_{m_1}$  is removed from the preference list of  $m_2$  (entry  $\mathcal{E}_{m_2}(\tau_{m_1})$  is removed from  $\mathcal{E}_{m_2}$ ). Consequently, since the preference list of  $m_1$  is not empty,  $m_1$  is added to the list of unpaired requests ( $UR$ ) and Algorithm 4-1 seeks a feasible slot for  $m_1$ .

However, during previous iterations the algorithm removed multiple entries from  $\mathcal{E}_{m_1}$  (removed entries are denoted by  $\times m_i, i = 1,2,3$  in Figure 4-4), hence requiring a reduced set of slots. Time slot  $t = 2$  lies on top of the preference list of request  $m_1$ , since the value of  $\mathcal{E}_{m_1}(2)$  outperforms the preference assigned by  $m_1$  to the other available requests. Hence,  $m_1$  is allocated to  $t = 2 = \tau_{m_1}$  and  $\mathcal{E}_{m_1}(2)$  is removed from the preference list of  $m_1$ .

This example suggests that the re-allocation of  $m_1$ , after the arrival of more important requests, is fast (since Algorithm 4-1 considers a subset of time slots) and does not compromise the stability of the schedule (the schedule remains Pareto optimal after the submission of  $m_2$ ). At this point, it is worth noting that a newly submitted request may create a ‘chain-effect’ and affect the allocations of multiple previously feasible request-to-slot assignments. Even at this case, Algorithm 4-1 keeps track of each request’s preference list and re-allocates all requests.

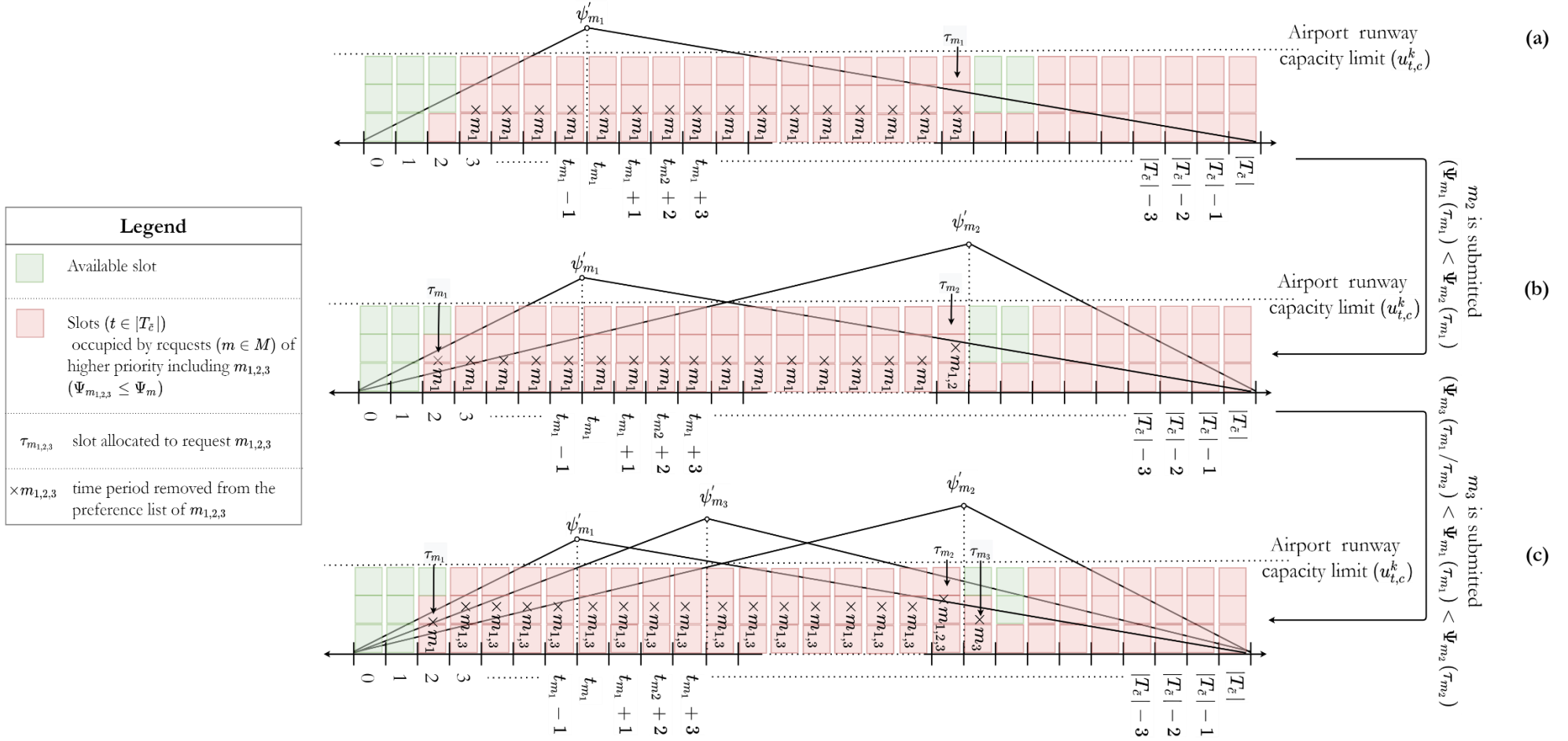


Figure 4-4: Demonstration of the memory property of Algorithm 4-1

Finally, in subplot (c) of Figure 4-4, request  $m_3$  is submitted and requests access to the airport. In this example,  $m_3$  is matched to  $\tau_{m_3}$  since all other slots with a higher value of preference (as per  $\mathcal{E}_{m_3}$ ) are occupied by more important requests. In addition, despite the increased importance of  $m_3$  ( $\psi'_{m_3}$ ) in relation to  $m_2$ , the proximity of  $t_{m_2}$  to  $\tau_{m_2}$  assigned increased importance to  $m_2$  in relation to  $m_3$  ( $\Psi_{m_2}(\tau_{m_2}) > \Psi_{m_3}(\tau_{m_2})$ ) thus the time slot is reserved for  $m_2$ . Through this series of examples, Figure 4-4 exhibits how the memory property of Algorithm 4-1 is capable of considering the real-time submissions of slot requests, re-allocating pre-existing requests, and producing stable airport slot schedules without re-iterating over the complete request set. In the following section we detail a multi-objective preference-based algorithm that integrates the DA algorithm proposed for the ASA problem

#### 4.4.2.2 A multi-objective preference-based algorithm for the ASA problem

Up to this point we have discussed how the DA algorithm that we propose for the ASA problem (as per Algorithm 4-1) adheres to the decision-making requirements of ASA decision-making. Yet, an important aspect of ASA decision-making is the existence of multiple objectives and scheduling performance metrics. To provide multiple schedules and inform decision-makers on the trade-offs between the multiple airport slot scheduling performance metrics considered in the literature and in practice, we propose a multi-objective, preference-based algorithm for the ASA problem.

Multi-objective DA algorithms and stable matching problems have recently emerged in the literature and consider the trade-off between the number of blocking pairs and the efficiency of the system under consideration (Gharote et al., 2019), i.e. investigating changes to the system efficiency when altering the number of

blocking pairs. Hence, the proposition of an algorithm that considers the number of stable assignments in conjunction with problem-specific efficiency metrics, to the best of our knowledge, is an approach that has not been previously proposed in the literature. In the proposed algorithm (see Algorithm 4-2), we introduce systematic compromises to the preference lists of the requests submitted to the airport and obtain stable schedules that exhibit different values with respect to displacement-related metrics. In addition to the input sets required for Algorithm 4-1, Algorithm 4-2 requires a list ( $PL$ ) with the preference list lengths that will be used to generate the stable schedules. Please note, that the preference lists of different requests are shaped based on the functions detailed in section 4.3.2.1, which differentiate among requests of different priorities and different operational characteristics.

<b>Input:</b> Request set ( $M$ ); Set of available airport slots ( $t \in T_{\bar{c}}$ ); Airlines' function for each request ( $m$ ) with respect to each time slot ( $t$ ) - $\mathcal{E}_m = \{\mathcal{E}_m(t)   \forall t \in T, \mathcal{E}_m(t)\}$ ; Coordinators' function for each request ( $m$ ) based on WASG - $\Psi_m = \{\Psi_m(t)   \forall t \in T, \Psi_m(t)\}$ ; List of preference list lengths to be considered ( $PL$ )	
<b>Output:</b> List of stable schedules concerning different lengths of preference lists ( $s$ )	
1	$s \leftarrow []$
2	<b>for</b> $i \in PL$ <b>do</b>
3	set $\varphi_m^{l(u)} = i \forall m \in M$
4	$s[i] \leftarrow$ Algorithm 4-1 ( $M, T_{\bar{c}}, \mathcal{E}_m \forall m \in M, \Psi_m \forall m \in M$ )
5	<b>if</b> $Z_1(s[i]) = 0$ <b>then</b>
6	<b>break</b>
7	<b>else</b>
8	$M \leftarrow \{Z_1(s[i])\}$
9	<b>return</b> $s$

**Algorithm 4-2:** A multi-objective DA algorithm for the ASA problem

The introduction of  $PL$  allows the algorithm to examine the trade-off between airport capacity utilisation and the maximum displacement of the requests in conjunction with the request/slot-specific prioritisation functions. For instance,  $PL = [0,10,20,35]$  will generate 4 stable schedules where the requests will not accept displacements (from their requested times) that exceed 0, 10, 20 and 35 scheduling

intervals respectively. Once the input is provided, the list of schedules is initialised so as to be empty (line 1), and the algorithm iterates over all preference list lengths in  $PL$  (line 2). During each iteration the algorithm sets the lower and upper flexibility bounds of each request ( $\varphi_m^{l(u)}$ ), hence adjusting the length of all requests' preference lists (line 3).

At the core of Algorithm 4-2 lies Algorithm 4-1, which is used to generate stable schedules based on the current preference list length ( $i$  defined in line 2) and the requests currently composing the pending list. At the outset of the algorithm, the pending list is identical to the request set. The pending list is updated after each iteration and considers requests that have not been able to receive a time slot during previous iterations, and requests that were unmatched during the current iteration and did not receive a slot. If the schedule generated during an iteration has no rejected requests (line 5) (obtained by substituting the solution of the current iteration  $s[i]$  in expression (4.6)), the algorithm terminates and returns the list of stable schedules (line 6). Alternatively, the algorithm will select the requests that were not able to receive a time slot (line 8) and proceed to the next iteration.

At this step, the pending list's size is reduced and considers only the requests that could not be accommodated based on the current preference list length ( $i$ ). During the next iteration, the size of the preference lists of the currently unscheduled requests (requests that belong to the pending list) will be increased (as per the current value of  $i$ ) and a new schedule will be created. Eventually, the algorithm will generate stable schedules for all list lengths composing  $PL$ . In the case that there are no rejected requests for a schedule, the algorithm terminates since there is no need to further compromise the preferences of requests (line 6). In the case that the algorithm terminates and there are still requests in the pending list, then the requests are permanently added to the pending list, signifying that

there is no available capacity for them. Algorithm 4-2 is based on the following logic. By increasing the range that requests accept to be scheduled to, there will be more stable pairs and hence the cardinality of the scheduled request set will be larger. This is explicitly stated in the following remark.

**Remark 4.2** As Algorithm 4-2 introduces compromises to the preference lists of the requests, the number of scheduled requests increases.

Based on Remark 4.2, there is a trade-off between the utilisation of airport capacity (expressed in terms of scheduled requests) and the requests' preferences. This observation is in accordance with the findings of Zografos et al. (2017), which observe a monotonous relationship between airport capacity utilisation and the maximum acceptable displacement threshold. In our paper, the range of acceptable displacement is an intuitive representation of the maximum displacement objective (see expression (4.7)), while the cardinality of the scheduled request set is the complement of the set of rejected requests (expression (4.6)). In addition, for each schedule in  $\mathcal{S}$ , we may estimate through substitution additional performance metrics of interest, i.e., the number of rejected passengers, the displaced requests, and the total displacement objectives. As a result, the proposed algorithm captures the trade-offs between the timing preferences of airlines and the multiple ASA performance metrics existing in the literature.

An additional property of Algorithm 4-2, is that the schedules that are generated are weakly dominated with respect to the objectives of maximum displacement and the number of displaced requests. This is formally proved as follows.

**Proposition 4.9** Algorithm 4-2 results in non-dominated and weakly-dominated solutions with respect to the maximum displacement and the number displaced requests' objectives.

*Proof.* This will be a proof by contradiction. It suffices to prove that Algorithm 4-2 will not generate dominated solutions with respect to objectives  $Z_1$  and  $Z_2$  (as defined in expressions (4.6) and (4.7)). Suppose a dominated schedule (denoted by  $s_1$ ) generated by Algorithm 4-2. Since the schedule is dominated, there must be another schedule (denoted by  $s_2$ ) exhibiting lower values for both the rejected requests ( $Z_1$ ) and the maximum displacement ( $Z_2$ ) metrics, such that  $Z_1(s_2) < Z_1(s_1)$  and  $Z_2(s_2) < Z_2(s_1)$ . However, as per Algorithm 4-2, the preference lists' size (a proxy of  $Z_2$ ) increases and hence additional capacity is made available to requests. As a result, for a unitary increase to the value of  $Z_2$  (from  $z_2$  to  $z'_2 > z_2$ ), the number of scheduled requests will either remain the same or increase. Hence, as the value of  $Z_2$  increases,  $Z_1$  either remains the same or decreases. Therefore, one cannot obtain schedules  $s_1, s_2$  such that  $Z_1(s_2) < Z_1(s_1)$  and  $Z_2(s_2) < Z_2(s_1)$  when solving Algorithm 4-2. That's a contradiction to the initial assumption. Consequently,  $s_1$  will either be weakly dominated by  $s_2$ , i.e.,  $Z_1(s_2) = Z_1(s_1)$  and  $Z_2(s_2) < Z_2(s_1)$ ; or be a non-dominated schedule. In addition, as we increase the length of the preference list, the average priority (expressed in terms of  $\Psi_m(t)$ ) of the requests allocated to slot  $t$  will either remain the same or improve. Thus, the scheduling efficiency improves as we introduce compromises to the preference list of the requests. This is proved in the following proposition.

**Proposition 4.10** Based on Algorithm 4-2,  $\forall t \in T_{\bar{c}}$ , the average value of  $\Psi_m(t) \forall m \in M: x_{m,t} = 1$  will either increase or remain the same, as  $\varphi_m^{l(u)}$  increase.

*Proof.* Assume an iteration of Algorithm 4-2, where the preference list of each request has a length of  $1 + 2i$  (the requested time, in addition to  $i$  time intervals of tardiness as per  $\varphi_m^u$  and  $i$  intervals of earliness as per  $\varphi_m^l$ ). Then assume a time slot  $t$  that was matched with  $n$  requests ( $|\{m \in M : x_{m,t} = 1\}| = n$ ). At the end of this iteration, the average priority of the requests that are currently scheduled to  $t$  is equal to  $(\sum_{m \in M} \Psi_m(t)x_{m,t})/n$ . By expanding the formula and removing zero elements (since requests that are not scheduled to  $t$  will have  $x_{m,t} = 0$ ), this may be written as follows:  $\Psi_{m_1}(t)/n + \dots + \Psi_{m_n}(t)/n$  (a). Now, in the next iteration of Algorithm 4-2, the preference list of each request submitted to the airport has a length of at most  $2(i + 1) + 1$  ( $i + 1$  time intervals of tardiness as per  $\varphi_m^u$  and  $i + 1$  intervals of earliness as per  $\varphi_m^l$ ). Hence, under the increased size of the preference lists, there may be request ( $\mu$ ) that was previously rejected (due to unavailable capacity during time slots lying in the preference list with length  $2i+1$ ) and now pre-empts at least one  $m_i$  (say  $m_n$ ) that was scheduled to  $t$  during the previous iteration such that  $\Psi_\mu(t) > \Psi_{m_n}(t)$ . As a result, the new mean priority of the requests assigned to  $t$  becomes:  $\Psi_{m_1}(t)/n + \dots + \Psi_{m_{n-1}}(t)/n + \Psi_\mu(t)/n$  (b). However, the only difference between expressions (a) and (b) is that  $\Psi_{m_n}(t)x_{m_n,t}/n$  has been substituted by  $\Psi_\mu(t)x_{\mu,t}/n$ . But we know that  $\Psi_\mu(t) > \Psi_{m_n}(t)$ , hence (a) < (b). Obviously, if there are no requests to take the place of the previously allocated requests, the average priority of  $t$  will remain the same. Hence, the average priority increases or remains the same when the length of preference list increases. The above proof holds for the case that the requests occupying a slot at a given iteration saturate the entirety of its capacity. However, Proposition 4.10 may be trivially generalised for cases that the slot's capacity is partially saturated. This can be done by substituting  $n$  in expressions (a) and (b) with  $\max_{k \in K} u_{d,t,\epsilon}^t$  (calculating the mean of the requests that are matched to  $t$  as  $(\sum_{m \in M} \Psi_m(t)x_{m,t})/\max_{k \in K} u_{d,t,\epsilon}^t$ ).



Proposition 4.10 proves that Algorithm 4-2 introduces compromises to the preferences of airlines' requests but allocates the airport's capacity to the requests that are valued the most based on WASG's prioritisation. Concurrently, requests are matched to the best possible time slot that is attainable for them (as per Proposition 4.8 ).

In what follows, we provide an example that details how Algorithm 4-2 operates and how it improves airport capacity utilisation through augmenting the size of the requests' preference lists (see Figure 4-5). In Step 0 of Figure 4-5, we detail the assumptions and the setup of the example. For simplicity, the capacity of each time slot is limited to 2 movements (regardless of their type). Let's assume that some of the slots' capacity has already been allocated to requests of higher priority (unavailable slot capacity is denoted by red squared boxes), yet at some point of Algorithm 4-2's operations, there are 8 requests which are yet to be scheduled ( $m_1, m_2, \dots, m_8$ ). The requests are prioritised based on the coordinators' function, i.e.,  $\Psi_{m_i}(t), i = 1, 2, \dots, 8$ . For their requested time slots, we know that requests  $m_1$  to  $m_8$  receive corresponding priorities  $\psi'_{m_1}, \dots, \psi'_{m_8}: \psi'_{m_1} < \psi'_{m_2} \dots < \psi'_{m_8}$  by the coordinator. In addition, requests  $m_1, m_2$  and  $m_4$  request time slot  $t = 0$ , request  $m_2$  requests time slot  $|T_{\bar{c}}| - 2$  and remaining requests require time slot  $t = 2$  (ceteris paribus).

In addition, we know that  $m_2$  (departure) and  $m_7$  (arrival) are two paired requests with a turnaround time of  $|T_{\bar{c}}|$ . Obviously, based on the available capacity (denoted by green squared boxes) there will be some requests that won't be able to receive their requested times, while at least one request will be rejected and remain in the pending list after the termination of the algorithm (there is capacity for 7 time slots but 8 requests). During the first step of Algorithm 4-2, each request proposes to their requested time (as per Algorithm 4-1). The preference lists of all

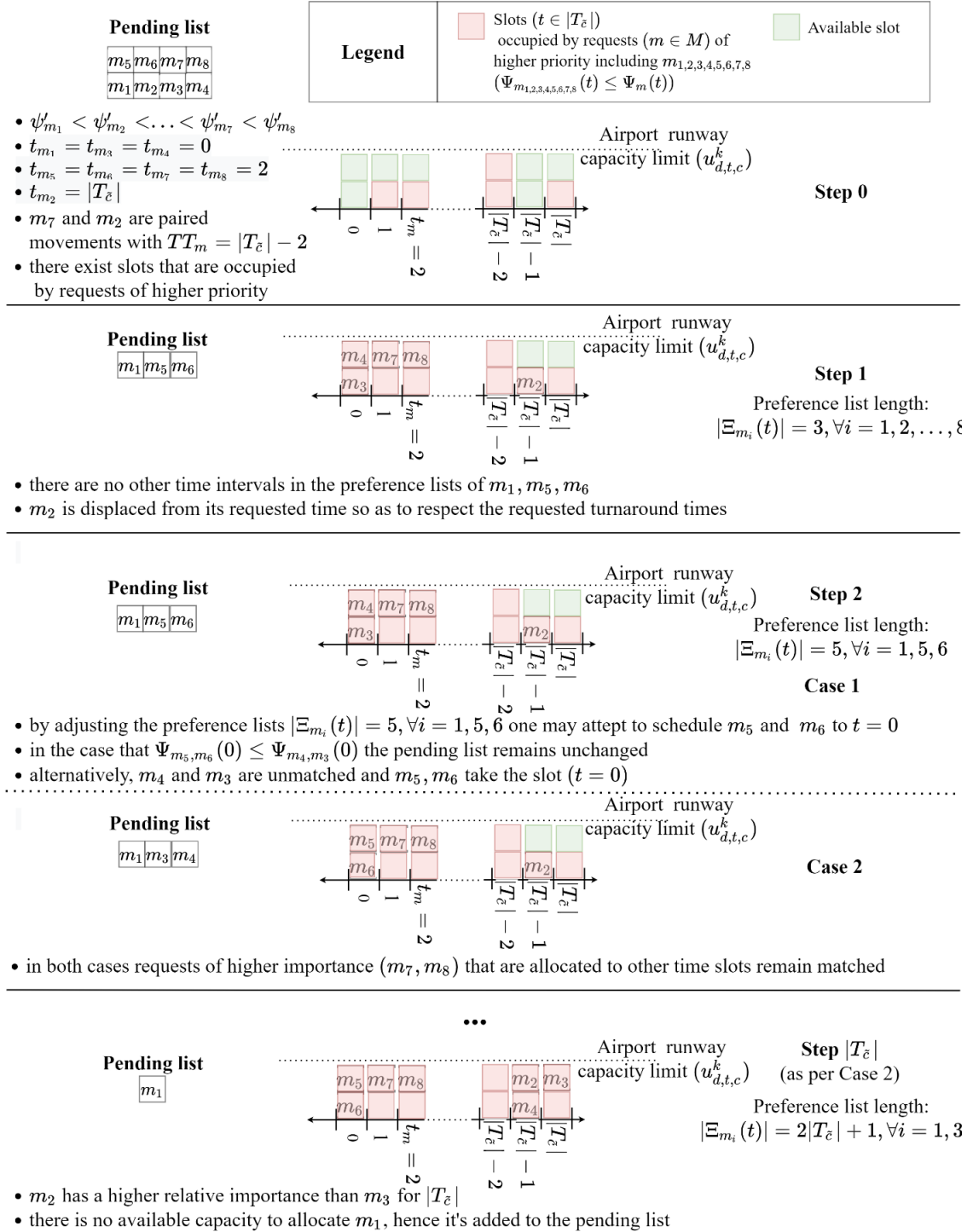


**Figure 4-5:** Demonstration of the multi-objective DA algorithm for the ASA problem

requests comprise 3 entries, which correspond to their requested time and  $\pm 1$  interval. Hence, each request  $m_i, i = 1, \dots, 8$  assigns a preference of  $\Xi_{m_i}(t_{m_i}) = \xi'_{m_i}$

to their requested time and a preference of  $\Xi_{m_i}(t_{m_i} \pm 1) < \xi'_{m_i}$  for the other 2 intervals lying in their preference lists. As a result,  $m_8$ , which receives the highest priority by the coordinator, will receive its requested time  $t = 2$  and consume the remaining capacity of that time.

Consequently,  $m_7$  is displaced to the only other time slot that belongs to its preference list, i.e.,  $t = 1$ , and consumes all the remaining capacity during  $t = 1$ . Concurrently, the algorithm schedules  $m_2$  to  $|T_{\bar{c}}| - 1$ . The displacement of  $m_2$  by 1 interval (from slot  $|T_{\bar{c}}|$  to  $|T_{\bar{c}}| - 1$ ), is done in accordance with the requested turnaround times and the allocation of its arrival pair ( $m_7$ ). Requests  $m_5$  and  $m_6$  that also requested time slot  $t = 2$  are added to the pending list, since requests of higher importance occupy all the capacity associated with the time slots that belong to their preference lists ( $t = 1, 2, 3$ ). The algorithm then attempts to schedule the slots that requested  $t = 0$ .  $m_3$  and  $m_4$  are scheduled to  $t = 0$  and  $m_1$  is added to the pending list, since  $\psi'_{m_1} < \psi'_{m_3} < \psi'_{m_4}$ .

Hence, at the end of the first step, the pending list is composed by  $m_1, m_5$  and  $m_6$ . In step 2, the preference lists of the requests that lie in the pending list are augmented by 2 intervals (accepting a 5-minute increase to their earliness/tardiness). In this case, one may attempt to schedule  $m_5$  and  $m_6$  to  $t = 0$ . In the case that  $\Psi_{m_{5/6}}(0) \leq \Psi_{m_{3/4}}(0)$ , the allocations obtained during the previous iteration/step will remain unchanged (Case 1). Alternatively (Case 2),  $m_5$  and  $m_6$  will take the place of  $m_3$  and  $m_4$  and the latter will be added to the pending list. After multiple steps, as per Case 2, at step  $|T_{\bar{c}}| - 1$ , request  $m_4$  will pre-empt  $m_3$  and  $m_1$  for time slot  $|T_{\bar{c}}| - 1$ . Finally, at step  $|T_{\bar{c}}|$  request  $m_3$  will receive the last available time slot (pre-empting  $m_1$ ) and hence  $m_1$  is rejected.

## 4.5 Application and computational results

SASAM and the DA algorithm were applied to data obtained from a real-world coordinated airport. Computational results considering alternative slot prioritisation schemes are presented. Furthermore, we conduct a series of statistical analyses that confirm the robustness of the proposed prioritisation functions (section 4.3.2.1) with respect to the load factor ( $lf_m$ ) parameter, and the ability of the functions' exponents to differentiate among requests sharing similar characteristics. This section consists of 5 subsections. Subsection 4.5.1 summarises the input data (requests, capacity parameters) and details the alternative ASA schemes considered for generating alternative schedules. Subsection 4.5.2 presents the statistical analyses regarding the exponents of the prioritisation functions. Subsection 4.5.3 conducts a comparative analysis between the schedules obtained by the ASA schemes detailed in subsection 4.5.1. Subsection 4.5.4 presents the complete frontier of stable schedules generated by Algorithm 4-2 and assesses the trade-offs among multiple non-dominated points. Finally, subsection 4.5.5 presents the output provided by the implementation of the DA algorithm and discusses its implications for decision-making.

### 4.5.1 Data and computational setup

The data used in the computational experiments that follow concern a European coordinated airport which is coordinated during the summer season of 2018. Herein we present the main datasets that are required for the slot allocation process and the computational experiments.

The first set of inputs concerns the request data and the priorities of the requests. Table 4-2 provides an analysis on the distribution of the submitted airline requests based on the request priority that they belong to. Over half of the submitted requests fall into the *Others* priority (*O*) and concern approximately

46% of the aircraft and passenger traffic. Furthermore, we observe that new entrant’s requests concern only 3.5% of the total season-wide movement and passenger traffic.

Priority	Action Code	Request series		Individual requests		Passengers concerned	
		# (unpaired)	%	#	%	#	%
Historic ( <i>H</i> )	F	561 (52)	22.5	20,659	28.6	3,705,266	28.7
Other ( <i>O</i> )	N	1,414 (170)	56.8	33,610	46.5	5,942,871	46.1
Changes to historic ( <i>CH</i> )	R	413 (70)	16.6	13,095	18.1	2,355,536	18.2
	L	60 (1)	2.4	2,310	3.2	450,296	3.5
New entrant ( <i>NE</i> )	B	43 (0)	1.7	2,538	3.5	454,216	3.5
<b>All</b>	<b>Total</b>	<b>2,491 (293)</b>	<b>100%</b>	<b>72,212</b>	<b>100%</b>	<b>12,908,185</b>	<b>100%</b>
<b>Notes:</b>	Changes to historic requests that accept slot times between the historic or the requested time (R), changes to historic requests that will only accept the historic slot if the requested time is not available (L), percentage (%), number (#).						

**Table 4-2:** *Distribution of requests and the concerned passengers across the different request priorities*

This observation in conjunction with the fact that requests for historic operations (*H*) correspond to 28.6% of the airport’s aircraft traffic, suggests that the rules for the slot pool, i.e., the capacity remaining after the allocation of historic requests, are not violated by new entrants’ movements, since after the allocation of historic requests, new entrants consume less than 50% of the remaining capacity. Please note the existence of requests for routes with Public Service Obligations (*PSO*). However, since all *PSO* requests are classified as *H*, there is no need to consider an explicit prioritisation (Katsigiannis and Zografos, 2021a).

Overall, 100 airlines submitted 2491 requests (4689 series of arrival/departure requests) relating to 72212 flights and about 13000000 passengers. Ergo, the considered data instance is challenging and one of the most complex in terms of submitted requests. The second dataset that is required is the declared capacity and the coordination parameters of the airport. This set of inputs is provided in Table 4-3.

With respect to the airport’s capacity, we observe that the airport may accommodate 8 movements every 20 minutes and a total of 22 movements per hour. This allows the airport to offer 114576 slots (24 hours  $\times$  22 movements/hour  $\times$  217 days in the scheduling season). Hence, one considers the requests submitted to the airport and the available slot capacity, the airport is severely congested and more than 63% of its capacity is requested by airlines’ requests. For the sake of reference, during the same season London Heathrow offered slots for 458,304 movements and airlines’ requests corresponded to approximately 260,000 movements (a request-to-slot-capacity ratio of 56.7%). Turnaround separations are set to be equal to the requested departure-arrival time difference.

<b>Model parameter</b> (notation)	<b>Comment</b>	20 min	60 min
Runway capacity ( $u_{d,t,c}^k$ )	Arrivals	-	10
	Departures	-	12
	Total	8	22
Turnaround constraints ( $TT_m$ )	Paired movements	$TT_m = t_{md} - t_{ma} + v_m  T_{\tilde{c}} $	
Coordination interval ( $\tilde{c}$ )	All movements	$\tilde{c} = 10$ mins ( $ T_{\tilde{c}}  = 144$ )	
Load factor ( $lf_m$ )	Scheduled/Charter requests	0.85/1	
Prioritisation functions ( $\Psi_m(t), \Xi_m(t)$ )	According to each requests’ priority ( $H, CH, NE, O$ )	As described in section 4.3.2.1	
Weights for the objectives in expressions (4.10) ( $\beta_j, j = 1,2,3,4$ )	The relative importance of each considered objective provided by the empirical study of Katsigiannis and Zografos (2021b)	$\beta_1 = 0.21,$ $\beta_2 = 0.25,$ $\beta_3 = 0.1,$ $\beta_4 = 0.24$	

**Table 4-3:** *Model parameters*

The coordination interval that we consider in the following experiments is 10 minutes, i.e., half of the length of the minimum rolling capacity constraint duration. Hence, each day of the scheduling season ( $d \in D$ ) comprises  $144 \times 10$ -minute intervals. Finally, the load factor considered for charter and scheduled operations is 100% and 85% accordingly. The prioritisation functions that we

considered for the solution of SASAM, and the multi-objective delay algorithm are identical to the descriptions provided in section 4.3.2.1.1. In expressions (4.10), the objectives are weighted using empirical preference data obtained from a previous study (Katsigiannis and Zografos, 2021b).

In the experiments that follow we consider four alternative ASA prioritisation schemes. These are described and identified in Table 4-4.

*u-MIP* represents an ASA scheme which corresponds to the modelling of the current WASG rules. In addition to constraints (4.1)-(4.5), this regime optimises (4.10) by considering the following constraints.

$$\sum_{t \in [t_m + \min\{0, \bar{t}_m - t_m\}, t_m + \max\{0, \bar{t}_m - t_m\}]} x_{t,m} = \sum_{t \in T_{\bar{c}}} x_{t,m} \quad \forall m \in M_{CR \cup H} \quad (4.31)$$

$$x_{\bar{t}_m, m} = 1 - x_{t_m, m} \quad \forall m \in M_{CL} \quad (4.32)$$

$$HM_{d,t,c} = \sum_{m \in M_H} \sum_{t' \in [t, t+c-1]} a_{m_k}^d x_{t', m} b_m \quad \forall d \in D, c \in C, t \in [0, |T_{\bar{c}}| - c] \quad (4.33)$$

$$NEM_{d,t,c} = \sum_{m \in M_{NE}} \sum_{t' \in [t, t+c-1]} a_m^d x_{t', m} b_m \quad \forall d \in D, c \in C, t \in [0, |T_{\bar{c}}| - c] \quad (4.34)$$

$$\sum_{d \in D} \sum_{t \in T_{\bar{c}}} NEM_{d,t,c} \leq \left\lfloor \frac{\sum_{d \in D} \sum_{t \in T_{\bar{c}}} (u_{d,t,c}^k - HM_{d,t,c}^k)}{2} \right\rfloor \quad \forall c \in C \quad (4.35)$$

$$\sum_{t \in T_{\bar{c}}} x_{t,m} |\psi_{t,m}| \leq \Psi \leq 60/\bar{c} \quad \forall m \in M_{Ne} \quad (4.36)$$

Constraints (4.31) ensure that requests for unchanged historic movements (*H* requests) will receive their historic time ( $\bar{t}_m$ ), i.e., the time that they received in the previous season. In addition, expressions (4.31) ensure that each *CH* request of *R* type (denoted by *CR*) will receive a slot lying between the time period defined by its requested ( $t_m$ ) and its previously allocated time slot ( $\bar{t}_m$ ). Constraints (4.32)

respect the rules for  $L$  type  $CH$  requests (denoted by  $CL$ ) and will only allocate the requested or the previously allocated time slot. Constraints (4.35) define the slot pool, i.e. the available slots after the allocation of historic requests (defined as per expression (4.33)), of whom up to 50% is allocated to movements of  $NE$  requests (defined as per expression (4.34)) with the remaining capacity being distributed to  $CH$  and  $O$  requests according to WASG.

ID	Variant	Description
u-MIP	Unstable MIP	Schedule generated by considering expressions (4.1)-(4.5) and (4.10). Requests are simultaneously allocated but prioritised based on the WASG rules, i.e., historic requests ( $H$ ) receive their requested time slots, new entrant requests are then allocated with a maximum displacement of 1 hour, changes to historic requests ( $CH$ ) receive time slots based on their willingness to accept alternative offers (based on $R, L$ action codes). Finally, other requests ( $O$ ) are allocated without any priority considerations.
s-MIP	SASAM	Schedule obtained by optimising expression (4.10) subject to constraints (4.1)-(4.5) and the stability constraints (4.21)-(4.30)
DA	DA schedule(s) (holistic)	Application of Algorithm 4-2 by considering all requests simultaneously. The lengths of priority lists considered are (lengths expressed in 10-min intervals): $PL = [0, 1, 3, 6, 9, 12, 15, 21, 24, 30, 36, 48, 60, 72, 84, 96, 108, 120, 132, 144]$
h-DA-MIP	DA + MIP schedule(s) (prioritised)	Application of Algorithm 4-2 after considering a hierarchical allocation of requests. This ASA scheme allocates $H$ requests to their requested times and updates the remaining airport capacity. Then, $NE$ requests are allocated using a maximum displacement of 1-hour. After the allocation of $NE$ requests, the capacity of the airport is updated, and the DA algorithm is applied for $CH$ and $O$ requests. The lengths of priority lists considered are (lengths expressed in 10-min intervals): $PL = [0, 1, 3, 6, 9, 12, 15, 21, 24, 30, 36, 48, 60, 72, 84, 96, 108, 120, 132, 144]$ . This is a hybrid approach which ensures that historic's requests will not be displaced. In the hybrid approach, the definition of the slot pool is more accurate since $CH$ and $O$ are allocated after the allocation of $NE$ requests. This approach illustrates how the proposed DA algorithm can be used in conjunction with existing MIP approaches

**Table 4-4:** Description of the slot allocation schemes considered for the computational experiments

During the pre-processing of the request data, if the total number of offered slots minus the number of the requested historic movements divided by two is greater than the number of new entrants' movements, then constraints (4.33),



(4.34) and (4.35) can be dropped, since the capacity remaining after the allocation of historic requests trivially satisfies the slot pool's allocation to new entrants (similar to the considered airport data instance). Finally, constraints (4.36) ensure that the maximum displacement for  $NE$  will be kept below 1 hour.

$s$ -MIP is an ASA scheme that optimises expression (4.10) subject to constraints (4.1)-(4.5) and the stability constraints defined in (4.21)-(4.30). Schedules relating to  $s$ -MIP are provided by the solution approach detailed in section 4.4.1.

$DA$  corresponds to the application of Algorithm 4-2 for different preference list lengths. In  $DA$  airline requests are considered in a holistic fashion (similar to WASG's requirements) and their prioritisation is enforced using the prioritisation functions detailed in section 4.3.2.1. Under this scheme, multiple schedules are generated by considering the concurrent allocation of all requests and the trade-offs between the requests' preference lists and airport capacity utilisation.

Finally,  $h$ - $DA$ -MIP is a hybrid ASA regime which allocates airports slots sequentially.  $H$  requests are allocated first; the airport's slot capacity is updated, and the remaining capacity is allocated to  $NE$  movements by keeping maximum displacement below 1 hour (according to WASG's rules for new entrants and constraints (4.36)). The allocation of  $NE$  and  $H$  movements is done by (4.10) subject to constraints (4.1)-(4.5), yet for each priority level only the corresponding requests are considered (a model considering  $m \in M_H$  is solved for the  $H$  level; and a model considering  $m \in M_{NE}$  is solved for the  $NE$  level). After the allocation of  $H$  and  $NE$  requests, the remaining capacity is allocated to  $CH$  and  $O$  requests using Algorithm 4-2 for different preference list lengths. Under this scheme, stability is considered only for  $CH$  and  $O$  requests and multiple schedules are generated by considering the trade-offs between the preferences of the  $CH$  and  $O$  requests and airport

capacity utilisation. h-DA-MIP is a hybrid approach that illustrates how the proposed DA algorithm can be used in conjunction with MIP formulations so as to generate multiple schedules in a multi-objective setting.

The detailed algorithms and ASA schemes are implemented using version 3.7.2 of the Python programming language (Van Rossum and Drake, 2009) using the Anaconda distribution. The MIP models were built and solved using version 9.1 of Gurobi solver (Gurobi Optimization, LLC, 2021) and the optimality gap considered for each solved MIP was equal to 0.1%. All computational experiments reported in sections 4.5.2-4.5.5, were conducted on a desktop computer with 8GB of RAM and an Intel(R) Core™ i5-6500T CPU @ 2.50GHz.

## **4.5.2 Sensitivity of the functions with respect to different parameters**

This subsection conducts statistical analyses regarding the load factor parameter and its influence on the exponents of the prioritisation functions. The main discussion revolves around the influence of the load factor parameter. Analyses and discussion on other parameters are also included wherever it is deemed appropriate.

### **4.5.2.1 Sensitivity analyses regarding the airline demand preference functions**

To demonstrate the suitability of (4.14) for shaping the preference function and differentiating between requests with different characteristics, in this subsection we provide a sensitivity analysis.

#### **Sensitivity with respect to the load factor**

Figure 4-6 exhibits the distributions of the  $\xi'_m$  index received by each airline (please note that for visualisation purposes the plot includes airlines with more than 1% of the total requests submitted to the airport). The rows of the figure represent alternative scenarios regarding the load factor of requests for scheduled operations.

The scenarios range between the load factor parameter considered in the airport under consideration (85%) and a load factor of 100% using 5% increments, hence resulting in four scenarios with the following load factors: 85%, 90%, 95% 100%.

The lowest value of the load factor parameter that is used to determine the scenario set is determined by the fact that system-wide load factors in the U.S. were approximately equal to 85% in 2018 and 2019 (before the impact of COVID19) (MIT and U.S. Department of Transportation, 2021), while in Europe system wide load factor was approximately equal to 85.4% (ICAO, 2019). In addition, Figure 4-6 differentiates between requests for charter and scheduled operations (denoted by blue and orange colour respectively). In all scenarios, the load factor of charter operations is set to 100% (as per the current commercial practices). As a result, the scenarios included in the statistical analyses that follow are listed below:

**Scenario 1:** Charter operations load factor = 100%, Scheduled operations load factor = 85%

**Scenario 2:** Charter operations load factor = 100%, Scheduled operations load factor = 90%

**Scenario 3:** Charter operations load factor = 100%, Scheduled operations load factor = 95%

**Scenario 4:** Charter operations load factor = 100%, Scheduled operations load factor = 100%

Figure 4-6 provides an overview of the distribution of  $\xi'_m$  for different airlines and different market types (Charter/Scheduled) under the 4 load factor scenarios. An initial observation is that within each scenario the values of  $\xi'_m$  of each airline are diverse and receive a wide spectrum of values. This suggests that the proposed tie-breaking exponent (as per expressions (4.14)) and its components may differentiate sufficiently between the requests of the submitted by airlines and capture the relative importance assigned to each request. The visual comparison facilitated by Figure 4-6 shows that the alternative load factor considerations lead

to imperceptible changes to the distributions of  $\xi'_m$  for all airlines. Subtle differences in different load factor scenarios are observed for two airlines that requested both charter and scheduled operations (A48 and A70).

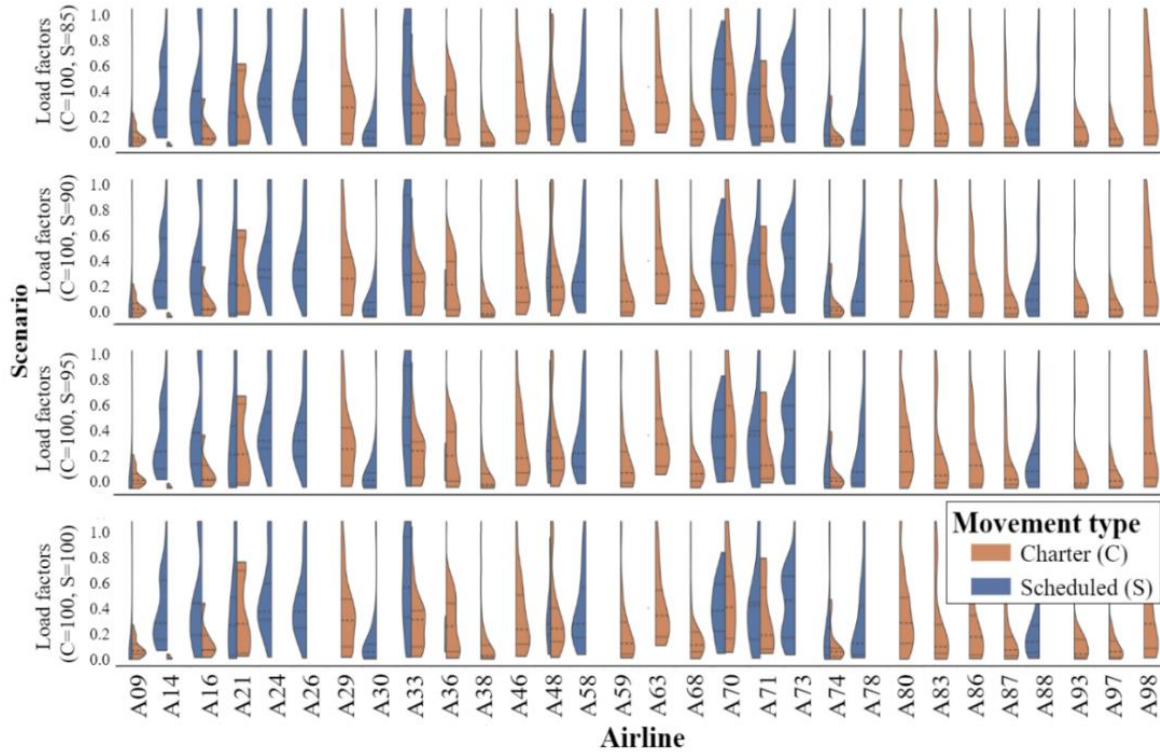


**Figure 4-6:** *Distribution of demand exponent's values for each airline under different load factor scenarios*

To provide conclusive results on the impact of the load factor on the value of  $\xi'_m$ , we conduct statistical tests which determine on whether there is a statistically significant difference between the means of  $\xi'_m$  under the different load factor scenarios or not. To do so, we conduct a series of paired tests using Tukey's Honestly Significant Difference (HSD) (Tukey, 1949). Tukey's HSD is superior to the one-way ANalysis Of VAriance (ANOVA), since not only it determines the existence of differences between the samples/scenarios, but it also indicates which samples are different, hence reducing the susceptibility of the comparisons to Type I errors (Barnette and McLean, 1998). Tukey's HSD produces a series of tests that

compare the mean value of  $\xi'_m$  in each scenario with the mean value observed in all other scenarios, thus producing a total of  $n(n - 1)/2$  comparisons. In this case, for the 4 considered scenarios, the test produces 6 comparisons. The hypotheses tested in this series of two-tailed tests are stated as follows:

$$H_0^{i,j}: \mathbb{E}(\xi'_m)_i = \mathbb{E}(\xi'_m)_j$$

$$H_1^{i,j}: \mathbb{E}(\xi'_m)_i \neq \mathbb{E}(\xi'_m)_j$$

Where,  $H_{0(1)}^{i,j}$  is the null (alternative) hypothesis regarding scenarios  $i, j$ ; and  $\mathbb{E}(\xi'_m)_i$ ,  $\mathbb{E}(\xi'_m)_j$  are the means of  $\xi'_m$  in scenarios  $i$  and  $j$ .

Scenario $i$	Scenario $j$	Mean difference	p-value	Rejection of $H_0^{i,j}$
4	1	-0.0022	0.899	False
4	2	-0.0012	0.9	False
4	3	-0.0006	0.9	False
1	2	0.001	0.9	False
1	3	0.0016	0.9	False
2	3	0.0006	0.9	False

**Table 4-5:** Statistical comparison between the mean value of  $\xi'_m$  under alternative load factor scenarios

The results of this series of tests suggest (see Table 4-5) that there is no difference between any of the considered scenarios (at the 99% significance level), since in all cases the test failed to reject the null hypothesis (which assumed equality of means). An additional test would be to examine on whether the alternative load factor scenarios lead to statistically significant differences to the values of each airline's  $\xi'_m$  or not. In this case, we cannot use parametric t-tests since there are several airlines whose submitted requests do not suffice to assume normality. Instead, we may use the *Wilcoxon signed-rank test* which is the non-parametric equivalent of the paired t-test (MacFarland and Yates, 2016).

Again, for all 100 airlines and scenarios, the test failed to reject the null hypothesis. This suggests that there are no airlines whose average value of  $\xi'_m$  (across the submitted requests) differed among the alternative load factor scenarios. The lowest p-value observed during this series of tests was 0.80 suggesting that the null hypothesis (the median  $\xi'_m$  for of each airline in a scenario is equal to the values observed in other scenarios) cannot be (and is far from being) rejected.

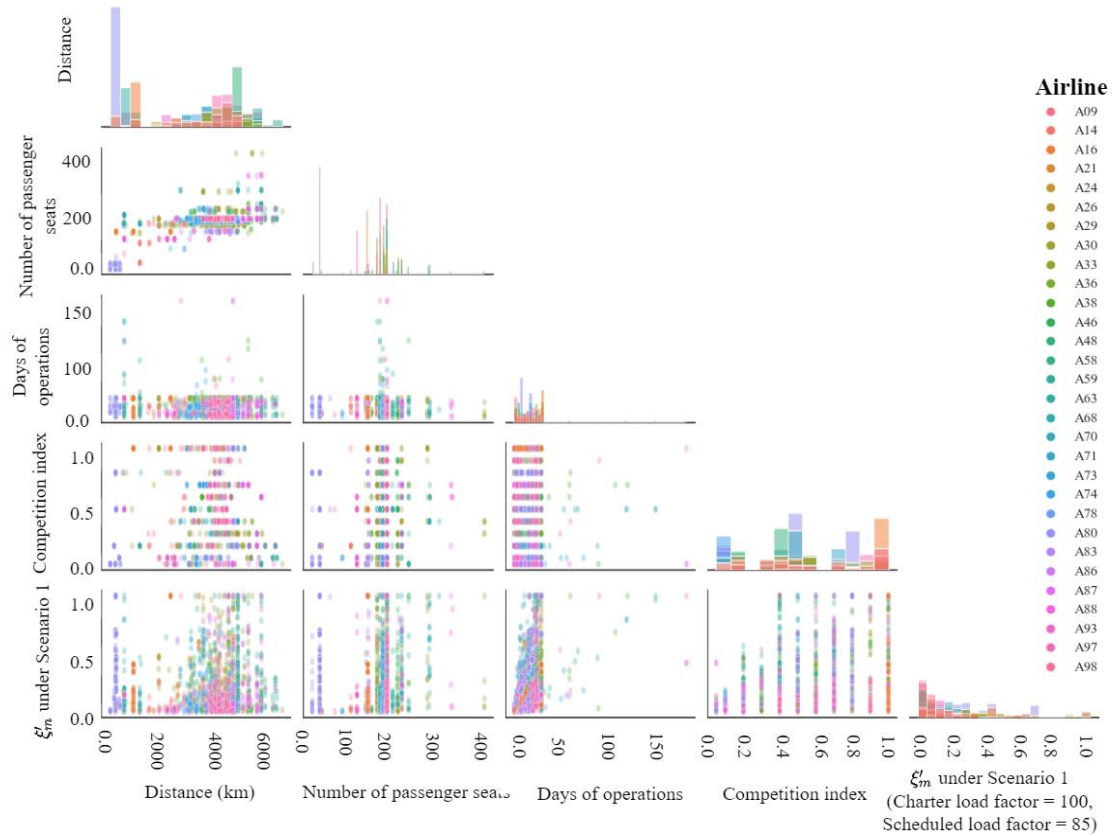


**Figure 4-7:** Scatter plot demonstrating the relationship between the components of  $\xi'_m$

### Relationship between the other parameters composing $\xi'_m$

One of the issues that is worthy of investigation is to examine how the proposed index ( $\xi'_m$ ) differentiates between the requests of the same airline, requests having the same distance, days of operations or passenger seats. In Figure 4-7 we demonstrate that for the same airline (represented by the hue of each point), the

$\xi'_m$  received a wide spectrum of values which depends on its structure and interaction of its components. The most interesting observation is extracted for airline A80 which only serves domestic destinations (similar distance) and has a homogeneous aircraft fleet (only two different aircraft types). As one can see in both Figure 4-6 and Figure 4-7,  $\xi'_m$  adequately differentiates among the requests of A80 since it also considers the effective period and the frequency of the associated operations. Similar observations are extracted for cases where an airline's requests have similar distances. In Figure 4-7 there are several airlines with requests of similar geographical reach but with significantly different values for the  $\xi'_m$  index. Accordingly, we observe that requests of the same airline with similar days of operations, may receive significantly different values for  $\xi'_m$ .

Overall, we observe that for each airline,  $\xi'_m$  can differentiate between the requests comprising the airlines' request portfolio. In Figure 4-8, we present the correlation (Pearson correlation is used since there are more than 2000 requests per scenario, which suffice to assume normality) of the  $\xi'_m$  values with each of the other components of the index. This figure suggests that there is no strict monotonicity between the index and its components.

For instance, the number of passenger seats, the distance between airports, the days of operations and the competition index appear to have weak correlations with  $\xi'_m$ . This finding suggests that  $\xi'_m$  does not single-handedly depend on a single request characteristic and thus it is able to differentiate between requests which have at least one different operational characteristic *ceteris paribus*. This statement is also supported by the fact that in the concerned dataset, there are no requests with similar characteristics (distance, weekly frequency, airline, etc) for whom the demand-prioritisation exponent results in similar values.

The only case of similarity that is observed, concerns 2+2 requests (out of the 2491 request submitted to the airport, i.e., 0.16% of the total request portfolio) with identical characteristics submitted for different days (2 requests of airline A48 and 2 requests of A93). However, in this case the requests of the two airlines concern different days of the scheduling seasons and the time-dependent components of the proposed functions and models can easily distinguish between them.

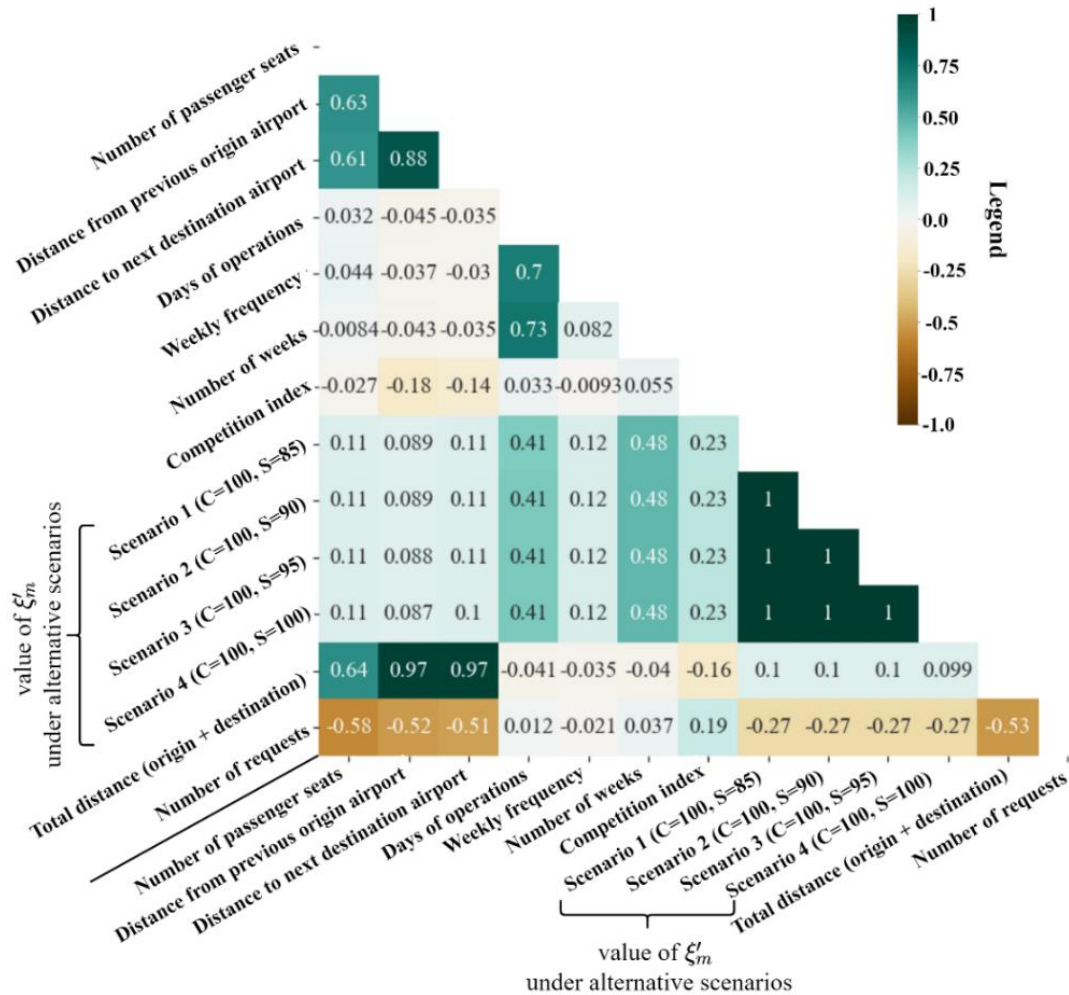


**Figure 4-8:** Heatmap illustrating the correlation among multiple metrics and the value of  $\xi'_m$



### 4.5.2.2 Sensitivity analyses regarding coordinators' function

Similar to the analysis presented for the exponent of the demand prioritisation functions, in this subsection we provide a sensitivity analysis on the influence of the different parameter values on the value of  $\psi'_m$ .

#### Sensitivity regarding the load factor

The goal again is to determine on whether different load factor considerations significantly alter the value of  $\psi'_m$  or not. Figure 4-9 exhibits the distributions of the values of  $\psi'_m$  under different load factor scenarios (the scenarios are identical to the ones considered for the demand exponent) for each airline that submitted more than 1% of the total submitted requests. The observations that we extract in this case are similar to the conclusions we reached for the demand function's exponent, i.e., there is no significant influence of the load factor on the value of  $\psi'_m$ .

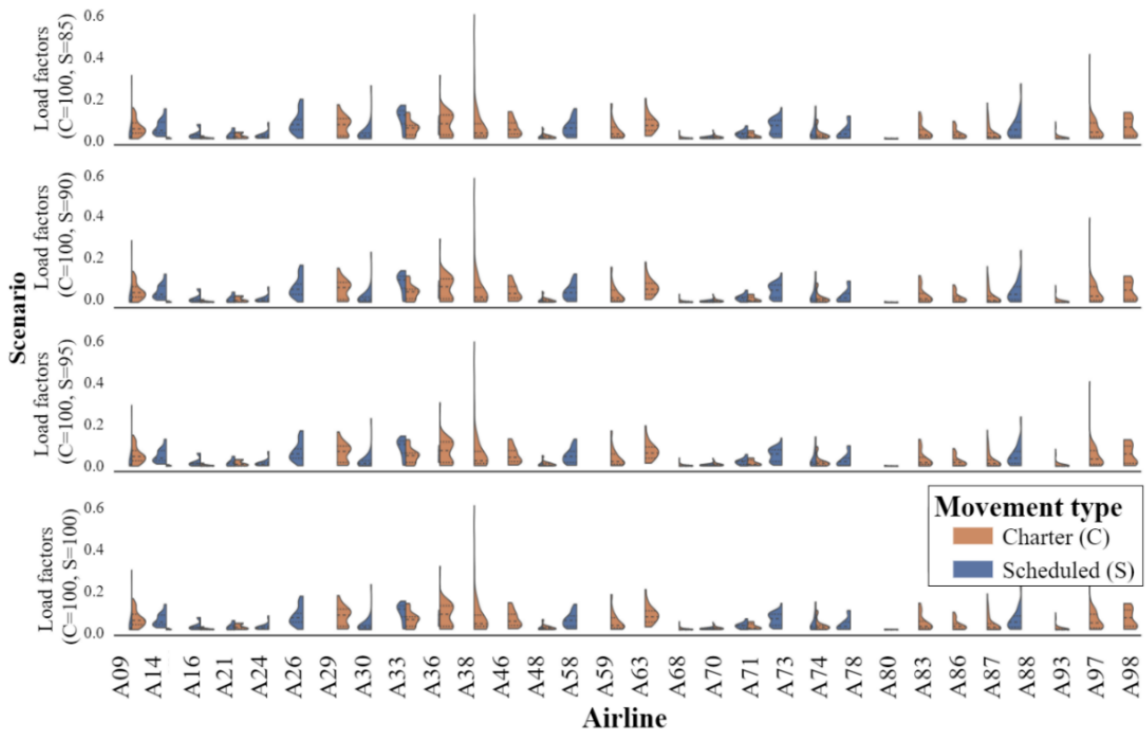


Figure 4-9: Impact of alternative load factors on  $\psi'_m$

Similar to the demand index (section 4.5.2.1), we construct 4 scenarios with different load factors for Charter (C) and Scheduled operations, i.e. Scenario 1: Charter operations load factor = 100%, Scheduled operations load factor = 85%, Scenario 2: Charter operations load factor = 100%, Scheduled operations load factor = 90%, Scenario 3: Charter operations load factor = 100%, Scheduled operations load factor = 95%, Scenario 4: Charter operations load factor = 100%, Scheduled operations load factor = 100%). In addition, since  $\psi'_m$  is determined by multiple parameters, it is less sensitive to the value of the load factor parameter (which is only one of the multiple components). This is statistically proved through an application of Tukey's HSD, which compares the mean values of  $\psi'_m$  obtained for each scenario.

The hypotheses tested in this series of two-tailed tests are similar to the hypotheses of the demand exponent and are stated as follows:

$$H_0^{i,j}: \mathbb{E}(\psi'_m)_i = \mathbb{E}(\psi'_m)_j$$

$$H_1^{i,j}: \mathbb{E}(\psi'_m)_i \neq \mathbb{E}(\psi'_m)_j$$

Where,  $H_{0(1)}^{i,j}$  is the null (alternative) hypothesis between scenarios  $i, j$ ; and  $\mathbb{E}(\psi'_m)_i, \mathbb{E}(\psi'_m)_j$  are the means of  $\psi'_m$  in scenarios  $i$  and  $j$ .

Scenario $i$	Scenario $j$	Mean difference	p-value	Rejection of $H_0^{i,j}$
4	1	0.0016	0.8517	False
4	2	0.001	0.9	False
4	3	0.0005	0.9	False
1	2	-0.0006	0.9	False
1	3	-0.0011	0.9	False
2	3	-0.0005	0.9	False

**Table 4-6:** *Statistical comparison between the mean values of  $\psi'_m$  under alternative load factor scenarios*

As with the demand exponent, all tests failed to reject the null hypothesis (99% significance level), suggesting that there is no significant difference in the value of  $\psi'_m$  when the load factor of requests for scheduled operations changes (see Table 4-6). Even between the two extreme scenarios (15% difference to the load factor of scheduled operations) the p-value reported by the statistical test was 0.852.

In order to test for differences for each airline, we again conduct a non-parametric test (*Wilcoxon signed-rank test*) comparing the value of  $\psi'_m$  for all airlines in each alternative scenario. The test failed to reject the null hypothesis (minimum p-value  $\sim 0.9$ ) thus confirming that the median (in non-parametric tests it is the median that is compared rather than the mean)  $\psi'_m$  of each airline is not significantly affected by the load factor's value. Hence, we conclude that the load factor does not significantly impact the value of  $\psi'_m$ .

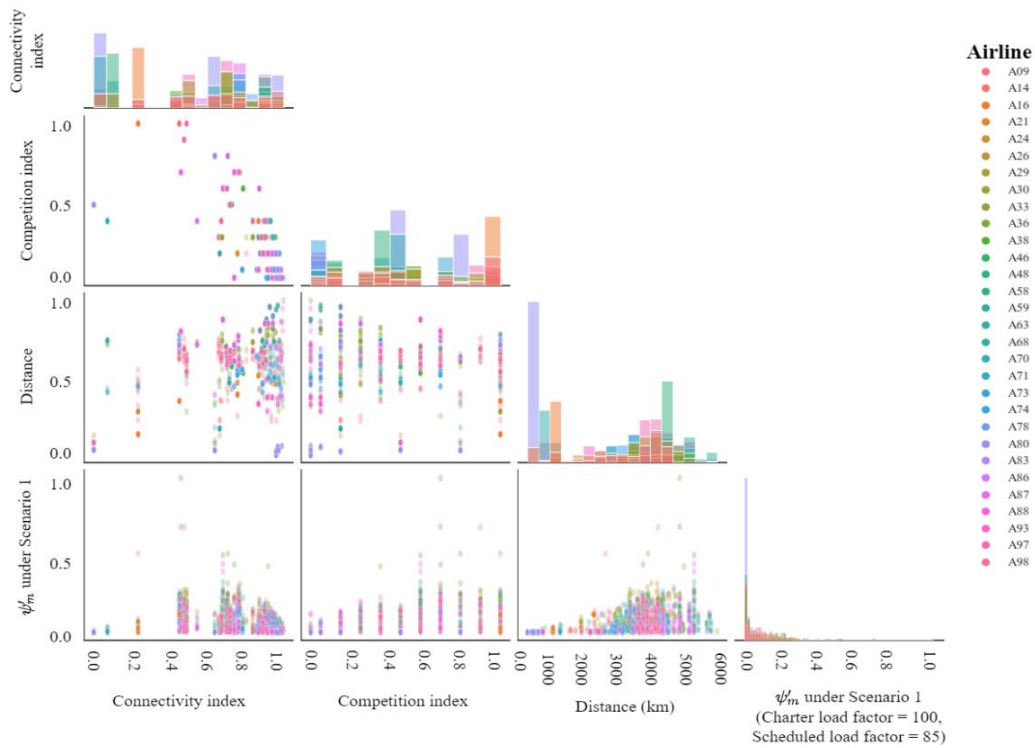


**Figure 4-10:** Scatter plot studying the relationships among the components of  $\psi'_m$

**Sensitivity regarding other parameters**

In studying the relationship between the components of  $\psi'_m$ , we observe that there is adequate differentiation between airlines' requests (i.e., for the same airline the exponent receives different values). This is validated by the following scatter plots (Figure 4-10) and the heatmap in Figure 4-11. A difference that we observe between  $\psi'_m$  and  $\xi'_m$ , is that  $\psi'_m$  provides distributions of values that lie closer to 0 (Figure 4-9 and Figure 4-10).

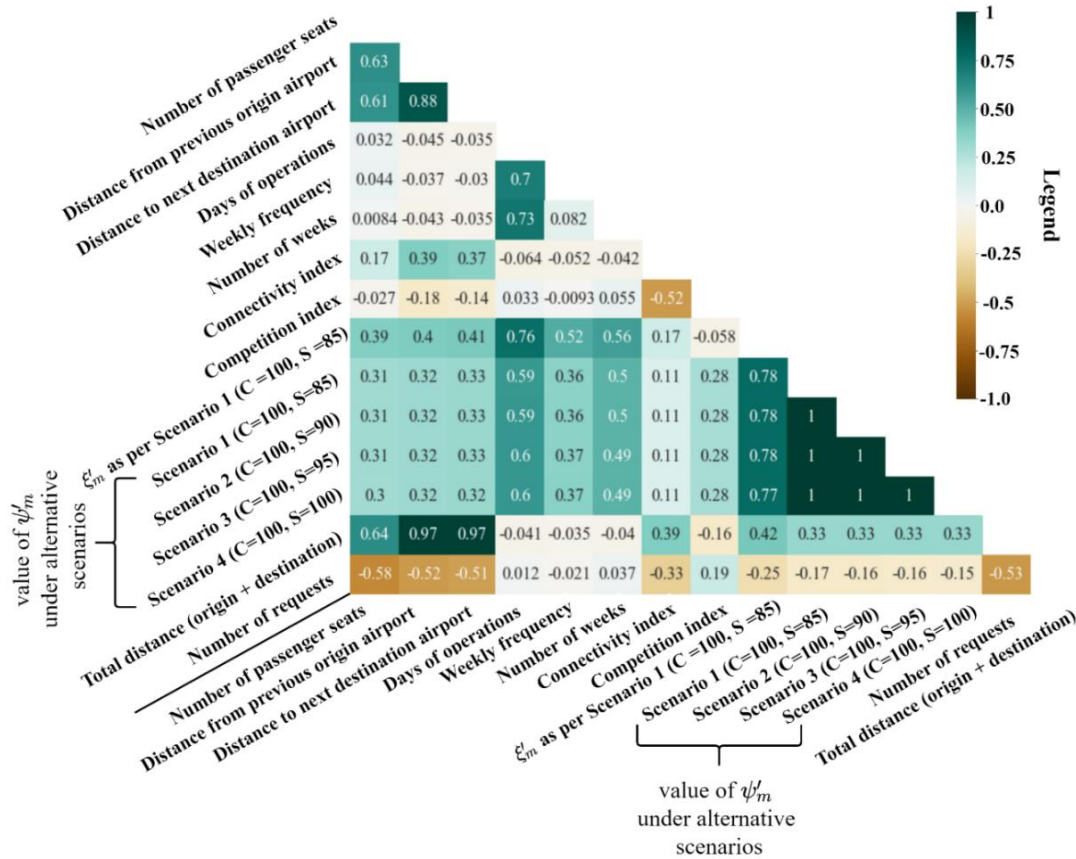


**Figure 4-11:** Correlation heatmap between the components of  $\psi'_m$

That is because  $\psi'_m$  is composed of three components which take values between 0 and 1 (connectivity/competition index and  $\xi''_m$ ) that cannot receive their maximum value simultaneously. This statement is supported by the heatmap in Figure 4-11 where we observe an important negative correlation between the connectivity and the competition index (a correlation of -0.52). In Figure 4-10 we

observe that  $\psi'_m$  (under all scenarios) is not entirely monotonous with any other parameter since it is determined by a series of interconnected parameters (no strong correlation). This finding in conjunction with Figure 4-10 suggest that  $\psi'_m$  can be used as a differentiating (tie-breaking) factor in the coordinators' function. Please note that this heatmap contains additional insights of interest, i.e., significant negative correlation between the number of requests submitted by an airline and the distance covered.

#### 4.5.2.3 Statistical evidence on the difference between $\psi'_m$ and $\xi'_m$

Having provided arguments on the robustness of  $\psi'_m$  and  $\xi'_m$  with respect to the load factor parameter, and their ability to differentiate between requests sharing similar characteristics, in this section we conduct a statistical comparative analysis between the two exponents. The purpose of this section is to confirm that there is a significant difference between the two exponents and further validate the need for considering the ASA problem as a two-sided matching game.

To compare  $\psi'_m$  and  $\xi'_m$  there is need to implement an unpaired test for comparing the means (the two samples are not related since they concern the prioritisation/importance assigned by two different sets of agents). For comparing the mean values of  $\psi'_m$  and  $\xi'_m$ , we may assume normality (more than 2000 requests per scenario) and use an unpaired t-test. The test rejected the null hypothesis with a p-value of 0.00 suggesting that the two exponents are significantly different from each other. Furthermore, we moved beyond this test and conducted a series of unpaired t-tests (significance level 99%) so as to determine on whether the two indices remain different from each other under alternative load factor scenarios or not. In all cases, the tests rejected the null hypothesis, suggesting that there is significant difference between the values of the two indices regardless the considered load factor scenario (Table 4-7).

Finally, to compare the exponents of each airline under each scenario, we created a custom testing routine using the unpaired non-parametric test of Kruskal Wallis (*H-statistic*). The routine conducted 400 tests based on the number of airlines requesting access to the airport and the number of alternative scenarios (100 airlines x 4 scenarios = 400 tests). The p-value for all airlines and all load factor scenarios was equal to 0.00, suggesting that there is no scenario under which any of the airlines may have similar values of  $\psi'_m$  and  $\xi'_m$ .

$\xi'_m$ -Scenario $i$	$\psi'_m$ -Scenario $j$	Mean difference	p-value	Rejection of $H_0^{ij}$
4	4	-0.2661	0.001	True
4	1	-0.2638	0.001	True
4	2	-0.2646	0.001	True
4	3	-0.2654	0.001	True
1	4	-0.2639	0.001	True
1	1	-0.2616	0.001	True
1	2	-0.2625	0.001	True
1	3	-0.2632	0.001	True
2	4	-0.2649	0.001	True
2	1	-0.2626	0.001	True
2	2	-0.2634	0.001	True
2	3	-0.2642	0.001	True
3	4	-0.2655	0.001	True
3	1	-0.2632	0.001	True
3	2	-0.264	0.001	True
3	3	-0.2648	0.001	True

**Table 4-7:** Comparison between the mean values of  $\psi'_m$  and  $\xi'_m$  under alternative load factor scenarios

#### 4.5.2.4 Discussion on $\psi'_m$ and $\xi'_m$

The statistical analyses presented in sections 4.5.2.1-4.5.2.3 have provided support on the suitability of the proposed functions' exponents. In particular, we have demonstrated that  $\psi'_m$  and  $\xi'_m$  are sufficient for distinguishing between requests and consider their importance from the airlines' perspective and the priority assigned by the coordinators' functions. Rather than proposing a limited subset of values for the requests of each airline, the proposed airline demand function

exponent captures the interrelation between several operational characteristics of each request, thus providing a surrogate estimate on the relative importance that a request receives in relation to the other requests comprising the airline's request portfolio. With respect to the  $\psi'_m$ , we observe that it captures latent relationships between its components without being single-handedly dependent on a single characteristic. The index is not correlated to a single index/component, rather it is valued based on the interactions between the connectivity and competition indexes, and the available seat kilometres as per  $\xi'_m$ .

On another note, we have placed special emphasis on the determination of the influence of the load factor ( $lf_m$ ) parameter on the exponents of both functions. That is because the load factors associated with each request are not known or are not disclosed by the airlines before the outset of the operations. The conducted statistical tests demonstrate that the load factor parameter has minimal influence on the value of the exponents. Even between scenarios where the load factor of scheduled requests is increased by more than 15%, the statistical comparisons suggest that the values of both  $\psi'_m$  and  $\xi'_m$  are insignificantly changed. This finding validates the robustness of the proposed functions with respect to the uncertainty of the load factor parameter (which is heavily influenced by the stochasticity of passenger demand).

As a result, the use of aggregate load factor estimates, i.e., differentiating between charter and scheduled operations based on the load factor estimates included in the declared capacity parameters, does not appear to affect the quality of the decision support capabilities of the proposed functions. This observation in conjunction with the fact that the load factor is solely used in the exponent of the function -which is mainly used for shaping the gradient of the time-dependent, delay discount functions - suggests that the assumptions made about this parameter

result in insignificant changes to the decisions made by the models that follow. Regardless of the assumptions made concerning the load factor, future research considering load factor estimates could either consider assumptions similar to the ones made in this study, or, in the case that higher fidelity is desired, use commercial data sources which may provide average load factor estimates for each route.

Finally, in section 4.5.2.3 we proved that  $\psi'_m$  and  $\xi'_m$  and their values are significantly different from each other. This analysis further supports the need for modelling the ASA problem as a two-sided matching game, since the agents on both sides of the problem have significantly different needs and priorities. The statistical analyses and the findings of this section coupled with the mathematical properties of the proposed prioritisation functions presented in section 4.3.2.1 suggest that the proposed prioritisation approaches can be sensible proxies with regards to (a) the airlines' side and (b) the coordinators' side.

### 4.5.3 Comparisons between the schedules obtained by u-MIP and s-MIP

In comparing the schedules provided by u-MIP and s-MIP (as identified in Table 4-4) we consider a wide array of ASA performance metrics. The schedules obtained by the two alternative MIP models are discussed with respect to their aggregate performance (measured with respect to all requests submitted to the airport) and their performance with respect to the different request priorities composing the ASA decision-making, i.e., historic ( $H$ ), new entrant ( $NE$ ), changes to historic ( $CH$ ) and other requests ( $O$ ).

The performance of the schedules obtained by solving s-MIP and u-MIP are provided in Table 4-8. An initial observation is that in both schedules  $H$  requests receive no-displacement. This validates the ability of the proposed prioritisation



functions (section 4.3.2.1) in capturing the priority rules associated with  $H$  requests. Regarding new entrants' requests, we observe that stability considerations (as introduced by s-MIP) result in increased displacement in comparison to u-MIP. That is because, in s-MIP, the allocation of  $NE$  is done by considering the stability of the allocations concerning requests of the following priority levels ( $CH$  and  $O$  requests). As a result, to prune blocking allocations across the whole schedule, s-MIP introduces additional displacement to the  $NE$  and the  $CH$  levels, which however does not compromise the model's compliance with WASG's requirements.

Performance metric	s-MIP				u-MIP			
	H	NE	CH	O	H	NE	CH	O
[1] Schedule displacement	0	222	25,501	196,533	0	97	8,338	305,900
[2] Schedule displacement (Schengen)	0	222	21,501	149,631	0	97	8,016	229,770
[3] Schedule displacement (Domestic)	0	0	2,749	17,806	0	0	828	43,239
[4] Displaced requests	0	2	98	235	0	2	82	756
[5] Displaced requests (season)	0	49	1,642	5,081	0	49	1,265	14,300
[6] Displaced passengers	0	275	17,285	42,130	0	275	14,416	132,123
[7] Displaced Passengers (season)	0	6750	295,000	932,041	0	6,750	226,045	2,508,918
[8] [1]/ [5]	0	4.53	15.53	38.68	0	1.98	6.59	21.39
[9] [1]/ [7]	0	0.03	0.09	0.21	0	0.01	0.04	0.12
[10] Rejected requests	0	0	0	48	0	0	0	17
[11] Rejected requests (season)	0	0	0	1,292	0	0	0	1,478
[12] Rejected passengers	0	0	0	5,354	0	0	0	3,342
[13] Rejected Passengers (season)	0	0	0	151,964	0	0	0	291,638
[14] Maximum displacement	0	6	16	51	0	3	16	101

**Notes:** [1], [2], [3] and [14] are measured in 10-minute intervals

**Table 4-8:** Comparison between the schedules obtained by solving s-MIP and u-MIP

For new entrants' requests we observe that s-MIP may adequately grasp existing policy rules and result in allocations that do not exceed the 1-hour displacement threshold. In the  $CH$  level we observe similar results. Despite

exhibiting the same maximum displacement that u-MIP reported, it appears that more  $R$ -type  $CH$  requests are displaced and hence all displacement-related metrics reported by s-MIP are increased in comparison to u-MIP. An interesting finding is that the constraints/rules of  $CH$  requests are adequately grasped by the proposed prioritisation functions, since the flexibility allowed by  $R$  requests is utilised so as to prune blocking pairs and hence result in an acceptable schedule.

For all upper priority levels ( $H, CH, NE$ ) both modelling variants reported no request rejections. This finding suggests that schedule acceptability can cater existing slot request prioritisation rules without leading to spilled airline and passenger demand for pre-existing and  $NE$  operations, ergo the price of stability for  $H, CH, NE$  does not appear to inhibit the applicability of s-MIP in practice. The results regarding  $O$  requests appear to deviate from this observation, since in order to achieve an acceptable schedule, the s-MIP rejected 48 requests (out of the 4689 arrival/departure series submitted to the airport), while the solution of u-MIP resulted in 17 rejected requests.

This observation signifies that  $O$  requests' acceptability requires the rejection of some requests. However, the requests that are rejected in s-MIP concern fewer days of operations and less passengers. Hence, under the s-MIP schedule, despite the larger number of displaced requests, the airport capacity is used more intensively and serves more passengers and movements throughout the scheduling season. On another note, the airport under consideration appears to be severely congested, since regardless the modelling variant, there several request rejections.

The compromises required so as to achieve scheduling stability are hereafter referred to as the '*price of stability*'. The price of stability, as per Table 4-8, suggests that the requests that are rejected by the stable modelling variant concern less passengers, routes with less competition and a shorter effective period. This is

supported by the fact that the unstable variant (u-MIP), despite reporting less request rejections, resulted in more spilled passenger demand and a larger number of season-wide request rejections in comparison to s-MIP. This observation suggests that the proposed prioritisation functions can support the definition of the pending list (the list of unaccommodated requests), by rejecting requests of low importance (expressed through a series of requests' operational characteristics) and scheduling requests that increase the airports' connectivity, serve more passengers and more competitive routes.

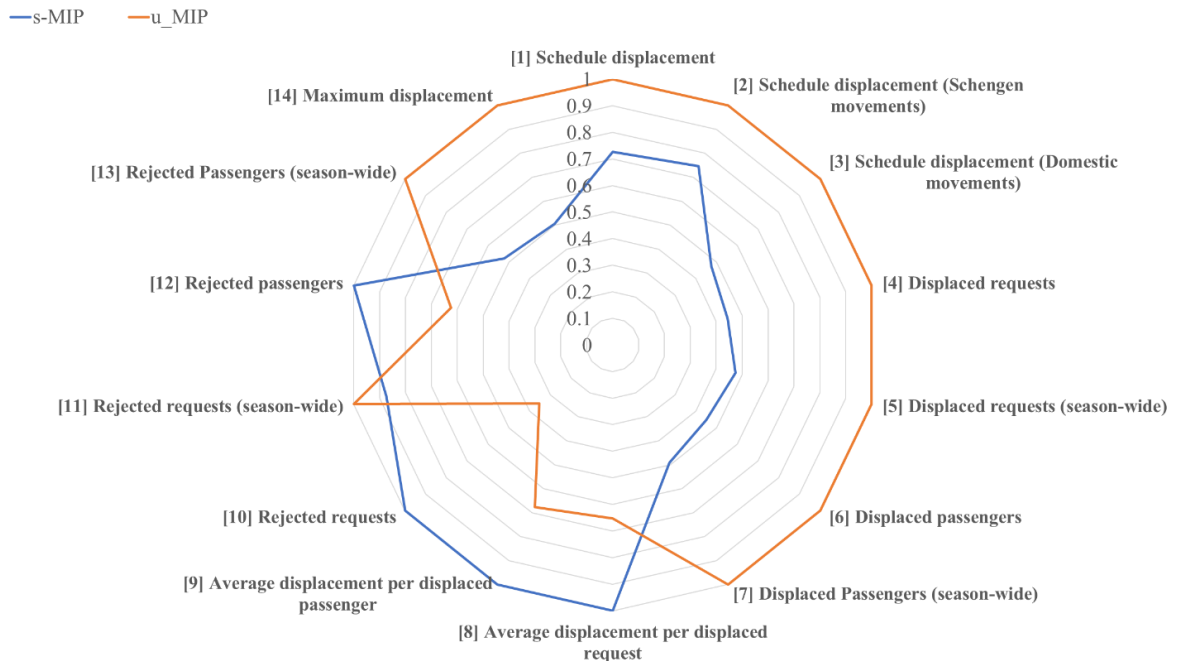


**Figure 4-12:** Schematic representation on the trade-off between airport capacity utilisation and scheduling performance for the schedules obtained by s-MIP and u-MIP

Overall, we observe that the price of stability is not prohibitive. This price translates to more rejected requests for the  $O$  priority and increased displacement for  $NE$  and  $CH$  requests. In exchange, the schedule provided by s-MIP, not only is guaranteed to be free of blocking allocations, but in achieving stability, it schedules the requests that matter the most (as per the assumptions made by the introduced

prioritisation functions). This set of observations suggests that there are significant trade-offs between airport capacity utilisation and airport efficiency. SASAM (s-MIP) captures these trade-offs and proposes acceptable allocations. This series of observations is diagrammatically articulated in Figure 4-12.

#### 4.5.3.1 Who pays the price? Comparison of the schedules given by u-MIP and s-MIP for each airline

To better grasp the implications of stability, this section discusses how airlines' objectives are affected by the integration of stability in ASA decision-making. Figure 4-13 compares the performance of the allocations received by airlines that submitted more than 0.5% of the total requests submitted at the airport, i.e., includes airlines  $a \in A: |M_a|/|M| \geq 0.005|M|$ . Blue bars denote improvements (decreases) after the consideration of stability as per s-MIP, while red bars indicate increases in s-MIP in comparison to u-MIP. An initial observation is that in s-MIP most airlines received improved values for the displaced passengers/requests and the total displacement objectives.

However, there are only 5 airlines which receive changed values with respect to the number of rejected passengers and requests. Airlines A80, A97, A16 receive an increased number of rejected requests and passengers. In contrast airlines A14 and A29 received improvements for both objectives. The reason behind this is that the rejected requests of airlines A80 and A16 mostly correspond to unpaired requests which concern a few days of operations and a low weekly frequency. The number of passengers and the competitiveness of the concerned routes of the rejected requests are lower than the requests of A14 and A19 that were rejected in u-MIP schedule.

With regards to A97, out of the 248 requests submitted by airline A97, s-MIP rejected 8 paired requests. A80 received 17 unpaired request rejections in s-MIP (out of 287 submitted requests) and A16 received 10 unpaired rejections (out

of 97 submitted requests). A16's rejections concerned unpaired requests for medium-haul operations and small-sized aircraft. Based on the considered prioritisation functions s-MIP reserved airport capacity for more important requests and hence these three airlines have received more rejections. Moreover, we observe that airlines submitting multiple requests (e.g., A80 and A97) are more prone to rejections. This is justified by the fact that an airline submitting multiple requests for the same origin-destination airport, will reduce the connectivity contributions for each of the requests serving the same route. Furthermore, in submitting multiple requests of low weekly frequency, requests' importance is reduced. This can be validated by the widely distributed values of  $\psi'_m$  and  $\xi'_m$  observed for airlines A80, A97 and A16. Please note that A80 exhibits some of the lowest values with regards to  $\psi'_m$  (see Figure 4-10).

On another note, for all three airlines that received an increased number of rejected requests (A80, A97 and A16), we observe significant improvements with respect to both total (A80 and A16) and maximum displacement. This finding has important implications for ASA decision-making, since, from an airline scheduling perspective, it may be worth offering fewer passenger seats (accepting less requests) in return for reduced schedule displacement. From an airport scheduling perspective, accepting less requests may result in improved airline acceptability and satisfaction for requests that are deemed of higher priority.

From a decision-making perspective, the final scheduling choice lies with the pertinent ASA stakeholders (airlines, airports, coordinators, air-traffic authorities) and their interests, who in order to reach to an informed decision, require additional information on the trade-offs among the considered objectives. Since SASAM and s-MIP require significant computational times so as to propose a single airport schedule, in the next section, we employ different variants of the DA algorithm (DA and h-DA-MIP as detailed in Table 4-4) and provide multiple non-dominated

stable schedules that can inform decision-making. Furthermore, we discuss on how the pertinent stakeholders may use the preference list length parameter of Algorithm 4-2 (*PL*) so as to reduce the number of scheduling alternatives, to a subset of schedules that express their preferences and needs.

Airline	Submitted requests (Arrival/Departure + Unpaired)	Displaced pasengers	Displaced requests	Maximum displacement	Total displacement	Rejected requests	Rejected pasengers
A80	287	2108	22	35	13574	-17	-766
A97	248	933	5	11	-4772	-11	-1624
A09	230	1566	9	48	667	0	0
A29	224	2205	10	-8	947	3	564
A48	190	5321	29	46	6625	0	0
A74	173	5728	31	52	13276	0	0
A68	170	603	3	4	-111	0	0
A38	164	894	5	-31	-6011	0	0
A93	148	3750	29	29	3747	0	0
A36	146	1980	11	-21	-5702	0	0
A33	134	5376	32	39	7849	0	0
A59	120	613	3	20	80	0	0
A87	108	189	1	-39	17281	0	0
A88	108	-136	0	-15	-1547	0	0
A16	97	3552	24	41	12261	-8	-854
A83	97	3205	21	-1	3110	0	0
A14	94	3062	21	19	1581	2	488
A70	86	945	4	16	1000	0	0
A73	82	-80	0	10	1983	0	0
A46	78	180	1	-38	-290	0	0
A78	74	180	1	-20	-273	0	0
A63	66	1540	7	-5	1002	0	0
A30	64	424	2	-21	-1045	0	0
A58	64	2340	13	38	10176	0	0
A71	64	348	2	28	384	0	0
A86	62	970	6	-16	-444	0	0
A98	62	1890	10	13	1864	0	0
A26	60	2268	12	-16	-2022	0	0
A15	56	358	2	-11	155	0	0

**Notes** Maximum and Total displacement are measured in 10-minute intervals

**Figure 4-13:** Bar-chart/table assessing the implications of stability for multiple airlines

#### 4.5.4 Assessment of the schedules obtained by the DA algorithm and comparison with s-MIP and u-MIP

The solution of s-MIP results in schedules with guaranteed acceptability but requires significant computational times for its solution. In fact, the MIP solution approach described in section 4.4.1 required more than 4 days of computations so as to provide a schedule with an MIP gap of 4.7% before resulting in a memory error. Even though the reported computational times appear to be reasonable for the considered airport instance, the solution of larger or more congested airport instances is expected to be intractable. To hedge against the computational complexity that arises from the introduction of stability considerations in ASA, in section 4.4.2, we have proposed a Deferred Acceptance algorithm (DA) and a multi-objective preference-based solution approach that has the ability to generate multiple schedules. The proposed DA algorithm and solution approach are solved based on two ASA schemes.

- the solution through the holistic consideration of all airport slot requests, prioritised through the functions of section 4.3.2.1 (identified as DA in Table 4-4); and
- the hybrid DA-MIP allocation scheme (identified as h-DA-MIP in Table 4-4), which first allocates *H* and *NE* requests using the model defined by expressions (4.1)-(4.5) and objective function (4.10) and then applies Algorithm 4-2 for *O* and *CH* requests.

The pure application of DA respects WASGs' prioritisation rules but allows more important requests of lower priorities, i.e., *CH, O* to displace *H* and *NE* requests. This approach enables one to study the impact of stability. On the other hand, h-DA-MIP ensures that all historic requests will receive their requested times

regardless of their functions' priority and allocates *NE* requests by considering an accurate definition of the slot pool. In h-DA-MIP, stability is solely enforced among *CH* and *O* requests.

DA and h-DA-MIP are solved using a list of preference list lengths (*PL*) that is equal to [0, 1, 3, 6, 9, 12, 15, 21, 24, 30, 36, 48, 60, 72, 84, 96, 108, 120, 132, 144]. Hence, for each entry in *PL*, DA and h-DA-MIP generate schedules by increasing the size of each requests' list length (introducing additional maximum displacement) so as to reduce spilled airline and passenger demand that are expressed through the rejected requests/passengers' objectives. This set of computational experiments also stands as a sensitivity analysis that enables one to study the impact of compromising requests' preferences on ASA performance. The results for both DA and h-DA-MIP and a comparison with the schedules obtained by the solution of s-MIP and u-MIP are facilitated by Figure 4-14. Figure 4-14 summarises the objective values reported by all considered ASA schemes with respect to multiple ASA performance metrics. During the generation of the schedules for DA and h-DA-MIP, we observed that the cardinality of the pending list and the list of scheduled requests was not altered after introducing preference list lengths of more than 108 intervals. This suggests that there is no need to consider maximum displacements of more than  $108 \times 10$ -minute intervals, since after that point compromises to requests' preferences result in no improvement for the considered ASA performance metrics. For the sake of clarity, the discussion regarding each performance metric is presented independently. Whenever deemed productive, cross-referencing allows the extraction of additional insights.

**Results regarding the average displacement per displaced passenger/request (subplots (a, b)):** These two metrics are expressed as the ratio between the schedule displacement and the displaced passengers/requests. An



initial observation is that s-MIP results in more displacement for both metrics than all other ASA schemes. That is because in s-MIP, for the same values of maximum/total displacement, there are less displaced passengers and requests, ergo implying that each displaced passenger/request is displaced more. This is justified by the fact that in objective function (4.10), the displaced requests' objective receives less priority than the rejected requests and total/maximum displacement objectives. In comparing the pure application of DA with h-DA-MIP, we observe that the pure application of DA results in less displacement per displaced passenger and request. However, the differences are more subtle for preference list lengths that are below 40 intervals. This signifies that the more one increases the size of the requests' preference list lengths, the pure application of DA can reduce the number of displaced requests and achieve improved displacement in comparison to h-DA-MIP. The reduced allocation flexibility allowed in h-DA-MIP results in more displacements and increased displacement per displaced request. On another note, the u-MIP schedule exhibits similar values to h-DA-MIP for approximately the same value of maximum displacement (101 intervals in u-MIP and 99 intervals in h-DA-MIP). This finding stands as validation on the ability of the proposed prioritisation functions to model the rules and priorities relating to *CH* requests (since for similar levels of maximum displacement the schedules exhibit similar objective values)

**Results regarding the displaced passengers/requests metrics (subplots (c, d)):** Since the number of displaced requests is considered as an explicit objective in the objective function of s-MIP, we observe that the schedule provided by s-MIP significantly outperforms all other ASA schemes with respect to both the number of displaced passengers and the number of displaced requests. For similar values of maximum displacement, i.e., 48-51  $\times$  10-minute intervals, it exhibits a reduction of

55% in relation to DA and 59% in relation to h-DA-MIP (for both metrics). This observation suggests that the ability of s-MIP to consider multiple objectives, results in improved scheduling performance with respect to these metrics. The DA algorithm proposed is limited to the consideration of maximum displacement in conjunction with the number of rejected requests and cannot integrate additional objectives. However, for the considered objectives, the DA algorithm variants produce schedules with values that are comparable to s-MIP. Again, for approximately equal values of maximum displacement, u-MIP demonstrates values that are comparable to the values of h-DA-MIP and the pure application of DA, ergo signifying the prioritisation functions' ability to model WASGs' rules and priorities.

**Results regarding the rejected passengers/requests metrics (subplots (e, f)):** These two metrics are explicitly considered in all ASA schemes. Notably, we observe that DA and h-DA-MIP result in values that are comparable to their MIP counterpart (s-MIP). For similar values of maximum displacement, the frontiers of DA and h-DA-MIP introduce at most 52 additional rejections, corresponding to 1% of the requests submitted to the airport. In fact, for increased values of maximum displacement DA and h-DA-MIP were able to outperform s-MIP with respect to both objectives. DA was able to propose a schedule with a maximum displacement of  $104 \times 10$  intervals and 26 rejected requests (4836 rejected passengers), while h-DA-MIP resulted in a schedule with  $99 \times 10$  intervals and 40 rejected requests (7492 rejected passengers). This finding suggests that the proposed DA algorithms constitute a tractable alternative to s-MIP and can generate multiple schedules from which the ASA decision-makers can later choose.

The improvements that result from the increase of maximum displacement, are more intense for maximum displacement values below  $40\text{-}60 \times 10\text{-minute}$

intervals but diminish after this threshold. This suggests that the airport capacity becomes more saturated as more requests are scheduled. Hence, even for large increases in terms of maximum displacement, the number of rejected requests is not significantly improved. Finally, for increased values of maximum displacement, the schedules proposed by DA and h-DA-MIP report objective values that are comparable to the schedules obtained by the unstable MIP (u-MIP). This suggests that the acceptability considerations in conjunction with the modelling of WASGs rules and priorities results in airport slot schedules that are comparable to current MIP solution approaches. This suggests that even after solving DA and h-DA-MIP the price of stability is not significant. For 23 (9) additional request rejections h-DA-MIP (DA) results in significant improvements with respect to all displacement-related metrics.

**Results regarding total displacement and total displacement of domestic movements (subplots (g, h)):** The more we increase the number of scheduled requests, the more is the total displacement of the airport slot schedules. This is a finding that is common for both (g) and (h), however, after exceeding  $60 \times 10$ -minute intervals of maximum displacement, it appears that the scheduling of additional requests results in diminishing increases with respect to total displacement. This finding is also evident in (e) and (f), where the increase of maximum displacement above the  $60 \times 10$ -minute maximum displacement threshold achieves insignificant reductions to the number of rejected requests.

Below the 60-minute threshold the trade-offs among all objectives are more intense. On another note, maximum and total displacement are monotonous, i.e., an increase (decrease) to the value of maximum displacement results in an increased (decreased) value of total displacement. The two objectives are known to be conflicting (Katsigiannis et al., 2021), yet this finding is justified by the following

conjecture. The increases to the size of the requests' preference lists result in increased maximum displacement but allows the accommodation of additional requests. Among the additional requests that are scheduled some will not be able to receive their requested times, ergo resulting in additional displacements. This observation also holds for sublots (c, d) and the displaced requests/passengers' objectives.

Overall, we observe that the DA algorithm variants (DA and h-DA-MIP) can ensure ASA stability by reporting objective values that are comparable to the values reported by s-MIP. In addition, it is evident that the sets of schedules generated by Algorithm 4-2 are not only acceptable and non-dominated with respect to each submitted request, but also constitute a Pareto front between the spilled airline/passenger demand and maximum displacement. From the analyses facilitated in Figure 4-14, it appears that the introduction of stability considerations is not prohibitive. This set of observations coupled with the computational tractability of Algorithm 4-2 suggest that DA algorithms may grasp the specificities of ASA, generate multiple stable schedules, and provide crucial decision-support to the ASA decision-making process.

From a decision-making perspective, when considering the DA algorithmic variants and the given list of preference list lengths ( $PL$ ) one generates at least 17 schedules per variant (17 for the DA and the h-DA-MIP). Hence, in the presence of multiple schedules, a question that arises concerns the reduction of the solutions presented to the decision-making process. Fortunately, by appropriately adjusting the  $PL$ , the proposed DA algorithm variants may consider the preferences of the stakeholders and propose a subset of stable schedules that can be easily assessed. An analysis demonstrating the solution space reduction facilitated by the adjustment of the  $PL$  is provided in the following section.

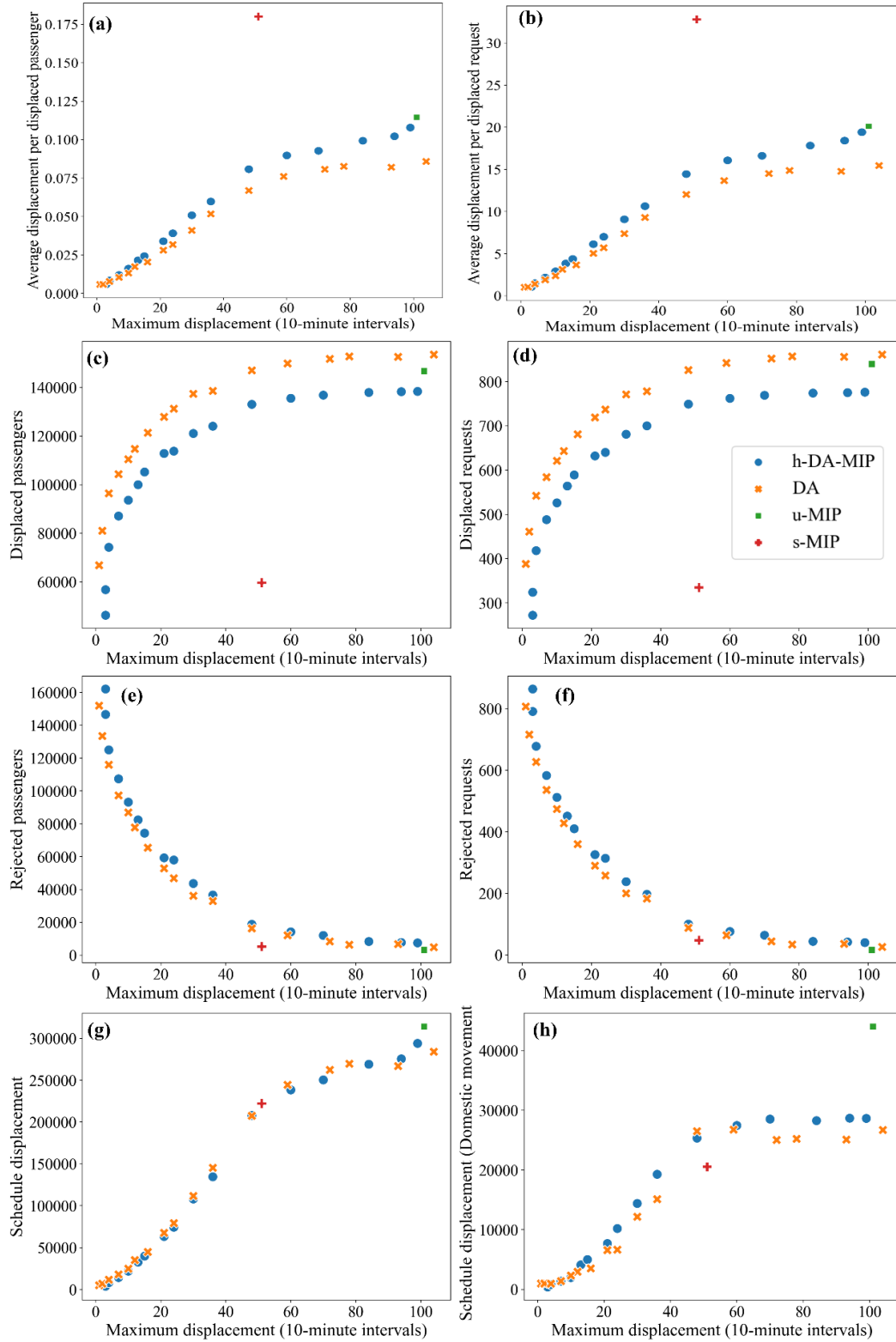


**Figure 4-14:** Comparison among the schedules generated by different slot allocation schemes

#### 4.5.4.1 Solution space reduction and decision-making support

The multi-objective scope and tractability of the proposed multi-objective DA algorithm variants enables the pertinent ASA stakeholders to reach to informed decisions by having more insights on the trade-offs among the ASA performance metrics of interest. However, as demonstrated in Figure 4-14, the DA algorithms may generate a large number of non-dominated schedules that cannot be easily assessed by the ASA stakeholders. In particular, each DA variant generates 17 stable schedules comprising multiple days of operations, and requests. Hence, by considering the decision-making capabilities of human beings (Miller, 1956) and the complexity of the ASA problem, there is need to provide a limited subset of schedules that can facilitate decision making. In order to represent the trade-offs among the ASA performance metrics of interest, we use the value paths associated with the non-dominated points generated by DA and h-DA-MIP and the schedules reported by s-MIP and u-MIP (see Figure 4-15).

The visualisation of multi-objective trade-offs using value paths provides improved decision support and aids the understanding of the properties of the alternative schedules (Weber and Desai, 1996; Weber et al., 1998; Dal Sasso et al., 2019) The horizontal axes in subplots (a)-(d) of Figure 4-15 consist of the ASA performance metrics of interest, while on the vertical axes they report the relative percentage gap of each schedule with respect to each metric (Dal Sasso et al., 2019). The relative percentage gap of each schedule ( $i$ ) with respect to each performance metric ( $j$ ), is calculated as per the following formula.

$$g_{i,j} = 100 \times \left( z_j(i) - \min_{\forall i \in I} z_j(i) \right) \left( \max_{i \in I} z_j(i) - \min_{\forall i \in I} z_j(i) \right)^{-1} \quad (4.37)$$

In expression (4.37),  $z_j(i)$  is the value reported by schedule  $i$  regarding performance metric  $j$ . In subplot (a) of Figure 4-15 one observes that the multiple

schedules generated by the variants of the DA algorithm, render the assessment of the trade-offs among the different performance metrics a challenging task. In subplot (a), it is evident (due to the intersection of the value paths) that the considered performance metrics are conflicting since the minimisation of one metric (e.g., maximum displacement) leads to increased values for other objective metrics (e.g., displaced passengers and the rejected requests). In assessing the schedules of the non-dominated set, one may address inherent decision complexity that stems from the multiple points through the filtering of solutions.

With respect to this aim, one could employ different filtering criteria, or adjust the *PL* input of the DA algorithms. For instance, one could consider the following criteria:

- Limit the value of the rejected requests so as to deviate at most 5% from the minimum value reported by u-MIP (subplot b);
- Adjust the *PL* of DA and h-DA-MIP so as to consider schedules that do not deviate more than 10% from the maximum displacement of s-MIP and/or u-MIP (subplots c and d).

Through the consideration of the above solution reduction criteria, the number of non-dominated points that are presented to the decision makers is reduced significantly. For instance, when limiting the number of rejected requests to deviate less than 5% from the value reported by u-MIP, the DA algorithms report 7 schedules as per subplot (b) of Figure 4-15 (3 for h-DA-MIP and 4 for the DA variant). In this case, the reported schedules demonstrate commonalities with the u-MIP schedule. The s-MIP schedule reports more rejected requests than all filtered schedules but exhibits fewer rejected requests/passengers during the scheduling season.

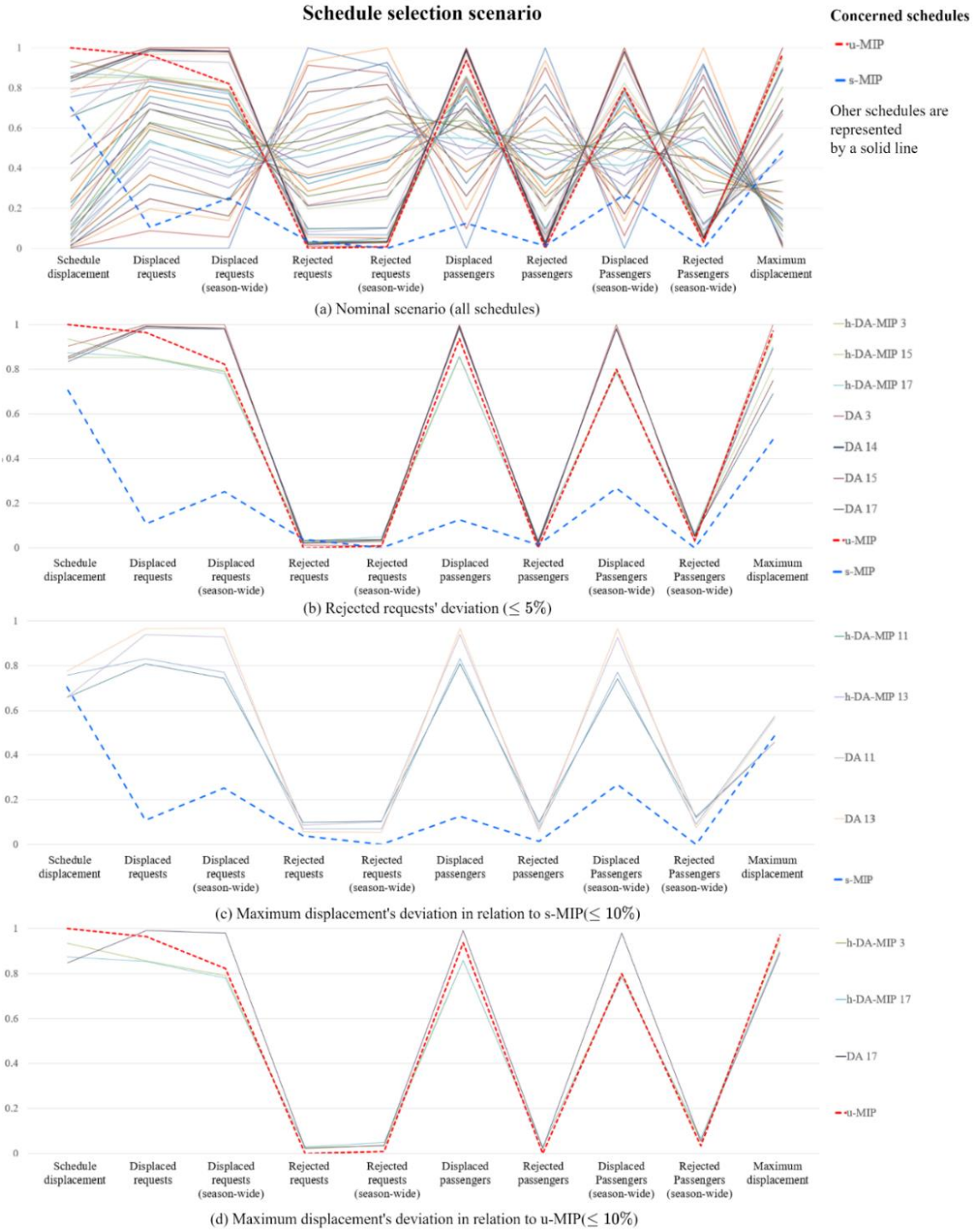


**Figure 4-15:** Value paths of alternative solution reduction scenarios

Another filtering approach could limit the number of schedules by accepting maximum displacement values that differ at most 10% the s-MIP or u-MIP schedules. When considering deviations within 10% from the maximum



displacement reported by s-MIP, the non-dominated set comprises 4 non-dominated points (2 schedules by the h-DA-MIP and 2 schedules by the DA). On the other hand, when considering schedules that have a maximum displacement that does not deviate more than the maximum displacement of u-MIP, the set of solutions is composed of 3 points (2 from the h-DA-MIP and 1 from the DA variant) as per subplot (d).

This filtration can be achieved by adjusting the preference list lengths included in  $PL$  and produce stable schedules that lie in proximity with s-MIP and u-MIP. Hence, the  $PL$  acts as a control valve on the number of points that can be generated by the solution algorithms and the range of the objective values that they report. Using this property, aiming to explore scheduling alternatives that are different from s-MIP and u-MIP, one could adjust  $PL$  so as to generate schedules that differ significantly in terms of the objective values that they report (e.g., maximum displacement, rejected requests). For instance, by limiting the DA algorithmic variant to generate solutions that are at least 20% different from the s-MIP and u-MIP schedules, one obtains 4 schedules that exhibit mild trade-offs among the objectives of interest (see Figure 4-16).

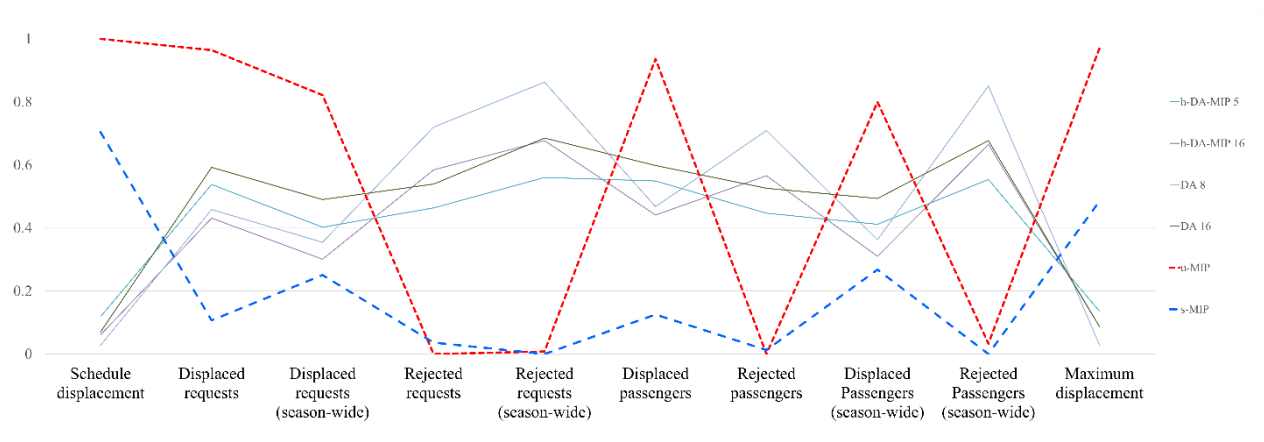


**Figure 4-16:** Selection of schedules that are different from s-MIP and u-MIP

Through the above analyses, we observe that the proposed DA algorithms integrate solution pruning capabilities that address the decision-making complexity associated with presenting multiple non-dominated points to the ASA decision-making. Having, schedules that comply with their decision-making requirements and the filtration criteria, ASA stakeholders can dive deeper on the schedules and examine the implications of alternative schedules on the request portfolios of different airlines (similar to the analysis presented in section 4.5.3.1). Having this additional, level of information available, airlines can convene with coordinators and evaluate the different solutions and the corresponding trade-offs. In what follows, the remainder of this section discusses the computational performance of the DA algorithm variants.

#### **4.5.4.2 Computational performance of the DA algorithm variants**

The DA algorithms can generate multiple schedules within tractable computational times. The performance profiles of the algorithms corresponding to the DA and h-DA-MIP ASA schemes, with respect to different lengths of preference lists, are presented in Figure 4-17. On the vertical axes Figure 4-17 plots the number of requests that are treated (scheduled or have empty preference lists) by the algorithms. Both subplots of Figure 4-17 share several commonalities. First, both variants have similar performance for all preference list lengths.

Furthermore, the larger the size of the requests' preference list length, the more time is needed to have a termination of the algorithms. For preference list sizes that concern maximum displacement values of less than 9 intervals, we observe that both algorithms terminate within 25 minutes. That is because small preference list sizes are parsed faster, and more requests are rejected. By examining Figure 4-17 in conjunction with Figure 4-14, the larger the number of scheduled requests, the more time is required for the algorithms to terminate.

Hence, the algorithms can support the definition of the pending list (list of unaccommodated requests) regardless the size of each request's preference list (see subplots (c, d) in Figure 4-14). The DA variant, which holistically considers all requests submitted to the airport, requires additional computational times for all preference list sizes. This is not only justified by the fact that it considers additional requests (h-DA-MIP considers only *CH* and *O* requests, since *H* and *NE* are pre-allocated by an MIP model), but also by the increased number of operations (as per Algorithm 4-1) that are required so as to reach to a stable schedule.

For both variants we observe that after allocating 80% of the requests, the airport's capacity becomes saturated, and the scheduling of an additional request requires the parsing of additional entries in their preference list. Under this observation, it appears that the allocation of 80% of the requests, results in a high saturation of the airport's capacity, hence forcing requests of lower priority to accept less beneficial timings and receive more displacement. For larger preference list sizes, DA and h-DA-MIP require larger computational times to converge, yet after examining and pruning entries from the requests' preference lists, they converge faster since there are less entries to consider. This is evident in Figure 4-17 when more than 95% of the requests are treated. This is justified by the fact that after the consideration of 95% of the requests, requests that remain unscheduled have reduced preference list sizes (the algorithms determined that multiple slots are unattainable for them).

In associating the computational performance of DA and h-DA-MIP with the solution space reduction techniques discussed in section 4.5.4.1, we observe that we may omit from *PL* preference list sizes that concern less than  $40 \times 10$ -minute intervals. That is because such preference considerations result in schedules with impractically large number of rejected requests. This observation may limit the

entries of  $PL$ , thus further expediting the solution times required for the convergence of DA and h-DA-MIP.

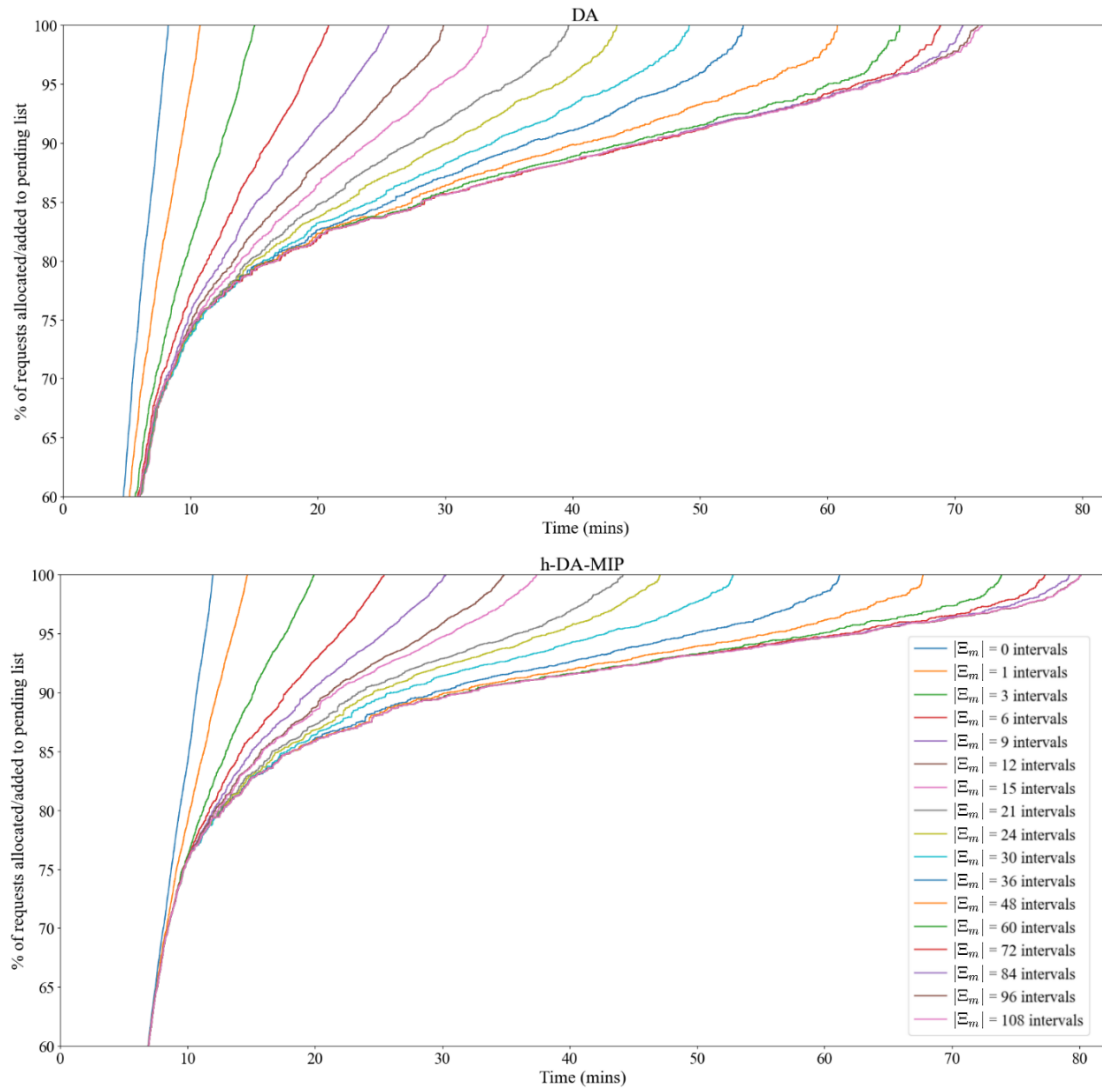


**Figure 4-17:** Performance profiles of DA and h-DA-MIP as a function of the requests' preference list size

To conclude, Algorithm 4-2 may be used to model alternative ASA schemes by combining alternative MIP formulation and the proposed DA algorithm (as in h-DA-MIP) and produce stable airport schedules within tractable computational times. The sets of schedules generated by the pure application of DA and h-DA-MIP required less than 12 hours of solution time. In considering, that s-MIP

required multiple days and did not prove optimality, DA algorithms stand as a viable solution for the generation of stable airport schedules. On a final note, Algorithm 4-1 and Algorithm 4-2 do not rely on the use of commercial solvers. Instead, they can be coded using any programming language and can be used by coordinators without requiring expensive licenses. This observation is significant since the use of expensive commercial solvers is an additional barrier that hinders the adoption of mathematical/computational-based ASA solutions in practice.

In the next section, we present a sample of the real-time output that is provided by Algorithm 4-1 and Algorithm 4-2 and its decision-making implications for practice and decision-making.

#### **4.5.5 Sample output and decision-making support**

A decision-support capability of the implementation of Algorithm 4-1 is that it generates real-time information on the provisional matchings, the requests that are added to the pending list and the displacements required so as to generate stable schedules. In Figure 4-18 we provide a screenshot with some output messages that are provided by Algorithm 4-1 during each iteration of Algorithm 4-2. The algorithm generates output for each operation (provisional allocation, displacement, rejection) and informs the user on the provisional allocations that are generated by identifying the requests that are concerned.

Furthermore, the output messages provide information on the type of the considered requests, i.e., unpaired arrival (a), unpaired departure (d) and paired movement (a, d). In cases that the allocation of a movement of a paired request is infeasible, the algorithm prints a message identifying the source of infeasibility, i.e., in displaying the following message: *there are blocking pairs (a, d) but the allocation to time slot 15 cannot be done after parsing all pairs (a),*

the algorithm identifies that the allocation of a paired request is infeasible since the arrival movement cannot be scheduled.

```

Allocation of 2018AIP180663 to time slots 8 and 12 is not possible
-----99.26% allocated-----
Allocation of 2018AIP180663 to time slots 136 and 140 is not possible
-----99.26% allocated-----
Request (a, d) 2018AIP180663 allocated to times 7 and 11 and request (a, d) 2018AIP180552 is unmatched
-----99.26% allocated-----
Allocation of 2018AIP181096 to time slots 126 and 130 is not possible
-----99.26% allocated-----
Request (a, d) 2018AIP181096 allocated to time 10 and request (a, d) 2018AIP180389 is unmatched
-----99.26% allocated-----
Allocation of 2018AIP180647 to time slots 22 and 26 is not possible
-----99.26% allocated-----
Request (a, d) 2018AIP180647 allocated to time slots 132 and 136
-----99.32% allocated-----
Allocated 2018AIP180099 only by removing the arrival blocking pair 2018AIP180746
...
allocation of 2018AIP180561 to time slots 85 and 91 is not possible
-----99.43% allocated-----
allocation to time slot 15 cannot be performed when trying unmatching (a, d) 2018AIP181900:
there are blocking pairs (a, d) but the allocation to time slot 15 cannot be done after parsing all pairs (a)
-----99.43% allocated-----
Allocation of 2018AIP180561 to this time slots 86 and 92 is not possible
...
-----99.66% allocated-----
Request (a, d) 2018AIP180555 added to pending list
...
-----99.94% allocated-----
Infeasible Turnaround Time for 2018AIP180663
-----99.94% allocated-----
Request (a, d) 2018AIP180663 allocated to time slot 2 and request (a, d) 2018AIP180552 is unmatched
-----99.94% allocated-----
Request (a, d) 2018AIP180552 allocated to time slots 1 and 7

```

**Figure 4-18:** Sample output from the execution of the proposed DA algorithm

Due to confidentiality concerns, in Figure 4-18, the identification of the requests is anonymous, but in reality, the IDs may be built using the airline and the flight code of the concerned requests. The output informs users on the overall completion of the algorithm, which is expressed as a percentage. This allows user to anticipate the completion of the algorithm. This set of features suggests that the DA algorithm proposed in this work is a user-friendly alternative to solver-based solutions and may constitute the basis for online coordination systems (see section 4.4.2.1) and slot coordination decision-support software.

## 4.6 Concluding remarks

To address the issue of acceptability in ASA decision-making, this paper proposes the Stable Airport Slot Allocation Problem (SASAP) which considers the interactions between airline demand and the coordinators' side when allocating airport slots so as to generate schedules that offer no incentives to airlines and coordinators to alter or reject the proposed request-to-slot assignments. These schedules are referred to as *stable* since they achieve equilibria between airlines' preferences and the coordinators' prioritisation, and lead to schedules that are Pareto optimal from the requests' perspective.

The proposed approach proposes request-to-slot assignments that are Pareto optimal per se, meaning that a request cannot receive an improved allocation without compromising the allocation efficiency of a more important request. In addressing SASAP, this paper proposed a game-theoretic MIP model (SASAM) and suitable preference-based solution algorithms. In doing so, the paper exploits prioritisation functions that model the interests of airlines and the policy rules considered by coordinators. In SASAP, ASA decisions are optimised through the consideration of stability/acceptability constraints that ensure that there will be no request-to-slot allocations that create incentives for airlines and coordinators to reject or alter the proposed schedules.

Under such schedules, there are no requests that would rather receive an alternative timing, or there will be no slots that may accommodate other requests of higher priority. The integration of stability constraints in ASA models and algorithms allows a better representation of the decision-making process applied by coordinators and considers airlines' preferences in conjunction with the limitations posed by the current ASA rules and priorities. Through extensive computational experiments we demonstrate that the proposed methodology allows a more efficient

utilisation of airport capacity, by decreasing unaccommodated flights (13% improvement) and passengers (40% improvement) during the entirety of the scheduling season.

The solution of SASAM is however a challenging task, since the stability constraints require the consideration of additional variables which often result in intractable formulations. To tackle this issue, the paper moves beyond the proposition of SASAM and implements a multi-objective, DA algorithm that can propose multiple Pareto optimal solutions. The efficiency of the DA algorithm was compared with SASAM and other alternative ASA prioritisation schemes. Despite the computational complexity of the problem, the preference-based algorithm may produce a large set of efficient schedules of comparable quality to the schedule proposed by SASAM, albeit requiring a fraction of the computational times required for the solution of SASAM. Computational experiments suggest that DA-based algorithms may provide schedules that achieve comparable values of total/maximum displacement and rejected/displaced requests.

Furthermore, the memory property of the proposed DA algorithm may constitute the backbone of a stable Online Coordination System (OCS) where requests are submitted by airlines dynamically, i.e., one at a time, and the coordinators have minimal participation. OCS is currently being used by multiple coordinators and airlines, providing real-time decision-support (for instance the online coordination system described in <https://www.online-coordination.com>). To the best of our knowledge the proposed DA algorithm is the first to store and update the feasible, stable allocations for each request, hence providing a modelling approach that can schedule requests dynamically and update their preference lists based on additional requests that may arrive. Besides, a distinguishing feature of the proposed DA algorithm is that, in contrast to existing ASA models and



algorithms, it does not have commercial solver and software dependencies. Hence, the proposed DA algorithm has less barriers for adoption in practice and can be readily applied by coordinators without requiring expensive software licenses.

The consideration of stable ASA decision-making creates ample room for future research. For instance, the proposition of multi-level solution approaches where DA algorithms are symbiotically combined with MIP formulations is another interesting pathway for future research. The adaptation of the airlines and coordinators' function to the decision-making context of different airports is a promising pathway for future research. On another note, the proposition of solution approaches that can store and update the preferences of airlines appears to be a promising research direction that can support current online coordination systems. As discussed in section 4.4.2.1 of this paper, the consideration of requests' timing preferences may facilitate on-line slot coordination and reduce computational times.

More realistic variants of SASAP may exploit commercial data sources (e.g., the data base of OAG - <https://www.oag.com/flight-data-seats>) or mine data to improve the fidelity of the proposed prioritisation functions (e.g., by estimating the average air fares per route through public datasets, i.e., the website of United States Department of Transportation, or by scrapping through the airlines' booking systems). Using such data sources, one could provide realistic estimates for the average load factors of each origin-destination pair and consider the average revenues of airlines across different routes. On another note, future game theoretic ASA approaches could benefit from the rich literature in stable matching theory so as to consider additional problem characteristics (Delorme et al., 2019; Ágoston et al., 2021) or propose improved formulations and pre-processing techniques (Pettersson et al., 2021).

Finally, the introduction of stability results in increased computational times that hinder the scalability of SASAM at large hub airports. To this effect, the proposition of more efficient MIP solution approaches that consider additional capacity parameters (e.g., passenger terminal constraints) and reduce the computational times required to solve SASAM is an important future research direction.



# Chapter 5: Conclusion

## 5.1 Summary

Airport demand management is the prevailing short-term solution for mitigating airport congestion, the associated delays, and their undesirable implications for passengers, airline profitability, and airport operations. The Airport Slot Allocation (ASA) process defined by WASG is the main administrative airport demand management mechanism that is applied in the majority of the world's most congested airports (also referred to as coordinated). The WASG-based ASA process is a multi-objective, multi-stakeholder problem that has attracted significant research interest.

During the last decade, researchers proposed mathematical/computational-based approaches that consider several problem characteristics and improve the efficiency of the ASA process defined by WASG. However, there exist several research questions that remain unaddressed (as identified by I–V in section 1.1). In considering questions (I)–(V) this thesis develops mathematical models and algorithms that generate information that would otherwise be unavailable to the decision-makers, ergo providing a pathway for further supporting the ASA decision-making and enhancing scheduling efficiency. A summary of the contributions of this thesis is provided below.

We have considered airlines' timing flexibility in ASA decision-making through time-dependent functions that model airlines' earliness/tardiness flexibility for each submitted request (research question I). The proposed flexibility functions are subsequently used as the basis of comprehensive airline utility functions that take into account several operational characteristics and competitive dynamics to approximate airlines' timing utility for each available time slot. The consideration

of airlines' timing flexibility and utility results in more extensive use of airport capacity without placing airlines in a disadvantageous position. Additionally, the thesis develops formulations that provide endogenous modelling of the capability of the airport's infrastructure to adapt dynamically to the characteristics (e.g., aircraft type) of airline demand (research question II). In addressing research questions (I) and (II) the thesis develops a model that can study the benefits that are brought upon by the isolated and the concurrent consideration of airlines' timing flexibility and the dynamic airport capacity constraints. Our analyses suggest synergies between (I) and (II) which result in more intensive use of the available airport capacity and reduced displacement. The benefit of considering (I) and (II) becomes more prominent in airports with limited infrastructure since it results in reduced spilled airline demand and hence improved connectivity.

Furthermore, by building upon the formulations developed for addressing I and II, the thesis developed a multi-objective, multi-stakeholder framework that considers the operational delays associated with strategic ASA decision-making. The framework generates the complete set of efficient schedules and provides estimates on the operational delays expected during peak days of operations (research question III). An intrinsic aspect of this framework is that it generates the complete set of non-dominated schedules for any linear, tri-objective ASA formulation; and then, by having full information on the available alternatives, mitigates decision-complexity through the proposition of representative airport slot schedules (research question IV) that do not compromise the information offered to the decision-makers. The proposed framework moves beyond this step and elicits a commonly-preferable schedule through the consideration of multi-stakeholder preferences (research question IV) concerning both operational delays and displacement-related metrics. With regards to (IV), the framework provides a look ahead on the implications of alternative schedules during peak days of operations

and quantifies the impact of the airport's current declared capacity setting. Overall, in addressing (III)-(IV) the thesis facilitates a more collaborative decision-making process and sheds light on the implications of alternative stakeholder preference considerations on ASA strategic and operational efficiency.

Finally, the thesis models the ASA as a two-sided matching game that considers the interactions between airlines timing flexibility and the WASG-based priorities assigned by the coordinators to each submitted request (research question V). In doing so, the thesis introduces a model (SASAM) that optimises an objective function that incorporates the multi-stakeholder considerations addressing research question (IV); and develops utility functions that approximate the value of each submitted airline request from the airline demand perspective and the WASG-based importance assigned to each request by the coordinators. The proposed functions extend the time-dependent flexibility functions concerning research question (I) and consider each request's operational characteristics (distance, effective period, available seat kilometres, competition, and connectivity) in conjunction with the policy-related priority of each request.

A multi-objective Deferred Acceptance (DA) algorithm enabling the generation of multiple stable airport slot schedules is developed and implemented. Overall, our analyses suggest that stability results in request-to-slot assignments that reduce the unaccommodated demand and result in improved displacement-related efficiency. This improvement is achieved at the expense of requests which concern fewer passengers and fewer days of operations. Furthermore, the developed DA algorithm has no commercial software dependencies, ergo reducing the barriers to adopting mathematics-based approaches in practice. Ultimately, we find that the proposed preference-based algorithm has beneficial properties for online airport slot scheduling and hence it may motivate and support future research in the area

The methodologies developed for addressing (I)–(V) are tested using data obtained from coordinated airports. Instance-specific results shed light on the implications of considering (I)–(V) in real-world ASA decisions and policy-making. In particular, a case study relating to research questions (I) and (II) suggests that the synergies achieved by the concurrent consideration of airlines timing flexibility and the dynamic airport capacity capabilities result in more efficient use of the existing airport capacity. This is demonstrated by improvements concerning multiple displacement-related efficiency metrics (ranging between 5 and 24% for the considered airport instance). Concerning (IV), one observes that the proposition of representative sets of airport slot schedules may reduce decision complexity without compromising the quality of the alternatives offered to the decision-makers. This claim is supported by a case study that achieves a 70% coverage in relation to the complete set of schedules through the use of 13% of the generated schedules. Computational results concerning the modelling of operational delays (research question III) and multi-stakeholder preferences (research question IV) recommend that schedules obtained under alternative preference considerations result in comparable levels of expected delays but improve significantly on the delays that would be experienced without the airport slot coordination process and the airport's declared capacity. Finally, in considering ASA decision-making as a two-sided matching game (research question V) one can achieve the scheduling of additional flights that serve more passengers (the number of unaccommodated flights and passengers throughout the scheduling season is reduced by 12% and 40% respectively). Based on the considered request and capacity data, this result requires the rejection of requests concerning fewer passengers and days of operations (rejection of an additional 1.2% of requests).

## 5.2 Recommendations for future research

During this research endeavour, we have uncovered additional ASA problem characteristics and research pathways that merit further investigation.

The thesis has mainly focused on exact models and solution algorithms to provide decision support for medium-sized regional airports. In modelling the airports' capacity, the thesis provides dynamic capacity constraints modelling both the landside and airside infrastructure. To provide decision-support for more challenging airport instances future research could employ pre-processing techniques that identify the bottlenecks of each airport's capacity (e.g., passenger terminal and/or runways) and appropriately reduce the size of the models by pruning redundant constraints. Furthermore, the proposition of efficient heuristic algorithms that consider multiple objectives and the problem aspects addressed by the thesis may reduce the solution times required for solving multi-objective formulations. With regards to this research direction, future studies could extend existing ASA heuristics (Androutsopoulos et al., 2019; Ribeiro et al., 2019) so as to propose multiple airport slot schedules that realistically consider the rules of WASG and study the trade-offs between the ASA scheduling objectives considered in literature and practice.

In addition, the thesis models the operational delays associated with strategic ASA decision-making through the evaluation of the operational implications of the generated schedules during days of peak demand. The explicit consideration of operational delays as an optimisation objective during the generation of the airport slot schedules is a research direction that can further improve the operational performance of strategic ASA decision-making, and better study the trade-offs between displacement-related and operational delay efficiency. In view of this research pathway, future studies may extend formulations that



jointly optimise schedule displacement and the expected queue lengths for a single day of operations under the U.S.-based ASA (Jacquillat and Odoni, 2015).

Meanwhile, in accordance with current practice, the formulations proposed in this thesis consider deterministic expressions of airport declared capacity. In acknowledging the uncertainty associated with airport operations, future studies could propose stochastic and/or robust expressions of airport declared capacity that takes into account the interrelationship of airport throughput and the stochasticity pertaining to weather conditions (Shone et al., 2019). Through the anticipation of weather stochasticity during operations, such approaches could provide a more accurate representation of the available airport capacity and provide schedules of increased operational performance that exhibit reduced operational delays without requiring significant displacements at the strategic ASA decision-making.

Finally, in modelling airlines' timing flexibility and utility for each submitted request, the thesis has provided approximation functions that leverage data that are made available during the ASA process. Future studies may extend the proposed functions by considering the revenues and aircraft utilisation associated with each request obtained through empirical data and commercial data sources. In the case that such data is unavailable, the representation of airlines' utility can be improved through data mining and machine learning techniques that will uncover airlines' scheduling behaviour and infer their timing preferences based on past request and allocation data.



# Bibliography

- ACI, 2019. 2019 Annual World Airport Traffic Dataset | ACI World [WWW Document]. ACI World Store. URL <https://store.aci.aero/product/annual-world-airport-traffic-dataset-2019/> (accessed 12.18.21).
- Adler, N., Yazhemsy, E., 2018. The value of a marginal change in capacity at congested airports. *Transportation Research Part A: Policy and Practice* 114, 154–167. <https://doi.org/10.1016/j.tra.2017.12.004>
- Ágoston, K.C., Biró, P., Kováts, E., Jankó, Z., 2021. College admissions with ties and common quotas: Integer programming approach. *European Journal of Operational Research*. <https://doi.org/10.1016/j.ejor.2021.08.033>
- Airport Coordination Limited, 2018. London Area Set For Continued Growth as ACL Maximises the Use of Available Capacity – Airport Coordination Limited [WWW Document]. URL <https://www.acl-uk.org/news/london-area-set-for-continued-growth-as-airport-coordination-ltd-maximises-the-use-of-available-capacity/> (accessed 7.3.19).
- Aloise, D., Deshpande, A., Hansen, P., Popat, P., 2009. NP-hardness of Euclidean sum-of-squares clustering. *Mach Learn* 75, 245–248. <https://doi.org/10.1007/s10994-009-5103-0>
- Androutsopoulos, K.N., Madas, M.A., 2019. Being fair or efficient? A fairness-driven modeling extension to the strategic airport slot scheduling problem. *Transportation Research Part E: Logistics and Transportation Review* 130, 37–60. <https://doi.org/10.1016/j.tre.2019.08.010>

- Androutsopoulos, K.N., Manousakis, E.G., Madas, M.A., 2019. Modelling and Solving a Bi-Objective Airport Slot Scheduling Problem. *European Journal of Operational Research*. <https://doi.org/10.1016/j.ejor.2019.12.008>
- Aull-Hyde, R., Erdogan, S., Duke, J.M., 2006. An experiment on the consistency of aggregated comparison matrices in AHP. *European Journal of Operational Research* 171, 290–295. <https://doi.org/10.1016/j.ejor.2004.06.037>
- Baïou, M., Balinski, M., 2000. The stable admissions polytope. *Math. Program.* 87, 427–439. <https://doi.org/10.1007/s101070050004>
- Ball, M., Barnhart, C., Dresner, M., Hansen, M., Neels, K., Amedeo, O., Peterson, E., Sherry, L., Trani, A., Zoo, B., 2010. Total Delay Impact Study.
- Baltagi, B.H., Griffin, J.M., Rich, D.P., 1995. Airline Deregulation: The Cost Pieces of the Puzzle. *International Economic Review* 36, 245–258. <https://doi.org/10.2307/2527435>
- Barnette, J.J., McLean, J.E., 1998. The Tukey Honestly Significant Difference Procedure and Its Control of the Type I Error-Rate.
- Barnhart, C., Cohn, A., 2004. Airline Schedule Planning: Accomplishments and Opportunities. *M&SOM* 6, 3–22. <https://doi.org/10.1287/msom.1030.0018>
- Barnhart, C., Fearing, D., Odoni, A., Vaze, V., 2012. Demand and capacity management in air transportation. *EURO J Transp Logist* 1, 135–155. <https://doi.org/10.1007/s13676-012-0006-9>
- Behzadian, M., Khanmohammadi Otaghsara, S., Yazdani, M., Ignatius, J., 2012. A state-of the-art survey of TOPSIS applications. *Expert Systems with Applications* 39, 13051–13069. <https://doi.org/10.1016/j.eswa.2012.05.056>

- Bichler, M., Littmann, R., Waldherr, S., 2021. Trading airport time slots: Market design with complex constraints. *Transportation Research Part B: Methodological* 145, 118–133. <https://doi.org/10.1016/j.trb.2021.01.003>
- Boland, N., Charkhgard, H., Savelsbergh, M., 2017. The Quadrant Shrinking Method: A simple and efficient algorithm for solving tri-objective integer programs. *European Journal of Operational Research* 260, 873–885. <https://doi.org/10.1016/j.ejor.2016.03.035>
- Boland, N., Charkhgard, H., Savelsbergh, M., 2016. The L-shape search method for triobjective integer programming. *Math. Prog. Comp.* 8, 217–251. <https://doi.org/10.1007/s12532-015-0093-3>
- Bråthen, S., Eriksen, K.S., 2018. Regional aviation and the PSO system – Level of Service and social efficiency. *Journal of Air Transport Management* 69, 248–256. <https://doi.org/10.1016/j.jairtraman.2016.10.002>
- Brunsch, T., Goyal, N., Rademacher, L., Röglin, H., 2014. Lower Bounds for the Average and Smoothed Number of Pareto-Optima. *Theory of Computing* 10, 237–256. <https://doi.org/10.4086/toc.2014.v010a010>
- Burghouwt, G., Redondi, R., 2013. Connectivity in Air Transport Networks: An Assessment of Models and Applications. *Journal of Transport Economics and Policy* 47, 35–53.
- Cao, Y., Smucker, B.J., Robinson, T.J., 2015. On using the hypervolume indicator to compare Pareto fronts: Applications to multi-criteria optimal experimental design. *Journal of Statistical Planning and Inference* 160, 60–74. <https://doi.org/10.1016/j.jspi.2014.12.004>

- Castelli, L., Pellegrini, P., 2011. An AHP analysis of air traffic management with target windows. *Journal of Air Transport Management* 17, 68–73. <https://doi.org/10.1016/j.jairtraman.2010.05.006>
- Castelli, L., Pellegrini, P., Pesenti, R., 2011. Airport slot allocation in Europe: economic efficiency and fairness. *International Journal of Revenue Management* 6, 28–44. <https://doi.org/10.1504/IJRM.2012.044514>
- Cavusoglu, S.S., Macário, R., 2021. Minimum delay or maximum efficiency? Rising productivity of available capacity at airports: Review of current practice and future needs. *Journal of Air Transport Management*. <https://doi.org/10.1016/j.jairtraman.2020.101947>
- Chiu, S.L., 1994. Fuzzy Model Identification Based on Cluster Estimation.
- Cohon, J.L., 1978. Multiobjective programming and planning. Courier Corporation.
- Council Regulation (EEC) No 95/93, 1993. Common rules for the allocation of slots at Community airports.
- Dächert, K., Klamroth, K., 2015. A linear bound on the number of scalarizations needed to solve discrete tricriteria optimization problems. *J Glob Optim* 61, 643–676. <https://doi.org/10.1007/s10898-014-0205-z>
- Dal Sasso, V., Djeumou Fomeni, F., Lulli, G., Zografos, K.G., 2019. Planning efficient 4D trajectories in Air Traffic Flow Management. *European Journal of Operational Research*. <https://doi.org/10.1016/j.ejor.2019.01.039>
- de Neufville, R., Odoni, A., 2003. AIRPORT SYSTEMS. PLANNING, DESIGN AND MANAGEMENT.

- de Neufville, R., Odoni, A.R., 2013. Airport Systems: Planning, Design, and Management, 2nd ed. Mc Graw Hill.
- Delorme, M., García, S., Gondzio, J., Kalcsics, J., Manlove, D., Petterson, W., 2019. Mathematical models for stable matching problems with ties and incomplete lists. *European Journal of Operational Research* 277, 426–441. <https://doi.org/10.1016/j.ejor.2019.03.017>
- Diebold, F., Bichler, M., 2017. Matching with indifferences: A comparison of algorithms in the context of course allocation. *European Journal of Operational Research* 260, 268–282. <https://doi.org/10.1016/j.ejor.2016.12.011>
- Dray, L., 2020. An empirical analysis of airport capacity expansion. *Journal of Air Transport Management* 87, 101850. <https://doi.org/10.1016/j.jairtraman.2020.101850>
- European Commission, 2018. Public Service Obligations (PSOs) - Mobility and Transport - European Commission [WWW Document]. Mobility and Transport. URL [https://ec.europa.eu/transport/modes/air/internal-market/pso\\_en](https://ec.europa.eu/transport/modes/air/internal-market/pso_en) (accessed 8.14.18).
- European Commission, 2017. Commission Notice — Interpretative guidelines on Regulation (EC) No 1008/2008 of the European Parliament and of the Council — Public Service Obligations (PSO).
- Fairbrother, J., Zografos, K.G., 2020. Optimal scheduling of slots with season segmentation. *European Journal of Operational Research*. <https://doi.org/10.1016/j.ejor.2020.10.003>

- Fairbrother, J., Zografos, K.G., Glazebrook, K., 2019. A slot scheduling mechanism at congested airports which incorporates efficiency, fairness and airline preferences. *Transportation Science*. <https://doi.org/10.1287/trsc.2019.0926>
- Feng, C.-M., Wang, R.-T., 2000. Performance evaluation for airlines including the consideration of financial ratios. *Journal of Air Transport Management* 6, 133–142. [https://doi.org/10.1016/S0969-6997\(00\)00003-X](https://doi.org/10.1016/S0969-6997(00)00003-X)
- Gale, D., Shapley, L.S., 1962. College Admissions and the Stability of Marriage. *The American Mathematical Monthly* 69, 9–15. <https://doi.org/10.2307/2312726>
- Gharote, M., Phuke, N., Patil, R., Lodha, S., 2019. Multi-objective stable matching and distributional constraints. *Soft Comput* 23, 2995–3011. <https://doi.org/10.1007/s00500-019-03763-4>
- Gillen, D., Jacquillat, A., Odoni, A.R., 2016. Airport demand management: The operations research and economics perspectives and potential synergies. *Transportation Research Part A: Policy and Practice* 94, 495–513. <https://doi.org/10.1016/j.tra.2016.10.011>
- Gurobi Optimization, L., 2018. Gurobi Optimizer Reference Manual.
- Gurobi Optimization, LLC, 2021. Gurobi Optimizer Reference Manual.
- Haimes, Y.Y., 1971. Modeling and Control of the Pollution of Water Resources Systems Via Multilevel Approach1. *JAWRA Journal of the American Water Resources Association* 7, 93–101. <https://doi.org/10.1111/j.1752-1688.1971.tb01681.x>



- Hanowsky, M., Sussman, J.M., 2008. Design of Ground Delay Programs Considering the Stakeholder Perspective (Working Paper). Massachusetts Institute of Technology. Engineering Systems Division.
- Hanowsky, M.J., 2008. A model to design a stochastic and dynamic ground delay program subject to non-linear cost functions (Thesis). Massachusetts Institute of Technology.
- Hickley, P., 2004. Great Circle Versus Rhumb Line Cross-track Distance at Mid-Longitude. *Journal of Navigation* 57, 320–325.  
<https://doi.org/10.1017/S0373463304002681>
- Hsu, W.L., Nemhauser, G.L., 1979. Easy and hard bottleneck location problems. *Discrete Applied Mathematics* 1, 209–215.
- Hwang, C.-L., Yoon, K., 1981. Multiple Attribute Decision Making, Lecture Notes in Economics and Mathematical Systems. Springer Berlin Heidelberg, Berlin, Heidelberg. <https://doi.org/10.1007/978-3-642-48318-9>
- IATA, 2021. Worldwide Airport Slots - Fact Sheet [WWW Document]. URL <https://www.iata.org/en/iata-repository/pressroom/fact-sheets/fact-sheet--airport-slots/> (accessed 11.15.21).
- IATA, 2020. Worldwide Slot Guidelines - 10th Edition [WWW Document]. URL <https://www.iata.org/policy/slots/Documents/wsg-edition-9-english-version.pdf> (accessed 4.16.19).
- IATA, 2019a. Worldwide Slot Guidelines - 9th Edition [WWW Document]. URL <https://www.iata.org/contentassets/4ede2aabfcc14a55919e468054d714fe/wsg-edition-9-english-version.pdf> (accessed 2.16.20).

- IATA, 2019b. Resolution: Airlines Urge Governments to Adhere to Global Slot Allocation Guidelines [WWW Document]. URL <https://www.iata.org/pressroom/pr/pages/2019-06-02-03.aspx> (accessed 7.24.19).
- IATA, 2018. Worldwide Airport Slots - Fact Sheet [WWW Document]. URL [https://www.iata.org/pressroom/facts\\_figures/fact\\_sheets/Documents/fact-sheet-airport-slots.pdf](https://www.iata.org/pressroom/facts_figures/fact_sheets/Documents/fact-sheet-airport-slots.pdf) (accessed 10.24.18).
- IATA, 2013. IATA ECONOMIC BRIEFING - Inefficiency in European Airspace [WWW Document]. URL <https://www.iata.org/en/iata-repository/publications/economic-reports/inefficiency-in-european-airspace/> (accessed 2.5.19).
- IATA/ACI/WWACG, 2020. Worldwide Airport Slot Guidelines [WWW Document]. URL <https://www.iata.org/en/policy/slots/slot-guidelines/> (accessed 9.22.20).
- ICAO, 2019. The World of Air Transport in 2019 (ICAO Annual Report) [WWW Document]. URL <https://www.icao.int/annual-report-2019/Pages/the-world-of-air-transport-in-2019.aspx> (accessed 9.20.21).
- Jacquillat, A., Odoni, A.R., 2015. An Integrated Scheduling and Operations Approach to Airport Congestion Mitigation. *Operations Research* 63, 1390–1410. <https://doi.org/10.1287/opre.2015.1428>
- Jacquillat, A., Vaze, V., 2018. Interairline Equity in Airport Scheduling Interventions. *Transportation Science*. <https://doi.org/10.1287/trsc.2017.0817>

- Jiang, Y., Zografos, K.G., 2021. A Decision Making Framework for Incorporating Fairness in Allocating Slots at Capacity-Constrained Airports. *Transportation Research Part C: Emerging Technologies*.  
<https://doi.org/10.1016/j.trc.2021.103039>
- Jiang, Y., Zografos, K.G., 2017. Modelling fairness in slot scheduling decisions at capacity-constrained airports.
- Jorge, D., Antunes Ribeiro, N., Pais Antunes, A., 2021. Towards a decision-support tool for airport slot allocation: Application to Guarulhos (Sao Paulo, Brazil). *Journal of Air Transport Management* 93, 102048.  
<https://doi.org/10.1016/j.jairtraman.2021.102048>
- Kahn, A.E., 1988. Surprises of Airline Deregulation. *The American Economic Review* 78, 316–322.
- Katsigiannis, F.A., Zografos, K.G., 2021a. Optimising airport slot allocation considering flight-scheduling flexibility and total airport capacity constraints. *Transportation Research Part B: Methodological* 146, 20–87.  
<https://doi.org/10.1016/j.trb.2021.02.002>
- Katsigiannis, F.A., Zografos, K.G., 2021b. A multi-criteria approach for optimising and assessing airport schedules. Presented at the 3rd IMA and OR Society Conference on Mathematics of Operational Research, Online.
- Katsigiannis, F.A., Zografos, K.G., Fairbrother, J., 2021. Modelling and solving the airport slot-scheduling problem with multi-objective, multi-level considerations. *Transportation Research Part C: Emerging Technologies* 124, 102914. <https://doi.org/10.1016/j.trc.2020.102914>

- Kirlik, G., Sayın, S., 2014. A new algorithm for generating all nondominated solutions of multiobjective discrete optimization problems. *European Journal of Operational Research* 232, 479–488. <https://doi.org/10.1016/j.ejor.2013.08.001>
- Kivestu, P.A., 1976. Alternative methods of investigating the time dependent M/G/k queue (PhD Thesis). Massachusetts Institute of Technology.
- Koesters, D., 2007. Airport scheduling performance—An approach to evaluate the airport scheduling process by using scheduled delays as quality criterion, in: *Proceedings of the Air Transport Research Society (ATRS) Annual World Conference*, June 21.
- Kumar, V., Sherry, L., 2009. Airport throughput capacity limits for demand management planning, in: *2009 Integrated Communications, Navigation and Surveillance Conference*. Presented at the 2009 Integrated Communications, Navigation and Surveillance Conference, pp. 1–10. <https://doi.org/10.1109/ICNSURV.2009.5172836>
- Lai, Y.-J., Liu, T.-Y., Hwang, C.-L., 1994. TOPSIS for MODM. *European Journal of Operational Research, Facility Location Models for Distribution Planning* 76, 486–500. [https://doi.org/10.1016/0377-2217\(94\)90282-8](https://doi.org/10.1016/0377-2217(94)90282-8)
- MacFarland, T.W., Yates, J.M., 2016. Wilcoxon Matched-Pairs Signed-Ranks Test, in: MacFarland, T.W., Yates, J.M. (Eds.), *Introduction to Nonparametric Statistics for the Biological Sciences Using R*. Springer International Publishing, Cham, pp. 133–175. [https://doi.org/10.1007/978-3-319-30634-6\\_5](https://doi.org/10.1007/978-3-319-30634-6_5)

- Madas, M.A., Zografos, K.G., 2010. Airport slot allocation: a time for change? *Transport Policy* 17, 274–285. <https://doi.org/10.1016/j.tranpol.2010.02.002>
- Manlove, D., 2013. *Algorithmics of matching under preferences*. World Scientific.
- Marler, R.T., Arora, J.S., 2004. Survey of multi-objective optimization methods for engineering. *Struct Multidisc Optim* 26, 369–395. <https://doi.org/10.1007/s00158-003-0368-6>
- Mavoian, G., Pilon, N., Allard/Valeane, E., 2016. *Optimised Airspace User Operations*.
- Miller, G.A., 1956. The magical number seven plus or minus two: some limits on our capacity for processing information. *Psychol Rev* 63, 81–97.
- Mirković, B., Tošić, V., 2017. The difference between hub and non-hub airports – An airside capacity perspective. *Journal of Air Transport Management* 62, 121–128. <https://doi.org/10.1016/j.jairtraman.2017.03.013>
- Mirković, B., Tošić, V., 2014. Airport apron capacity: estimation, representation, and flexibility. *Journal of Advanced Transportation* 48, 97–118. <https://doi.org/10.1002/atr.1250>
- MIT, U.S. Department of Transportation, 2021. Airline Data Project [WWW Document]. URL <http://web.mit.edu/airlinedata/www/Traffic&Capacity.html> (accessed 9.20.21).
- Morisset, T., Odoni, A., 2011. Capacity, Delay, and Schedule Reliability at Major Airports in Europe and the United States. *Transportation Research Record* 2214, 85–93. <https://doi.org/10.3141/2214-11>

- Morrison, S.A., Winston, C., 1990. The Dynamics of Airline Pricing and Competition. *The American Economic Review* 80, 389–393.
- Odoni, A.R., 2020. A Review Of Certain Aspects Of The Slot Allocation Process At Level 3 Airports Under Regulation 95/93 [WWW Document]. URL <https://www.aeroport.fr/uploads/documents/etude-de-m.-odini-du-mit.pdf?v12> (accessed 12.5.20).
- Pellegrini, P., Bolić, T., Castelli, L., Pesenti, R., 2017. SOSTA: An effective model for the Simultaneous Optimisation of airport Slot Allocation. *Transportation Research Part E: Logistics and Transportation Review* 99, 34–53. <https://doi.org/10.1016/j.tre.2016.12.006>
- Pettersson, W., Delorme, M., García, S., Gondzio, J., Kalcsics, J., Manlove, D., 2021. Improving solution times for stable matching problems through preprocessing. *Computers and Operations Research*. <https://doi.org/10.1016/j.cor.2020.105128>
- Pyrgiotis, N., Malone, K.M., Odoni, A., 2013. Modelling delay propagation within an airport network. *Transportation Research Part C: Emerging Technologies, Selected papers from the Seventh Triennial Symposium on Transportation Analysis (TRISTAN VII)* 27, 60–75. <https://doi.org/10.1016/j.trc.2011.05.017>
- Pyrgiotis, N., Odoni, A., 2015. On the Impact of Scheduling Limits: A Case Study at Newark Liberty International Airport. *Transportation Science* 50, 150–165. <https://doi.org/10.1287/trsc.2014.0564>
- Qualtrics Survey Software [WWW Document], 2020. . Qualtrics. URL <https://www.qualtrics.com/uk/> (accessed 9.8.20).

- Ramanathan, R., Ganesh, L.S., 1995a. Using AHP for resource allocation problems. *European Journal of Operational Research* 80, 410–417. [https://doi.org/10.1016/0377-2217\(93\)E0240-X](https://doi.org/10.1016/0377-2217(93)E0240-X)
- Ramanathan, R., Ganesh, L.S., 1995b. Energy resource allocation incorporating qualitative and quantitative criteria: An integrated model using goal programming and AHP. *Socio-Economic Planning Sciences* 29, 197–218. [https://doi.org/10.1016/0038-0121\(95\)00013-C](https://doi.org/10.1016/0038-0121(95)00013-C)
- Ramanathan, R., Ganesh, L.S., 1994. Group preference aggregation methods employed in AHP: An evaluation and an intrinsic process for deriving members' weightages. *European Journal of Operational Research* 79, 249–265. [https://doi.org/10.1016/0377-2217\(94\)90356-5](https://doi.org/10.1016/0377-2217(94)90356-5)
- Ribeiro, N.A., Jacquillat, A., Antunes, A.P., 2019a. A Large-Scale Neighborhood Search Approach to Airport Slot Allocation. *Transportation Science*. <https://doi.org/10.1287/trsc.2019.0922>
- Ribeiro, N.A., Jacquillat, A., Antunes, A.P., Odoni, A., 2019b. Improving slot allocation at Level 3 airports. *Transportation Research Part A: Policy and Practice* 127, 32–54. <https://doi.org/10.1016/j.tra.2019.06.014>
- Ribeiro, N.A., Jacquillat, A., Antunes, A.P., Odoni, A.R., Pita, J.P., 2018. An optimization approach for airport slot allocation under IATA guidelines. *Transportation Research Part B: Methodological* 112, 132–156. <https://doi.org/10.1016/j.trb.2018.04.005>
- Rossum, G. van, 1995. Python tutorial (No. CS-R9526). Centrum voor Wiskunde en Informatica (CWI), Amsterdam.

- Roth, A.E., Rothblum, U.G., Vate, J.H.V., 1993. Stable Matchings, Optimal Assignments, and Linear Programming. *Mathematics of Operations Research* 18, 803–828.
- Saaty, T.L., 2015. Rank Preservation and Reversal in Decision Making. *Journal of Advances in Management Sciences & Information Systems* 1, 34–37.
- Saaty, T.L., 2008. Decision making with the analytic hierarchy process. *International Journal of Services Sciences* 1, 83–98.  
<https://doi.org/10.1504/IJSSci.2008.01759>
- Saaty, T.L., 1989. Group Decision Making and the AHP, in: *The Analytic Hierarchy Process*. Springer, Berlin, Heidelberg, pp. 59–67.  
[https://doi.org/10.1007/978-3-642-50244-6\\_4](https://doi.org/10.1007/978-3-642-50244-6_4)
- Schoner, B., Wedley, W.C., 1989. Ambiguous Criteria Weights in AHP: Consequences and Solutions\*. *Decision Sciences* 20, 462–475.  
<https://doi.org/10.1111/j.1540-5915.1989.tb01561.x>
- Shone, R., Glazebrook, K., Zografos, K.G., 2019. Resource allocation in congested queueing systems with time-varying demand: An application to airport operations. *European Journal of Operational Research* 276, 566–581.  
<https://doi.org/10.1016/j.ejor.2019.01.024>
- Sidiropoulos, S., Majumdar, A., Han, K., 2018. A framework for the optimization of terminal airspace operations in Multi-Airport Systems. *Transportation Research Part B: Methodological* 110, 160–187.  
<https://doi.org/10.1016/j.trb.2018.02.010>



- Stamatopoulos, M.A., Zografos, K.G., Odoni, A.R., 2004. A decision support system for airport strategic planning. *Transportation Research Part C: Emerging Technologies* 12, 91–117. <https://doi.org/10.1016/j.trc.2002.10.001>
- Stan Schenkerman, 1994. Avoiding rank reversal in AHP decision-support models. *European Journal of Operational Research* 74, 407–419. [https://doi.org/10.1016/0377-2217\(94\)90220-8](https://doi.org/10.1016/0377-2217(94)90220-8)
- Swaroop, P., Zou, B., Ball, M.O., Hansen, M., 2012. Do more US airports need slot controls? A welfare based approach to determine slot levels. *Transportation Research Part B: Methodological* 46, 1239–1259. <https://doi.org/10.1016/j.trb.2012.03.002>
- Tableau [WWW Document], 2021. URL <https://community.tableau.com/s/> (accessed 4.10.21).
- Tomashevskii, I.L., 2015. Eigenvector ranking method as a measuring tool: Formulas for errors. *European Journal of Operational Research* 240, 774–780. <https://doi.org/10.1016/j.ejor.2014.07.050>
- Tukey, J.W., 1949. Comparing Individual Means in the Analysis of Variance. *Biometrics* 5, 99–114. <https://doi.org/10.2307/3001913>
- Van Rossum, G., Drake, F.L., 2009. *Python 3 Reference Manual*. CreateSpace, Scotts Valley, CA.
- Vaze, V., Barnhart, C., 2012. Modeling Airline Frequency Competition for Airport Congestion Mitigation. *Transportation Science* 46, 512–535. <https://doi.org/10.1287/trsc.1120.0412>

- Vossen, T., Ball, M., 2006. Optimization and mediated bartering models for ground delay programs. *Naval Research Logistics (NRL)* 53, 75–90.  
<https://doi.org/10.1002/nav.20123>
- Vowles, T.M., 2006. Airfare pricing determinants in hub-to-hub markets. *Journal of Transport Geography* 14, 15–22.  
<https://doi.org/10.1016/j.jtrangeo.2004.10.004>
- Weber, C.A., Current, J.R., Desai, A., 1998. Non-cooperative negotiation strategies for vendor selection. *European Journal of Operational Research* 108, 208–223. [https://doi.org/10.1016/S0377-2217\(97\)00131-8](https://doi.org/10.1016/S0377-2217(97)00131-8)
- Weber, C.A., Desai, A., 1996. Determination of paths to vendor market efficiency using parallel coordinates representation: A negotiation tool for buyers. *European Journal of Operational Research* 90, 142–155.  
[https://doi.org/10.1016/0377-2217\(94\)00336-X](https://doi.org/10.1016/0377-2217(94)00336-X)
- Wei, W., Hansen, M., 2003. Cost Economics of Aircraft Size. *Journal of Transport Economics and Policy (JTEP)* 37, 279–296.
- WWACG, 2019. WWACG Guideline - Coordination Parameters [WWW Document]. <http://www.wwacg.org/>. URL  
<http://www.wwacg.org/up/files/WWACG%20Guidelines/WWACG%20Guideline%20-%20Coordination%20Parameters.pdf> (accessed 5.4.20).
- Yadav, V., Karmakar, S., Kalbar, P.P., Dikshit, A.K., 2019. PyTOPS: A Python based tool for TOPSIS. *SoftwareX* 9, 217–222.  
<https://doi.org/10.1016/j.softx.2019.02.004>

- Zeng, W., Ren, Y., Wei, W., Yang, Z., 2021. A data-driven flight schedule optimization model considering the uncertainty of operational displacement. *Computers & Operations Research* 133, 105328. <https://doi.org/10.1016/j.cor.2021.105328>
- Zio, E., Bazzo, R., 2011. A clustering procedure for reducing the number of representative solutions in the Pareto Front of multiobjective optimization problems. *European Journal of Operational Research* 210, 624–634. <https://doi.org/10.1016/j.ejor.2010.10.021>
- Zitzler, E., Thiele, L., Laumanns, M., Fonseca, C.M., Fonseca, V.G. da, 2003. Performance assessment of multiobjective optimizers: an analysis and review. *IEEE Transactions on Evolutionary Computation* 7, 117–132. <https://doi.org/10.1109/TEVC.2003.810758>
- Zografos, K.G., Androutsopoulos, K.N., Madas, M.A., 2017a. Minding the gap: Optimizing airport schedule displacement and acceptability. *Transportation Research Part A: Policy and Practice*. <https://doi.org/10.1016/j.tra.2017.09.025>
- Zografos, K.G., Jiang, Y., 2019. A Bi-objective Efficiency-Fairness Model for Scheduling Slots at Congested Airports. *Transportation Research Part C: Emerging Technologies* 102, 336–350. <https://doi.org/10.1016/j.trc.2019.01.023>
- Zografos, K.G., Jiang, Y., 2016. Modelling and solving the airport slot scheduling problem with efficiency, fairness, and accessibility considerations. Presented at the 9th Triennial Symposium on Transportation Analysis (TRISTAN16), Aruba.

- 
- Zografos, K.G., Madas, M.A., Androutsopoulos, K.N., 2017b. Increasing airport capacity utilisation through optimum slot scheduling: review of current developments and identification of future needs. *J Sched* 20, 3–24. <https://doi.org/10.1007/s10951-016-0496-7>
- Zografos, K.G., Madas, M.A., Salouras, Y., 2013. A decision support system for total airport operations management and planning. *Journal of Advanced Transportation* 47, 170–189. <https://doi.org/10.1002/atr.154>
- Zografos, K.G., Salouras, Y., Madas, M.A., 2012. Dealing with the efficient allocation of scarce resources at congested airports. *Transportation Research Part C: Emerging Technologies* 21, 244–256. <https://doi.org/10.1016/j.trc.2011.10.008>

